Title
NUCLEAR SCIENCE DIVISION ANNUAL REPORT 1979-1980

Author
Cerny, J.

Publication Date
1980

Peer reviewed

LBL-11588
UC-34

NUCLEAR SCIENCE

ANNUAL REPORT
1979-1980

March 1981

LAWRENCE BERKELEY LABORATORY
UNIVERSITY OF CALIFORNIA

Prepared for the U.S. Department of Energy under Contract W-7405-ENG-48

Contents

Part 1. Research Programs

Part 2. Progress Reports

I. Experimental Research

A. Nuclear Structure

B. Nuclear Reactions and Scattering

1. Microscopic

2. Macroscopic

II. Theory of Nuclear Collisions

III. Instrumentation

A. SuperHILAC and 88 Inch Cyclotron

Part 3. Appendices

INTRODUCTION

This annual report describes the scientific research carried out within the Nuclear Science Division (NSD) during the period between July 1, 1979 and June 30, 1980. The principal objective of the division continues to be the experimental and theoretical investigation of the interactions of heavy ions with target nuclei, complemented with programs in light ion nuclear science, in nuclear data compilations, and in advanced instrumentation development.

Directly affiliated with the division during this period were 5 faculty senior scientists, 16 staff senior scientists, 22 staff scientists, 3 divisional fellows, 15 post-doctoral fellows, 21 graduate students, 46 visitors (the majority from 12 foreign countries), and 24 technical, administrative and clerical support staff. The FY 1980 operating budget was $8,165,000. Ninety-four journal articles and reports were published by division members, and three Ph.D. degrees were awarded to Nuclear Science Division students.

During this period there have been some progressive changes in the division. Two Assistant Division Heads were appointed: Michael Zisman oversees the planning and development of the division's many equipment, computer, and instrumentation projects while Janis Dairiki's responsibilities lie in the general area of scientific administration. There have also been some welcome staff additions:

> Howel Pugh has joined the NSD staff as the Scientific Director of the Bevalac. He was previously Head of the Nuclear Science Section at the National Science Foundation. Because of his responsibility for the research program at the Bevalac, which cuts across LBL division lines, and as co-chairman (with Tom Elioff) of the VENUS Planning Committee, he plays an important liaison role. In addition, he has joined with Andres Sandoval, Lee Schroeder and Reinhard Stock (GSI) in a program of relativistic heavy ion research.
>
> Robert Stokstad has come from Oak Ridge National Laboratory to become co-leader of the Harvey-Stokstad group at the 88-Inch Cyclotron where he is pursuing a program to study heavy ion reaction mechanisms in the intermediate energy region (10-20 MeV/amu).

With these gains there was also a loss: David Scott left LBL to accept a Hannah Chair of Physics and Chemistry at Michigan State University.

During this period a number of awards and honors were bestowed upon NSD scientists:

> Arthur Poskanzer received the 1980 American Chemical Society Award in Nuclear Chemistry at the Society's Houston meeting, March 24-28, "...for his pioneering use of high-energy nuclear reactions to produce light nuclei far from beta stability and for his experimental contributions to the understanding of the mechanism of nuclear reactions induced by protons and heavy ions of relativistic energy." A one-day symposium on High Energy Reactions and Nuclei Far From Stability was organized in Art's honor by Earl Hyde, LBL Deputy Director.
>
> Dick Diamond and Frank Stephens were awarded the 1980 Tom W. Bonner Prize in Nuclear Physics, sponsored by the American Physical Society. The award, presented at the Washington APS meeting in April, has a citation that reads, "Their studies of multiple Coulomb excitations with heavy ions, of multiple gamma-ray cascades, and of the effects of the Coriolis coupling in rotational spectra are important ingredients in our understanding of rapidly rotating nuclei."
>
> Bernard G. Harvey became Chairman of the Division of Nuclear Physics of the American Physical Society in April for a one-year term, having been elected to serve as Vice-Chairman for a year in April 1979. He also received an honorary degree from the University of Science and Medicine in Grenoble, France on October 26, 1979.
>
> Glenn T. Seaborg was awarded an L.H.D. degree from Augustana College in Rock Island, Illinois on May 25, 1980.

NSD members Bill Myers, Jorgen Randrup, and Gary Westfall organized the first Winter Workshop on Nuclear Dynamics held at Granlibakken, March 17-21. This successful conference was a stimulating blend of physics (with emphasis on the macroscopic aspects of nuclear collisions), sparkling snow, and fresh mountain air.

The division continues to operate the 88 Inch Cyclotron as a major research facility that also supports a strong outside user program. Both the SuperHILAC and Bevalac accelerators, operated as national facilities by LBL's Accelerator and Fusion Research Division, are also important to NSD experimentalists. Domestic and foreign cooperative efforts are underway at all three accelerators; in particular, major collaborations with our German and Japanese colleagues continue to flourish at the Bevalac. In May the division hosted a delegation from the People's Republic of China; discussions explored possible collaborative research projects.

The next few years promise exciting advances in heavy ion physics. High energy uranium beams, soon to be available at LBL for the first time anywhere, will open up a new area of heavy-ion research with the study of nuclear systems of high charge and mass under conditions of extremely high density and temperature. An Electron Beam Ion Source (EBIS), currently under study, would significantly extend the performance of the 88 Inch Cyclotron for medium mass ions in the 10-30 MeV/amu range. Fusion-type reactions will continue to be pursued in the search for the elusive superheavy elements. Knowledge of particle-creation effects in the nuclear equation of state under conditions of extreme nuclear densities will be sought at the Bevalac. Such experiments and others planned in the division will be of substantially increased technical and conceptual complexity. They will be aided by strong interactions with the division's nuclear theorists and by the increased effort devoted to development of sophisticated detectors and data analysis systems.

Joseph Cerny

Joseph Cerny
Nuclear Science Division Head

PART 1. RESEARCH PROGRAMS

EXOTIC NUCLEI AND NUCLEAR REACTIONS

Joseph Cerny

A. Bice*
M. Cable*
R. Parry*
H. Thierens
J. Wouters*

For a number of years this group has been actively exploring the properties of nuclei near the limits of nucleon stability. These investigations test the various theoretical models used to predict the ground state masses and level schemes of exotic light nuclei and permit one to search for new radioactive decay modes, such as direct proton radioactivity or the still unobserved two-proton radioactivity. Techniques for observing the products of very low yield reactions have been developed. The studies primarily concern the lighter elements, since one expects to reach the onset of general nuclear instability first in this region, and particularly among the neutron-deficient nuclides.

Current research at the 88 Inch Cyclotron focuses on employing the on-line mass separator RAMA (for Recoil Atom Mass Analyzer) in the study of exotic nuclei far from the valley of beta-stability. RAMA employs a helium-jet to transport radioactive nuclides from the target area to a hollow cathode ion source; following extraction and magnetic analysis, the mass of interest is collected either on carbon foils in the focal plane (for beta-delayed proton studies) or on a tape transport system (for beta and γ-ray studies). With RAMA, one more (previously unknown) $T_z = -2$ beta-delayed proton emitter, ^{36}Ca($T_{1/2}$ = 100 ms), has been discovered (complementing the discovery of the decays of ^{20}Mg and ^{24}Si reported last year), thereby completing the heaviest isospin quintet possible with established techniques and stable targets. Excellent agreement is observed in this heavy mass system with the predictions of the isobaric multiplet mass equation. Future studies are planned on both neutron-deficient and neutron-excess light isotopes.

Another part of the program in studying nuclei far from stability is the initiation of a series of experiments to determine total decay energies of isotopes in the vicinity of the doubly magic nucleus ^{100}Sn. Mass excess determinations for nuclides in this region should highlight the influence of the closed shells on the decay energies and establish whether such proton-rich magic nuclei follow the same mass systematics as do those nuclei nearer stability. The decays of $^{103-106}In$ have been observed following their production via 110 MeV ^{14}N on Mo targets and on-line mass analysis. The simple decay schemes for $^{103,105}In$ have permitted the determination of their mass-excesses for comparison with various theories of the mass surface.

In previous work in nuclear reactions this group has observed the nuclear structure of light nuclei via the two-nucleon pickup (p,t) and (p, ^3He) reactions. Currently, they are developing techniques to detect, under optimum conditions, unbound resonant states as nuclear reaction products. An example is the observation of the unbound system ^2He; its successful detection permits such measurements as two-neutron stripping via the (^4He, ^2He) reaction which has led to the observation of the preferential population of states with $(d_{5/2})^2_4$ and $(f_{7/2})^2_6$ character. Recent studies have utilized this technique in the investigation of scattering and transfer reactions induced by heavy ions in which transitions to specific, unbound, excited states of the outgoing heavy ion can be observed.

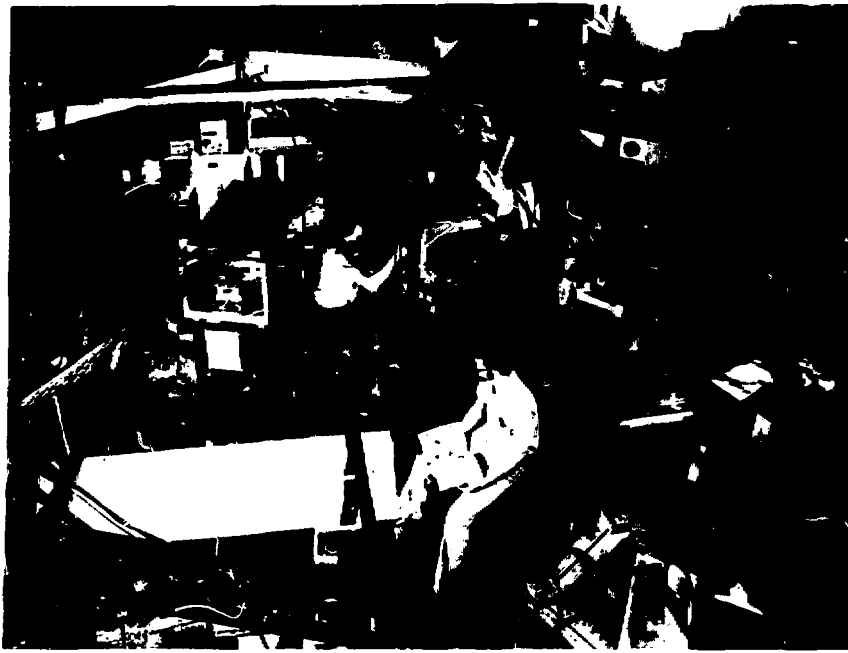

[illegible]

HEAVY ION REACTIONS

B G Harvey and R G Stokstad

J Mahoney
M J Murphy
W D Rae

R Legrain Saclay France
J Cole Grenoble France

This new research group continues the study of heavy ion reactions that was begun by its predecessors (Harvey, Hendrie, Scott) at the 88 Inch Cyclotron.

The foundation of much of the current and proposed work rests on the surprising discovery of Scott et al. that the heavy ion fragmentation process sets in very rapidly between 10 and 20 MeV/A. Already at 20 MeV/A, cross sections and momentum widths are close to their values at 2 GeV/A. From these and subsequent results, it is clear that the physics of peripheral collisions is remarkably similar at these two energies. As Scott emphasized in his ICNP lecture, high energy heavy ion physics begins at 15 MeV/A.

This group's research program is designed to look for additional similarities and to try to understand why 15 MeV/A is such an important frontier. Experiments at ORNL and the Bevalac showed that the reaction cross section σ_R for the ^{12}C + ^{12}C system rises rapidly just above the Coulomb barrier but becomes much lower at Bevalac energies. De Vries interprets this observation in terms of the nucleon-nucleon cross sections, which also drop. The group has recently measured σ_R at energies intermediate between the ORNL and Bevalac points and the preliminary results do indeed confirm that σ_R reaches a maximum and then falls off. The peak value seems to fall in the critical region around 15 MeV/A. Is this indeed due to the increasing role of nucleon-nucleon collisions that replaces the nuclear mean field description?

Experiments and theoretical work by Wilczynski et al. draw attention to the importance of the critical angular momentum in determining whether nucleon transfers or fragmentation will occur in peripheral collisions. When applied to the system ^{16}O + ^{208}Pb that was studied by Scott et al., the Wilczynski criterion predicts that fragmentation will start at 15 MeV/A, exactly as observed. The Harvey/Stokstad group has studied the mechanism for fragmentation of ^{16}O into ^{12}C + ^{4}He using a ^{12}C target and oxygen energies of 8.5 and 20 MeV. They find that even at 20 MeV/A fragmentation occurs predominately by inelastic excitation of ^{16}O to α-decaying states between 10 and 20 MeV/A and not by a direct single-step process. Thus, the transition from inelastic excitation (i.e., resonant fragmentation) to prompt fragmentation appears in this case to occur at bombarding energies above 20 MeV/A.

In order to get a more complete picture of heavy ion reactions in the intermediate energy region, they have begun to use a small streamer chamber to measure the multiplicity of charged fragments in coincidence with an identified forward-going particle. If the streamer chamber proves to be as useful as expected, further experiments will be planned with a more elaborate trigger system, perhaps using γ-rays to identify the residual target fragments.

A simple semi-classical model of massive transfer (or incomplete fusion) reactions can be used to calculate the excitation energy and angular momentum of the final nucleus. It has been very successful in predicting the γ-ray multiplicities that are measured in coincidence with quasi-elastic fragments. The model predicts that massive transfer reactions will populate final states in a narrow band of excitation energy and angular momentum. This is in sharp contrast with the (H.I.,xn) complete fusion reactions that are being used to produce high-spin states. In these reactions, all angular momenta are formed from zero to a maximum value. High-spin spectroscopy would benefit enormously by the use of reactions that produce a narrow region of angular momenta centered around a value that can be predicted and varied by changing the beam energy and the reaction. Consequently, this group plans to make futher experimental tests of the semi-classical model to test its predictive power. In order to reach really high spins, they will eventually require beams of heavier ions such as Ar, Kr, and Xe at 10-20 MeV/A. These will become available from advanced ion sources.

NUCLEAR STRUCTURE

R. M. Diamond and F. S. Stephens

D. Lebeck
H. Kluge, Hahn Meitner Institute,
Berlin, West Germany
H. Lindeberger
S. Shih, Shanghai, Institute of Nuclear Research,
Shanghai, China
J. O. Newton, Australian National University,
Canberra, Australia
C. Schuck, C.S.N.S.M. Orsay, France

The aim of this group is to study and understand some of the important aspects of nuclear structure and, particularly at the present time, the changes that occur with increases in angular momentum. They use beams of very heavy ions (^{40}Ar through ^{208}Pb) from the SuperHILAC and of smaller ions (^{4}He through ^{40}Ar) from the 88 Inch Cyclotron. They exploit the particular properties of heavy ions, namely, their large nuclear charge, the large recoil velocities of the composite system, and the high spin of the composite system.

The high nuclear charge makes the heaviest ions (^{136}Xe and ^{208}Pb) especially suitable for Coulomb excitation studies. States with spins up to 30 ℏ can be excited by multiple excitations. The large recoil velocities given to product nuclei under heavy-ion bombardment makes heavy-ion projectiles the choice for determining lifetimes by Doppler-shift methods (10^{-10} to 10^{-14} seconds), for g-factor measurements, and for a variety of other techniques requiring implantation of the recoiling nuclei in special materials.

The high angular momentum imparted in heavy-ion fusion reactions leads to nuclei in spin states greater than 60 ℏ. Studies of the de-excitation of these states by continuum γ-rays gives information about the moment of inertia and the shape of these nuclei as a function of spin. In certain cases (non-rotational nuclei), discrete states may be seen up to spins of 36-37 ℏ. Such studies comprise one of the most exciting fields in recent nuclear structure research.

The Nuclear Structure Group's sum spectrometer. From left to right: ... C. Shuck, E. Dines, and S. Shuang-Hui.

POLARIZATION PHENOMENA IN NUCLEAR PHYSICS

H E Conzett

R M Larimer

P von Rossen, University of Bonn, West Germany

This group's research uses the polarized beams from the 88 Inch Cyclotron, and it is concerned with spin-polarization effects in nuclear scattering and reaction. It particularly addresses such fundamental questions as parity violation by the weak interaction component in $\vec{p}p$ scattering, time-reversal invariance in reactions, charge symmetry of the nucleon-nucleon interaction, and the three nucleon problem.

They have essentially completed a program to measure the various polarization observables in p+d scattering for comparison with exact three-nucleon calculations. With the exception of the tensor analyzing powers, the agreement between experiment and theory was perfect. An improvement in the input nucleon-nucleon tensor potential and the inclusion of an F-wave interaction in calculations (by Doleschall) have now resulted in good agreement with the measured tensor analyzing powers as well. Thus, the exact three-nucleon calculations, with the known nucleon-nucleon input interactions, are now most successful in reproducting the three-nucleon experimental results.

From accurate measurements of the cross section and tensor analyzing powers in $\vec{d}p$ scattering at 35 and 45 MeV, they have determined, in a model-independent analysis, an accurate value for an important deuteron D-state parameter. This paramenter, the asymptotic D- to S-state ratio of the deuteron wave function has been determined to an accuracy of 5%. This result has significant impact in several areas. It establishes constraints on the nucleon-nucleon intermedite and long range tensor force, and, thus, on the various nucleon-nucleon potential models, both the phenomenological and the modern meson-exchange types. These constraints are also important in exact calculations of the triton binding energy and in the determination of the saturation properties of nuclear matter, both of which are very sensitive to the deuteron D-state probability.

A most important feature of polarization effects is that they often display uniquely the operation of a basic symmetry property of the nuclear interaction. They are pursuing several fundamentally important experiments of this nature: (1) They have prepared a longitudinally polarized proton beam and the experimental apparatus for a major experiment on the basic nucleon-nucleon interaction, i.e., a determination of the weak interaction parity non-conserving part of this interaction from a measurement of the longitudinal anaylzing-power component in $\vec{p}p$ scattering at 50 MeV. Calculations predict a maximum value (3×10^{-7}) at 50 MeV, and theirs is one of the three existing polarized-beam facilities in the world with the capability to do the experiment at that energy. (2) They have been engaged in a collaborative experiment at TRIUMF to determine the level of validity of charge symmetry in the nucleon-nucleon interaction, which implies an equality of the neutron and proton polarizations in $\vec{n}p$ scattering. The experiment is designed to check this equality to an accuracy of 10^{-3}. One experimental run has taken place in $\vec{p}p$ scattering which verifies that this accuracy is possible. (3) They have started a collaborative experiment with a group from Laval University to test the principle of time-reversal invariance in nuclear reactions. This principle results in the polarization-analyzing power equality, i.e., the polarization in a reaction $A(\vec{a},b)B$ is equal to the analyzing power in the inverse reaction with polarized projectile $B(\vec{b},a)A$. Polarizations have been measured at Laval in several (^{3}He,p) reactions, and measurements have begun here of the analyzing powers in the corresponding (p, ^{3}He) inverse reactions. Previous checks of time-reversal invariance in nuclear reactions have been limited to tests in elastic proton scattering.

In the future work they plan to continue to focus on experiments with polarized particles which examine the operation of the basic symmetries of the nuclear interaction, i.e., parity conservation in $\vec{p}p$ scattering, charge symmetry in $\vec{n}p$ scattering, and time-reversal invariance in nuclear reactions. The increased polarized beam intensities of 2-3 microamperes, to be provided by our FY 1980 Accelerator Improvement Project, will be particularly important for these experiments which demand high statistical accuracy and overall precision. They will also continue studies of the consequences of particle identity and charge symmetry in nuclear reactions.

SPIN, ISOSPIN AND ENERGY FLUCTUATION IN HEAVY ION REACTIONS

L G Moretto

J Hunter
R J McDonald
D J Morrissey
L G Sobotka*

A J Pacheco*
G J Wozniak
C C Hsu, Beijing
Peoples Republic of China

During the last several years this group has been investigating the short-lived dinuclear system, or intermediate complex, which is formed in heavy ion collisions. The short lifetime of this dinuclear system allows one to classify its excited collective modes in terms of their relaxation times. From short to long they are: neutron to proton ratio, energy damping, angular momentum transfer, and the mass asymmetry degree of freedom. Associated with each of these equilibration processes are quantal or classical fluctuations. These fluctuations can be measured and general conclusions can be drawn about either the equilibrium distribution and/or the equilibration process. Recently, the group has focused its theoretical and experimental attentions on spin, isospin and energy fluctuations. Information on spin fluctuations is contained in the γ-ray and α-particle angular distributions arising from the decay of one or both of the primary reaction products. For very asymmetric systems, energy fluctuations greatly enhance the statistical emission of fast light particles from deep-inelastic processes. Isospin fluctuations are associated with a variety of giant isovector modes and can be studied by means of isobaric charge distributions.

THE TRANSFER, ALIGNMENT AND PARTITIONING OF ANGULAR MOMENTUM WITHIN THE DINUCLEAR SYSTEM

Elementary dynamical considerations suggest that the angular momentum transferred to the reaction products should be perpendicular to the reaction plane. However, thermodynamical considerations also suggest that some amount of angular momentum misalignment should arise from the excitation of angular momentum bearing collective modes of the intermediate complex. For a system of two touching spheres in the equilibrium statistical limit, these modes have been identified as bending, twisting, tilting and wriggling. For this simple system, the second moments of the fragment spins and the spin depolarization have been calculated. If the fragment angular momentum is carried away mainly by stretched E2 transitions, one can learn about the degree of misalignment by measuring the out-of-plane angular distribution of the γ rays. In a study of the ^{165}Ho + ^{165}Ho system at 8.5 MeV/A, a very strong correlation between the γ anisotropy and the reaction Q-value was observed which indicated a rapid buildup of aligned spin in the quasi-elastic region and a decrease in the aligned component at very large Q-values. A quantitative comparison of the data with model calculations indicates that the spin depolarization introduced by the angular momentum bearing collective modes is the primary cause of the fall of the anisotropy at large Q-values.

The out-of-plane angular distribution of α particles emitted by deep-inelastic fragments can be used to investigate the partitioning of angular momentum within the dinuclear system. This can be done because in certain kinematic regions only light particles emitted from the target-like nucleus are observed and the out-of-plane distribution of these light particles is sensitive to the spin of the emitter nucleus. In addition, the sum of the spins of both fragments can be determined from γ-ray multiplicity measurements. For the 664-MeV ^{84}Kr + ^{nat}Ag system, the group has determined that for fully damped events the intrinsic spin of the dinuclear complex is partitioned between the two product fragments as one would expect for rigid rotation of an intermediate complex consisting of substantially deformed spheroids.

ENERGY FLUCTUATIONS

Light particles with velocities substantially greater than the beam velocity have been reported in inclusive measurements of heavy ion reactions. The production mechanism of such fast particles has been a lively subject of discussion and the data have been interpreted as evidence for "hot spots" and "PEP jets." The group has recently studied proton emission from the ^{20}Ne + ^{nat}Cu system at 12.5 MeV/A. Although simple evaporation calculations underpredict the intensity of fast protons, including statistical fluctuations in the equilibrated excitation energy gives the correct spectral shape of the fast protons. For this asymmetric system, fluctuations in the partitioning of the exitation energy of the dinuclear complex can produce a substantial increase in the excitation energy of the Ne-like fragments. The resulting higher temperature gives rise to protons with velocities comparable to that of the beam which, when coupled to the velocity of the projectile-like fragment, yield values of up to twice the beam velocity in the lab system.

ISOSPIN FLUCTUATIONS

Recently, the group has suggested that the isobaric charge distributions carry information regarding giant isovector modes in the intermediate complex. The group investigated the role of the higher order isovector modes in the exactly solvable problem of a cylinder split at various asymmetries. The role of the higher isovector multipoles becomes more and more important as the asymmetry increases. While the cylinder model is much too schematic to be realistic, it points to the mass asymmetry and to the higher isovector modes as essential components of a comprehensive theory.

*Graduate student

G.J. Woznick with the scattering chamber and gamma-anisotropy set up used in the Moretto-Diamond-Stephens collaboration. Note the two Pb-shielded large volume (5 x 8 inch) NaI detectors in the radial plane and a third at 30° to this plane. In addition, an array of eight 3 x 3 inch NaI detectors is positioned at 45° above the radial plane to enable selection of high spin events.

HEAVY ELEMENT RESEARCH

A. Ghiorso and J. M. Nitschke

M. J. Nurmia
L. P. Somerville
S. Yashita
E. K. Hulet, LLNL
R. W. Lougheed, LLNL
J. F. Wild, LLNL
D. C. Hoffman, LASL
M. Leino, University of Helsinki, Finland

The Heavy Element Research group studies the synthesis of new elements and isotopes and investigates their radioactive and chemical properties. An important adjunct to this effort is training students in advanced methods and techniques of experimental nuclear physics. The group conducts experiments at the 88 Inch Cyclotron and the SuperHILAC, and is collaborating with other American laboratories in experiments at GSI Germany. Research at the 88 Inch Cyclotron has focused on the synthesis of neutron-rich actinide isotopes with very heavy targets (^{244}Pu, ^{248}Cm, ^{249}Bk, ^{249}Cf, and ^{254}Es) and high intensity light ion beams. These reactions do not necessarily proceed according to the classical concept of compound nucleus reactions with the subsequent evaporation of a few neutrons or α-particles. To gain a better understanding of the reaction mechanisms involved it has included the study of transfer reactions in its program. The identification of the reaction products is predominantly achieved through their characteristic α-particle decay but in some cases unique features of fission decay have given important clues as to the nature of the reaction mechanisms involved. The instrument most useful for the study of the spontaneous fission (SF) decay properties of short-lived isotopes has been the MG system, which has been used in paricular for a systematic investigation of the SF properties of Fm isotopes.

The discovery of several new SF emitters in the neutron rich actinide region was made possible through the development of an instrument that is capable of reducing the background of unwanted long-lived SF emitters by several orders of magnitude compared to previous experiments. This instrument is able to detect SF emitters with ms half-lives that are formed with sub-nanobarn cross sections, and it will eventually allow searches for exotic nuclei like ^{264}Rf which is a key nucleus for the understanding of shell effects in the SF process of heavy elements.

The group's efforts at the SuperHILAC are directed towards the use of complete fusion reactions to produce and analyze new elements and isotopes with half-lives as short as 1 μs. For this purpose it has been successful in bringing on line a gas-filled magnetic spectrometer (SASSY) after a necessarily protracted development period. This system has an acceptance angle of about two degrees in the beam direction and has proved able to completely suppress the bombarding particles in most cases of interest. The heavy recoils are brought to a focus four meters downstream from the target at a focal plane where two types of detectors have been used, either solid state recoil/alpha/fission detectors or recoil-detecting gaseous ionization chambers. Two avalanche counters with extremely thin windows intercept the recoil path to provide START/STOP signals for velocity (TOF) measurements.

Using a solid state detector array and parastic beams of ^{40}Ar and ^{56}Fe from the SuperHILAC short-lived alpha radioactive species from Po to Ac have been produced. Several new neutron-deficient isotopes of Po and At have been discovered with SASSY using this technique. With a multiple grid chamber as the detector an unexpected, complicated structure in the TOF spectra when ^{175}Lu and ^{174}Yb are bombarded by ^{40}Ar ions was found. This structure does not appear with ^{169}Tm bombardments, only the compound nucleus spectrum being observed. The analyses of these reactions have not yet been completed, so there is no explanation for the phenomenon as yet.

It appears that SASSY has now been developed to the point at which one more definitive search for superheavy elements can be made, this time down to half-lives as short as a fraction of a microsecond. Early in 1981 it is planned to bombard ^{248}Cm with ^{48}Ca ions because it still appears from theroretical considerations that this is the best reaction to try.

A program of a somewhat different nature is being pursued with the SuperHILAC on-line isotope separator. The scope of research is not limited to the investigation of the heaviest elements or the use of complete fusion reactions, but spans the whole range of the periodic table. The reaction mechanisms utilized for the production of isotopes far from the line of beta stability include beside complete fusion, deep inelastic collisions and multi-nucleon exchange reactions.

Several aspects of the separator are still under development, in particular the detection system; but it is expected that in a year's time on-line β-γ-spectroscopy will be possible in addition to the present particle detection. The measured efficiencies and separation times are sufficient to study isotopes with half-lives as short as one second and production cross sections below 1 mb.

A final aspect of their research concerns the study of heavy and superheavy elements in deep inelastic reactions. For this purpose they have undertaken a collaborative experiment with

LLNL, ORNL, and GSI to bombard ^{248}Cm targets with high intensity ^{238}U beams at the Unilac in Germany. Compared to ^{238}U, the yield with ^{248}Cm targets for the production of heavy actinides was enhanced by a factor of 10^3 to 10^4. This enhancement, however, was not sufficient to discover superheavy elements. In the future the studies of the deep inelastic reaction mechanism and the process of nuclear diffusion will be continued using ^{238}U and other heavy ion beams from the SuperHILAC with targets as heavy as ^{254}Es and ^{257}Fm.

J.M. Nitschke and L. Archambault with the on-line isotope separator at the SuperHILAC.

SUPERHEAVY ELEMENT INTERLABORATORY CHEMISTRY (SHEIKS)

G. T. Seaborg

K. Aleklett, Swedish Research Council, Sweden
L. Frank[*]
B. Jacak[†]
R. McFarland[*]
P. McGaughey[*]
K. Moody[*]
Y. Morita[*]
D. Morrissey
M. Nurmia
M. Perry[†]
M. Schulman[†]
L. P. Somerville
R. Welsh[†]
S. Yashita[*]
D. Hoffman, LASL
Luis Cheng, Beijing, Peoples Republic of China
W. Loveland, Oregon State University
H. Von Gunten, University of Bern, Switzerland
H. Groening, Simon Bolivar University

This group uses all three of the LBL accelerators to identify and characterize new elements and isotopes, to study nuclear reaction mechanisms, to study the chemical properties of rare known elements, and to train students in modern radiochemical techniques. Currently its reasearch is focused toward (1) the synthesis and identification of new isotopes and elements in the actinide and transactinide region, along with attempts to synthesize superheavy elements, (2) the study of low energy heavy ion reaction mechanisms potentially useful in the synthesis of new elements and isotopes such as massive transfer, complete fusion and deep inelastic scattering, (3) the characterization of the mechanisms operating in intermediate energy (10-100 MeV/A) and relativistic ($\gtrsim$250 MeV/A) heavy ion reactions through studies of the target fragment yields, energies, angular distributions, etc.

With light (A < 25) heavy-ion reaction studies at the 88 Inch Cyclotron, the primary emphasis has been on the use of "transfer" reactions to produce heavy actinides and the study of the mechanism of these reactions. Preliminary studies have indicated suprisingly large probabilities for the synthesis of all the nuclear species ranging in mass from the target mass to that of the compound nucleus. The group is systematically exploring these reactions by studying the variation of product yields, energies, angular distributions, etc., with projectile and target mass and energy.

Members of the group have also used the 88 Inch Cyclotron, the low-energy beam line at the Bevalac and the SC synchrotron at CERN to study the transition between low energy and high energy heavy ion reaction mechanisms. In particular, they are concerned with studies of the target fragment yields, energies and angular distributions in light ion-heavy target reactions. Preliminary results show large dramatic changes in the product yield distributions at projectile energies ~40 MeV/A.

Research at the SuperHILAC has been directed at the use of deep inelastic transfer processes to produce new isotopes or elements, and obtain an understanding of the mechanisms involved. Efforts have been concentrated on the reaction of the heaviest projectiles (Kr, Xe) with very heavy targets (^{244}Pu, ^{248}Cm). Future work will involve the use of heavier projectiles such as ^{238}U. Current results seem to indicate no significant advantage in the use of Kr or Xe projectiles as compared to the use of ^{48}Ca and other lighter ions in these synthesis studies.

Research on target fragmentation at the Bevalac has shown that (1) the target fragment yields have been measured in the interaction of relativistic heavy ions (RHI's) and are in good agreement with the predictions of current models of RHI interactions (such as the firestreak, intranuclear cascade), (2) the target fragment energies, momenta, etc., exceed those of fragments from relativistic p-nucleus collisions and are not well described by current models of these interactions, (3) there are indications of sidewise peaked fragment angular distributions in some of these reactions, suggesting compression of nuclear matter in the RHI-interaction. Futher work in this area will be concentrated in (2) and (3).

[*]Graduate students
[†]Undergraduate students

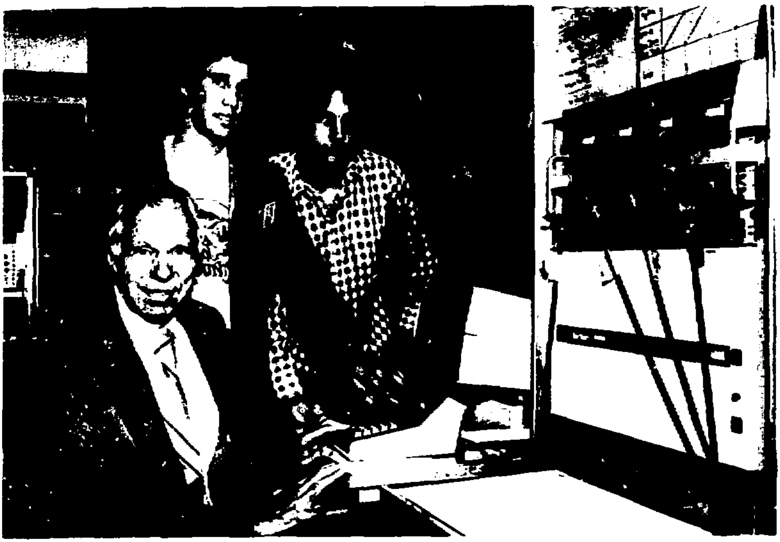

Undergraduates L. Frank and ?. Sayler with prof. [illegible] spectrum from the chemical [illegible]

HIGH ENERGY NUCLEAR COLLISIONS

A. M. Poskanzer and H. H. Gutbrod GSI

A. Baden*
H. Loehner University of Marburg
M. Maier University of Marburg
J. Meneses
J. Peter Orsay France
H. Ritter GSI
H. Steltzer GSI
R. Stock GSI
A. Warwick
F. Weik GSI
H. Wieman GSI
K. Wolf ANL

The work of this group is directed to the study of central collisions of relativistic heavy ions with the aim of learning about nuclear matter at high temperature and density. The group is a continuing collaboration between GSI, the University of Marburg, and LBL. An experiment was performed together with a nuclear chemistry group from the Argonne National Laboratory and, in addition, there were two visitors from the Kurchatov Institute of Moscow.

In the year before this, both a ΔE-E telescope of silicon and thick germanium detectors and a gas ΔE-silicon E telescope were used in conjunction with an 80-counter multiplicity array. All the single particle inclusive p, d, and t data have been published and also some multiplicity selected p and π^+ data. The heavy fragment results, together with their correlations with the fast fragments, have been published. The remainder of the π^+ data is ready for publication.

This year another experiment was performed to study the correlations between slow and fast fragments. For the slow fragments an array of 40 detectors, consisting of silicon counters, gas ΔE counters, and avalanche counters, was used. For the fast fragments the 80-counter multiplicity array plus a new piece of equipment, the Plastic Wall, were used. This year A. Poskanzer was on leave at CERN and performed various experiments with the ISOLDE group on exotic light nuclei and also measured yields from the reaction of 80 MeV/A ^{12}C ions with uranium. The future work at LBL will be centered exclusively around the combination of the Plastic Ball with the Plastic Wall. This is an attempt to make a much more exclusive measurement of realtivistic heavy ion interactions to search for collective phenomena.

p, d, AND t

Inclusive energy spectra of protons, deuterons, and tritons were measured with a telescope of silicon and germanium detectors at kinetic energies up to 200, 250 and 300 MeV, respectively. Fifteen sets of data were taken using projectiles ranging from protons to ^{40}Ar on targets from ^{27}Al to ^{238}U at bombarding energies from 240 MeV/nucleon to 2.1 GeV/nucleon. An estimation of the sum of nucleonic charge emitted as protons plus composite particles was obtained as a function of energy in the interval from 15 MeV/nucleon to 200 MeV/nucleon. For low energy fragments at foward angles the protons account for only 25% of the nucleonic charges. Comparisons of some cases with firestreak, cascade, and fluid dynamics models were made. In addition, associated charged particle multiplicities and azimuthal correlations were measured with an 80-counter array of plastic scintillators. It was found that the associated multiplicities were a smooth function of the total kinetic energy of the projectile.

CORRELATIONS BETWEEN SLOW AND FAST FRAGMENTS

Analysis has finished on earlier Bevalac measurements of low energy heavy fragments and fission fragments in coincidence with fast light particles. These measurements were made with a variety of projectiles from protons to ^{20}Ne and a range of bombarding energies from 0.4 GeV/n to 2.1 GeV/n on three targets (uranium, gold and silver). Some of the results of this work include charged particle multiplicity distributions that show fission fragments from realtivistic nuclear collisions are predominatly produced in low multiplicity events. There is, however, a component with high multiplicities indicating that even in violent reactions binary fragments are produced. It was also found that low-z fragments are associated only with events of high multiplicity. Another feature observed in the data was the anomalously low apparent Coulomb barrier encountered by emitted fragments from interactions with both light and heavier projectiles. This lowered apparent Coulomb barrier appears to drop with increasing incident kinetic energy.

This experimental program has been expanded with additions of equipment and personnel. The apparatus is now composed of four ion chamber-silicon telescopes plus two large area silicon arrays. Two avalanche detectors used in conjunction with the silicon arrays and two of the ion chamber-silicon telescopes provide TOF information for mass identification of the fragments. The Plastic Wall, later to be used with the Plastic Ball, has been added to the setup to measure coincident fast particles scattered into the foward cone between 2° and 9°. A multiplicity array of 80 scintillator paddles provides coincident fast particle counting over the full solid angle from 9° to 90°.

For the future, the scattering chamber and multiplicity array of scintillators will be removed from the Bevalac to make way for the

*Graduate student

Plastic Ball. It is under consideration, however, to move this apparatus to the Fermi laboratory where high energy proton nucleus interactons can be studied to augment our work with heavy ions at the Bevalac.

PLASTIC BALL

The major future project of the collaboration with GSI and the University of Marburg is the Plastic Ball. Bevalac research has passed from the stage where one was satisfied to measure one particle from each event to a stage where one would like to measure all the charged particles from each event in order to look for the collective effects. The Plastic Ball will cover 94% of 4π with 815 modules, each consisting of a CaF_2 ΔE detector and a plastic scintillator E detector. The two scintillators are observed by the same photomultiplier tube and the signals are separated electronically by taking advantage of their different decay characteristics. In addition positive pions will be identified by their $\pi^+ - \mu^+ - e^+$ decay as has been done previously. The small forward angle region will be covered by the Plastic Wall placed 6 m downstream. The wall consists of 176 plastic scintillators and will identify particles by their time of flight and energy loss.

It is expected that the first configuration of the Plastic Ball/Wall system will be completed before FY 1981 and that the first round of experiments using this facility will be in operation during the FY 1981-82 period. The first experiment for this apparatus will be a measurement of excitation functions for charged particle multiplicities and their correlations, where for each event all the charged particles ($\pi^{\pm}$, p, d, t, ^3He, ^4He) are identified in the Ball as to their mass, charge, energy and scattering angles θ and ϕ. The targets will be ^{40}Ca and ^{208}Pb and the projectiles will be ^{12}C and ^{40}Ar with energies ranging from 100 MeV/n to 1000 MeV/n.

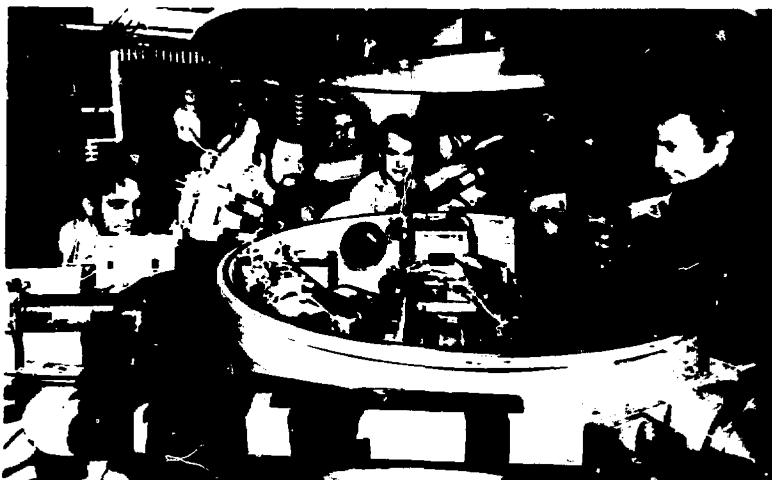

[illegible]

RELATIVISTIC HEAVY ION PHYSICS

H. H. Heckman

E. Friedlander
R. Gimpel
Y. Karant
D. Tittle
H. Yee
D. Olson, LLNL
M. Bloomer, UC Space Sciences Laboratory

E. Ganssauge, University of Marburg, West Germany
N. Klein, University of Marburg, West Germany
B. Judek, National Research Council, Ottawa, Canada

This group initiated some of the first heavy ion experiments at the Bevatron/Bevalac to explore the phenomenon of projectile fragmentation, i.e., the break-up of heavy ion beam projectiles from collisions with target nuclei, in which the fragments of the incident nucleus are charecterized by their near-beam velocities and small production angles. The group's early works were concerned with the systematics of the projectile fragment production cross sections, the longitudinal and transverse momentum distributions, total reaction cross sections, fragmentation mechanisms, etc. The immediate results of these early experiments were the concepts of "limiting fragmentation" and "factorization" which were found to be relevant to heavy ion collisions. Use of these concepts led to a great simplification in the ordering of cross section data and are the bases for estimating isotope production cross sections in any target material.

Other direct consequences of the projectile fragmentation experiments were (1) the immediate application of the cross sections to cosmic-ray studies, (2) the realization that the Boltzman distribution for high energy reactions should have the form $\sqrt{E}\exp(-E/kt)$ rather than $E\exp(-E/kT)$, as clearly demonstrated by the Gaussian-shaped longitudinal momentum distributions of projectile fragments, (3) factorization is strongly violated for high-Z targets, where the Weizsäcker-Williams virtual-photon field induces photodisintegration of the projectile via the giant dipole resonance, (4) the "fragmentation model" explains well fragmentation reactions and (5) practical applications of the fragmentation mechanism led to the development of isotopic beams of ^{11}C for biomedical applications, the development and calibration of cosmic-ray heavy-ion detectors, and recently, projectile fragmentation was employed successfully in searches for new neutron-rich isotopes using ^{40}Ar and ^{48}Ca beams.

ACCOMPLISHMENTS AND OUTLOOK

The group's Bevalac experiments during this fiscal year have marked the beginning of a series of second-generation experiments on projectile fragmentation. These experiments include (1) the interaction properties of secondary, tertiary and later generations of projectile fragments of 2 A GeV ^{16}O and ^{56}Fe beam nuclei, (2) the observation of enhanced production cross sections for ^{17}N, ^{17}O and ^{16}O from the fragmentation of ^{18}O in high-Z targets, indicative of the photoexcitation (via the Weizsacker-Williams effect) and the unique decay of the giant resonance states of the ^{18}O projectile nucleus, and (3) the production and identification of 14 new neutron-rich isotopes. In addition, the isotopic composition of cosmic ray heavy nuclei is being investigated in a satellite experiment supported by NASA. Expanded discussions of these activities are presented below.

Interaction Properties of ^{16}O and ^{56}Fe at Bevalac Energies

The interaction properties of relativistic projectile fragments are being investigated in cooperation with B. Judek, National Research Council of Canada, and E. Ganssauge, University of Marburg, West Germany. To date, some 1500 extra-nuclear cascades induced by ~ 2 A GeV ^{16}O and ^{56}Fe beams in nuclear research emulsions have been followed through all generations involving fragments $Z > 3$ in order to obtain estimates of the reaction mean-free paths (mfp) of projectile fragments in the different generations. The results of the experiment show that the mfp's of later generations of fragments are significantly shorter than those of "primary" accelerator beams of the same charge, an effect that is interpretable under the simplest assumption that a small (~ 6%) fraction of the fragments interact with a mfp ~ 2.5 cm, independent of charge of the fragment. Such a mfp corresponds to a cross section 5-10 times larger than geometric for the fragments considered. The extent of these differences between the mfp's of the primary and secondary (and later generation) fragments cannot be explained within the framework of conventional nuclear physics.

This observation of anomalous fragment nuclei is surprising in that they (1) are produced at beam energies as low as 2 A GeV in relatively peripheral collisions and (2) have lifetimes as long as ~ 10^{-11} sec. Of highest priority is to pursue further experimentation on this new effect to elucidate (1) its dependence on the order of generation in the extra-nuclear cascade, (2) the semi-inclusive properties of the collision parameters for production and subsequent interaction of the anomalous component, and (3) to investigate the lifetime of the state(s). A complex of exposures of emulsions to a variety of Bevalac beams was recently approved by the PAC and carried out in July 1980.

Concurrently other features of relativistic heavy ion fragmentation, already under study--especially angular correlations of projectile fragments and their multiplicity distributions--are being investigated with considerably better statistics than have hitherto been possible.

Coulomb Dissociation of Projectile Nuclei

The effect of the electromagnetic interaction on the fragmentation of ^{18}O beam nuclei at 1.7 A GeV is being investigated in collaboration with B.L. Berman (LLNL). The electromagnetic contribution to the single proton and the one- and two-neutron removal fragmentation cross sections have been determined and they agree with calculations based on virtual-photon theory, given the minimum impact parameter deduced from the Coulomb dissociation of ^{12}C and ^{16}O.

There are two overall results of this experiment. First, the process that enhances certain fragmentation cross sections on high-Z targets is clearly identified as electromagnetic in origin. The quantity that is measured is the integrated virtual-photon-weighted photonuclear dissociation cross section. Second, because the physics of this process is understood, one can use the relativistic heavy ion technique, developed here to study the photonuclear cross sections and branching ratios of a variety of stable and unstable beam particles, thereby expanding greatly experimental data on photonuclear processes. Such information on unstable nuclei is impossible to obtain by conventional methods.

With the verification of the Coulomb-field induced excitation and decay of ^{18}O, an experiment to study the specific reaction $^{16}O(\gamma,p)^{15}N$ by use of HISS is under preparation. In this experiment, the group expects to detect and momentum-analyze both the ^{15}N (and possibly any de-excitation γ-rays from the ^{15}N) and proton in order to determine the photoexcitation energies of the ^{16}O nucleus to about 1-2 MeV accuracy. The experiment will determine the virtual photon-weighted cross section for the $^{16}O(\gamma,p)^{15}N$ reaction and will also verify the role played by excited states of ^{15}N in the photodissociation of ^{16}O, the only nucleus for which such information is available.

The possibility of extending these measurements to β-unstable nuclei is intriguing, particularly the extension to isobars of the stable oxygen isotopes (mass 16, 17 and 18). From both the photonuclear and electron scattering work done on these nuclei, it is clear that isospin considerations play a major role in our understanding of their structure, and their unstable isobars cannot be studied by conventional techniques.

Production of Neutron-Rich Nuclides

In this experiment, done in collaboration with other groups from LBL, Michigan State University, and the U.S. Naval Research Laboratory, the yields of neutron-rich projectile fragments were measured at 0° for the reaction of 0.212 A GeV ^{48}Ca ions on an 890 mg cm^{-2} Be target. The first experimental evidence for the particle stability of fourteen nuclides was obtained: ^{22}N, ^{26}F, $^{33,34}Mg$, $^{36,39}Si$, $^{41,42}P$, $^{43,44}S$, and $^{44,45}Cl$. The existence of ^{37}Si, ^{40}P, and $^{41,42}S$ was also confirmed.

Clearly established by this experiment is the fact that the fragmentation of high energy nuclei is a practical means for the production of nuclei far from stability. Observations of such nuclei are useful for making quantitative tests of mass formulae, for studies of microscopic level structure, and for elucidation of production mechanisms.

Cosmic Ray Heavy Nuclei

Data from the LBL (Heckman/Greiner)-Samuel Silver Space Sciences Laboratory (M. Wiedenbeck) instrument aboard the ISEE-3 spacecraft has continued to be of high quality (launch date August 12, 1978) and are being used to investigate the isotopic composition of galactic cosmic rays. The spaceflight instrument used for this experiment, which was fully calibrated with Bevalac beams, is the outgrowth of our interrelated cosmic ray and Bevalac research.

After a one-year accumulation of data, sufficient statistics have been obtained on the rare ^{10}Be isotope to permit the determination of a definitive cosmic-ray age. Also, from measurements of cosmic-ray carbon, nitrogen and oxygen nuclei the group has concluded that the cosmic-ray source abundances do not contain a large overabundance of the rare isotopes ^{13}C, ^{17}O and ^{18}O. The abundance of ^{15}N is consistent with a solar-like composition, although a $^{15}N/N$ ratio substantially greater than the solar system value of 0.004 is permitted by the data. Furthermore, conventional propagation models adequately describe the observed abundances of the CNO isotopes. In contrast to these results, they find for the composition of Ne in the local interplanetary space the ratios $^{22}Ne/^{20}Ne = 0.64 \pm 0.07$ and $^{21}Ne/^{20}Ne < 0.30$. These observations are inconsistent with a solar-like composition, for which $^{22}Ne/^{20}Ne = 0.122$.

The successful operation of the LBL-SSL instrument and, indeed, the ISEE-3 satellite itself, has led to an extension of this program beyond that originally planned by NASA. The plan here is to continue studies on the isotopic composition of nuclei through Fe, a program that will necessarily require cross section information obtained from Bevalac experiments to interpret the data in terms of cosmic-ray sources and propagation mechanisms.

BEVALAC RESEARCH

H G Pugh,
L S Schroeder

A Sandoval GSI Darmstadt
R Stock, GSI, Darmstadt

TASS
J Geaga
R Koontz
R Treuhaft*
J W Harris, GSI, Darmstadt, West Germany
J Engelage*, Louisiana State University
P N Kirk, Louisiana State University
C Ruiz, Louisiana State University
G Roche Clermont Ferrand, France

Streamer Chamber:
J P Brannigan
E H McCann
I W Muskovich
M Raff
L M Tinay
J W Harris, GSI, Darmstadt
J Miller, GSI, Darmstadt
H Stroebele GSI, Darmstadt
R E Renfordt University of Marburg
K L Wolf, ANL
M Brandan University of Mexico
A Dacal, University of Mexico
A Menchaca Rocha, University of Mexico
M Mazari, University of Mexico
M Ortiz, University of Mexico
T Bowen, University of Arizona
A G Pifer, University of Arizona

During 1980 this new group was formed from two smaller groups to respond to the common interests of the members in studying nuclear collisions at Bevalac energies. The research of the group is in two areas, presently associated with the LBL streamer chamber and with the newly-operating Two-Arm Spectrometer System (TASS). With the use of both visual and purely electronic techniques a broad range of experiments from exploratory to follow-up of specific predictions are being undertaken. Both the TASS and Streamer Chamber research are conducted in collaboration with outside researchers.

TASS

The Two-Arm Spectrometer System (TASS) consists of two fully rotatable magnets, with accompanying wire chambers and scintillation hodoscopes for particle detection and identification. The first experiment on TASS, a collaborative LBL and Louisiana State University effort, was run in July 1980.

The first experiment (444H), a follow-up of an earlier experiment (351H) on particle production (π^+,p,d,t) at 180°, involved measuring the angular and momentum correlations between high energy particles (π^+,p,d) emitted in the forward and backward hemispheres. The majority of the running involved 2.1 GeV proton-carbon interactions. Particle production at backward angles is of considerable interest since it is either strictly forbidden (e.g., nucleon scattering) or severely constrained (e.g., pion production, where $p^{\pi}_{max} \lesssim 300$ MeV/c) in "free" N-N collisions. Thus, the observation of correlations between forward and backward particle particle emission provides a tool to probe possible exotic or cooperative production mechanisms, that is, study the short-range behavior of nucleons in nuclear matter. The data are being analyzed, with particular attention being given to that portion of the data that is sensitive to the incident proton scattering from two or more nucleon correlations in the target nucleus. These correlation studies will be continued in early 1981 with a proton beam, and for comparison, with a heavier beam such as carbon.

Future directions with TASS will involve measurements of $\pi\pi$ and πN correlations to ascertain the contributions of both meson and baryon resonances to the pion spectrum observed in heavy-ion collisions. Also correlations between particles emitted at large $p_{\perp}$ will be studied to probe features of A-A central collisions. Finally, we feel that a study of di-lepton production (e^+e^- or $\mu^+\mu^-$) might be a very sensitive test of whether exotic states of nuclear matter are being formed in central collisions. Being weakly interacting, the leptons will not suffer the large attenuation that pions, nucleons, and to some extent kaons experience in traversing the nuclear medium from their creation point in the collision process. The group presently hopes to conduct such a search starting early in 1982.

STREAMER CHAMBER

This already active group has been formally established as an independent sub-effort this year, both by GSI and LBL, to coincide with an expansion of activity and support. In addition, the groups of K. Wolf at Argonne and A. Dacal at the University of Mexico have made major new commitments to this effort. The University of

*Graduate student

Arizona group of T. Bowen will be involved in our future program on strange baryon production.

Recent work by the group has included the following experiments.

401H. Study of the multiplicity of charged pions produced in Ar + KCl central collisions to obtain an estimate of the space and time extent of the source emitting the pions by interferometry techniques. In addition, the negatively charged pion multiplicity excitation function has been obtained for bombarding energies from 0.4-1.8 GeV/n (see Phys. Rev. Lett. 45, 874 (1980)). This type of data can be used to test various models of central collisions such as hydrodynamic, cascade, thermal, etc. The group is also investigating the yields of Λ^0 hyperons by observing their decays (appearance of "vee" shaped tracks) in the streamer chamber. At 1.8 GeV/n the large statistics central collision running has provided a sample of about 60 Λ^0's, enough to extract their production cross-section as well as gross features of their *momentum and* angular distributions.

400H. This experiment used a 2.1 GeV proton beam with the streamer chamber being triggered on a backward going Λ or p. This work, which complements the backward particle production studies on TASS, provides a more exclusive look at the production mechanisms responsible for backward particle emission. An early indication from this study is that a large sample (~ 50%) of the events with a backward particle have an associated pion, suggesting that simple N-N quasi-elastic scattering is not the dominant mechanism at these energies.

In 1981 the group will conduct a new experiment (564H) using a 2.1 GeV/n ^{40}Ca beam to study strange particle (particularly Λ^0) *production in both the inelastic and central* collision modes. There are plans for a high statistics run of 50-100 K pictures. Data from this experiment will also be used to provide a more detailed study of negative pions. An experiment (557H) looking at the reaction mechanisms of ~ 100 MeV/n Ar beams on various targets is scheduled for early 1981. During 1981, the group will start a program of upgrading the streamer chamber at LBL that will include the following:

(1) Replacement of the present camera system by image intensifier cameras, and testing digital image processing.

(2) Investigation of the operating characteristics and possible limitations of the chamber when exposed to beams heavier than Ar, in anticipation of the heavy beams available *after the Bevalac upgrading.*

(3) Determination of the limit in a single event of multiple tracks that can be successfully studied in *the* chamber.

(4) Surrounding the chamber with detectors (e.g., scintillators or solid state counters) to improve particle identification. This will mark the beginning of use of the streamer chamber in a hybrid configuration.

(5) Reactivation of the PEPR semi-automatic measuring facility of the University of Heidelberg, and with this to start proton measurement and π^+ - p discrimination.

R. Stock and A. Sandoval using a leak detector to check the window seals on the streamer chamber.

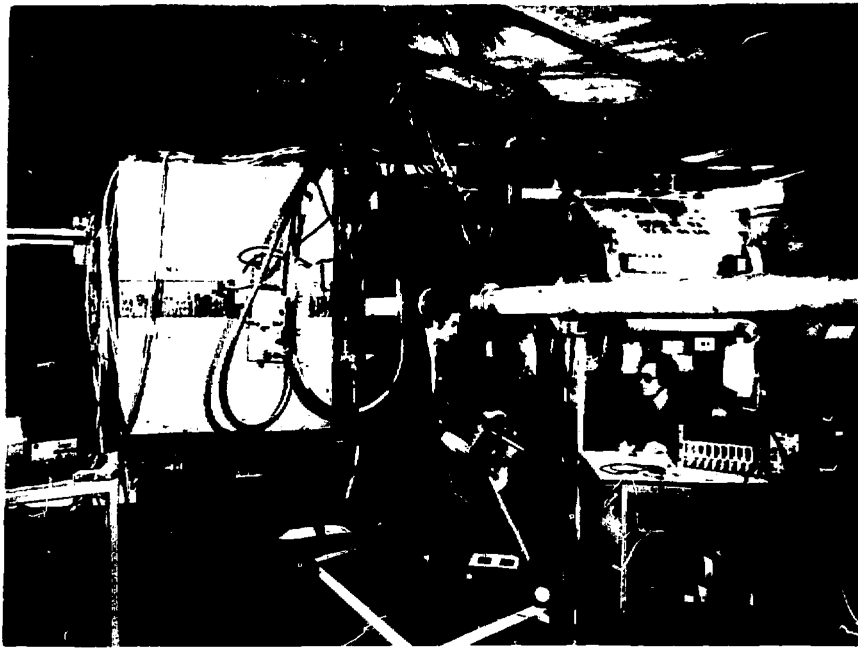

G. Roche, on leave from Clermont-Ferrand for a year to work at the Bevatron, adjusts the oscilloscope while U.C. Berkeley graduate student P. [illegible] prepares to write down the calibration data. They are calibrating [illegible] detectors for the two-arm spectrometer (TASS) shown in the background.

STUDY OF CENTRAL COLLISIONS

H. Steiner and S. Nagamiya

O Chamberlain, LBL-UC Berkeley
H Hamagaki, INS, University of Tokyo
S. Kadota, INS, University of Tokyo
R Lombard, CEN de Saclay
Y Miake, Osaka University
E. Moeller, Freie Universitat Berlin
S. Schnetzer
G Shapiro, LBL UC Berkeley
Y. Shida, INS, University of Tokyo
I. Tanihata, INS, University of Tokyo

The main research objective of this group is to study reaction mechanisms in nuclear collisions at high energies by measuring the spectra of light fragments and their mutual correlations over a wide range of fragment energies and emission angles.

In Experiment 299H the inclusive spectra of pions, protons, deuterons, tritons, ^{3}He, and ^{4}He, as well as two-proton correlations and the spectra of light fragments at high event multiplicities, have been measured. These data, combined with the proton-nucleus data measured by the group, have been used to study reaction mechanisms, especially those responsible for central collisions.

The mean free path of protons inside the nucleus was evaluated from the proton-nucleus data. Composite particle emission turned out to be consistent with the coalescence model from which interaction radii of heavy-ion collisions were estimated. From the observed mean free path and interaction radius one learns that heavy-ion collisions, involve both single nucleon-nucleon collisions and multiple nucleon-nucleon collisions. The fraction of each of these processes was studied in restricted kinematical regions in the two-proton correlation experiment and over a wider kinematical region by analyzing the proton spectra of high-multiplicity events. The group also looked for but did not find evidence for shock-like behavior or other startling new features in either the two-particle correlation data or the high multiplicity events.

In Experiment 471H kaon production has been measured. The data-taking for 2.1 GeV/A Ne, 2.1 GeV protons and for 4.8 GeV protons had been completed. Cross sections predicted on the basis of thermal models exceed the observations by factors of 10 or more. Futher data analysis is still in progress.

Another experimental program, which is in the process of taking data, is Experiment 472H, in which two-particle correlations are studied in detail over a wider kinematical region than was possible in the previous experiment. A new detector system has been installed. It consists of (1) a beam counter bias on high-event multiplicity, (2) four sets of time-of-flight counters to cover forward angles, (3) 18 sets of ΔE-E counter telescopes to cover backward angles. Some data have already been obtained with this system but the major data run is now scheduled for January 1981.

In Experiment 493H a preliminary study of delayed-particle emission in heavy-ion collisions will be done by using rf-bunched Bevalac beams. Beam time will be scheduled sometime in 1981.

In FY 1981 another main activity of the group will be Experiment 512H, in which fragments with very large transverse momenta and their mutual correlations will be measured using the HISS magnetic spectrometer. To carry out these studies they plan to install 5 sets of 3-dimensional multiwire proportional chambers and 30 sets of time-of-flight and dE/dx detectors. Most of this hardware construction will be conducted under the Institute for Nuclear Study, Universits of Tokyo-LBL Collaboration Program.

In the future the group intends to undertake an experimental program to learn more about the production of excited baryonic states and the mutual interactions between these excited baryons, using a large solid-angle device.

Apparatus for two-particle correlation measurements in high-energy nuclear collisions being performed by a collaboration LBL and INS (University of Tokyo). On the left are S. Kadota, I. Tanihata, and in front, Y. Miake. The others (left to right) are M. Echard, R. Lombard, S. Schnetzer, and the group leaders, S. Nagamiya and H. Steiner.

HEAVY ION STUDIES/PION STUDIES

K. M. Crowe and J. O Rasmussen

J. A. Bistirlich
R. Bossingham
H. R. Bowman
K. A. Frankel
C. J. Martoff
D. L. Murpy*
J. P. Sullivan*
E. Yoo*
W. A. Zajc

O. Hashimoto, INS Tokyo
M. Koike, INS, Tokyo
J. Peter, Orsay, France
J. Quebert, University of Bordeaux, France
P. Truoll, SIN, Zurich

The Berkeley research activities of this group center mainly around the study of charged pions produced in high-energy heavy-ion collisions at the Bevalac. The technical approach involves a large (~ 1.5 meter long) magnetic spectrometer (JANUS) and combinations of fast scintillators and wire chambers interfaced with computer data systems. One major part of their work is the determination of the cross sections (with an exploration of the angular dependence) for pion production in heavy-ion reactions. The existence of both positively and negatively charged pions facilitates determinations of simple Coulomb effects and therefore the charge density evolution in heavy-ion collisions by observation of the π^+/π^- ratio as a function of pion energy, bombarding energy, and target-projectile charges. In fact they have found that pions produced with low energy in the projectile frame have large π^-/π^+ ratios due to the Coulomb fields of the fragments. Systematic observations of the sharp anomaly are being made to compare with various models for production. The effects due to esoteric mechanisms, i.e., condensates, etc., are expected to modify the conventional modes, and these phenomena are being explored.

They are also studying the production cross section for low-energy π^- and π^+ at 90° in the center of mass, where an enhancement in the π^+ production has been observed. They want to ascertain that this 90° peak does disappear at low energy and to attempt to measure the threshold for its appearance. They have undertaken thick target studies in order to evaluate the practicality of heavy-ion production of useful π^- beams.

The second major part of their work is an experiment to look at the Hanbury-Brown-Twiss effect for like charged pions made by heavy-ion collisions in events where many pions are produced. They look at the production of a pair of closely related pions +,+ or -,- at the lab angle 40°. In the past ten years, such exotic phenomena as pion condensation, pionic lasing and quark matter have been predicted as possible for nuclear matter in a heavy-ion collision. Gyulassy, Koonin and others have pointed out that one possible way to see the effect of pion instabilities in heavy-ion collisions is to look for the correlation of like pions in the situation when the relative momentum is extrapolated to zero.

More quantitatively, one studies the correlation function $C_m(k,\cdots k_m)$ for m pions. For the case of two pions, $C_2(k,k) = 0$ for coherent sources. Highly coherent pions will have a different distribution in relative momenta than that expected for chaotically produced pions, and the range of coherence depends on the size of the interaction region. This technique of pion interferometry has been employed to measure the size and lifetime of the pion source formed in the collision of 1.8 GeV/A ^{40}Ar + KCl. The values obtained provide useful constraints on models detailing the pion production mechanism. The Bose-Einstein enhancement for low relative momentum was observed.

Future work that this group intends to pursue will utilize the experimental techniques and apparatus that they have built. The availability of Bevalac beams of the heavier elemnts (Au, Pb, or U) will call for new pion spectroscopic measurements to search for evidence of highly compressed nuclear matter effects, such as pion condensation, quark matter, etc. The π^+/π^- ratios will again be exploited for heavier beams to measure the dynamic charge evolution in relativistic heavy-ion collisions.

Studies of several new areas of research are being considered for work to exploit the Bevalac. Among them are the following topics: measurement of deuteron ground state to excited state (virtual) ratio as a probe of spin correlations associated with pion condensation, and the study of strange particle production.

Kamae and Fujita, Jaffe, Kerman, and Chin have suggested that the system of six quarks including two strange quarks may be exceptionally stable with binding energy of order 80 MeV or greater. The reduction in decay channels may produce significantly different objects, including tightly bound di-lambda, and hyperstrange quark matter.

As a first step in searching for exotic strange fragments the group plans to develop a multipurpose K^+ trigger. Such a trigger might be used in a streamer chamber collaboration to study strange particle production. The multipurpose K^+ trigger may also find application in JANUS or HISS spectrometer experiments.

*Graduate students †Undergraduate student

After the completion of the scheduled upgrading of the Bevalac to accelerate essentially any element, they plan to undertake a new type of experiment, the coherent resonance Coulomb excitation of the 14 keV transition (of wide usage in Mossbauer effect) in a ^{57}Fe beam. This would be a collaboration with Y. Okorokov of the U.S.S.R. and C. Moak of Oak Ridge.

They intend to use partially stripped ^{56}Fe beams at lower Bevalac energies to study atomic processes. These are of considerable interest in their own right (see earlier Bevalac studies of Raisbeck, Crawford, et al.) and also lay the groundwork for the special single-crystal resonance excitation experiment with ^{57}Fe beams mentioned in the preceding paragraph.

Various members of the group are involved in collaborative work centered at other laboratories: pion or muon experiments at LAMPF; theoretical studies on muon fission with collaborators in China; theoretical nuclear studies by the Classical Limit S-Matrix Method with collaborators at the University of Tennessee, Brazil, and Kuwait; and hybrid plastic and emulsion studies of relativistic heavy ions with collaborators in Nagoya and Cairo.

The two-meter wire chambers of the JANUS magnetic spectrometer used for two-pion interferometry experiments at the Bevalac. Holding one of the connector boards is E. Yoo, a summer undergraduate physics assistant working with the Crowe-Rasmussen Group.

NUCLEUS-NUCLEUS COLLISIONS

P. B. Price

S. P. Ahlen
E. K. Shirk
M. Solarz
J. D. Stevenson
G. Tarle
M. Budiansky*
K. Kinoshita*
T. Liss*
J. Musser*
M. Salamon*
M. Tincknell*
S. Levin†
K. Martin†
J. Martinis†
H. Nelson†
J. Zelinsky†

All of this group's offices and equipment are located in Birge Hall on the UCB campus, which makes it easy to attract new students, but restricts to some extent interaction with Nuclear Science Division staff. Current research falls into the following three principal areas:

1. Relativistic heavy ion research (DOE support):
   a. Production of heavy fragme ts, including exotic neutron-rich nuclides near the dripline.
   b. Production of high-energy gamma rays.
   c. Search for Lee-Wick matter.
   d. High-order effects in electrodynamics of slowing heavy ions.
   e. Response of various detectors to heavy ions, and development of new detectors.
   f. Hadron calorimetry for nucleus-nucleus collisions.

2. Search for highly ionizing particles in e^+e^- annihilation (PEP-2 experiment, supported by NSF):

3. Cosmic ray astrophysics (NASA support):
   a. Relative abundances of isotopes of very heavy cosmic rays.
   b. Abundances of cosmic rays in the vicinity of uranium and beyond.
   c. Design of future, large-area detectors for long-duration space exposures.
   d. Study of highly ionizing particles with anomalously long interaction lengths at mountain altitudes.

Drs. Ahlen, Stevenson, and Tarle play a major role in conceiving new experiments and in training students. There is a great deal of overlap among the various projects. Detectors devised to solve one problem frequently make possible part or all of the solution of another problem. A result obtained with plastic detectors may stimulate the construction of an electronic system to do a second-generation experiment. Expertise gained in resolving isotopes in a balloon-borne cosmic ray experiment may be used at PEP or the next-generation neutron-rich nuclide experiment. In all these projects, both post-graduate and pre-graduate students play an active part.

Among the experiments planned for the next two years at the Bevalac are a high-energy gamma ray experiment with 10^2 higher collecting power; detection of many new nuclides delineating the neutron dripline; hadron calorimetry with large solid angle; search for Lee-Wick matter in U-U collisions; measurement of higher-order electrodynamics in dE/dx and Cerenkov radiation by ions up to U; and determination of the response of plastic track detectors to relativistic ions up to U (the latter being of crucial importance for the proof that cosmic rays come from freshly synthesized supernova debris).

*Graduate students
†Undergraduate students

NUCLEAR THEORY

N K Glendenning

J Botuta
M Gyulassy
Y Karant*
S K Kauffmann
C. M. Ko
G. Mantzouranis
W D Myers
J. Randrup
M. Redlich
H Ruck

W * Swiatecki
S Bohrmann, MPI, Heidelberg West Germany
H Flocard, CNRS, Orsay France
J Knoll, GSI, Darmstadt West Germany
A Lumbroso, CEN, Saclay France
C Noack, University of Bremen West Germany

There are three general themes in the research of the theory group. One of these works close to the boundary between nuclear, particle and astrophysics, and includes the study of hadronic matter at extreme densities and the search for phase transitions. The next is an investigation of the properties of ordinary nuclei treated as a system of relativistic interacting fields. The third concerns nuclear collisions from the Coulomb barrier to Bevalac energies.

HADRONIC AND QUARK MATTER

Several lines of investigation are being pursued. The first, appropriate to an intermediate range of densities from normal up to a few times normal density, employs a relativistic Lagrangian field theory to describe nuclear matter. In this density range, the nuclear forces can be regarded as arising through the exchange of the mesons having various spin and isospin quantum members. This theory has been formulated and solved for symmetric nuclear matter with particular emphasis on the possible phase transition to the so called pion condensed state. For the first time, this much discussed state of matter has been shown to be compatible with the constraints imposed on the theory by the bulk properties of normal nuclei. The constraints severely limit the magnitude of the condesate energy, although the amplitude of the spin-isospin density wave to which it corresponds attains almost its maximum possible value. This work is being extended to finite temperature and preliminary work suggests two very interesting phenomena. Although of minor importance at zero termperature, the pion condensate creates a density isomer above a critical temperature of a few MeV. Secondly the pressure in the condensed state is not isotropic, but is greater along the direction of the spin-isospin lattice. This is very encouraging for it implies that dense matter in which a condensate has been induced would disassemble, in bulk, preferentially along this direction. Asymmetric matter or neutron star matter is currently being formulated. The rho meson has to be introduced because of the asymmetry, and accounts in part for the symmetry energy. Technically, this is a considerably more complicated problem.

The other research in this catergory investigates quantum chromodynamics in a one dimensional model. The success of this project so far is that the theory has been demonstrated to lead to quark confinement. Currently a quark matter state of the theory is being sought.

RELATIVISTIC FIELD THEORY OF NUCLEI

This research, like that described above, is a relativistic interacting field theory. In this case the field equations are solved for finite nuclei. The theory has so far been demonstrated to account successfully for saturation, the spin-orbit interaction, single-particle levels, charge distributions, Λ-hyper nuclei, the level density parameter for finite nuclei, and the energy dependence of the optical potential. The theory also makes a prediction for the anti-nucleon nucleus optical potential, which turns out to have a greater range than the nuclear optical potential. The spin-orbit interaction is introduced phenomenologically in the usual Schroedinger description of nuclear physics but in this theory arises naturally as a relativistic effect. Particular attention is being focused on whether there are other nuclear properties that specifically require relativity.

NUCLEAR COLLISIONS FROM THE COULOMB BARRIER TO BEVALAC ENERGIES

A large number and diversity of projects are underway in this area, including the development a new type of dynamic large-scale shape evolutions (with applications to the production of super-heavy nuclei); progress toward the unification of transport-type theories of nuclear collisions through the use of parameterless "proximity" expressions for the transport coefficients (analogous to the proximity force and proximity friction); the detailed study of the time-dependence of the charge-equilibration degree of freedom in fission and nucleus-nucleus collisions; and the refinement and application of TDHF methods to (resonant) nuclear collisions. In the high energy region, the research includes the study of the role of non-equilibrated dynamics via cascade simulation, the analysis of $\pi^-\pi^-$ correlations and pp correlations; theory of the composite fragment production, dynamics of pion and kaon production; role of final state interactions such as Coulomb. These topics are described in more detail.

*Graduate student

Futher progress has been made in developing and applying a new macroscopic theory of nuclear dynamics in which the nuclear shape evolution is largely dominated by dissipation (of the "one-body" type). A global survey of different types of nucleus-nucleus reactions that follow from this theory is under way. In addition to criteria for compound-nucleus and deep-inelastic processes a new type of reaction emerges from such studies, probably to be identified with fast-fission or quasi-fission processes suggested by recent experiments. The theory has also been applied to estimating the optimum reactions for producing super-heavy elements.

A theory has been developed for the effect of nucleon transfer on the dynamics of the dinuclear complex formed in a damped nuclear collision. Some hitherto puzzling features of the experimental data appear now to be well understood on this basis. This theory, together with the above mentioned shape dynamics, form a useful reference model for the dynamical evolution of a damped nuclear collision and its numberical implementation has already proved successful in the data analysis. The validity of the Fokker-Planck treatment of transport in nuclear collisions is being explored by performing a direct dynamical simulation of the individual nucleon transfers.

Various studies relating to the role of giant modes in the dinuclear complex have been carried out. For damped collisions, the charge asymmetry has been treated as a collective quantal mode analogous to the Giant Dipole mode in spherical nuclei. In this connection, separate studies have been made of the inclusion of damping effects into the time-dependent Schrodinger equation. The quantal treatment of the collective charge-asymmetry mode has been incorporated into the dynamical collision model mentioned above, allowing reasonably realistic calculations to be made. For the case of fission, the dependence of the charge dispersion on the dynamical trajectory has been examined. A separate study has shown that isovector modes of higher multipolarity can be important for the charge distribution in damped collisions. Progress on the charge distribution in static nuclei has been made within the Droplet Model.

The current low-energy program also includes studies within the Hartree-Fock approximation. The possibility of exciting high-lying modes in nuclear collisions has been studied in TDHF. A search for periodic TDHF solutions has been carried out; a general numerical code has been developed and applied to monopole vibrations of magic nuclei. The use of TDHF codes with an imaginary time for solving the static problems has also been explored.

The theoretical pursuit of problems relating to the Bevalac has been continued over a broad front. The dynamics of relativistic nuclear collisions has been studied within the framework of conventional multiple-collision cascade models. These studies are providing useful insight into the equilibration process and permit the test of various idealized treatments. One current project is the study of proton-proton correlations. A special aspect here is whether critical scattering phenomena might manifest themselves in the correlation function via the dependence of the elementary cross section on the nuclear medium. These studies are to be extended to pion-proton correlations as well.

Extensive theoretical development on $\pi^-\pi^-$ correlations has been completed. The goal here is to test for coherent pion fields produced in nuclear collisions. Numerical calculations of the role of Coulomb final state interactions have been completed. The recent data on $\pi^-\pi^-$ correlations are now being analyzed in light of these calculations.

A first calculation of kaon production in relativistic nuclear collisions has been made in a multiple-collision cascade model. Kaons are produced in relatively violent nucleon-nucleon collisions (above 1.6 GeV) and have a small interaction cross section so that once produced they are likely to leave the interaction zone rather unperturbed. Kaons are therefore particularly suitable for probing the early collision stage where the highest degree of compression and excitation occurs. Futher work on kaon production is anticipated when the analysis of a recent experiment is completed.

Recent interest has focused on the empirical square law of deuteron production. A new line of attack on the problem based on a microcanonical ensemble approach has begun that will complement the previously developed macrocanonical chemical-thermal equilibrium models.

The effect of Coulomb interactions on the π^-/π^+ and n/p ratio has been calculated. In addition the question of π^+ focusing has been analyzed. The simple analytical formulas that have been derived compliment the numerical studies at other laboratories. The hope in this time of research is to use the well understood Coulomb interactions to gain insight into the dynamics of nuclear collisions.

A current topic under investigation is why there are so few pions produced in nuclear collisions. Statistical models systematically predict twice the observed number of pions. Yet temperatures predicted are correct. There is an energy balance problem to be solved. Does this mean more transparency in nuclear collisions than we expect?

[illegible] Myers and [illegible] Theory Group.

HEAVY ION SPECTROMETER SYSTEM (HISS) GROUP A

D E Greiner

M Banks
E Beleal
M Bronson
P Lindstrom
F Bieser U C Space Sciences Laboratory

H Crawford, U C Space Sciences Laboratory
C McParland U C Space Sciences Laboratory

HISS Group A was formed this year to spearhead the experimental program at the Heavy Ion Spectrometer System. The major effort in 1980 has been to direct construction of HISS, develop and coordinate the first five experiments to be performed at HISS, and to oversee design and construction of the Phase I detector system to be used in these experiments.

The HISS facility will be on the air by the end of FY 1980. The numerous attendant difficulties in getting this large project moving have been overcome in this year. The group has been responsible for overseeing the construction of the dipole, experimental housing and beam lines. They have been directly responsible for the computer system and beam line diagnostics. The design and construction of the Phase I detectors for HISS has been a cooperative effort between the groups that will perform the first five HISS experiments; the HISS Group has played a major role in forming and encouraging this collaboration. The thirty-five people involved consist of twenty-five physicists, 50% outside users, and represent eight institutions.

The first five experiments on HISS will be performed between October 1980 and June 1981. It is hoped that it will be possible to perform these experiments (totaling 750 hours of Bevalac time) before the shutdown for the Bevalac improvement project. These five experiments could not be done without HISS; all require the large magnetic volume and solid angle that HISS provides to make multi-particle measurements. These long-awaited multipartical measurements will provide the information necessary to probe the underlying assumptions of presently available interaction models and bring us closer to our understanding of the reaction mechanism and its time evolution.

During FY 1980 this group has also performed numerous services for the laboratory. They have provided the management for the Division effort to develop general purpose software for Bevalac users. In this area a system has been put together at low cost from borrowed pieces and is proving itself indispensable to a growing number of experimenters. They assisted the Accelerator Division and many Bevalac users in the preparation of new beam lines and in the determination of the characteristics of these lines. They also support an active outside user program and several times a year special runs for short exposures (emulsions, plastics, etc.) and NASA calibrations are handled by this group on the 0° spectrometer in Beam 40.

In this group's experimental program during FY 1980, data collection and analysis was completed on Bevalac experiment 350H. This experiment is a detailed examination of the photodisintegration of ^{18}O in the photon fields of heavy targets. Earlier experiments had indicated that there is an enhacement proportional to Z^2 of the target in the nucleon removal which could be attributed to Coulomb effects. By using ^{18}O this assumption could be strongly verified because of precise knowledge of the photon-induced disintegrations $^{18}O(\gamma,p)\,^{17}N$, $^{18}O(\gamma,n)\,^{17}O$ and $^{18}O(\gamma,2n)\,^{16}O$. Preliminary analysis indeed shows and enhanced rate for $^{18}O(\gamma,2n)\,^{16}O$ which gives the proper increase with target charge. This work was done in collaboration with H. Heckman (LBL) and B. Berman (LLNL).

In another experiment this year the advantage of using relativistic heavy ions to investigate the limits of stability of nuclear matter was clearly demonstrated by the discovery of 14 new isotopes within the space of a few hours. The experiment was quite simple; it involved fragmenting ^{48}Ca, then dispersing and indentifying the fragments. (This work was done in collaboration with the Scott-Symons group of LBL). Fragment identification was made using the solid state detection technique which the group developed for satellite use.

In FY 1981 the Phase I HISS experiments begin. The HISS Group will carry out three of the five experiments that will be completed within this period. These experiments each exploit the same basic method: the examination of exclusive or near-exclusive final states of the projectile fragments.

The first experiment at HISS will be an examination of the exclusive states of ^{12}C fragmentation (exp. 513H). The relativistic energies provide kinematic focusing of projectile fragments, allowing measurement of branching ratios to states totaling ~ 40 of the nuclear fragmentation channels with the relatively small HISS Phase I detectors. On an event-by-event basis the hypothesized excitation stage of the reaction will be reconstructed. This stage, unlike the evaporation stage, has properties such as excitation energy, mass ratios and momentum distributions that are clearly predicted by the available models and will allow us for the first time to distinguish between the various reaction models.

This powerful analysis method will also be applied at HISS to the fragmentation of ^{56}Fe in experiment 516H, were the primary goal will be a search for abnormal states. Possible signatures for such states are (1) structure in the invariant mass spectrum, (2) correlations in fragment emission, (3) planer emission, of fragments, and (4) short-lived states, all of which can be investigated for the first time with HISS.

An additional goal of this group is to provide HISS users with the documentation and advice necessary to allow efficient use of the facility. They will be supplementing the available software tools and keeping the common-use detector arrays in operating condition. They also expect to continue to cooperate with the Acceleration Division to ensure smooth operation of the experimental program as well as continuing support for outside users (NASA) in Beam 40.

In 1981 a fraction of their time will be spent in designing and prototyping the Phase II detector system for HISS. In particular, the schedule calls for extensive prototype tests of the energy flow calorimeter in FY 1981. Experience gained in the Phase I experiments will futher support an optimum design for the Phase II detectors. The timing is excellent as the shutdown for the Bevalac vacuum improvement project will allow them to ensure that the Phase II detectors are suitable for the high charge available from the upgraded Bevalac.

Checking construction details for the recently assembled HISS [illegible] are [illegible] Tuttle, P. Lindstrom, and H. Crawford.

NUCLEAR ELECTRONICS

F S Goulding

F Gin
E Haller
D Landis
P Luke
J Meng
D Pehl
H Sommer
J Walton
Y Wong

This group specializes in the development of detectors and associated electronics for nuclear science. It is also involved in the development of improved data acquisition and reduction systems based on Mod Comp IV and Classic computer systems.

The bulk of the detector work centers on semiconductor detectors (both silicon and germanium). At the base of the germanium detector work is the high-purity germanium materials program. This program has made unique contributions to the development of high-purity germanium for radiation detectors and to the understanding of purification processes and of the role of defects in germanium. Of particular recent importance has been the discovery of the role of hydrogen and its association with crystal defects and with impurities such as carbon and silicon. The extreme purity of the germanium ($10^{1?}$. provides a unique environment for studies of such interactions and the results achieved are of considerable interest in solar cell processing where hydrogen can play an important part in the electrical behavior of amorphous layers.

Another focus of the germanium detector program is on studies of radiation damage and annealing of damage in high-purity detectors. This work is of particular importance in the application of multi-detector telescopes for long-range particle identification and spectroscopy. In these experiments the detectors are severely damaged, and the practicality of the method rests on the ability to conveniently repair the damage (preferably in situ). This type of experiment also demands reliable detectors, exhibiting only very thin dead layers in both contacts. An amorphous germanimum coating has been developed to provide surface protection for such detectors, and it has demonstrated its ability to provide surface protection. The group has also developed thin ion-implanted contacts (both p and n type) and is continuing work to improve these contacts.

An outgrowth of this research and development program has been the provision of specialized germanium detectors and germanium detector telescopes that are the basis for experiments in several laboratories in the United States and Europe. For example, much of the work at the University of Indiana Cyclotron uses multi-detector telescopes supplied by this group.

The silicon detector program covers the complete range of detectors but has recently focused on very large area detectors (up to 7 cm diameter) of uniform thickness (~ 10 μm in 5 mm) and with very thin dead layers. These detectors are used at the Bevalac, in space experiments measuring the isotopic composition of cosmic rays and in many laboratories in the United States and Europe. The work has recently been expanded to producing position-sensitive versions of these large area detectors, and work is continuing in this direction.

A significant interest is developing in the fabrication of large position-sensitive silicon detector arrays for 4π detection of the products of high-energy particle reactions. The resolution of gas detectors is limited to > 100 μm while that of semiconductor detectors can, in principle, be much smaller. This improvement in resolution can be reflected in a smaller 4π detector assembly and a large reduction in the cost of the whole detector system. Our detector capability will be used in the future to explore some of the possiblities in this area.

The work on signal processing for detectors is substantially smaller now than it was a few years ago. The group has been responsible in the past for many of the processing methods and hardware design now in common use. Work continues on special processing techniques such as gated-integrators to improve resolution at high-counting rates. Work on pulsed-reset preamplifiers for high-rate system and particularly for work on pulsed machines is also presently being carried out. The group expects to be working in the next two years on the application of CMOS and VMOS switching devices to simplify and improve the analog/digital part of our data acquisition systems. This work will include development of analog multiplexers, very fast ADCs and cheap multichannel ADCs.

The present digital work is aimed mainly toward the development of a highly interactive data sorting system that uses specialized hardware associated with Mod Comp Classic computer system. It is expected that this work will result in a throughput for typical experimental data that is between 10 and 100 times that of conventional systems of similar cost. The savings arise mainly from the provision of multiple programmable sorting and arithmetic modules and from complex hardware to handle random demands on memory and processors in an efficient way. This program is expected to continue intensively for the next three years with demonstrations of portions of the system in mid-1981 and completion of the whole system in 1982 or 1983.

The group also provides much of the specialized maintenance and design effort for experiments in the Nuclear Science Division. Considerable time is spent in consultation with experimental groups about new experiments or proposed instruments, the proposed crystal or liquid-xenon ball being an example that will involve much design effort by the group.

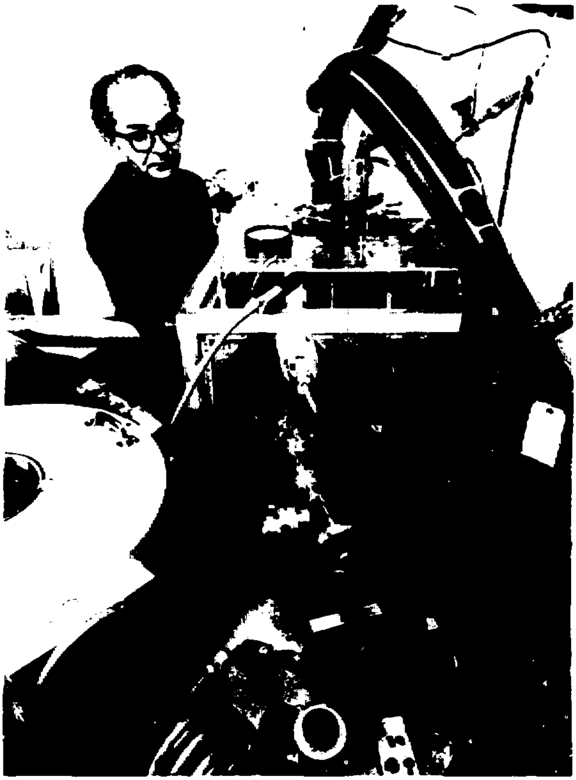

V. Roach with the experimental [illegible] angle detector system.

ISOTOPES PROJECT

J M Dairiki

E Browne
R B Firestone

C M Lederer
V S Shirley

This group compiles and evaluates nuclear structure and decay data and develops compilation methodology. The majority of effort is directed to the evaluation of experimental data, based on knowledge of the experimental methods, of the experimenters themselves, and of the relationships and constraints imposed upon the data by nuclear theory and systematics. Considerable effort is also devoted to the selection and presentation of data in formats most convenient for users.

The Isotopes Project coordinates its nuclear data evaluation effort with those of other data centers via national and international nuclear data networks. The group is currently responsible for the evaluation of mass chains A = 146-152 and A = 163-194; all evaluated data are entered into the international Evaluated Nuclear Structure Data File (ENSDF) and are published in Nuclear Data Sheets.

During the past year the evaluation of nuclear-structure data for all nuclei with mass A = 163 has been published.[1] The mass A = 191 evluation has been reviewed and accepted for publication, and the mass A = 193 evaluation has been submitted for review. Evaluations of four additional mass chains (A = 188, 189, 190, and 192) are nearing completion. Those for masses A = 169, 174, 185, 181, 168, 170 and 171 will be started in 1981.

In addition to the evaluation effort, the Isotopes Project will produce, on behalf of the U.S. Nuclear Data Network (NDN), a "Radioactivity Handbook" for applied users. The purpose of the handbook is to provide a compilation of recommended decay data that is detailed enough for use in sophisticated applications, but that is organized clearly so as to be usable in simple routine applications. The handbook will be produced at four-year intervals, beginning in 1982. Recommended decay data will be taken from the current version of ENSDF, with no further updating. Additional calculations and evaluation will be done to provide recommended data on atomic radiations and conversion electrons. Each mass chain will be referenced to the most recent evaluation in Nuclear Data Sheets, as the source for futher details and references to the original papers.

Copies of a "Handbook Sample"[2] illustrating the contents and format proposed by the group were distributed to the other data centers for their comments and approval. Additional copies (and a two-page questionnaire requesting specific comments on the proposed format) were also sent to about 5000 members of several professional societies, including the nuclear divisions of both the American Physical Society and the American Chemical Society and four divisions of the American Nuclear Society. A further mailing of about 900 was handled by the National Nuclear Data Center (BNL). Additional suggestions and comments on the format were obtained from the IAEA Advisory Group on Nuclear Structure and Decay Data during its Vienna meeting in April 1980.

Since publication of the Table of Isotopes[3] in 1978, continued development of data handling techniques has been directed to support the objectives of the NDN, especially the handbook production and the evaluation effort.

Work has begun on the computer codes needed to produce the handbook; this involves retrieval of the desired data from ENSDF and their presentation in the final publication formats. The first step involves modification of the data in ENSDF so that each decay data set will contain the "best" values for γ-ray and level properties, independent of the decay parent. Nonuniformities and holes in the ENSDF data are being corrected as work proceeds. The existing level-scheme graphics program (used for the Table of Isotopes) is being modified to handle data in ENSDF formats.

Programming tools to aid the evaluation effort have also been developed. The physics analysis programs, written by the Nuclear Data Project (ORNL) for data in ENSDF formats, have been adapted and extended into an interactive package for use on the CDC-7600 computer. The resulting PACK program enables immediate calculation of quantities such as internal conversion coefficients, energy fits, and log ft values and level feedings in radioactive decay. It also permits manipulation of the data to give, for example, energy-ordered γ-ray listings and to allow on-line editing. As a further aid in the evaluation effort, programs have been developed for the TI-59 calculator to permit desk-top calculation of log ft values, rotational band parameters, and Weisskopf photon half-lives.

The seventh edition of the Table of Isotopes, published in 1978, continues to be the most up-to-date general reference source available for nuclear data. Sales of the seventh edition through January 1980 total 5101 copies (2371 clothbound and 2730 paperback). The Nuclear Wallet Cards,[4] produced in 1979 by the Isotopes Project on behalf of the NDN, have proved to be very popular; about 6500 copies have been distributed.

The Isotopes Project also compiles and publishes every 3-4 years the Table of Nuclear

Moments, the only such table maintained on a continuing basis. The most recent version was published as an appendix to the Table of Isotopes. Work will begin in 1981 on the fifth edition. Like previous editions it will be a comprehensive compilation of nuclear magnetic and quadrupole moments. New features will be the inclusion of "adopted" or "recommended" values, the addition of values for higher-order nuclear moments and the inclusion of the magnitudes of such non-uniform corrections as those due to the Knight shift.

During the past year the database prepared for the Index of the Table of Isotopes was modified and expanded to produce the Table of Nuclides.[5] In addition, the Table of Isotopes level-scheme file has been restructured into a searchable database. It is the most up-to-date file of nuclear structure data and can readily be used for horizontal compilations and systematic studies of nuclear properties.

The Project also maintains a library containing comprehensive data files and the major nuclear physics journals.

References

1. J. M. Dairiki, E. Browne, and V. S. Shirley, Nucl. Data Sheets 29, 653 (1980).

2. E. Browne, J. M. Dairiki, C. M. Lederer and V. S. Shirley, LBL-97111, 126 (1980).

3. Table of Isotopes, 7th edition: C. M. Lederer and V. S. Shirley, editors; E. Browne, J. M. Dairiki, and R. E. Doebler, principal authors; A. A. Shihab-Eldin, L. J. Jardine, J. K. Tuli, and A. B. Buyrn, authors, John Wiley and Sons, Inc., New York (1978).

4. V. S. Shirley, C. M. Lederer, E. Browne, J. M. Dairiki, R. E. Doebler, A. A. Shihab-Eldin, L. J. Jardine, J. K. Tuli, A. B. Buyrn, J. M. H. Chong, and D. P. Kreitz, Nuclear Wallet Cards, produced by the Isotopes Project on behalf of the U. S. Nuclear Data Network (1979).

5. V. S. Shirley and C. M. Lederer, Table of Nuclides, LBL-10436 (1980). [Prepared for publication in the book Nuclear and Radiochemistry (3rd edition); Gerhart Friedlander, Joseph W. Kennedy, Edward S. Macias, and Julian Malcolm Miller, John Wiley and Sons, Inc., New York (1980).]

Y. Ellis-Akovali, V. Shirley, and P. Firestone at the Isotopes Project computer console.

SUPERHILAC RESEARCH

R. M. Diamond and M. S. Zisman

The SuperHILAC is one of two LBL accelerators (the other being the Bevalac) designated as national facilities. This means that a substantial portion of the research, more than 50%, is performed by outside users. At present, this research can be divided into five major categories: nuclear reactions (59%), nuclear structure (14%), exotic nuclei (11%), atomic physics (15%), and biomedicine (1%). The first three of these categories correspond to research sponsored by the Nuclear Science Division, while the latter two are sponsored mainly by other LBL divisions.

Research in nuclear reactions, the most heavily used area, primarily involves study of the deeply inelastic scattering (DIS) process. The questions that are being addressed are: What are the mechanisms and time scales for the equilibration of various nuclear degrees of freedom in DIS? What are the magnitude and alignment of the angular momentum transferred to the target-like and projectile-like fragment in DIS? What are the time scales and mechanisms for the emission of light charged particles (protons, alphas, etc.) and neutrons? In addition, the field of heavy ion induced fusion reactions is also under investigation. The questions to be answered here are related to limitations to the fusion process and details of the competition between complete and incomplete fusion.

The nuclear structure program at the SuperHILAC involves mainly the study of Coulomb excitation reactions. Because of our unique (in the U.S.) ability to produce beams of very heavy projectiles, such as ^{136}Xe, ^{165}Ho, and ^{208}Pb, these experiments are well suited to the SuperHILAC. By Coulomb-exciting nuclei up to very high spin states, a great deal can be learned about B(E2) values of collective excitations. Other areas under study involve the use of heavy beams to measure g-factors of high spin states with transient field techniques. This work populates high-spin states via an "inverse" reaction such as $^{28}Si(^{134}Xe,4n)^{158}Er$. The high recoil velocity in such a reaction greatly enhances the transient field effect and also allows the implantation of the recoil ions into a non-perturbing medium in times as short as 0.5 psec.

Investigation of exotic nuclei involves two different experimental techniques. The first technique utilizes radiochemical investigations of various heavy ion reaction products. Heavy targets are irradiated with high intensity heavy beams from the SuperHILAC and then chemically separated and counted offline. Although the ultimate goal of the program is to synthesize superheavy elements, exploration of the reaction mechanisms of heavy projectiles with heavy targets is also emphasized, since it will lead to better knowledge about the stability of very heavy nuclei and provide important tests of nuclear structure models in this mass region. A second technique, suitable for half-lives as short as 1 μsec, involves use of a spectrometer called SASSY (Small Angle Separator System). The device consists of a gas-filled dipole magnet, a quadrupole doublet for refocusing the recoil products, and two avalanche detectors for time-of-flight measurements. Because of the very different magnetic rigidities of beam particles and recoil ions as they pass through the spectrometer, it is possible to collect recoil products at 0° while suppressing the beam particles by as much as 10^{-12}. Various target-projectile combinations such as ^{248}Cm + ^{48}Ca and ^{238}U + ^{76}Ge are being looked at, since these are predicted theoretically to lead to formation of compound nuclei near the superheavy island of stability.

In the next few years, there are plans to expand our experimental facilities in several areas. For one thing, a new area for gamma-ray experiments is planned. This new beam line, in the North Cave area, will relieve some of the overcrowding in the present Coulex area and also provide space for any user with a large experimental apparatus (which is difficult to accomodate in any of the existing caves). A second planned expansion, already well underway, involves construction of an on-line isotope separator for the study of exotic nuclei. The device will employ an ion source to ionize recoil atoms and an extraction system to accelerate these ions into a 180° spectrometer. (Details may be found in the article by J.M. Nitschke in this annual report.) It is hoped that this device will become an outside user facility and a tape transport system is being planned that will allow low background beta- and gamma-spectroscopy of the mass-separated recoil products. A new scattering chamber will be added for the nuclear reaction program along with various special detection systems such as large-area position sensitive avalanche detectors (for fast timing) and one or more large-area total energy ionization chambers (such as a Bragg curve spectrometer, designed at LBL, or a Sann chamber, designed in Germany). These new devices will allow the nuclear reaction groups the ability to take full advantage of the proposed SuperHILAC beam buncher, now under development by the LBL Accelerator and Fusion Research Division, which is expected to provide beam bunches as narrow as 200-300 psec FWHM in selected target areas.

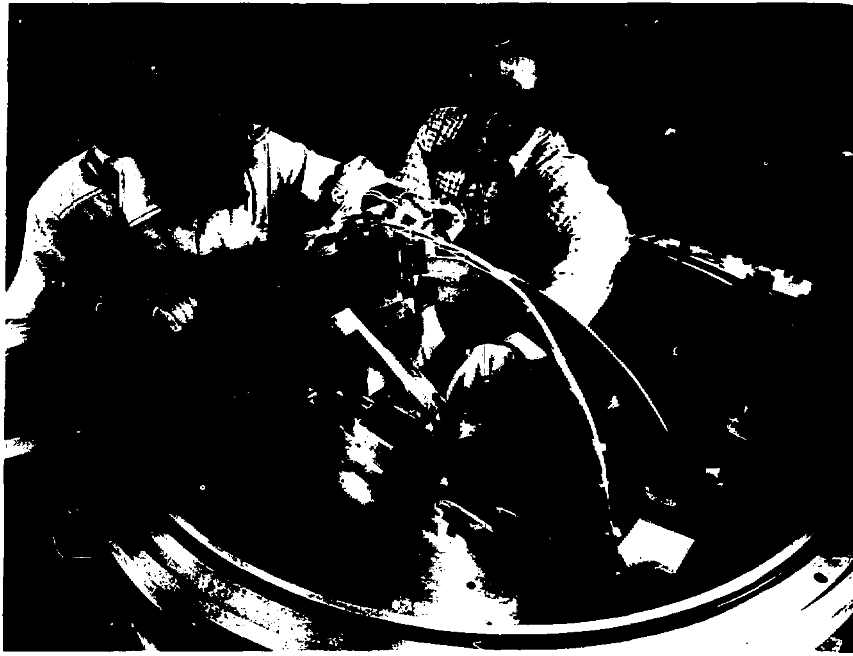

Start of an experimental setup in the SuperHILAC user's 30-inch scattering chamber. Shown are D. Logan (left) from Carnegie-Mellon University and M. Zisman, LBL SuperHILAC users liaison. The device mounted inside the chamber is a detector arm that allows measurements to be made out of the reaction plane.

88 INCH CYCLOTRON OPERATIONS

R. A. Gough and D. J. Clark

D. Elo
L. Glasgow

R. Lam
P. von Rossen

The 88 Inch Cyclotron, operated by the Nuclear Science Division, provides a large fraction of the beam time that is used by LBL scientists. Variable energy, high resolution beams from hydrogen through argon are produced and used for studies of nuclear structure and nuclear reaction mechanisms. The 88 Inch Cyclotron is also the laboratory's major source of medical isotopes and its only source of polarized proton and deuteron beams.

The large energy constant, K, recently increased to 160, permits the acceleration of ions as heavy as ^{40}Ar to energies useful for nuclear physics. The lighter heavy ions reach energies up to 30 MeV/A . The cyclotron and its almost identical twin at Texas A&M remain the only sources in the world of variable energy heavy ions in the important region around and above 15 MeV/A where low-energy nuclear phenomena disappear very suddenly.

These beams, as well as the polarized proton beams, are extensively used by outside groups from many institutions in the U.S. and abroad. In recent years, about 25% of the operating time has been taken up by outside users, almost as many hours per year as they receive at Super-HILAC. Proposals are made by letter and are informally reviewed by two outside consultants. Approval can be made within two weeks and the experiment can be scheduled within two weeks thereafter. This economical and flexible system is much appreciated by the users.

The past year has seen substantial progress in the completion of accelerator improvement projects, especially by the raising of the main magnetic field to K = 160 and by the first successful operation of the external PIG heavy ion source. These and other improvements are described in the report that follows.

The rapid increase in electric power rates in 1980 has had an impact upon present and future operation by diverting funds that were needed for engineering and technical support. Although the impact is not immediately apparent, in the future it will seriously slow the completion of ongoing improvement projects and the design stages of new ones. A serious problem for the future will be the allocation of resources between present operations and future development.

OPERATIONS

In the year ending June 30, 1980, the cyclotron was scheduled for 20 eight-hour shifts per week for experiments in nuclear science, isotope production and machine development. One eight-hour period per week was scheduled for routine maintenance. In addition there were five weeks of shutdown for general maintenance, machine improvements and because of budgetary restrictions. Accelerator time distribution is shown in Table 1. The list of beams available is shown in Table 2, while Fig. 1 shows the particle distribution of light and heavy ion beams over the past 12 years. The ratio of heavy ion to light ion beam time has stabilized at 2:1 in the last several years.

As previously mentioned, the cyclotron magnetic field was increased to increase the energy or K value from 140 to 160. A design study was done of the main and trimming coils to determine that they would tolerate the increased mechanical forces and dissipate the aditional heat generated by the greater current. The main coil power supply was revised and a 25 V, 3250 A booster power supply was added in late August 1979. The electrical cables from the power supplies to the magnet were replaced with higher current cables. The whole system was checked out in Spring 1980. The current has been run up to 3250 A for an extended period with all electrical components working within the design ratings. A new regulator was designed and installed to improve regulation and reliability. Beam tests of acceleration and extraction were done using main magnet currents up to 3230 A. Beams of C^{4+}, C^{5+} and O^{4+} were extracted at K values ranging up to approximately 160 for C^{4+}. Some changes had to be made in the calculated trim coil settings to obtain beam extraction for the highest energy C^{4+} beams due to slight errors in extrapolation of measured magnetic fields to these higher levels.

A 750 kVA capcitor bank and its associated switching circuitry were installed to bring the full load power factor from 60% to about 89%. This modification has cut down about 15% of reactive current in the load center and has reduced the heating of the transformer considerably.

A new 4648 rf power tube was installed in January 1980. A smaller diameter water separator was used in the anode cooling circuit. This modification has greatly reduced the number of flushings required. New regulators have been installed to replace the old tube type regulators in the defelector supplies and as a result of this improvement the ac ripple has been reduced by a factor of at least 50 and the reliability of the system has been greatly improved.

The polarized ion-source weak-field and intermediate-field oscillators have been modified so that they can be remotely turned on or off by a control signal from the counting area. A regulator circuit has also been added to the screen power supply to stablize the 331 MHz or 468 MHz power output. To stabilize the position of the polarized beam on target, a set of low inductance steering magnets and a set of high current driving amplifiers have been designed and installed in the vault for Cave 5 beam centering feedback control. This system has greatly stablized the beam on target in spite of fluctuations on the deflector and dee voltages.

An order was placed for a new ionizer for the polarized ion source. Installation will be made early in 1981 when it is anticipated that the factor of 10 increase in the intensity of polarized beams will be obtained.

All components of the new external PIG ion source and beam line have been completed, installed and aligned. The system has been used to inject heavy ions into the cyclotron and external accelerated beams have been obtained. Futher testing is required to maximize the overall efficiency from source to extracted beam. A new cryopumping unit has been purchased for this system and will be installed when preliminary testing is complete.

Design work is continuing on a passive magnetic deflection channel that will provide radial focusing for all beams and greater deflection strength for the higher K, high charge/mass beams; it will replace the third element in the present electrostatic deflector. Studies have included magnetic design of the channel and orbit tracking of phase space ellipses through the channel. This is a cooperative project with the Cyclotron Institute at Texas A&M University, where Don May is carrying out the orbit tracking studies. Mechanical design of the channel will begin later in 1980.

A second cryopump on the cyclotron acceleration chamber was connected to its compressor, given a thorough leak check and is now in the final stages of debugging. The unit will provide an additional 10,000 liters per second pumping speed in the dee tank. Full operation is expected later in 1980.

A project was begun in 1976 to systematize the prediction of cyclotron set-up parameters for any requested new ion and energy and provide them on a single sheet to the cyclotron operators. It was completed this year by adding the capability to store values of the currents in the 17 trim coils. The task of entering values for these coils for some 400 reference beams up to K = 160 will be completed in 1980. This was implemented by the recent acquisition of a dual floppy disk drive for the PET computer.

Planning is underway for an advanced heavy ion source for the cyclotron. The goal is to provide useful beam intesities of 10^9-10^{10} particles/sec on target with energies of 2-3 times those of present heavy ion beams with masses between nitrogen and xenon at values up to 40 MeV/u for the lower masses. The two leading candidates for sources are the Electron Beam Ion Source (EBIS) and the Electron Cyclotron Resonance (ECR) source. The EBIS uses a well collimated electron beam on a solenoid axis in high vacuum to produce very high charge states (Ar^{18+}, Kr^{34+}). It is a pulsed device whose duty factor can be 10-50%. The ECR source uses a microwave-generated plasma with magnetic mirror confinement to produce high charge states. It gives higher intensities at the lower charge states than EBIS, but lower intensities at the highest charge states. Our choice is the EBIS because its higher charge states provide a greater energy range for the cyclotron.

Research and development to build a test bench EBIS was begun in January 1980, under the direction of the plasma group in the LBL Accelerator Division. The goal is to reproduce the high electron beam densities observed by the Orsay group. This will require careful alignment of the electron gun and magnet system, and high vacuum technology. To use existing hardware as far as possible, it will use an electron gun on loan from the Cyclotron Institute, Texas A&M University. A normal conducting coil system, using three 16-inch inside diameter coils, will be used to generate a 10 kG field on the axis of the 50 cm long source. A series of iron "homogenizing rings" inside the coils will provide a straight magnetic axis. A vacuum chamber and drift tube system will each be independently adjustable in position transverse to the axis. A time-of-flight mass analyzer will be designed and built for the system by R. Kenefick of Texas A&M. This test bench will give valuable information on the requirements for high charge state production, which will be used to design the final source to be installed on the axial injection system of the cyclotron.

Table 1. 88 Inch Cyclotron time distribution including total calendar time except holidays (7/79-6/80).

	Hours	Percent of total
Operating		
Experimental Program	6404	75.1
Beam Development	390	4.6
Subtotal	6794	79.7
Maintenance		
Routine	552	6.5
Scheduled Shutdown	974	11.4
Unscheduled Shutdown	208	2.4
Subtotal	1734	20.3
	8528	100.0

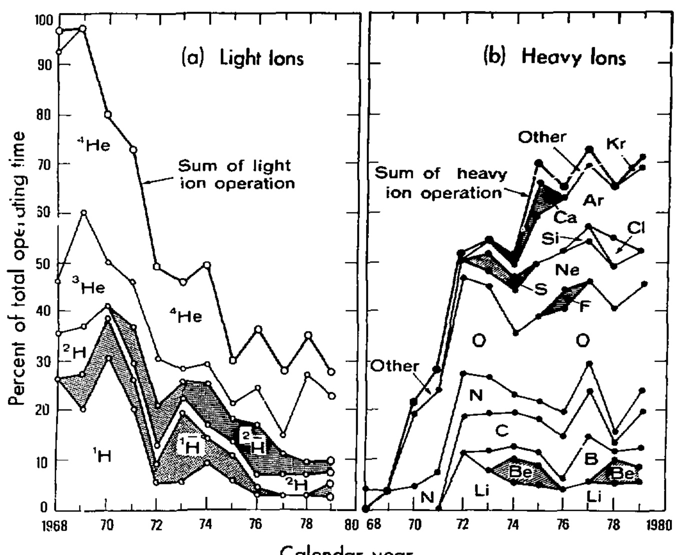

Fig. 1. (XBL 809-1999)

Table 2. 88 Inch Cyclotron beam list, July 1980.

Ion	Energy[a] (MeV)	Ext. Beam Intensity (euA[b])
p	0.2 - 55	100 - 20
p (polarized)	6 - 55	0.3
d	0.5 - 65	100 - 20
	65 - 70	~0.5
d (polarized)	10 - 70	0.3
$^{3}He^{1+}$ (d)	2 - 47	>20
$^{3}He^{2+}$ (d)	4 - 140	100 - 10
$^{4}He^{2+}$	3 - 130	100 - 10
	130 - 140	~0.5
$^{6}Li^{1+}$ (d)	2 - 23	10
$^{6}Li^{2+}$ (d)	23 - 93	5
$^{6}Li^{3+}$ (d)	93 - 195	0.5
$^{7}Li^{2+}$	20 - 80	5
$^{7}Li^{3+}$	80 - 180	0.5
$^{9}Be^{2+}$	15 - 62	5
$^{9}Be^{3+}$	62 - 140	2
$^{9}Be^{4+}$	140 - 249	0.05
$^{10}B^{2+}$ (d)	14 - 56	10
$^{10}B^{3+}$ (d)	56 - 126	50
$^{10}B^{4+}$ (d)	126 - 224	0.3
$^{10}B^{5+}$ (d)	224 - 320	0.001
$^{11}B^{2+}$	12 - 51	10
$^{11}B^{3+}$	51 - 115	50
$^{11}B^{4+}$	115 - 204	0.3
$^{12}C^{2+}$	12 - 47	>20
$^{12}C^{3+}$	47 - 105	30
$^{12}C^{4+}$	105 - 212	5 - .5
$^{12}C^{5+}$	187 - 306	0.01-.001
$^{12}C^{6+}$	292 - 384	10^5 p/sec
$^{13}C^{3+}$ (d)	43 - 97	>20
$^{14}N^{2+}$	10 - 40	20
$^{14}N^{3+}$	40 - 90	15
$^{14}N^{4+}$	90 - 160	15
$^{14}N^{5+}$	160 - 250	2
$^{14}N^{6+}$	250 - 360	10^6 p/sec
$^{14}N^{7+}$	360 - 448	100 p/sec
$^{15}N^{4+}$ (d)	84 - 150	15
$^{16}O^{1+}$	9	1
$^{16}O^{2+}$	9 - 35	>5
$^{16}O^{3+}$	35 - 79	20
$^{16}O^{4+}$	79 - 155	30-.2
$^{16}O^{5+}$	140 - 219	5
$^{16}O^{6+}$	219 - 315	0.3
$^{16}O^{7+}$	315 - 429	10^7 p/sec
$^{16}O^{8+}$	429 - 512	0.2 p/sec
$^{18}O^{3+}$ (d)	31 - 70	20
$^{18}O^{4+}$ (d)	70 - 124	>10
$^{18}O^{5+}$ (d)	124 - 194	5

Ion	Energy[a] (MeV)	Ext. Beam Intensity (euA[b])
$^{19}F^{3+}$	30 - 66	5
$^{19}F^{4+}$	66 - 118	10
$^{19}F^{5+}$	118 - 184	2
$^{20}Ne^{3+}$	28 - 63	>10
$^{20}Ne^{4+}$	63 - 112	10
$^{20}Ne^{5+}$	112 - 175	5
$^{20}Ne^{6+}$	175 - 252	1
$^{20}Ne^{7+}$	252 - 343	0.01
$^{20}Ne^{8+}$	343 - 448	~50 epA
$^{22}Ne^{5+}$ (d)	102 - 159	>5
$^{22}Ne^{6+}$ (d)	159 - 229	1
$^{24}Mg^{4+}$	50 - 93	2
$^{24}Mg^{5+}$	93 - 146	0.2
$^{25}Mg^{4+}$ (d)	50 - 90	2
$^{26}Mg^{4+}$ (d)	48 - 86	2
$^{28}Si^{5+}$	80 - 125	1
$^{28}Si^{6+}$	125 - 180	0.2
$^{28}Si^{7+}$	180 - 245	0.05
$^{32}S^{6+}$	100 - 158	2
$^{32}S^{7+}$	158 - 214	0.2
$^{35}Cl^{7+}$	144 - 196	0.5
$^{35}Cl^{8+}$	196 - 256	0.05
$^{37}Cl^{6+}$	95 - 136	0.3
$^{37}Cl^{7+}$	136 - 185	0.08
$^{40}Ar^{2+}$	3.5 - 14	0.4
$^{40}Ar^{6+}$	32 - 126	2
$^{40}Ar^{7+}$	126 - 172	[illegible]
$^{40}Ar^{8+}$	172 - 224	0.5
$^{40}Ar^{9+}$	224 - 280	10^5 p/sec
$^{40}Ar^{10+}$	280 - 350	10^3 p/sec
$^{40}Ca^{6+}$	37 - 126	[illegible]
$^{40}Ca^{7+}$	126 - 172	0.2
$^{56}Fe^{10+}$	195 - 250	[illegible] p/sec
$^{63}Cu^{9+}$	142 - 180	5 enA
$^{63}Cu^{10+}$	180 - 222	0.1 enA
$^{63}Cu^{11+}$	222 - 269	5×10^3 p/sec
$^{84}Kr^{2+}$ (c)	1.6 - 6.6	0.001
$^{84}Kr^{8+}$	92 - 107	0.250
$^{84}Kr^{9+}$	107 - 135	0.120
$^{84}Kr^{10+}$	135 - 167	0.030
$^{84}Kr^{11+}$	167 - 202	0.002
$^{197}Au^{13+}$	102 - 120	3 p/sec
$^{197}Au^{14+}$	120 - 140	0.1 p/sec

a) Heavy ion energy range shows nominal maximum energy for a particular charge state down to the energy which can be reached by the next lowest charge state. Beams can also be run at energies below 1 Mev/nucleon.

b) Electrical microamperes except as noted.

c) 15th harmonic

d) Isotopically enriched source feed

BEVALAC OPERATIONS AND RESEARCH

H. G. Pugh and G. D. Westfall

The Bevalac, operated by the Accelerator and Fusion Research Division's Accelerator Operations Group headed by R.J. Force, provides beams of heavy ions from 50 MeV/amu to 2.1 GeV/amu and is available approximately 2000 hours per year for nuclear science experiments

Currently active experiments in nuclear science involve outside users from 20 U.S. institutions and from 17 foreign groups. Major international collaborations exist with GSI Darmstadt, W. Germany; INS Tokyo, Japan; and UNAM, Mexico. In addition there is a collaborative program with the Kurchatov Institute, U.S.S.R.

Experiments are approved by a Program Advisory Committee of the following people: H. Feshbach, MIT, Chariman; S. Koonin, Caltech; J.P. Schiffer, ANL; R. Stock, GSI, W. Germany; W.A. Wenzel, LBL; T. Yamazaki, University of Tokayo, Japan; and ex officio members.

A Users' Association Executive Committee conducts monthly telephone conferences with local management. Nuclear science representatives on the committee are R.T. Poe, UC Riverside, chairman-elect, and K.L. Wolf, ANL. In conjuction with the annual meeting of the Users' Association, in February 1980, three workshops were held, on "Experiments Detecting High Energy Photons or Electrons," "Low Energy Experiments," and "Experiments Using Visual Techniques," as well as discussions concerning progress on HISS and planning for VENUS.

In addition to the annual Users' Association meeting and the semiannual meetings of the Program Advisory Committee, it has become a tradition to hold a major workshop every two years, such as the 1st Workshop on Ultra-Relativistic Nuclear Collisions, held in 1979, and the 5th High Energy Heavy Ion Summer Study, planned for May 18-22, 1981. These workshops are planned in conjunction with GSI Darmstadt, who have recently hosted similar workshops in the alternate years.

The major facilities at the Bevalac include the Streamer Chamber, the Zero-Degree Spectrometer (Beam 40), the Low Energy Beam Line, and several magnetic spectrometer systems in Beam 30. Almost ready to operate are the GSI Plastic Ball/Wall system involving over 1000 different detector telescopes and the HISS system, which consists of a 2 meter diameter, 1 meter gap superconducting spectrometer with a 3 tesla field. Both of these systems are expected to take data during the 1981 running period.

An electronics pool is maintained for users. The Bevalac Software Group, led by Chuck McParland and Everett Harvey, coordinates standardized experimental software.

The past year has been one of continued development of new beams lines and rearrangement of the experimental area in preparation for HISS. The Low Energy Beam Line was used for several experiments and will be further improved in 1980 under the direction of David Hendrie. Improvements will include installation of a large scatter chamber on loan from the University of Maryland. In Beam 30 the Two-Armed Magnetic Spectrometer system (TASS) was installed and used for experiments. Machine development included operation with a single motor-generator to save electric power and testing a "mezzanine" mode of operation that should permit prime beam sharing between biomedical and nuclear science users during the daytime shifts. A radioactive ^{19}Ne beam was developed and used for biomedical work.

Upgrading of the Bevalac to provide intense beams of heavier particles (uranium capability) is now underway and is expected to be completed during a shutdown for the latter half of 1981.

The research program during the past year has be characterized by a close interaction between theory and experiment. The striking π^-/π^+ ratio near projetile velocity drew attention to the strong effects of the nuclear charge under some circumstances. The large n-p ratio observed in inclusive spectra presented a puzzle until it was recognized that the light particle stable nuclei emitted in collisions have low isospin and thus deplete the supply of neutrons and protons about equally, magnifying the n-p ratio among those nucleons left unbound. The streamer chamber provided a quantity of systematic data on multipion production, while "bounce-off" multiparticle correlation may be the first clear hydrodynamical effect to the identified at the Bevalac.

All of the above observations are characterized by a close relationship to theoretical calculations and provide critical tests for some theories. On the other hand, the observation of anomalous behavior of projectile fragment mean free paths is a major puzzle and will require futher experimental work to provide clues for its interpretation.

VENUS PLANNING

H G Pugh and T Elioff

A committee was formed in December 1979, under the present co-chairmanship of the above, with the following (condensed) charge: "VENUS is an acronym which describes a proposed major accelerator for the Laboratory. While the name is associated with a specific design, the parameters of the accelerator have not been frozen and will depend on the scientific program to be executed with it ... the VENUS Planning Committee will conduct further study of the options available, in consultation with the full spectrum of potential users of such an accelerator ..." The membership, consisting originally of the co-chairmen and Miklos Gyulassy, Lee Schroeder, James Symons, Christoph Leeman and Frank Selph, with Joseph Cerny, Hermann Grunder, and Norman Glendenning as ex officio members, was subsequently expanded to include Bernard Harvey and Jorgen Randrup.

ACTIVITIES

A circular requesting suggestions, comments, and help was widely circulated and responses were received from over 100 people from outside the Laboratory. Interest was expressed in research programs related to atomic physics, astrophysics, and biomedicine. Taking into account these responses and after an intensive reexamination of the proposed scientific program the committee arrived at some preliminary conclusions, which have ben presented at a variety of meetings inside and outside the Laboratory.

The proposal basically covers three regions of heavy ion physics. One is the domain of colliding beams, for which the design energy of 20 GeV/amu against 20 GeV/amu is reconfirmed by the committee as being close to an ideal choice. Interactions in this energy region will be dominated by particle creation and will require quantum chromodynamics for their description. Secondly, the maximum energy of 20 GeV/amu for the fixed target capability is considered necessary to explore the full range of possibilities of nuclear phase transitions involving rearrangements of the quarks present in the target and/or projectile as opposed to conglomerates of created quarks. In addition the region up to 20 GeV/amu covers a range of interesting particle creation thresholds. Thirdly, the lower end of the fixed-target range, below a few hundred MeV/amu, is the natural region for evolution of programs at the 88 Inch Cyclotron and the SuperHILAC. The committee considered that in view of the variety of the interesting phenomena to be anticipated in the region of 10-40 MeV/amu and the presence in that region of significant energies such as the Fermi energy and the energy corresponding to the velocity of sound in nuclear matter, it would be desirable to extend the lowest energy of the accelerator down to 10 MeV/amu if possible.

On the technical side, the committee examined some of the practical desirabilities for the accelerator. The flexibility of the design for multiple beams and independent variation of them was much appreciated, and it was concluded that three independent fixed-target beams should be simultaneously operable, and three intersection regions for the colliding beam capability. However, the fact that the colliding beams and fixed target operation are mutually exclusive in this design is a disadvantage for the low energy segment of the research program. To address this problem, and also the above mentioned desirability of extending the energy range downwards, futher designs are being investigated, including boosters, subsidiary rings, and the existing LBL accelerators in a variety of configurations. Current objectives are listed in Table 1.

PROSPECTS

In July-August 1979 the DOE/NSF Nuclear Science Advisory Committee, chaired by Professor Herman Feshbach, held a major long range planning study and projected national construction and operating budgets for the coming decade. The Advisory Committee stated that $100 million

Table 1. Current objectives for VENUS design.

Fixed target mode	10 MeV/amu to 20 GeV/amu: 3 beams independently variable in ion, energy, duty factor, and intensity.
Colliding beam mode	2 GeV/amu to 20 GeV/amu (1 TeV/amu fixed target equivalent): 3 intersection regions.
Proton capability	50 GeV fixed target or colliding beam (5 TeV/amu fixed target equivalent)

projects such as VENUS, or a kaon-antiproton facility, would require funds supplemental to those projected for the national base program, and would have to "be justified separately as required by important national goals, requiring special constructon allocations, and ... substantial (additional) operating costs." The Advisory Committee recommended that research and development be conducted on such facilities, noting, "It is essential in all these cases that the R&D is not confined only to accelerator and other technical developments. A serious investigation into the scientific case ... must be mounted .... Scientfic feasibility, that is, the demonstration that one will be able to obtain results, is equally essential."

These considerations form the basis of current LBL planning for VENUS. We look foward to adoption by the government of the Advisory Committee's Long Range Plan and to the opportunity to compete for the supplementary construction funds that would be needed.

PART 2. PROGRESS REPORTS

I. EXPERIMENTAL RESEARCH

A. NUCLEAR STRUCTURE

NUCLEI AT HIGH ANGULAR MOMENTUM*

R. M. Diamond and F. S. Stephens

Nuclei have some of the classical properties of liquid drops, as attested by the success of the liquid-drop model, but are finite quantal systems. This imposes certain restrictions on their rotation. In addition, there is a competition between the single-particle motion and a collective rotation to carry angular momentum most efficiently. This interplay becomes increasingly important at high spin where a compromise between the two limiting situations appears to occur. That is, at lower spins we may observe in well-deformed nuclei relatively pure collective rotation that follows the geometrical relationships very well, or we may find in nuclei near closed shells that the shell model does an excellent job in explaining states up to several MeV in excitation and carrying tens of units of angular momentum. But at spins above ~40 $\hbar$, nuclei seem to have some characteristics from each of these limiting cases, and it is of interest to understand this compromise.

An important nuclear parameter whose behavior it is necessary to understand is the moment of inertia. The cranking-model calculations of Inglis give the rigid-body value, which is 2-3 times too large for the ground-states of real nuclei. Now it is understood that this is mainly due to the neglect of the pairing correlations. With an increase in spin, these correlations are reduced (Coriolis anti-pairing), leading to a rise in the moment of inertia towards the rigid-body value. The suddent increase in the moment of inertia observed in some rare-earth nuclei between spins 14-20 $\hbar$ (backbending) in 1971 is now recognized to be due usually to the crossing of the ground band by an excited band with two unpaired but aligned high-j particles. The aligned single-particle angular momentum allows the collective spin of this band to be reduced over that of the ground band for the same total angular momentum. In fact, this sharing of angular momentum between the collective and single-particle motions appears to be the most efficient way of carrying angular momentum in deformed nuclei above spins of around 20 $\hbar$; at still higher spin, bands with still more aligned particles appear to become lowest in energy. For some nuclei, theory predicts that there should be a very marked backbend above spin 50-60 $\hbar$ caused partly by the rapid stretching of nuclei at these spins, as suggested by the liquid-drop model, and partly by the large shell effect at such spins favoring a prolate nucleus with axes in the ratio of 2:1.

A new technique for studying high-spin states involves determining the γ-ray energy correlations obtained with pairs of γ-ray detectors. The resulting γ-γ correlation diagrams or contour plots, after subtraction of the uncorrelated events (mainly Compton-scattered events in one or both detectors) show structure extending well above transition energies of 1 MeV. In well-deformed nuclei there is a valley along the diagonal, corresponding to the fact that in a pure rotational nucleus each transition has a different energy and spin. In rare-earth nuclei the first backband shows up clearly as a bridge across the valley at 500-600 keV, and there is evidence for a second one at higher energy, and then more bridges at still higher energies. It is clear that a whole new spectroscopy of high-spin states is developing.

*Condensed from Ann. Rev. Part. Sci. 30, 85 (1980).

CORRELATION STUDIES OF ROTATIONAL BEHAVIOR AT VERY HIGH ANGULAR MOMENTUM*

M. A. Deleplanque, F. S. Stephens, O. Andersen, J. D. Garrett, B. Herskind

R. M. Diamond, C. Ellegaard, D. B. Fossan, D. L. Hillis, H. Kluge, M. Neiman, C. P. Roulet, S. Shih,

and R. S. Simon

Nuclear structure studies, based on the analysis of γ-rays, are limited at the present time to spins below ~ 70 $\hbar$ in the mass region around A=160, since for higher spins the compound nucleus fission prior to γ-ray emission. For the deformed rare earth region, detailed spectroscopic measurements extend now up to a spin 30 $\hbar$, above which the γ-ray spectrum can no longer be resolved. Many measurements have shown that this "continuum" γ-ray spectrum consists of an exponentially decreasing high-energy tail composed of statistical γ-rays which cool the nucleus toward the yrast line, and a lower-energy bump extending up to 1.5-1.8

MeV depending on the nucleus. This bump is formed by "yrast-like" γ-rays which deexcite the nucleus through many pathways roughly parallel to the yrast line, and which remove the angular momentum of the system. This yrast-like cascade contains nuclear structure information, and in deformed nuclei, it is dominated by stretched E2 rotational transitions, whose energies are correlated. The correlations can be studied in some detail, even in an unresolved spectrum, by a method which isolates correlated events from an uncorrelated background. Although these events cannot isolate individual rotational bands, they are sensitive to certain features, in particular the single-particle angular-momentum alignment, shared by many bands.

The measurement was performed at the 88 Inch Cyclotron. It consisted essentially of γ-γ coincidences, but four Ge(Li) detectors were used simultaneously, which gave six times the coincidence rate of one pair.

We have studied the deexcitation of the ^{164}Er compound system from the reaction of ^{124}Sn + ^{40}Ar at 185 MeV ^{40}Ar energy. A background of "uncorrelated" events was subtracted from the γ-γ matrix of 40 million events.

A contour plot of the correlated two-dimensional coincidence spectrum is shown in Fig. 1. It is symmetric about the 45° diagonal because the two independent halves of the ΔN_{ij} matrix have been added to improve the statistics. In the low-energy region (up to E ≈ 1 MeV), there is an absence of counts along the diagonal, which produces a valley. This valley reflects the absence of γ-ray transitions having the same energy, which is a property of a rotational band with a constant moment-of-inertia. Fig. 1 shows that the valley can be

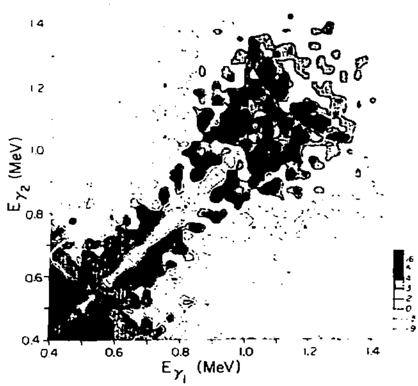

Fig. 1. Correlated γ-ray spectrum. The contour levels are statistically significant up to ~ 1.2 MeV along the diagonal. (XBL 803-481)

seen up to 1250 keV, although it is largely filled beyond about 1 MeV and even completely in some locations.

The width of this valley measures a "collective" moment-of-inertia, $\mathcal{I}$, and can be combined with $\mathcal{I}_{eff}$ to determine the aligned angular momentum, j_a. Previous measurements of moment-of-inertia at high spins have always measured $\mathcal{I}_{eff}$ and found it to be near the rigid-body value. It appears that $\mathcal{I}_c$ must be significantly lower if j_a is large, which simply reflects the fact that single particles cannot contribute fully both to the aligned angular momentum and to the collective moment-of-inertia. Data of the present type are not easy to interpret quantitatively along this line, but seem generally consistent with these ideas.

The observed filling of the valley in the high energy region (>1 MeV) probably implies many band crossings. It is clear from Fig. 1 that there are irregularities in the valley ("bridges") and also along the ridges ("gaps"). There are only a limited number of these, at least discernable within the present statistics. In the lower spin region, the bridges correspond to known band crossings. This has been established from the detailed spectroscopic studies of many nuclei in this region. These band crossings occur at specific rotational frequencies ($\hbar\omega = E_\gamma/2$) which depend, in a given nucleus, only on which orbitals are crossing. A given orbital crossing can occur in many bands differing in the rest of the configuration, and thus produce a feature in the correlation spectrum even though one cannot resolve individual bands. For example, the known first backbend in the ^{160}Er region (at $\hbar\omega \approx 0.3$ MeV) corresponds to the crossing of a 2-quasi-particle $i_{13/2}$ neutron state with the vacuum (ground band), and the second backbend (at $\hbar\omega \approx 0.41$ MeV) involves a 2-quasi-particle $h_{11/2}$ proton configuration crossing the vacuum. Both of these crossings can be involved in many bands and produce readily observable bridges in Fig. 1 at E_γ = 0.6 and 0.82 MeV, respectively.

In the high energy region (where pairing correlations probably no longer exist) one expects crossings with large angular momentum transfer due to only a few strongly aligned configurations based on the high-j orbitals. If these configurations are filled at high rotational frequencies, they will experience a band crossing (as the frequency decreases during the deexcitation of the nucleus) and empty at a characteristics orbital-crossing frequency irrespective of the rest of the state configuration. We propose that these characteristic frequencies are related to those where the few bridges and gaps are observed in Fig. 1.

Footnote and References

*Condensed from Phys. Rev. Lett. 45, 172 (1980).

1. O. Andersen, J. D. Garrett, G. B. Hagemann, B. Herskind, D. L. Hillis, and L. L. Riedinger, Phys. Rev. Lett. 43, 687 (1979).

LINEAR POLARIZATION AND ANGULAR CORRELATION OF CONTINUUM γ-RAYS

H. Hubel,* R. M. Diamond, F. S. Stephens, B. Herskind,† and R. Bauer†

The investigation of very high spin states ($I \approx 30$-70) involves studies of continuum γ-ray spectra emitted in heavy-ion compound-nucleus reactions. If sufficient angular momentum is brought into the nucleus there exists a broad structure in the spectra around ~ 1.2 MeV (the "yrast bump") which is mainly composed of highly collective stretched E2 transitions. At higher energies where the spectrum falls exponentially with energy (the statistical cascade) the radiation is probably mainly stretched and non-stretched E1. At energies below the E2-bump there appears a dipole component which varies in intensity depending on the properties of the particular system. An important question is whether this dipole contribution to the continuum spectrum is mainly electric or magnetic in character. If M1 it probably originates in collective phenomena, whereas E1's would likely indicate statistical processes.

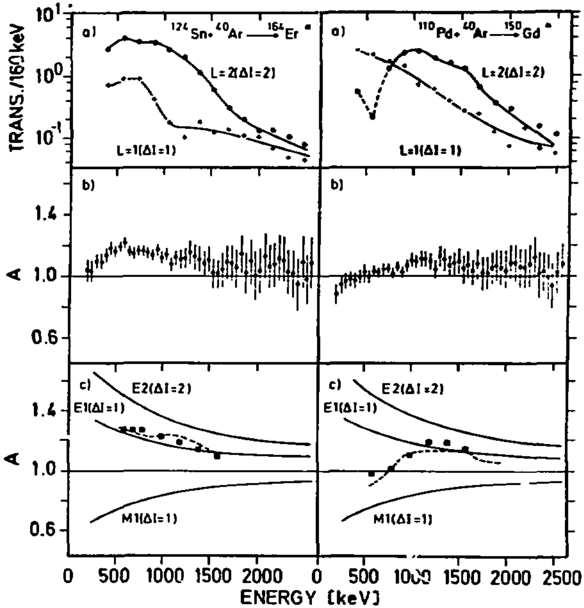

Fig. 1. (a) Multipole spectra for stretched quadrupole and dipole components from angular correlation measurements.

(b) Linear polarization asymmetry double ratios $A = \frac{N\perp(90°)}{N\parallel(90°)} / \frac{N\perp(0°)}{N\parallel(0°)}$ from measurements at $\theta = 90°$ and $0°$ to the beam direction (direct experimental points). (c) Linear polarization asymmetry double ratios A after unfolding (■), and calculations for pure stretched M1, E1, and E2 (solid curves) and for a mixture of the E2 and M1 components of the decay (dashed curve) with the L = 2 and L = 1 amounts taken from the upper part of the figure. (XBL 807-10661)

We have measured the angular correlation and the linear polarization of continuum γ-rays in two ^{40}Ar induced reactions. They were $^{110}Pd + {}^{40}Ar \rightarrow {}^{150}Gd^*$ and $^{124}Sn + {}^{40}Ar \rightarrow {}^{164}Er^*$ done with 170 MeV ^{40}Ar beams from the LBL 88 Inch Cyclotron. The experimental results of the linear polarization experiment are shown in the center part of Fig. 1. For each 50 keV interval the double ratio $A = \frac{N\perp(90°)}{N\parallel(90°)} / \frac{N\perp(0°)}{N\parallel(0°)}$ of the vertical ($N\perp$) and horizontal ($N\parallel$) coincidence counting rates measured at θ = 90° and 0° to the beam is plotted.

For a number of reasons we have restricted the further analysis to stretched dipole and E2 transitions, and have considered pure transitions only; the results from the angular correlation experiments are shown in the upper part of Fig. 1. Below ~ 1.5 MeV, the spectrum of the $^{164}Er^*$ compound system consists of 80-90% quadrupole transitions. For the $^{150}Gd^*$ compound system there is ~ 80% quadrupole radiation in the bump at 1.5 MeV; at lower energies, however, the dipole transitions become more prominent, even dominant (85% L = 1 at 0.5 MeV). The amounts of stretched dipole and quadrupole radiation were then used in the analysis of the linear polarization experiments to determine the electric or magnetic character of the dipole component. The result is that it appears to be predominantly M1 between 1.6 and 0.5 MeV, and likely at still lower energies. The dashed curves in the lower part of Fig. 2 are the linear polarization asym- metry ratios calculated under the assumption of 100% M1 for the dipole component in the spectrum.

Our angular corrleation and linear polarization data, as well as those of Vivien et al.[1] and Trautmann et al.,[2] show that the main features of the investigated cases are thefollowing: (1) The dominant fraction -- between 50% (for nuclei near closed shells) and 80% for deformed nuclei -- of the radiation consists of stretched E2 transitions. This component reaches 90% in the region of the E2 bump for deformed nuclei.

(2) The remaining part of the radiation at low energies and up to the E2 bump is composed of stretched M1 transitions in good rotors, and is predominatly M1 with some E1 transitions admixed in nuclei near closed shell.

Footnotes and References

*Institute für Strahlen- und Kernphysik, Universität Bonn, D-5300 Bonn.

†The Niels Bohr Institute, Copenhagen, Denmark

1. J.P. Vivien, Y. Schulz, F.A. Beck, E. Bozek, T. Byrski, G. Gehringer, and J.C. Merdinger, Phys. Letters 85B, 325 (1979).

2. W. Trautmann, J.F. Sharpey-Schafer, H.R. Andrews, B. Haas, O. Häusser, P. Taras, and D. Ward, Phys. Rev. Letters 43, 991 (1979).

THE DIPOLE COMPONENT IN THE YRAST CASCADE AND THE MULTIPLICITY OF STATISTICAL γ RAYS*

S. H. Sie, R. M. Diamond, J. O. Newton and J. R. Leigh

It had been observed that for $E_\gamma \lesssim 0.4$ MeV, the nature of the continuum γ rays in a number of deformed nuclei changed from being predominantly stretched E2 to predominantly dipole. The principal objective of the present measurements was to further study this dipole component. The reactions used were $^{149}Sm(^{16}O,3n)^{162}Yb$, $^{150}Sm(^{16}O,4n)^{163}Yb$, $^{154}Sm(^{16}O,4n)^{166}Yb$, $^{122}Sn(^{16}O,4n)^{124}Ce$ and $^{110}Pd(^{16}O,4n)^{122}Xe$ induced by ^{16}O beams from the 14 UD Pelletron at the ANU. The γ rays were detected in a movable 7.6 x 7.6 cm NaI(Tl) or Ge(Li) detector in coincidence with a fixed Ge(Li) detector. The movable detectors were set alternately at 0° and 90° with respect to the beam direction. The unfolded continuum γ-ray spectra are shown in Fig. 1. In the summed spectra (0° + 2 x 90°), which are essentially proportional to the isotropic spectra, the main features of the continuum cascades can be readily seen, namely, the exponentially falling statistical tail and the yrast bump.

The number of γ rays with $E_\gamma > 1.9$ MeV is related to the number of statistical γ rays, though the actual relationship depends on the shape of the spectrum below 1.9 MeV. This quantity is shown plotted against $\bar{M}_T$ in Fig. 2, where it is apparent that there is a correlation between $\bar{M}_T$ and $\bar{M}(>1.9)$; for each reaction the latter quantity increases with $\bar{M}_T$.

The quantity $2[N(E_\gamma)_{0°} - N(E_\gamma)_{90°}]$ is proportional to the value of A_2 and is shown for the various cases in Fig. 1. Data obtained at the higher bombarding energy show in all cases a pronounced bump with positive A_2, attributable to the yrast cascade. For the strongly deformed Yb nuclei this bump has A_2 0.25, in accordance with the value expected for the stretched E2 transitions thought to constitute the main part of the yrast cascade for such nuclei.

All the cases also show a smaller bump at lower energies than the main quadrupole bump and separated from it by a small dip. This bump has a negative A_2 and thus is probably a dipole component.

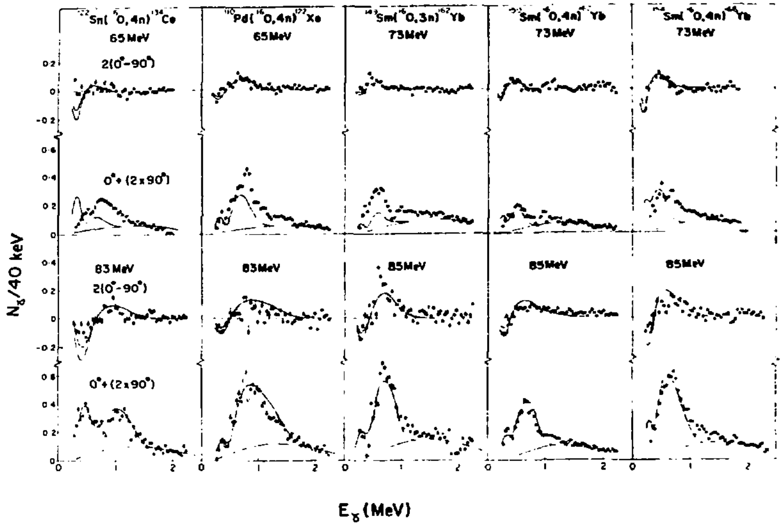

Fig. 1. Angle-integrated γ-ray spectra obtained by unfolding the continuum pulse-height spectra are shown in the lower parts of the figure. The curves were calculated from the model described in the text. A function $E^3e^{-E_\gamma/T}$ was assumed for the shape of the statistical spectrum. The upper parts of the figure show the 2(0°-90°) spectra which, when normalized, approximate the A_2 coefficients of the angular correlations. The calculated lines correspond to A_2 = -0.6 and -0.4 for the "dipole" component and A_2 = 0.25 for the quadrupole components.
(XBL 807-10662)

The spectra in Fig. 1 can be discussed in terms of a simple model[1] in which the yrast cascade is assumed to originate from decay through collective rotational bands roughly parallel to the yrast line. This cascade is approximated by decay through a single "average" deformation-aligned band, and the dipole component arises from the I → I - 1 transitions. The relative intensities of these to the cross-over transitions and the E2/M1 amplitude mixing ratios δ are proportional to $(g_K - g_R)^2K^2/Q_0$ and $Q_0/(g_K - g_R)$, respectively. The results of the calculations are shown by the full lines in Fig. 1.

In summary it can be said that a component with negative A_2, and hence presumably dipole, with average E about half of that for the main yrast bump, does occur in all four final nuclei, even though two are only weakly deformed and possibly triaxial. It suggests that the low-energy dipole component may be a fairly general phenomenon since it has now been observed in Xe, Ce, Yb and W nuclei. The realtive magnitudes of the dipole and quadrupole components of the yrast cascade do appear to vary from case to case, which suggests that nuclear structure information on the states well above the yrast line may be derived from their study.

The measurements also suggest that the multiplicity of the statistical cascade $\bar{M}_S$ increases with increasing angular momentum input (Fig. 2). This can be explained as arising from a corresponding increase in average excitation energy for gamma emission above the yrast line, and calculations with the evaporation code GROGI2 do show agreement with this expectation. The change in the number of statistical γ rays with increasing bombarding energy or angular momentum input depends on the relative rate of increase of the excitation energy and the yrast line with spin; the results might be different in a light nucleus.

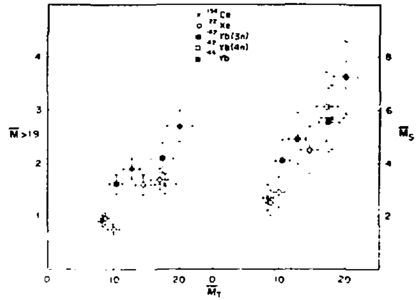

Fig. 2. The number of a) γ rays with $E_\gamma > 1.9$ MeV b) statistical gamma rays $\bar{M}_S$ estimated with the function assumed plotted in Fig. 1 against the total multiplicity $\bar{M}_T$. (XBL 807-10663)

Footnote and Reference

*Work performed at the Department of Nuclear Physics, the Australian National University, Canberra, ACT 2600, Australia.

1. J.O. Newton, S.H. Sie and G. D. Dracoulis, Phys. Rev. Lett. 40, 625 (1978).

E1 TRANSITION PROBABILITIES FROM $K^\pi = 0^-$ AND $K^\pi = 1^-$ OF ^{238}Pu*

C. Michael Lederer

An experimental study of ^{238}Np β^- decay and ^{242}Cm α decay has revealed previously unobserved transitions, established new multipolarity assignments and mixing ratios based on measured internal conversion coefficients, and improved the accuracy of the relative γ-ray intensities. Much of the information on ^{242}Cm α decay is new; the α-decay hindrance factors and conclusions based on them will be reported elsewhere.

A new method is developed for analysis of the γ-ray branching from the $K^\pi = 1^-$ band, in which the interband E2 transition rates to the $K^\pi = 0^-$ band are calculated from a mixing model and used to estimate the rates of competing E1 transitions. The model also yields estimated E1 transition rates from the $K^\pi = 0^-$ band. In ^{238}Pu, E1 transitions to the ground state from either octupole-vibrational band have half-lives on the order of 5 ps, corresponding to hindrance factors around 10^4. Although the required data are absent or less precise for other heavy nuclei, estimates can be made for five of them including ^{236}U, for which the model agrees with a direct *measurement of highly retarded E1 transition* probabilities from the 0^- band. Table 1 summarizes the results of the calculations. A description of them and a discussion of the limitations of the model are included in the full paper.

Table 1. Estimated E1 transition probabilities from octupole-vibrational states of heavy nuclei.

Nucleus	Weisskopf Hindrance Factor $\Delta K = 0$	$\Delta K = 1$
^{224}Ra	2×10^4 [a]	
^{230}Th	4×10^3	9×10^3 [b]
^{236}U	4.5×10^7	3.1×10^6 [c]
	2.2×10^7 [d]	
^{238}U	$\simeq 10^5$	$\simeq 10^7$ [e]
^{238}Pu	1.5×10^4	4.3×10^4

[a] By direct comparison with intraband E2 transitions.
[b] Geometric mean of 17×10^3 for the $K I^\pi = 11^-$ state, 4.5×10^3 for the 12^- state.
[c] For the 11^- state. γ-ray branching from the 13^- state is inconsistent with the model.
[d] From the measured half-life for the 01^- state (2).
[e] Approximate value; branching from the 11^-, 12^-, and 13^- states yield values that vary by two
orders of magnitude. (The data for ^{238}U are suspect.)

Footnote and References

* Condensed from reference (1).

1. C. Michael Lederer, to be submitted to Phys. Rev. (1982).

2. C. M. Lederer, J.M. Jaklevic, and S.G. Prussin, Nucl. Phys. A135, 36 (1969).

OBSERVATION OF THE DECAY OF THE $T_z = -2$ NUCLEUS ^{36}Ca†

M. D. Cable, J. Äystö,†† R. F. Parry, J. M. Wouters, and J. Cerny

The β^+-delayed proton decay of ^{36}Ca has been observed. From the energy of the proton group, it was possible to deduce the mass of the lowest T =2 excited state in ^{36}K (See Fig. 1). Measurement of this mass completed the mass 36 isospin quintet.

The masses of analog states in an isospin multiplet are given in first order by:

$$M(A,T,T_z) = a(A,T) + b(A,T)T_z + c(A,T)T_z^2$$

This Isobaric Multiplet Mass Equation (IMME) arises via first order perturbation theory from the assumptions that the wave functions of the members of an isospin multiplet are identical and that only two body forces are responsible for charge dependent effects in nuclei. Possible deviations from this quadratic form can be due to higher order Coulomb or other charge dependent effects as well as to various isospin mixing effects. These deviations are generally represented by the additional terms $d(A,T) \cdot T_z^3$ and $e(A,T) \cdot T_z^4$ and can only be studied with isospin multiplets having $T \geq 3/2$.

In general, extensive studies of isospin quartets and more recently quintets, have shown excellent agreement with the quadratic form of the IMME. Persistent deviations have been observed, however, in the mass 8 and mass 9 multiplets. These multiplets have members which are unbound to particle decay, so it is of interest to study higher mass multiplets in which all members are bound to isospin-allowed particle decay. The mass 36 quintet is, to date, the highest mass quintet that has been completed.

^{36}Ca was produced with the ^{40}Ca(^{3}He,α3n)^{36}Ca reaction at 95 MeV. Because of the simultaneous production of other strong β^+-delayed proton emitters, the on-line mass separator, RAMA, was used to isolate the mass 36 nuclei from the other reaction products. The ^{36}Ca experiment was made exceptionally difficult both by the expected low yield of the reaction and by possible interference by β^+ delayed protons from ^{36}K. Fortunately, a detailed study of ^{36}K by Eskola et al.[1] was available. With the RAMA ion source operating in a mode that enhanced alkali metal production, the ^{36}K groups were observed. Operation of the ion source in a mode that enchanced Ca ionization produced a new group that was not observed in the ^{36}K studies. This group, at an energy of

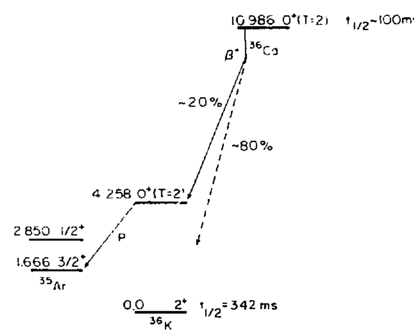

Fig. 1. A proposed decay scheme for ^{36}Ca.
(XBL 793-910)

Table 1. Properties of the A = 36 isobaric quintet and coefficients of the IMME.

Nucleus	T_z	Mass excess [MeV]	Ex [MeV]
^{36}Ca	-2	- 6.440 ± 0.040	0
^{36}K	-1	-13.168 ± 0.022	4.258 ± 0.023
^{36}Ar	0	-19.3795 ± 0.0022	10.8518 ± 0.0022
^{36}Cl	+1	-25.2229 ± 0.0013	4.2989 ± 0.0013
^{36}S	+2	-30.6659 ± 0.0015	0

Coefficients for the IMME: $M = a + b \cdot T_z + c \cdot T_z^2 + d \cdot T_z^3 + e \cdot T_z^4$

a	b	c	d	e	χ_ν^2 (a)
-19.3795(20)	-6.0437(37)	0.2003(16)	--	--	1.90
-19.3801(22)	-6.0446(40)	0.2030(46)	-0.0011(17)	--	3.42
-19.3795(22)	-6.0434(74)	0.1997(92)	--	0.0001(14)	3.80
-19.3795(22)	-6.018(15)	0.177(15)	-0.0097(50)	0.0075(41)	--

(a) Reduced $\chi_\nu^2 = \chi^2/\nu$.

2519 21 ke' , we attribute to the super-allowed β^+ decay of the 0^+, T = 2 ground state of ^{36}Ca to the 0^+, T = 2 state in its daughter, followed by proton emission. This energy, together with the mass of ^{35}Ar, yields a value of -13,168 22 keV for the mass excess of the T = 2 state in ^{36}K.

Table 1 shows the results of fitting the mass 36 data with possible forms of the IMME. The best fit to the data is seen to be the quadratic IMME. Four parameter fits result in a d or e coefficent consistent with zero. More precise measurements of the ^{36}Ca and ^{36}K points are necessary to determine any possible significance of the non-zero d and e coefficients found in the five paramenter fit.

Footnotes and Reference

†Condensed from LBL-11193.
††Present address: University of Jyväskylä, Finland.

1. K. Eskola, M. Rihonen, K. Vierinen, J. Honkanen, M. Kortelahti and K. Valli, Res. Rept. HU-P-177, Department of Physics, Univ. of Helsinki, Finland; to be published in Nucl. Phys. 1980.

BETA ENDPOINT MEASUREMENTS OF ^{105}In AND ^{103}In

J. Wouters, J. Aysto,† M. Cable, P. Haustein,‡ R. Parry and J. Cerny

In a continuing series of experiments[1] to determine beta endpoints we have now measured the beta endpoint of ^{105}In and ^{103}In. The ^{105}In beta endpoint of 3.88 ± 0.150 MeV is a new measurement while that of ^{103}In, 4.08 ± 0.250 MeV is a corroboration of a previous measurement by G. Lhersonneau et al.[2] Comparison of these measurements with the various mass formula predictions enables the observation of any effects on the mass surface due to the nearby double shell closure.

The beta endpoint measurements were conducted using the RAMA mass separator system together with standard β^+-γ coincidence techniques for data collection. Preliminary

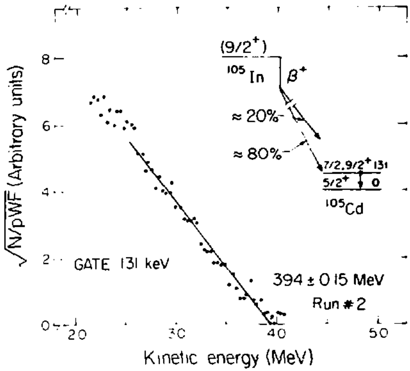

Fig. 1. Fermi Kurie plot and partial decay scheme for ^{105}In. Beta-branching ratios were determined from the γ-spectrum in coincidence with positrons. (XBL 799-2801)

results, including a detailed description of the techniques used, were reported at the 6th International Conference on Atomic Masses and Fundamental Constants.[3] We have since repeated the experiments with the following refinements. The beta-telescope was calibrated with the endpoints of the strongest allowed decay branches of ^{123}Cs (3.410 ± 0.122 MeV), and ^{124}Cs (4.574 ± 0.150 MeV) produced in ^{14}N on Cd at 110 MeV, and ^{80}Rb (4.069 ± 0.025 MeV), ^{79}Rb (1.837 ± 0.041 MeV), and ^{78}Rb (3.41 ± 0.37 MeV) produced in ^{14}N on Zn at 150 MeV. ^{105}In and ^{103}In were produced by bombarding 1 mg/cm^2 natural Mo and separated ^{92}Mo targets, respectively, with 110 MeV ^{14}N ions. The data were collected using hardwire coincidences between the beta-telescope detectors and the gamma detector and analyzed using software gates on known γ-rays of the daughter nucleus to project out a single component beta spectrum.

The resulting beta spectra were anlayzed two ways. The spectra were plotted in Fermi-Kurie form using a computer code that also corrects for the response function of the beta detector. Linear least squares fits of the resulting spectrum determined the endpoints (See Fig. 1). Secondly the spectra were analyzed using the shape function fitting technique of Davids et al.[4]

A summary of our measurements and the mass excesses of ^{105}In and ^{103}In are presented in Table 1. Deviations of the experimental values from a semiempirical shell model formula by Liran and Zeldes, and from a Garvey-Kelson transverse equation are given[5] for comparison. In the main, these predicted masses agree fairly well with the experimental measurements. An interesting disagreement of -1.0 MeV of the ^{103}In mass excess from the Liran-Zeldes calculations is inconsistent with the good agreement of their approach in predicting the other experimentally known In mass excesses. Further systematic studies are required to understand both this behavior and whether it might have any possible relationship with the nearby double shell closure.

Table 1. Summary of Q_{EC} determinations and comparison to different mass predictions.

Nuclide	Decay Energy [MeV] This work	Decay Energy [MeV] Literature	Mass excess [MeV]	Δ=Me(Exp) - Me(theory)[5] [MeV] L-Z	Δ=Me(Exp) - Me(theory)[5] [MeV] G-K
^{103}In	5.56±0.35	5.8±0.5[2]	-75.04±0.38	-1.00	-0.61
^{105}In	5.12±0.130		-79,22±0.13	0.24	0.55

Footnotes and References

†Permanent address: University of Jyvaskyla, Finland.

‡Permanent address: Brookhaven National Laboratory, Upton, NY.

1. Nuclear Science Division Annual Report for 1978-1979, LBL-9711, p. 21.

2. G. Lhersonneau, G. Dumont, K. Cornelis, M. Huyse, and J. Verplancke, Phys. Rev. C 18, 2688 (1978).

3. J. Cerny et. al., Lawrence Berkeley Laboratory preprint LBL-9876.

4. C. N. Davids, C. A. Guliardi, M. J. Murphy, and E. B. Norman, Phys. Rev. C 19, 1463 (1979).

5. S. Liran and N. Zeldes, At. Data and Nucl. Data Tables 17 (1976) 431; J. Janecke, ibid. 17 (1976) 455.

B. NUCLEAR REACTIONS AND SCATTERING

1. Microscopic

TEST OF PARITY CONSERVATION IN pp SCATTERING AT 46 MeV*

P. von Rossen,* U. von Rossen,* and H. E. Conzett

It has been calculated[1] that the parity non-conserving weak-interaction part of the nucleon-nucleon interaction should result in a non-zero value of the longitudinal analyzing-power A_z in p-p scattering. A_z is given by

$$A_z = (1/P_z)(\sigma^+ - \sigma^-)/(\sigma^+ + \sigma^-)$$

where p_z is the beam polarization and $\sigma^+(\sigma^-)$ is the cross section for incident protons of positive (negative) helicity. The calculations predict A_z to have a broad maximum near 50 MeV with a value of at most a few times 10^{-7}. Thus, extreme care and precision are required in order to reduce the experimental error to such a level.

The present experiment is done with a 50-MeV polarized proton beam from the 88 Inch Cyclotron. Since the polarization direction is provided by the magnetic field, the beam from the cyclotron has only transverse (vertical) polarization. As shown in Fig. 1, a solenoidal

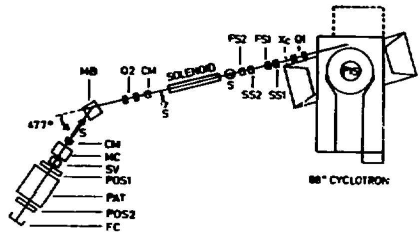

Fig. 1. The beam line and the experimental set-up. Q, quadrupole magnets; FS, fast steering magnets; SS, slow steering magnets; CM, centering magnets; MB, bending magnet; MC, monitor chamber; POS, beam position sensors; PAT, target-detector assembly. (XBL 8011-3901)

Table I. Summary of errors and results.

Systematic effect	Value	Contribution to error in $p_z A_z$ $(\times 10^7)$
(1) Intensity modulation $(I^+ - I^-)/(I^+ + I^-)$	$-1.3(3) \times 10^{-7}$	0.2[a]
(2) Position modulation $\langle x_1^+ - x_1^- \rangle$	$-0.03(4) \times 10^{-2}\mu m$	0.2
$\langle y_1^+ - y_1^- \rangle$	$-0.2(1) \times 10^{-2}\mu m$	0.2
$\langle x_2^+ - x_2^- \rangle$	$0.4(2) \times 10^{-2}\mu m$	0.2
$\langle y_2^+ - y_2^- \rangle$	$1.6(4) \times 10^{-2}\mu m$	0.2
(3) Emittance modulation $\delta Q/Q$	$\sim 10^{-5}$	0.5
(4) Transverse polarization components		1.0
(5) Electronic asymmetry		0.3

measured $|p_z| A_z$ with statistical error $(-1.0 \pm 1.2) \times 10^{-7}$
$|p_z| A_z$ with combined errors $(-1.0 \pm 1.8) \times 10^{-7}$

[a]Includes estimate for β-decay asymmetry.

magnetic field is used to precess the spin axis 90° into the horizontal plane, after which a dipole magnet bends the beam through an angle of 47.7° and precesses the spin axis into the beam direction. Thus, spin-reversal at the ion source results in proton helicity reversal at the target.

Since integrated scattering rates of 10^9 to 10^{10} per second are obtainable, it is not difficult to achieve a statistical accuracy at the level of 10^{-7}. The severe challenge is to reduce the systematic effects, which provide false asymmetries, to a comparable level. The systematic errors arise from coherent changes of the beam properties with spin reversal. Two beam-position sensing elements, consisting of secondary electron monitors in a quadrant geometry, are used both to monitor and control the beam in position and angle through the target. Improvements have been made on the polarized ion source and on the cyclotron in order to minimize instabilities which affect the ultimate accuracy obtainable with our experimental apparatus.

In contrast with the approach used by the Zurich group,[2] our design is to control the coherent beam modulations to such an extent that the remaining effects are not influencing the measured asymmetry in a signficant way. The success of this apprach is seen in Table 1, where our coherent beam position and intensity modulation amplitudes are two to three orders of magnitude smaller than those of Ref. 2.

Our present results, which are summarized in Table 1, were achieved in 3-4 days of data acquisition. The measured asymmetry is

$$\epsilon = |p_z|A_z = (-1 \pm 1.8) \times 10^{-7},$$

which, with a value of p_z = 0.80 gives the result

$$A_z = (-1.3 \pm 2.3) \times 10^{-7}$$

The listed error is the root square sum of the statistical and systematic errors. The main contributions to total error are the statistical error and the systematic error due to transverse polarization components. These both can be reduced substantially when a new ionizer for the polarized ion source is installed in a few months. A factor of ten increase in the polarized beam intensity is anticipated.

Footnotes and References

*Condensed from LBL-11122. Presented at the 5th International Symposium on Polarization Phenomena in Nuclear Physics, Santa Fe, NM, August 11-15, 1980.

†Present address: Institute of Nuclear Physics, University of Bonn, D-5300 Bonn, West Germany.

1. M. Simonius, Phys. Lett. 41B, 415 (1972); Nucl. Phys. A220, 269 (1974). V. R. Brown, E. M. Henley, and F. R. Krejs, Phys. Rev. C 9, 935 (1974).

2. R. Balzer et al, Phys. Rev. Lett. 44, 699 (1980).

CONCERNING TESTS OF TIME REVERSAL INVARIANCE VIA THE POLARIZATION-ANALYZING POWER EQUALITY*

Homer E. Conzett

It has long been established that time reversal invariance (TRI) is a sufficient condition for the general polarization-analyzing power equality.[1] That is, the polarization (P) of an outgoing particle from a (binary) nuclear reaction is equal to the analyzing-power (A) for those polarized particles incident in the inverse reaction. Since elastic scattering is its own inverse process, it has been used in essentially all of the tests of TRI that use the polarization-analyzing power equality.

In particular, the most sensitive test by this method was made on p + ^{13}C elastic scattering.[2] It is necessary to scatter from a nucleus with a non-zero spin value, because otherwise parity conservation alone ensures that P = A. By making the measurements for ^{13}C relative to ^{12}C, it was not necessary to measure either the absolute beam polarization or the absolute analyzing power, and the result that P = A to ± 2.5% was achieved.

As is shown in Ref. 2, the P-A difference is given by

$$P(\theta) - A(\theta) = (\sigma^{-+}(\theta) - \sigma^{+-}(\theta))/\sigma(\theta) \qquad (1)$$

where

$$\sigma(\theta) = (\sigma^{++}(\theta) + \sigma^{+-}(\theta) + \sigma^{-+}(\theta) + \sigma^{--}(\theta))/2$$

and $\sigma^{-+}(\theta)$ is the cross section for the scattering of a proton from an initial negative spin state to a final positive spin state. Using the Madison convention,[3] the positive (+y) direction is up for a proton scattered to the left in the horizontal plane. Since the time-reversed process of $\sigma^{-+}(\theta)$ is $\sigma(\theta)^{+-}$, eq. (1) becomes $P(\theta) - A(\theta) = 0$ if the strong interaction is invariant under time reversal. Thus, the ref. 2 result for the elastic scattering of 32.9-MeV protons from ^{13}C at θ_L = 60° was interpreted as satisfying TRI within the ± 2.5% accuracy of the experiment.

It is clear, however, from eq. (1) that another reason for $P(\theta) - A(\theta) \approx 0$ could be the very small values of the individual spin-flip probabilities, even if they were not equal as required by TRI. And, it is now known from measurements of the depolarization in elastic p-nucleus scattering that this is, indeed, the case.[4] Since the depolarization parameter is given by

$$D(\theta) = 1 - 2S(\theta) \tag{2}$$

with the (total) spin-flip probability

$$S(\theta) = (\sigma^{+-}(\theta)+\sigma^{-+}(\theta)/2\sigma(\theta) \tag{3}$$

measurements of $D(\theta)$ provide determinations of $S(\theta)$. It is now possible to estimate a value of $S(\theta)$ in p - ^{13}C scattering at 32.9-MeV and $\theta_L = 60°$ from determinations of $D(\theta)$ in p - ^{9}Be scattering at 25 MeV. That is, for the same qR, with q the momentum transfer and $R = r_0A^{1/3}$, the nuclear radius, one has $D = 0.94 \pm 0.02$.[6] I take this to be the lower limit of D(32.9 MeV, $\theta_L = 60°$) for p - ^{13}C scattering, since the quadrupole spin-flip mechanism[7] is not available here because of the spin-1/2 value of ^{13}C. Thus,

$$2S \leq 0.06. \tag{4}$$

Assume now that

$$\sigma^{+-} = 2\sigma^{-+}, \tag{5}$$

which would be a clear and substantial breaking of TRI. From eqns. (1), (3), (4), and (5) it follows that even then

$$|P-A| \leq 0.02, \tag{6}$$

which is smaller than the experimental error. Hence, the experiment did not provide a test of time reversal invariance.

It is immediately obvious from this discussion that tests of TRI using the polarization-analyzing power equality should be made through measurements in a reaction and its inverse where the spin-flip probability is expected or known to be large. Such measurements are presently underway in a Laval-Berkeley collaboration.[8]

I am grateful to H. S. Sherif for the suggestion to estimate D in p - ^{13}C scattering from the p - ^{9}Be results.

Footnote and References

*LBL-11087. Presented at the 5th International Symposium on Polarization Phenomena in Nuclear Physics, Santa Fe, NM, August 11-15, 1980.

1. R. J. Blin-Stoyle, Proc. Phys. Soc. A65, 452 (1952); G. R. Satchler, Nucl. Phys. 8, 65 (1958).

2. E. E. Gross, J. J. Malanify, A. van der Woude, and A. Zucker, Phys. Rev. Lett. 21, 1476 (1968).

3. Polarization Phenomena in Nuclear Reactions, eds. H. H. Barschall and W. Haeberli (Univ. of Wisconsin Press, Madison, 1971), p. xxv.

4. See, for example, H. S. Sherif, Proc. Fourth Int'l. Symposium on Polarization Phenomena in Nuclear Reaction, eds. W. Gruebler and V. Konig (Birkhauser Verlag, Basel, 1976), p. 189.

5. J. Birchall, H. E. Conzett, J. Arvieux, W. Dahme, and R. M. Larimer, Phys. Lett. 53B, 165 (1974).

6. From a linear interpolation, using the three data points of ref. 5 between $\theta_C = 60°-100°$.

7. J. S. Blair, M. P. Baker, and H. S. Sherif, Phys. Lett. 60B, 25 (1975).

8. R. J. Slobodrian, C. Rioux, R. Roy, H. E. Conzett, P. von Rossen, and F. Hinterberger, to be published.

TEST OF CHARGE SYMMETRY IN n-p SCATTERING

G. Greeniaus,* G. A. Moss,* G. Roy,* H. Coombes,* R. Abegg,†
N. E. Davison,† W. T. H. van Oers,† and H. E. Conzett

An experiment has been proposed to TRIUMF to investigate the isospin-mixing charge-symmetry breaking (CSB) component in the n-p interaction. The experiment will measure the difference ΔA between the neutron and proton analyzing power A_n and A_p in n-p elastic scattering at 500 MeV. Designed as a null-measurement requiring no accurately known polarisation standards, the experiment will determine the difference in angle at which A_n and A_p cross through zero. It will provide an unambiguous test for the existence of CSB effects to the level of $\Delta A \simeq 0.001$, corresponding to a laboratory angle difference at zero crossing of $\simeq 0.05°$.

During the summer of 1979 a test measurement of the p-p analyzing power crossover was made. This test was undertaken to provide some firm evidence that a precision comparable to the desired n-p experiment could be obtained, and to yield quantitative estimates of potential background. A polarized proton beam was incident on a CH_2 target. Protons were detected in coincidence in symmetric multiwire proportional chamber (MWPC) counter telescopes having central lab angles of 41.65°. The MWPC's allowed track reconstruction to be made. The NaI detectors were sufficiently thick to stop the p-p elastic protons that entered them. Figure 1 shows the coincidence yield as a function of the opening

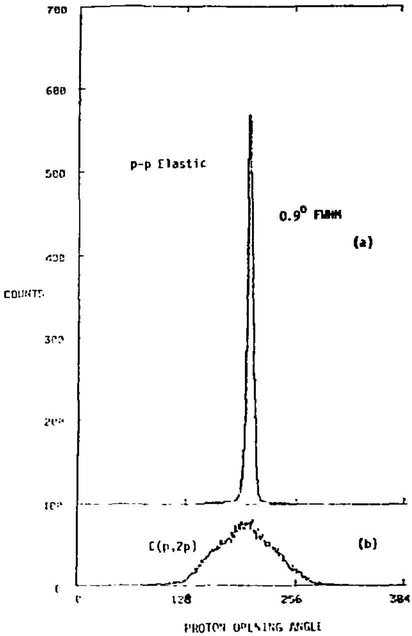

Fig. 1. (XBL 8011-3902)

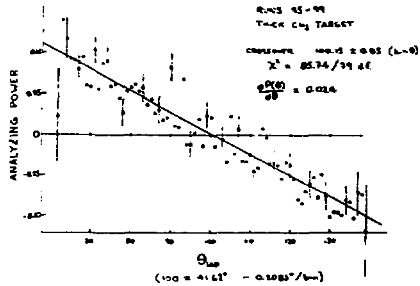

Fig. 2. (XBL 8011-3903)

angle between the coincident protons. When appropriate cuts are made, the C(p,2p) events are reduced by at least a factor of 7 relative to the p-p elastic events. The p-p scattering asymmetry observed for 5 consecutive runs and averaged for the left and right telescopes is shown in Fig. 2. The bins are 0.1083° wide (lab angle). The fit yields a crossover at bin 100.15 · 0.85. The expected value is at bin 100. The error is purely statistical. The five runs represent about 25% of the data for the thick target. Systematic errors in geometry are probably less than 0.05° at this stage of the analysis. These results are summarized in Table 1.

Footnotes

*Physics Department, University of Alberta, Canada

†Physics Department, Univeristy of Manitoba, Canada

Table 1.

	p-p experiment at 500 MeV	n-p experiment
Quasi-elastic scattering background	<<1%	probably < 1%
Background asymmetry	Small and similar to free p-p	Probably as favorable as the p-p case
Effect of background on crossover	$\Delta\theta_0 \lesssim 0.005°$ pessimistically	Probably similar to the p-p case.
	p-p experiment at 500 MeV	n-p experiment
Crossover determination for 5 run sample.	$\theta_0 = 41.64°$ 0.09° $\chi^2 = 85.74/79$ d.f. $\frac{dP(\theta)}{d\theta_{lab}}$ -0.024	

ANALYSIS OF ^{3}He + ^{4}He ELASTIC SCATTERING BETWEEN 18 and 70 MeV WITH THE RESONATING GROUP METHOD OF BROWN AND TANG*

A. D. Bacher,† H. E. Conzett, R. de Siniarski,‡ F. G. Resmini§ and T. A. Tombrello||

The elastic scattering of ^{3}He by ^{4}He has been well described at least for low energy ^{3}He particles by the resonating-group method of Brown and Tang[1] in the one-channel approximation. Indeed phase-shifts calculated by this method have been found in good agreement with those determined from typical phenomenological analysis of ^{3}He + ^{4}He elastic scattering at least up to $E_{^3He}$ = 31.5 MeV (ref. 2). The purpose of this experiment was to obtain data at higher energies to provide an extensive comparison with the resonating-group formalism which a priori should be less successful since an increasing number of reaction channels are expected to open as the energy increases. Another purpose of this experiment was to investigate the possible existence of high lying excited states of ^{7}Be. A recent ^{3}He + ^{4}He elastic scattering for incident ^{3}He particles between 27 and 43 MeV has indeed shown that the resonating-group method describes the data only in a rather general quantitative fashion.[3]

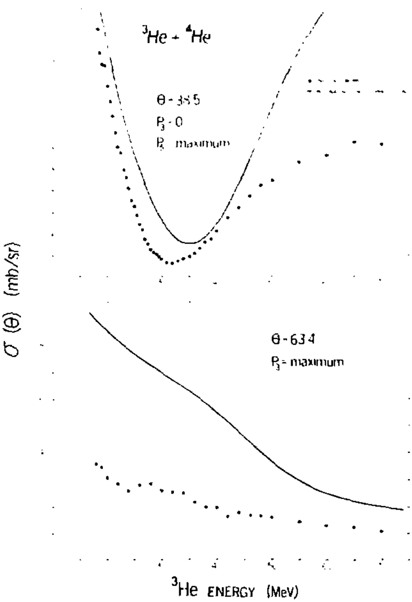

Fig. 1. (XBL 698-1242)

In this paper we present the differential cross-section of the ^{3}He + ^{4}He elastic scattering at certain angles and for 44 energies between 18 and 70 MeV. The range of excitation energies of ^{7}Be covered is between 11.8 and 41.5 MeV. Most of the low-lying states in ^{7}Be have already been observed in low energy ^{3}He + ^{4}He elastic scattering. For ℓ < 4 only f-wave phase shifts show resonance structure for E(^{3}He) < 18 MeV corresponding to the 4.57 MeV ($7/2^-$), the broad 6.73 MeV ($5/2^-$) and the 9.27 MeV ($7/2^-$) states in ^{7}Be (refs. 2,5). The 7.21 MeV ($5/2^-$) level has not been seen in elastic scattering. Besides these levels and states at 9.9 MeV ($3/2^-$) and 11.01 MeV ($3/2^-$) which have been obtained through various reactions,[2,4] no other levels in ^{7}Be have yet been clearly assigned. Recently[5] however a broad resonance structure at E(^{3}He) = 34 MeV has been seen in rough agreement with the resonating-group prediction.[6] Resonating-group calculations[7] employing an ℓ-dependent phenomenological imaginary potential reproduce the cross-section data over a wide range of energy and predict a broad ℓ = 2 level at 11.6 MeV and both ℓ = 4 and ℓ = 5 levels near 25 MeV excitation. In this paper we will compare the resonating-group calculations with the excitation function obtained at some particular angles, such as the zeros or maxima of the Lengendre polynomials which contribute to the partial wave expansion. Since we are dealing with a spin 1/2 particle elastically scattered on a spin zero target it is important to recall that for any level of given spin and parity only one partial wave contributes. We observe indeed marked changes in the shape of the angular distribution which are best reflected, as we shall see, in the behavior of the excitation functions. Figure 1 presents the excitation function at two angles corresponding to zeros or maxima of the Legendre polynomials which are compared to the resonating-group calculations. This figure shows the behavior at 38.5° (P_3= 0, P_5 = maximum) and θ = 63.4° (P_3 = maximum) compared to the resonating-group calculations. The increase in the cross-section in the upper one suggests that the ℓ = 5 wave could be involved, however the slow decrease in the lower one rules out the possibility of a significant contribution from the ℓ = 3 wave.

In conclusion, we can say that the resonating-group predictions follow generally the behavior of the excitation functions, at least for the shape of these functions. These calculations are also in relatively good agreement with the phase-shift with the exception of the p-wave δ_1. From our analysis and experiment, we can suggest the existence of a possible ℓ = 1 level around 20-30 MeV and most certainly broad ℓ = 4 and ℓ = 5 levels above 30 MeV in agreement with recent theoretical calculations. The resonating-group method describes the ^3He + ^4He elastic scattering for ^3He energies between 18 and 70 MeV only in a rather general qualitative fashion. Polarization measurements using either a polarized ^3He beam or a polarized ^3He target will provide the possibility of a complete and unique phenomenological analysis of the scattering data, especially when the polarization data will be extended to higher energies.

Footnotes and References

*Condensed from Helv. Phys. Acta 51, 680 (1978).

†Present address: Physics Department, University of Indiana, Bloomington, U.S.A.

‡Present address: Institut des Sciences Nucleaires de Grenoble, France.

§Present address: University of Milan, Italy.

Present address: California Institute of Technology, Pasadena, California, U.S.A.

1. R. E. Brown and Y. C. Tang, Phys. Rev. 176, 1235 (1968). Y. C. Tang, E. Schmid, K. Wildermuth, Phys. Rev. 131, 2631 (1963).

2. R. J. Spiger and T. A. Tombrello, Phys. Rev. 163, 964 (1967). J. S. Vincent, E. T. Boschitz and R. E. Wagner, Bull. Amer. Phys. Soc. 12, 17 (1967).

3. P. Schwandt, B. W. Ridley, S. Hayakawa, L. Put and J. J. Kraushaar, Phys. Lett. 30B, 30 (1969).

4. F. Merchez et al., J. of Phys. 29, 968 (1968); F. Ajzenberg-Selove and T. Lauritsen, Nucl. Phys. Rev. A227, 1 and references therein (1974).

5. R. E. Brown, E. E. Gross, A. van der Wounde, Phys. Rev. Lett. 25, 1346 (1970).

6. C. G. Jacobs, R. E. Brown, Phys. Rev. 1C, 1615 (1970).

7. J. A. Koepke, R. E. Brown, Y. C. Tang and D. R. Thompson, Phys. Rev. 9C, 823 (1974).

FROM TRANSFER TO FRAGMENTATION*

Bernard G. Harvey

Studies of the system ^{16}O + ^{208}Pb seem to indicate that quasi-elastic fragments of the projectile (those with beam velocity) are produced by fragmentation at energies greater than about 20 MeV/A but by a different mechanism (probably multi-nucleon transfer) at low energies.[1] The change in mechanism appears to occur rather abruptly in the region of 15 MeV/A.

Semiclassical calculations based on the matching conditions for momentum and angular momentum in transfer reactions[2] predict that the transfer cross section will be greatest when the ejectile retains almost the projectile velocity, and that the angular momentum of the heavy nucleus will be $mvR/\hbar$, where m is the transferred mass, v is the relative velocity of projectile and target nucleus and R is the radius of the final nuclus. Measurements of the average γ-ray multiplicity $\langle M_\gamma \rangle$ in coincidence with quasi-elastic fragments[3] show that $\langle M_\gamma \rangle$ is indeed proportional to m and v at energies up to 10 MeV/A, but not at higher energies.

At some value of v, the angular momentum of m around the core must become so great that the "transferred" nucleons cannot remain bound long enough for their angular momentum and energy to be taken up by the whole system. At this point, some or all of the transferred mass will presumably be promptly re-emitted, carrying away a substantial part of the angular momentum and excitation energy.

Figure 1 shows semiclassical transfer calculations of the angular momentum of the final

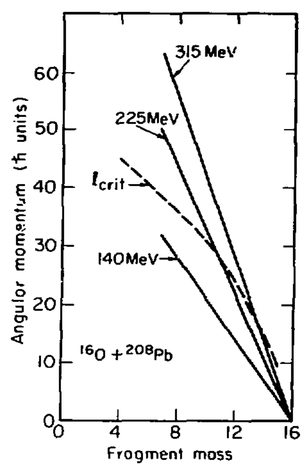

Fig. 1. Semiclassical calculation of angular momentum as a function of mass transferred. (XBL 808-1631)

heavy nucleus in the $^{16}O + ^{208}Pb$ system as a function of the mass of the observed quasi-elastic fragment. The dashed line shows the critical angular momentum ℓ_{crit} from the Wilczynski semi-empirical systematics.[4] For E_{16O} of 140 MeV, the angular momentum of the final heavy nucleus is always below ℓ_{crit}, and transfer is not limited by this criterion. At E_{16O} of 315 MeV, only one or two nucleons can be transferred before the angular momentum exceeds ℓ_{crit}. At E_{16O} of 225 MeV (14 MeV/A), as many as six nucleons can be transferred before the angular momentum exceeds ℓ_{crit}. It is therefore at about this beam energy that transfer reactions should begin to give way to the fragmentation mechanism.

It is instructive to look also at the excitation energy E_{ex} of the final nucleus. Figure 2 shows E_{ex} as a function of the mass of the observed quasi-elastic fragment for the same three beam energies. The slopes of the lines correspond to the excitation energy per transferred nucleon, E_{ex}/m. When that quantity exceeds the binding energy per nucleon, it seems likely that prompt re-emission will occur. At the three beam energies shown in Fig. 2, the excitation energies per nucleon are respectively 4.3, 9.0, and 14 MeV. This result suggests again that true transfer should cease in the vicinity of 14 MeV/A.

Further experiments are required to sort out the relative importance of the excitation energy and of the angular momentum in determining where transfer changes over into fragmentation. At least for the $^{16}O + ^{208}Pb$ system, both criteria suggest that this will occur at about 14 MeV/A, in agreement with the experiment.

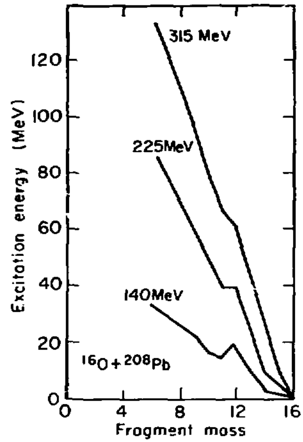

Fig. 2. Semiclassical calculation of excitation energy as a function of mass transferred. (XBL 808-1632)

Footnote and References

*B. G. Harvey, Notas de Fisica 3 No. 1, 99 (1980).

1. C. K. Gelbke et al., Phys. Rep. 42, 312 (1978).

2. D. M. Brink, Phys. Lett., 40B, 37 (1972).

3. L. W. Richardson, contribution to this Annual Report.

4. J. Wilczynski, Nucl. Phys., A216, 386 (1973).

MOLECULAR RESONANCES AND THE PRODUCTION OF FAST α-PARTICLES IN THE REACTION OF ^{16}O WITH $^{12,13}C$ NUCLEI*

W. D. Rae, R. G. Stokstad, B. G. Harvey, A. Dacal,[†]

R. Legrain,[‡] J. Mahoney, M. J. Murphy, and T. J. M. Symons

Recently Nagatani et al.[1] presented experimental results that suggest the direct population of molecular resonance states by ^{12}C transfer in the reaction $^{12}C(^{16}O,\alpha)$ at ^{16}O = 145 MeV. The inclusive spectra presented in Ref. 1 show structure in the yield of fast α-particles on top of a large underlying continuum. In contrast, these structures are not observed in the singles α-spectra obtained by bombarding ^{13}C with ^{16}O. The higher energy resonances observed in the $^{12}C + ^{12}C$ system are estimated to have large partial widths for decay into the ^{12}C g.s. + ^{12}C g.s.,[2] so for the $^{16}O + ^{12}C$ system an experiment in which carbon ions are detected in coincidence with α-particles could be expected to include events from the decay of a resonant $^{12}C + ^{12}C$ final state. To this end the following experiments were performed:

A beam of 140-MeV $^{16}O^{4+}$ from the LBL 88 Inch Cyclotron was used to bombard a 620 $\mu g/cm^2$ natural carbon target and a ^{13}C target of 285 $\mu g/cm^2$ thickness enriched to 99% in ^{13}C. Alpha particles were detected in a ΔE-E telescope while ^{12}C and ^{13}C ions were detected in either a second ΔE-E telescope or in the QSD magentic spectrometer.

Data were taken at 22 angle pairs covering 7.5° to 30° in the laboratory for the ^{12}C telescope and -4° to -18° for the α telescope. Figure 1 shows typical spectra obtained using the two telescopes and the ^{12}C target. Only events in which all three particles emerged in their ground states (Q = -7.16 MeV) are shown. Analysis of all the data showed that the dominant peaks are not constant in E_α or E_C as a function of either θ_α or θ_C. Also shown in Fig. 1 are $^{16}O^*$ excitation spectra. The energies of the peaks in these spectra are found to be independent of both θ_α and θ_C, and the relative angles θ_α-θ_C. On the basis of these results we conclude that the coincidence data are dominated by inelastic excitation of discrete α-unbound states of the ^{16}O projectile followed by their decay.

For a comparison of reactions with ^{12}C and ^{13}C targets we used the magnetic spectrometer to detect the carbon ions. Figure 2 compares typical spectra obtained with the ^{12}C and ^{13}C targets. The Q-value spectra for α-^{12}C coincidences and the energy spectra of the α-particles show similar structures. Analysis of data taken at different angles showed that the coincident yield of α + ^{12}C is dominated by the excitation and subsequent decay of $^{16}O^*$ regardless of whether the target is ^{12}C or ^{13}C.

Differences between the data from ^{12}C and ^{13}C targets were observed in the coincident yeild of α + ^{13}C (Figs. 1(c) and (d)). This

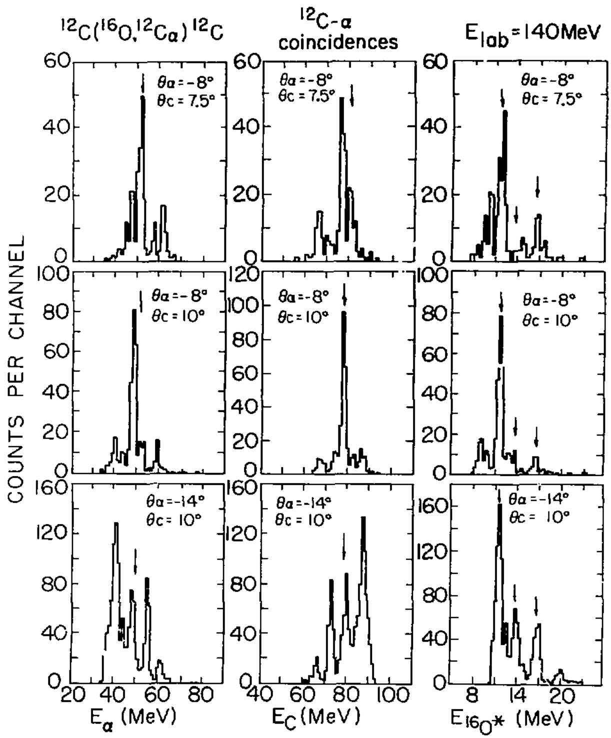

Fig. 1. Coincident counts vs E_α, E_C and $E_{^{16}O^*}$ are shown in columns 1-3. Each row shows a different pair of detector angles.
(XBL 806-3394)

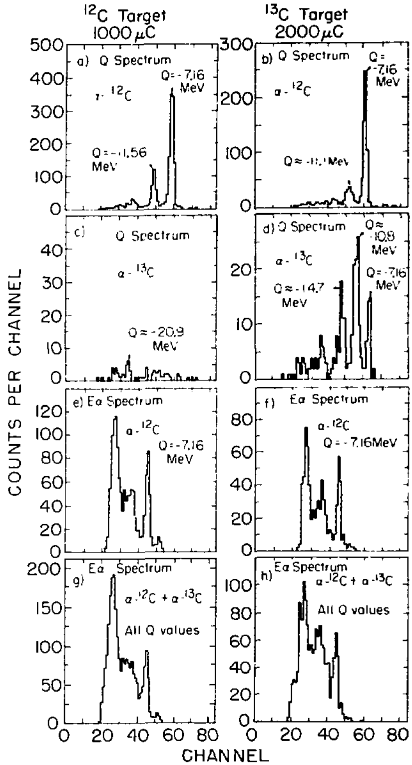

Fig. 2. A comparison of the coincidence data obtained in ^{16}O induced reactions on ^{12}C and ^{13}C at $\theta_\alpha = -14.5°$ and $\theta_C = 10°$.
(XBL 806-3395)

was explained by the respective Q-values for neutron pick up by the projectile. Another difference, the larger relative cross-section for the production of coincident fast α particles by a ^{12}C target, (Figs. 1(g) and (h)), is not understood at this time.

The inclusive alpha spectra of Ref. 1 suggest the population of highly excited states in ^{24}Mg, and this has been interpreted in terms of resonances in the ^{12}C + ^{12}C system.[1] The present coincidence experiments do not reveal a ^{12}C + ^{12}C final state interaction. The possibility exists that the small differences observed in the coincidence data on ^{12}C and on ^{13}C might account for the absence of structure in the α singles data on ^{13}C.[1] Alternatively, (1) the resonant breakup of the projectile might obscure a ^{12}C + ^{12}C interaction, or (2) the states formed in ^{24}Mg may have a small width for decay into ^{12}C + ^{12}C.

Footnotes and References

*Condensed from LBL-11135

†Instituto de Fisica, UNAM, Mexico.

‡DPhN-Be, CEN Saclay, 91190 Gif-sur-Yvette, France.

1. K. Nagatani, T. Shimoda, D. Tanner, R. Tribble and T. Yamaya, Phys. Rev. Lett. 43 (1979) 1480.

2. D. A. Bromley, Proc. Int. Conf. on Resonances in Heavy Ion Reaction, Hvar, Yugoslavia, (1977), ed N. Cindro, North Holland Pub. Co., 1978. See also T. M. Cormier et al., Phys. Rev. Letters. 40 (1978) 924 and A. J. Lazzarini, et. al Phys. Rev. Letters 40 (1978) 1426.

^{13}C* PRODUCTION IN THE 187 MeV ^{12}C + ^{208}Pb REACTION

A. N. Bice, A. C. Shotter[1] and Joseph Cerny

The reaction mechanisms involved in the production of fast light particles and projectile like fragments in the interaction of very assymetric systems are currently under extensive study. Several single particle inclusive, angular correlation and particle-γ experiments[1] have been performed with 10-20 MeV/nucleon B, C, N, and O beams on heavy targets. In general, these studies seem to indicate that the process of projectile excitation and decay is of relatively minor importance in explaining the observed inclusive yield of beam velocity particles. Indeed, it recently has been suggested by Wu and Lee[1] that the mechanism of incomplete fusion following projectile fragmentation must be a dominant process in complex projectile induced reactions. A recent investigation[2] of the $^{12}C + ^{208}Pb$ system at 187 MeV found that the process of projectile excitation and subsequent decay (in the $^{12}C^* \to \alpha + ^{8}Be$ channel) contributes significantly to inclusive ^{8}Be measurements. Presented here is data for another strong sequential breakup channel, i.e., the $^{13}C^* \to \alpha + ^{9}Be$ transition from the $^{208}Pb(^{12}C, ^{13}C^*)\ ^{207}Pb(g.s.)$ reaction at 187 MeV.

This study was performed by bombarding a 1.4 mg/cm^2 ^{208}Pb target with a 187 MeV ^{12}C beam. The production of $^{13}C^* \to \alpha + ^{9}Be$ was observed by detecting the decay products in coincidence with a two telescope system. Further experimental details of this detection system may be found elsewhere.[2]

Coincidence between α and ^{9}Be reaction products were measured between 13° and 30° in the laboratory system. The summed energy spectra of $\alpha + ^{9}Be$ fragments at all angles are dominated by a single transition that is kinematically consistent with a neutron pickup by the ^{12}C projectile leaving ^{207}Pb in its ground state and an excited ^{13}C product, which then decays into $\alpha + ^{9}Be$ fragments. This interpretation is further supported by the observed α - ^{9}Be relative energies of ~ 1.2 and ~2.7 MeV, which is close to the relative energies expected for a ^{13}C nucleus excited to the first two groups of alpha decaying states above the $\alpha + ^{9}Be$ breakup threshold. Our detection system geometry did not allow clear observation of α - ^{9}Be relative energies above 2.7 MeV.

Figure 1 shows the measured $\alpha + ^{9}Be$ yield (for the ^{207}Pb (g.s.) transition) versus the laboratory angle of the two telescope detection system. As was observed in the $(^{12}C, ^{12}C^*)$ reaction channel the $\alpha + ^{9}Be$ production peaks near the grazing angle (~ 20°). The shape of the $(^{12}C, ^{13}C^*)$ angular distributions were interpretable in terms of a peripheral reaction mechanism.

The observation of a strong neutron pickup channel to states unbound with respect to alpha decay suggests that direct nucleon transfer to unbound levels, in general, could strongly influence single particle inclusive measurements. For the $^{12}C + ^{208}Pb$ reaction it has been found that the sequential breakup process can significantly affect other reaction channels such as inclusive ^{8}Be measurements. From the observed $^{13}C^* \to \alpha + ^{9}Be$ transitions we have estimated that ~ 10-15% of the near beam velocity ^{9}Be inclusive cross section comes from this neutron transfer and subsequent decay channel.

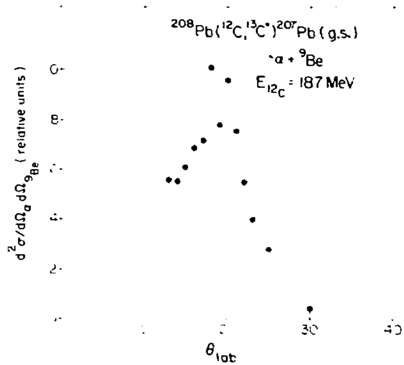

Fig. 1. The relative yield of $^{13}C^* \to \alpha + ^{9}Be$ production for α-^{9}Be relative energies less than ~ 3 MeV. Transitions from two groups of excited states of ^{13}C contibute to the observed $\alpha + ^{9}Be$ coincident yield.

(XBL 808-1755)

Clearly, further investigations of sequential breakup and direct nucleon transfer reactions producing unbound outgoing systems are necessary before a complete understanding of fast particle production can be achieved.

Footnote and References

†On leave from the Physics Department, University of Edinburgh, Edinburgh EH93JZ, United Kingdom.

1. J. R. Wu and I. Y. Lee, Phys. Rev. Lett. 45, 8 (1980), and references therein.

2. A. C. Shotter, A. N. Bice, D. P. Stahel and Joseph Cerny, to be published.

3. J. S. Larsen et al., Phys. Lett. 42B, 205 (1972).

^{16}O – ^{12}C ELASTIC SCATTERING AND TOTAL REACTION CROSS SECTION AT $E_{c.m.}$ = 60, 93 and 135 MeV.

M. E. Brandan,* A. Dacal,* A. Galinda,* A. Menchaca-Rocha.*

B. G. Harvey, R. Legrain, J. Mahoney, M. Murphy, W. D. M. Rae, and T. J. M. Symons

Angular distributions have been measured for the elastic scattering of ^{16}O from ^{12}C at ^{16}O energies of 140,218 and 315 MeV for angles up to 46° c.m. The data were analyzed in terms of a six-parameter W-S optical potential. The determination of the optical parameters at each energy showed the ambiguities already known for heavy ions. The real part is well determined only between ~ 6.6 and 7.4 fm., this sensitive radial region being the same for the three energies. Figure 1 shows the data with a representative optical model fit.

Some of the ambiguities disappeared when the three sets of data were analyzed simultaneously assuming an energy-independent potential. The quality of the fits however, was poorer, X^2/N being 2 to 5 times larger than the best individual fit at each energy.

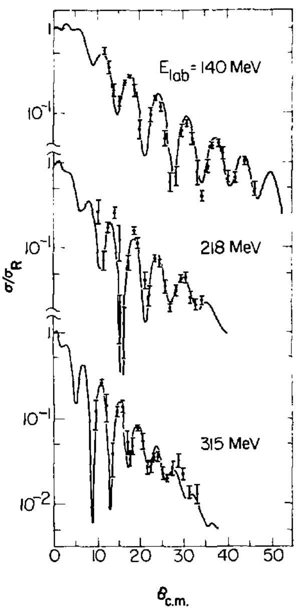

Fig. 1. (XBL 809-1841)

Total reaction cross sections $\sigma_R(E)$ were obtained from the optical model analysis of the elastic data. Since the parameters are not uniquely detemined it is not possible to unambiguously derive a value for σ_R. An averaging procedure was followed, based on the strong correlation that was found between σ_R and the imaginary diffuseness a_i. Figure 2 presents the values of $\sigma_R(E)$ with uncertainties calculated from the statistical distribution of σ_R values corresponding to different a_i. The data show that $\sigma_R(E)$ does not simply level off and stay at the geometrical value (= 1.39 b) but they are consistent, within the uncertainities, with parameter-free calculations[1] (solid line) based on nucleon-nucleon data, which show increased nuclear transparency in heavy-ion reactions at medium energies.[2]

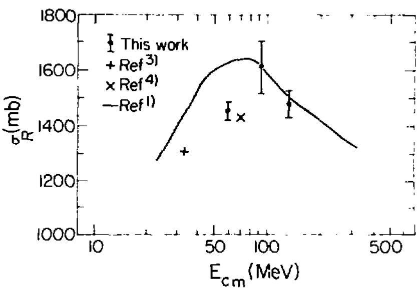

Fig. 2. (XBL 809-1840)

Footnote and References

*IFUNAM, A.P. 20-364, Mexico 20 D.F.

1. R. M. DeVries and J. C. Peng, private communication.

2. R. M. DeVries and J. C. Peng, Phys. Rev. Lett. 43, 1373 (1979), to be published in Phys. Rev. C.

3. H. H. Gutbrod et al, Z. Phys. 262, 373 (1973).

4. R. H. Bassel et al, Nucl. Phys. 89, 419 (1976).

STUDY OF HIGH ENERGY ^{7}Li + ^{28}Si ELASTIC SCATTERING

M. S. Zisman, J. G. Cramer,* R. M. DeVries,† D. A. Goldberg,‡ and A. Seamster*

As a continuation of our previous studies of high energy elastic scattering, we have now looked at the ^{7}Li + ^{28}Si system at 140.7 MeV using a $^{7}Li(3+)$ beam from the LBL 88 Inch Cyclotron. Based on our earlier work,[1] it is known that ^{6}Li exhibits behavior similar to that of light ions such as ^{4}He. For example, the high energy ^{6}Li elastic data show evidence for a back angle enhancement due to nuclear rainbow scattering, and global fits indicate the need for markedly energy dependent potentials. In contrast, for heavier projectiles such as ^{9}Be, ^{12}C, or ^{16}O there is no evidence[1,2] for nuclear rainbow scattering at high energies, and it is possible to find energy-independent optical potentials that fit the data over a very wide energy range.

Because ^{7}Li shares many properties in common with ^{6}Li and ^{9}Be (such as having a small binding energy and a non-zero spin), comparison of the present results with those from Refs. 1 and 2 might ultimately be expected to shed some light on whether the "transition" in elastic scattering properties outlined above depends primarily on these features. In addition, Satchler and Love[3] found in their global folding model analysis that both ^{6}Li and ^{9}Be are anomalous in the sense of requiring a substantial renormalization of the real potential (N ~ 0.5) to fit existing data. On the other hand, existing low energy ^{7}Li elastic scattering data on various targets do not appear to show such an anomaly.[3] Thus, it is very interesting to compare the real potential derived from the present ^{7}Li + ^{28}Si data with the high energy ^{6}Li + ^{28}Si potentials[1,2] obtained previously.

Figure 1 shows our preliminary ^{7}Li + ^{28}Si elastic scattering angular distribution at E_{Lab} = 140.7 MeV, along with optical model calculations employing both a deep (V_0 ~ 150 MeV) and a shallow (V_0 ~ 15 MeV) Woods-Saxon real potential. As can be seen, the back angle data appear to show evidence for rainbow enhancement. This feature can be fully reproduced with a deep potential, but is only approximately reproduced when a shallow potential is used. In contrast to the difference between ^{6}Li and ^{7}Li reported by Satchler and Love,[3] we find that the real potentials required to fit high energy ^{6}Li + ^{28}Si data (Ref. 1) and the present ^{7}Li + ^{28}Si data are very similar. One consequence of this similarity of the real potentials is that the fusion barriers that they predict are nearly the same. Interestingly, the values obtained for both systems agree rather well with predictions based on the systematics of Vaz and Alexander.[4]

As regards the imaginary potential for the ^{7}Li + ^{28}Si system, our preliminary analysis indicates that it is considerably less diffuse than that required to fit the high energy ^{6}Li + ^{28}Si data[1] and looks more like the sort of imaginary potential found[2] in fits to low energy ^{6}Li + ^{28}Si data. This suggests that whatever process causes the long tail on the ^{6}Li imaginary potential is less important in the case of ^{7}Li scattering. Insofar as breakup is the most likely candidate,[2,3] the differences between ^{6}Li and ^{7}Li would presumably be related to the different separation energies (1.47 MeV for ^{6}Li, 2.47 MeV for ^{7}Li) for the two ions. Firm conclusions on this point necessarily await more data as well as more detailed analysis of the present data.

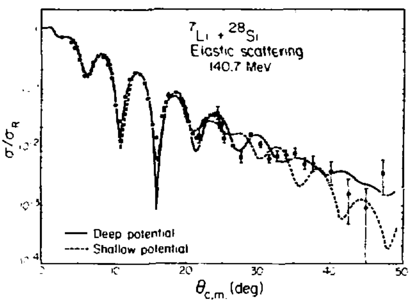

Fig. 1. ^{7}Li + ^{28}Si elastic scattering angular distribution at E_{Lab} = 140.7 MeV. The solid curve represents an optical model calculation employing a deep Woods-Saxon real potential (V_0 ~ 150 MeV) and the dashed curve represents a calculation using a shallow real calculation potential (V_0 ~ 15 MeV).
(XBL 808-1664)

Footnotes and References

*University of Washington, Seattle, WA 98195

†Los Alamos Scientific Laboratory, Los Alamos, NM 87545

‡University of Maryland, College Park, MD 20742

1. J. G. Cramer, R. M. DeVries, D. A. Goldberg, M. S. Zisman, and C. F. Maguire, Phys. Rev. C 14, 2158 (1976); R. M. DeVries, D. A. Goldberg, J. W. Watson, M. S. Zisman, and J. G. Cramer, Phys. Rev. Lett. 39, 450 (1977).

2. M. S. Zisman, J. G. Cramer, D. A. Goldberg, J. W. Watson, and R. M. DeVries, Phys. Rev. C 21, 2398 (1980).

3. G. R. Satchler and W. G. Love, Phys. Rept. 55, 183 (1979).

4. L. C. Vaz and J. M. Alexander, Phys. Rev. C 18, 2152 (1978).

THE QUASIELASTIC BREAKUP $^{12}C \rightarrow \alpha^{8}Be$ at 132 MeV AND 187 MeV

A. C. Shotter,* A. N. Bice and Joseph Cerny

In the last few years there has been increased interest in breakup reactions of light ions scattered from nuclei. Such reactions are of interest in their own right but it is also important to understand the breakup mechanism since it can have an influence on other reaction channels. In the case of light ions, it is normal to consider only a direct breakup process, i.e., a rapid fragmentation of the projectile at the nuclear surface. However, it is also possible for the breakup to occur following excitation of the projectile to discrete states that are above the corresponding breakup thresholds. We have undertaken an experiment designed to study the breakup characteristics of 132 and 187 MeV ^{12}C ions on ^{208}Pb, in which it is found that for quasi-elastic events in which the relative energy between the fragments is below 2.3 MeV, the breakup proceeds primarily through discrete states of ^{12}C.

The experiment was performed using ^{12}C beams produced by the 88 Inch Cyclotron. The only breakup channel of ^{12}C above 7.37 MeV, and below 15.96 MeV, is $^{12}C \rightarrow {}^{8}Be + \alpha$; these breakup fragments are confined to a cone of an angular width that is determined by their relative energy, ε, and the laboratory energy of the excited projectile, E. Maximum efficiency for the detection of the $^{12}C^*$ breakup fragments was achieved by constructing two $\Delta E \times E$ telescopes in close vertical geometry, with one telescope above and the other below the reaction plane. These telescopes consisted of pairs of ΔE and E detectors manufactured on the same silicon wafer such that the minimum vertical angular separation of the telescopes was 1.5°. Reject detectors placed behind the E detectors were employed to veto high energy events.

The differential cross sections for the breakup of ^{12}C into the $^{8}Be + \alpha$ channel, for which the target remains unexcited, is shown in Fig. 1 for 132 and 187 MeV ^{12}C energies. The grazing angle for these two reactions are 32°, 20°. It is seen that the experimental angular distributions are at a maximum near these angles. The shape of these distributions are also similar to other surface reactions such as $^{208}Pb(^{12}C,^{13}C)^{207}Pb$, which supports the interpretation that the breakup reaction is a peripheral phenomenon.

An investigation of the breakup cross section with incident energy should provide valuable data for testing various breakup theories, and complementary data for incomplete fusion reactions.[1]

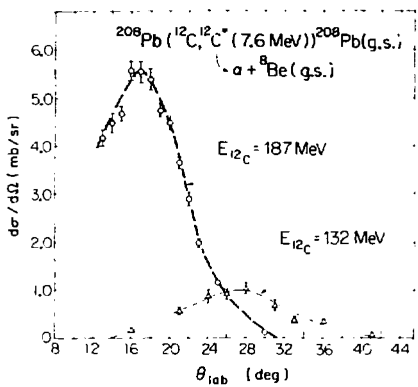

Fig. 1. The measured differential cross section for the $^{208}Pb(^{12}C,\alpha^{8}Be)^{208}Pb$ (g.s.) reaction at 132 and 187 MeV. (XBL 809-1906)

Footnote and Reference

*On leave from the Physics Department, University of Edinburgh, Edinburgh EH93JZ, United Kingdom.

1. K. Siwek-Wilszynska et al., Phys. Rev. Lett. 42, 1599 (1979).

FUSION CROSS SECTIONS DERIVED FROM OPTICAL POTENTIALS

M. S. Zisman

In recent years detailed studies of heavy ion elastic scattering[1,2] and also fusion excitation functions[3,4] have appeared in the literature. One interesting question which these data allow us to investigte is whether or not the optical potentials obtained from fits to elastic scattering data are also capable of reproducing the measured fusion excitation function for the same system. This question has been addressed previously by Vigdor et al.[3] for the $^{16}O + {}^{40}Ca$ system. They were successful in simultaneously fitting both the fusion excitation function data and the elastic scattering data at one energy (55.6 MeV) with a single real potential. However, this potential was incapable of providing good fits to the higher energy elastic scattering data (extending up to 214.1 MeV).

In the present study a somewhat different approach is used, namely to emphasize the high energy elastic data in the fit procedure. It turns out for most light heavy ion systems that the high energy elastic data are sensitive to a rather broad radial range, and that this region of sensitivity extends well inside of the $\ell = 0$ fusion barrier.[2] Thus, insofar as there is a single interaction potential between the ions which determines both elatic scattering and fusion, it is the high energy elastic data which are sensitive to that region of the potential which is important for low energy fusion data.

Examples of optical model fits to the elastic scattering in the $^{16}O + ^{28}Si$ system, utilizing both a Woods-Saxon (WS) and a proximity radial form are shown in Fig. 1. Fusion cross sections were calculated for each of the potentials shown in Fig. 1 using various friction-free models. The first involves a simple sharp cutoff (SCO) model in which $\sigma_f(E) = \pi\lambda^2(\ell_{cr} + 1)^2$, where ℓ_{cr} is the highest partial wave for which the maximum

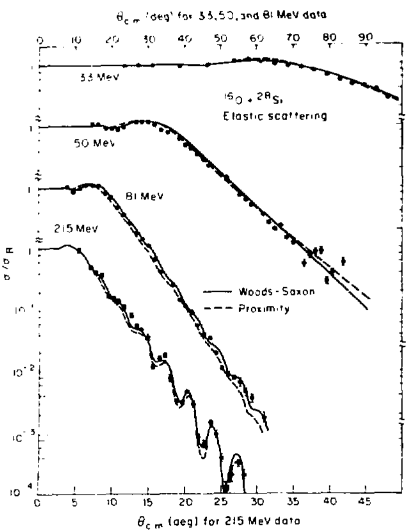

Fig. 1. Optical model fits to the elastic scattering of $^{16}O + ^{28}Si$ at several laboratory energies. The solid lines correspond to a Woods-Saxon parametrization of the real potential and the dashed lines to a proximity form for the real potential. (XBL 804-619)

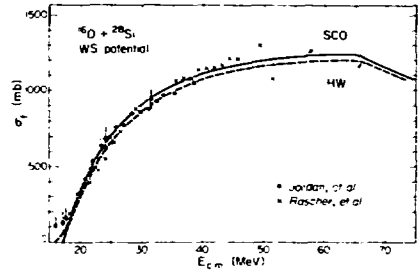

Fig. 2. Predicted fusion cross sections for the $^{16}O + ^{28}Si$ system based on the WS potential shown in Fig. 1. The solid curve represents a sharp cutoff calculation while the dashed curve represents a calculation including Hill-Wheeler barrier penetration effects. (XBL 803-518)

in the real potential (nuclear + Coulomb + centrifugal) is below energy E. In addition, calculations including barrier penetrability have been performed using the Hill-Wheeler expression[4] for passage through a parabolic barrier. In both cases the barrier height and position for each partial wave were determined by explicitly differentiating the appropriate optical potential.

Shown in Fig. 2 are calculated fusion cross sections for the $^{16}O + ^{28}Si$ system using the WS potential from Fig. 1. The solid points and crosses represent measured fusion data from Ref. 5. As can be seen, the agreement is quite gord and indicates that for this system it is possible to find a single interaction potential which simultaneously reproduces both elastic scattering and fusion data. Similar studies have been performed for the $^{16}O + ^{27}Al$ and $^{16}O + ^{40}Ca$ systems with comparably good results.

References

1. J. G. Cramer, R. M. DeVries, D. A. Goldberg, M. S. Zisman, and C. F. Maguire, Phys. Rev. C 14, 2158 (1976); R. M. DeVries, D. A. Goldberg, J. W. Watson, M. S. Zisman, and J. G. Cramer, Phys. Rev. Lett. 39, 450 (1977).

2. M. S. Zisman, J. G. Cramer, D. A. Goldberg, J. W. Watson, and R. M. DeVries, Phys Rev. C 21, 2398 (1980).

3. S. E. Vigdor, D. G. Kovar, P. Sperr, J. Mahoney, A. Menchaca-Rocha, C. Olmer, and M. S. Zisman, Phys. Rev. C 20, 2147 (1979).

4. L. C. Vaz and J. M. Alexander, Phys. Rev. C 18, 2152 (1978).

5. W. J. Jordan, J. V. Maher, and J. C. Peng. Phys. Lett. 87B, 38 (1979); R. Rascher, W. F. J. Müller, and K. P. Lieb, Phys. Rev. C 20, 1028 (1979).

ANALYZING POWERS OF $^3He(\vec{p},p)^3He$ ELASTIC SCATTERING BETWEEN 30 AND 50 MeV*

J Birchall† and W T H van Oers†

H E Conzett, P von Rossen‡ and R M Larimer

J Watson,§ R E Brown

In a recent phase-shift analysis[1] of p-^{3}He scattering data unusual behaviour of the $^1S_0$, $^1P_1$, and $^1D_2$ phases was observed in the energy range between 20 and 50 MeV. With a view to enlarging the data base and to obtain improved phase parameters, we have made measurements of the $^3He(\vec{p},p)^3He$ analyzing powers at laboratory angles between 20° and 160° at proton energies of 32.4, 35.1, 37.6, 40.1, 45.0, 47.6 and 49.6 MeV. These angular distributions complement those[2] at 21.4, 24.8, 27.3, and 30.1 MeV and differential cross section[3] and total reaction cross-section data[4] as well as data obtained with a polarised ^{3}He target.[5]

The polarised proton beam from the 88 Inch Cyclotron of the Lawrence Berkeley Laboratory was transported to a gas cell containing ^{3}He gas at pressures between 1 and 2 atmospheres. Beam currents on target were varied between 10 nA and 100 nA while the beam polarization was typically 0.8.

The gas target was contained in a scattering chamber, at the entrance and exit of which collimation slits were fitted. Current falling on the left and right components of these slits was monitored and beam transport parameters adjusted to ensure that these currents were equalised. In the first series of runs (at 32.4, 35.1, 37.6, 40.1 MeV) these adjustments were made by hand. An automatic control system was installed for subsequent runs.

The scattering chamber contained arrays of detectors placed symmetrically at either side of the beam. Four detector systems in the first and two in the second series of runs were used.

An absorber wheel downstream of the scattering chamber was used to reduce the beam energy to that appropriate for the beam polarimeter. The polarimeter was immediately downstream from the absorber wheel. One detector system at either side of the beam detected protons elastically scattered from the polarisation analyser, which was ^{4}He gas for the first and a ^{12}C foil for the second set of measurements. The ^{4}He and ^{12}C analyzing powers were taken from the data of Bacher et al.[6] and Kato et al.[7]

Beam was collected in a Faraday cup and charge integrated. The beam polarisation was reversed at the source a few times per second on the basis of equal Faraday cup charge per spin state.

The results of the measurements are shown in Fig. 1. Corrections for finite geometry were very small (usually less than 0.001) and have been incorporated into the data only at 32.4 and 35.1 MeV. The statistical error bars when not shown are smaller than the size of the dots.

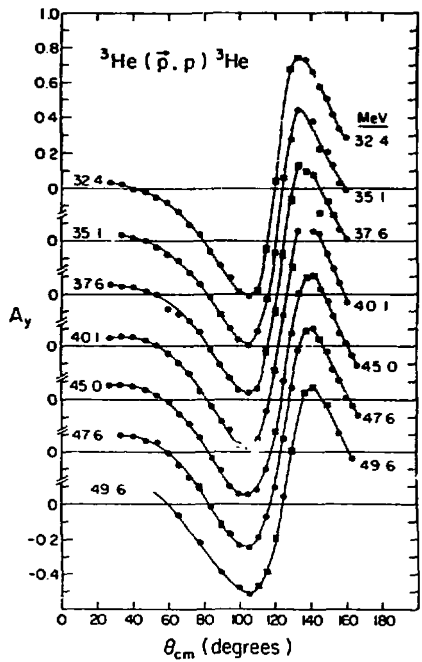

Fig. 1. Analyzing powers A_y for $^3He(\vec{p},p)^3He$ between 30 and 50 MeV. The curves are to guide the eye. (XBL 8011-3900)

Footnotes and References

*LBL-11121. Presented at the 5th International Symposium on Polarization Phenomena in Nuclear Physics, Santa Fe, NM, August 11-15, 1980.

†Department of Physics, University of Manitoba Winnipeg, Manitoba R3T 2N2, Canada.

‡Institute of Nuclear Physics, University of Bonn, D-5300 Bonn, West Germany.

§Department of Physics, Kent State University, Kent, Ohio 44242.

Los Alamos Scientific Laboratory, Los Alamos, NM 87545.

1. R. E. Brown, B. T. Murdoch, D. K. Hascll, A. M. Sourkes and W. T. H. van Oers, Few Body Systems and Nuclear Forces, ed. H. Zingl, M. Haftel and H. Zankel (Springer, Berlin, 1978), vol. 1, p. 292.

2. J. W. Watson, H. E. Conzett, R. M. Larimer, B. T. Leemann and E. J. Stephenson, Bull, Am. Phys. Soc. 22, 531 (1977).

3. B. T. Murdoch, D. K. Hasell, A. M. Sourkes, W. T. H. van Oers and R. E. Brown, (1980) to be published.

4. A. M. Sourkes, A. Houdayer, W. T. H. van Oers, R. F. Carlson and R. E. Brown, Phys. Rev. C13, 451 (1976).

5. R. H. McCamis et al. Contribution to this Conference.

6. A. D. Bacher, G. R. Plattner, H. E. Conzett, D. J. Clark, H. Grunder and W. F. Tivol, Phys. Rev. C5, 1147 (1972).

7. S. Kato, K. Okada, M. Kondo, A. Shimizu, K. Hosono, T. Saito, N. Matsuoka, S. Nagamachi, K. Nisimura, N. Tamura, K. Imai, K. Egawa, M. Nakamura, T. Noro, H. Shimizu, K. Ogino and Y. Kadota, Nucl. Instr. Meth. 169, 589 (1980).

ROTATIONAL ENERGY EXPRESSIONS AND LEAST-SQUARES FITTING OF BACKBENDERS AND SIMILAR NUCLEI*

J. O. Rasmussen, M. W. Guidry,† T. E. Ward,‡ C. Castaneda,§ L. K. Peker,** E. Leber,** and J. H. Hamilton‡‡

With the increasing knowledge of states near the yrast line in deformed even-even nuclei, it appears that irregularities in spacings (backbending or upbending) may be associated with band crossing. The band that crosses the ground band (g-band) at some critical spin I_c will here be referred to as the S-band (for "superband" or "Stockholm band"). The band-mixing picture has been invoked in numerous studies.

Stephens et al[2] especially have advanced the picture that the S-band involves the decoupling of a pair of particles in a high-j orbital to a resultant $J_p = 2j - 1$ angular momentum, to which the core angular momentum adds in stretched fashion to yield the resultant spin I. In its purest form the decoupled S-band should show a band-head spin of J_p (=2j - 1) and energies of

$$E_s(I) = E_0 + \frac{\hbar^2}{2\mathscr{I}_s} R(R + 1), \qquad (1)$$

with

$$R = I - J_p. \qquad (2)$$

The limiting case of two bands, degenerate in the absence of Coriolis interaction, has a simple analytical solution.

Consider the case of a deformed even-even nucleus with neutron chemical potential between Ω and $\Omega + 1$ orbitals of high j. We suppose that the $i_{13/2}$ neutrons play the major role in the backbending phenomenon and that essential features are dominated by the two nearest-lying $i_{13/2}$ orbitals. From these orbitals we can generate an excited 1^+ band and an excited 0^+ band that involve, respectively, promotion of one and two nucleons across the Fermi surface from $j\Omega>$ to $j\Omega + 1>$. To avoid spurious 0^+ states we treat the problem in a particle, not quasiparticle, representation. The three bands (including ground 0^+) will interact via pairing and Coriolis interactions. The physical nature we postulate for the important bands allows us to treat them by successive 2 x 2 diagonalizations. If we approximate the upper K = $0^{+\prime}$, and K = 1^+ bands as degenerate before Coriolis interaction, we get simple energy solutions with maximal 50:50 state mixing,

$$W_1 = E_0 + AI(I + 1) \mp H_{cor.}, \qquad (3)$$

where $A = \hbar^2/2\mathscr{I}$, the rotational constant, and the Coriolis matrix element is $H_{cor.} = 2A[j(j + 1) - \Omega(\Omega + 1)]^{1/2}[I(I + 1) - \Omega(\Omega + 1)]^{1/2}$. Taking the lower (minus) sign we have our approximate expression for the superband energies in the absence of mixing with the ground band.

In the limit of low Ω we get the "decoupled band" expression of eq. (2). This is the idealized Stephens decoupling limit.

Having derived a simple analytical expression for S-band energies, we now wish to introduce mixing with the ground band. The mixing matrix elements with the ground band should consist of (a) spin-independent terms coupling th 0^+ components and coming from pairing force and $j_1 \cdot j_2$ recoil and (b) of Coriolis terms with the K = 1 component having the spin dependence $\sqrt{I(I+1)}$. We shall constrain the Coriolis term to have the same $\langle \Omega + 1 | j_+ | \Omega \rangle$ matrix element as in the unmixed S-band expression. The spin-independent term will be a variable to be determined by fitting.

Table 1 gives a sample of least square fits obtainable with six free parameters.

In our model sharp backbending requires that the two large mixing terms nearly cancel at the virtual band crossing. The spin-independent term we believe arises from the pairing interaction coupling to the K = $0^{+\prime}$ component of the S-band wave function, and the other term is Coriolis coupling to the K = 1^+ component.

Table 1. Some experimental and fitted transition energies for cases where data exist in both crossing bands on either side of the crossing point[a]

I_i	I_f	^{164}Er		^{160}Yb		^{168}Hf	
		ΔE_{exp} (keV)	ΔE_{th} (keV)	ΔE_{exp} (keV)	ΔE_{th} (keV)	ΔE_{exp}	ΔE_{th} (keV)
2	0	91.4	113.5	102.3	116.0	124.0	141.6
4	2	208.1	212.2	228.1	222.3	261.7	250.7
6	4	315.9	311.9	337.5	327.2	371.3	358.3
8	6	410.0	405.0	430.3	422.5	456.7	452.0
10	8	493.5	489.4	507.6	505.7	522.2	529.0
12	10	564.5	563.2	569.5	574.7	570.1	584.1
14	12	619.8	621.0	603.5	617.9	551.5	547.8
16	14	560.5	565.1	494.5	491.8	453.0	462.2
18	16	505.5	512.4	509.1	515.3	522.2	525.9
20	18	577.1	579.4	588.8	584.9	607.7	595.5
22	20	654.4	650.7				
24	22	729.0	719.3				
16′	14	708.6	711.1	689.0	696.4		
14	12	355.7	359.0				
18′	16′	710.0	715.9	712.0	701.2		
14′	12	792.0	787.3			684.6	682.8
20′	18			724.0	721.4		

[a]The convention above is that the lowest level of a given spin (yrast) is unprimed and the next level of a given spin is primed.

Footnotes and References

*Condensed from Ref. 2

†Physics Department, University of Tennessee, Knoxville, TN 37916

‡Indiana University Cyclotron Facility, Bloomington, IN 47401

§Physics Department, University of California, Davis, CA 95616

**Data Group, Brookhaven National Laboratory, Upton, NY 11973

†† American Public Power Association, 2600 Virginia Avenue, NW Washington, DC 20037

‡‡ Department of Physics and Astronomy, Vanderbilt University, Nashville, TN 37240

1. It may be rationalized that retention in the zeroth order Hamiltonian of the diagonal matrix elements of pairing could make the $0^{+\prime}$ band degenerate with the 1^+.

2. J. O. Rasmussen, M. W. Guidry, T. E. Ward, C. Castenada, L. K. Peker, E. Leber, and J. H. Hamilton, Nuclear Physics, A332, pp. 82-94 (1979).

3. F. S. Stephens and R. S. Simon, Nucl. Phys. A138, p. 25 (1972).

THEORETICAL ROTATIONAL SIGNATURES FOR NEUTRON PICKUP REACTIONS TO $(i_{13/2})^2$ BANDS*

J. Almberger,† I. Hamamoto,‡ G. Leander,§ and J. O. Rasmussen

We show with the particle-rotor model that non-yrast low-spin states, which are structurally related to the rotation-aligned $(i_{13/2})^2$ band causing backbending at higher spins, can be populated selectively by means of $l = 6$ neutron pickup from an odd-neutron target with an appropriate ground-state configuration.[1]

We suggest that lower-spin states with relatively large spin alignment can be located selectively by (^{3}He, α) reactions on even-odd target nuclei having the odd neutron in an $i_{13/2}$ state, i.e. ^{161}Dy $5/2^+$, ^{167}Er $7/2^+$, ^{179}Hf $9/2^+$. The value of performing such experiments has been pointed out earlier[2], and experimental work is now in progress[3]. These large-Q neutron-transfer reactions are known to favor high-j orbitals, in contrast to (d,p) and (d,t), where lower-j orbitals are favored.

We used the parameters of the "$i_{13/2}$ model" as employed in Ref. 4. The results are summarized in Figs. 1 and 2.

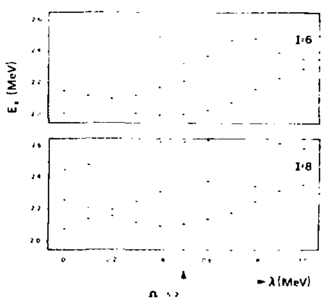

Fig. 1. Spectroscopic factors calculated from the particle-rotor model for I = 6 and 8. The Fermi level λ is varied through eleven values in a MeV range around the Ω = 5/2 orbital, whose position on the abscissa is arbitrarily set to 0.5 MeV. The states with an excitation energy between 2.0 and 2.7 MeV above the calculated I = 0 ground states are marked by dots. The spectroscopic factor is indicated by the length of the horizontal bar on each dot.

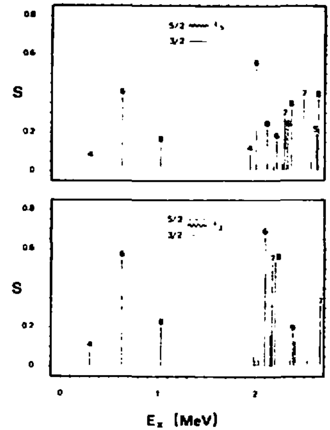

Fig. 2. Theoretical rotational signatures for $i_{13/2}$ *neutron pickup* The *results for spin 6* and 8 from fig. 2 at $\lambda = \lambda_2$ and λ_5 are displayed again in the lower and upper parts of the figure, respectively. In addition the states of the ground band and states with spin 4, 5, 7 and 9 are included. The lower plot might be approximately relevant for a ^{161}Dy target. For $\lambda = \lambda_2$ there are three spin-aligned states, closely spaced at an energy which the present calculation may be predicting somewhat inaccurately, which have as large spectroscopic factors as the I = 6 member of the ground band.

Footnotes and References

*Condensed from Ref. 1.

†Research Institute for Physics, Stockholm, Sweden

‡NORDITA, Copenhagen, Denmark

§Department of Mathematical Physics, Lund Institute of Technology, Lund, Sweden.

1. J. Almberger, I. Hamamoto, G. Leander, and J. O. Rasmussen Phys. Letters 9DB (1,2) pp. 1-5 (1980)

2. B. R. Mottelson, private communication.

3. J. Garrett, G.-M. Jin, G. Lövhöiden, J. Rekstad, T. F. Thorsteinsen and J. Waddington, private communication.

4. J. Almberger, I. Hamamoto and G. Leander, Phys. Lett. 80B, p. 153 (1979).

SURFACE STRUCTURE OF DEFORMED NUCLEI BY RADIAL AND ANGULAR LOCALIZATION IN HEAVY ION SCATTERING*

R. E. Neese,[†] M. W. Guidry,[†] R. Donangelo,[‡] and J. O. Rasmussen

The development of the classical-limit S-matrix (CLSM) formalism[1] has made tractable the analysis of inelastic scattering data for heavy-ion systems and has provided simple and accurate semiclassical models for the excitation mechanism. These calculations[1] demonstrate that (1) because both Coulomb and nuclear forces contribute to the excitation, scattering in this region should probe both charge and mass parameters; (2) at energies below the barrier a relatively clean separation can be made between the effects of the real and imaginary parts of the potential; (3) the short wavelength of the heavy-ion system implies radial localization; (4) the large transfer of angular momentum to the target nucleus implies localization in the orientation of the deformed rotor.

In Fig. 1 we show excitation functions for the system $^{40}Ar + ^{160}Gd$ in the range $E_{lab} = 100$-160 MeV. Assuming the 1 MeV contour defines a surface which is generated by deforming a sharp charge radius $r_c = 1.2\ A^{1/3}_2$ fm and assuming a spherical projectile, we deduce that $\beta_2 \sim 0.34$ and $\beta_4 \sim 0.03$, in reasonable agreement with other determinations of these quantities (e.g., Ref. 3). However, we believe the potential contours shown in Fig. 2 are more fundamental than such model-dependent parameters and provide a direct method of comparing theoretical deformed potentials (e.g., folded or proximity) with a minimum of a priori assumption. For instance, a deformed folded potential can be tested by its ability to reproduce the potential contours of Fig. 2

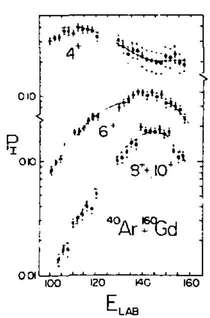

Fig. 1. Excitation functions for various states in the ground band of ^{160}Gd excited by ^{40}Ar projectiles scattered at $\theta_{lab} \sim 170°$. The lines represent fits by our theory. Below ~ 135 MeV the excitation is purely Coulomb.

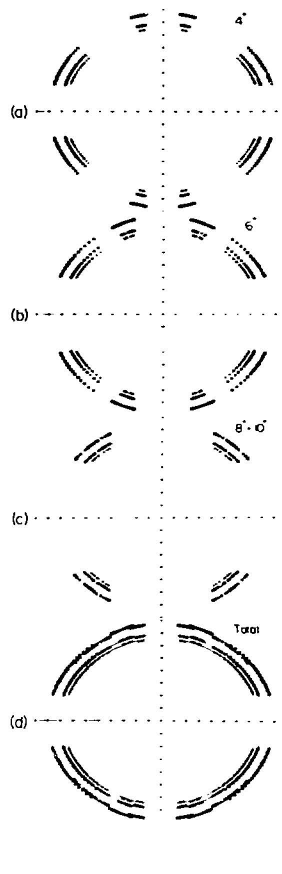

Fig. 2. The deformed ion-ion potential contours. Figs. (a)-(c) represent the contribution of each state, and fig. (d) is the composite nuclear potential energy surface for the ion-ion interaction. Each radial unit is 2 fm. The solid lines are spherical harmonic representations of each contour.

without including the folded potential explicitly in the scattering calculation. We may expect that results such as those in Fig. 2 will encourage the extension of folded and proximity potentials to include an adequate treatment of deformed systems. Such a program has recently been initiated by Randrup and Vaagen for proximity potentials.[4]

Footnotes and References

*Condensed from Ref. 1.

†Department of Physics and Astronomy, The University of Tennessee, Knoxville, TN 37916, USA and Oak Ridge National Laboratory, Oak Ridge, TN 37830, USA.

‡Universidade Federal do Rio de Janeiro, Rio de Janeiro, Brasil.

1. R. E. Neese, M. W. Guidry, R. Donangelo, and J. O. Rasmussen, Phys. Letter, 85B (2,3), pp. 201-205 (1979).

2. M. W. Guidry et al., Nucl. Phys. A274, 183 (1976); H. Massmann and J. O. Rasmussen, Nuclear Phys. A243, 155 (1975); M. W. Guidry et al, Nucl. Phys. A295, 482 (1978).

3. K. A. Erb et al., Phys. Rev. Lett 29, 1010 (1972).

4. J. Randrup and J. S. Vaagen, Phys. Lett. 77B, 170 (1978).

GIANT RESONANCE POLARIZATION TERMS IN THE NUCLEUS-NUCLEUS POTENTIAL*

J. O. Rasmussen, P. Möller,[†] M. Guidry,[†] and R. Neese[†]

Effective polarization potentials for adiabatic Coulomb coupling to giant resonances are derived for heavy-ion collisions (see Table 1). The isovector giant dipole resonance and isoscalar giant quadrupole resonance are found to contribute attractive terms varying as $Z_1^2 Z_2^2/r^4$ and $Z_1^2 Z_2^2/r^6$ respectively to the effective nucleus-nucleus potential. Because of the strong Z-dependence these terms become significant in the collision of very heavy ions, dominating the far tail of the ion-ion potential. Analysis of a recently determined surface potential for $^{40}Ar + ^{160}Gd$ suggests the presence of such polarization terms. We calculate that for a $^{208}Pb + ^{208}Pb$ collision the adiabatic polarization potential exceeds the real nuclear ion-ion potential estimated by the proximity theorem for center-of-mass separation distances $r \gtrsim 1.4\ (A_1^{1/3} + A_2^{1/3})$. Furthermore, at the point where the polarization and nuclear potentials become equal $-V_{pol}$ may be 2-3 MeV for very heavy systems (see Fig. 1). Therefore the adiabatic polarization represents a measurable effect that may be expected to play a significant role for heavy-ion reactions in which discrete final states are observed.

Table 1. Polarization potential at grazing distance $1.6\ (A_p^{1/3} + A_t^{1/3})$ Fm.

Projectile	Target	R(Fm)	V_{VDR}(MeV) G-Dipole	V_{SQP}(MeV) G-Quadrupole
$^{40}_{18}Ar$	$^{40}_{20}Ca$	10.9	0.040	0.011
	$^{140}_{58}Ce$	13.8	0.129	
	$^{208}_{82}Pb$	15.0	0.182	
	$^{238}_{92}U$	15.4	0.203	
$^{86}_{36}Kr$	^{140}Ce	15.4	0.311	
	^{208}Pb	16.5	0.453	
	^{238}U	17.0	0.511	
^{208}Pb	^{208}Pb	19.0	1.230	0.237
	^{238}U	19.4	1.404	
^{238}U	^{238}U	19.8	1.607	0.307

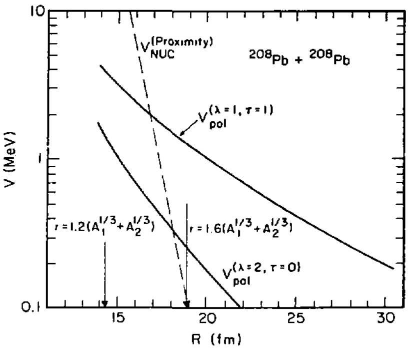

Fig. 1. Calculated polarization potentials (giant modes) for the system of two ^{208}Pb nuclei and comparison to the nuclear proximity potential. Note that by this estimate the polarization potential may reach several MeV before being masked by the real nuclear potential. (XBL 7910-12119)

Footnotes and Reference

*Condensed from Neils Bohr Institute report NBI-79-40 and Ref. 1.

† Lund Institute of Technology, Lund, Sweden

‡ Department of Physics, University of Tennessee, Knoxville, Tennessee

1. J. Rasmussen, P. Möller, M. Guidry, and R. Neese, Nuclear Physics A341, No. 1, p. 149 (1980).

2. Macroscopic

PRODUCTION OF HEAVY ACTINIDES FROM INTERACTIONS OF ^{16}O and ^{18}O with ^{248}Cm

Diana Lee, Barbara Jacak, Matti Nurmia, Cheng Quo, Glenn T. Seaborg
and
Darleane C. Hoffman*

The transfer of many nucleons from heavy-ion projectiles to target nuclei is a phenomenon that has been known for some time. A variety of techniques has been used to measure details of the product kinetic energies and angular distributions. Hahn et al.[1] have investigated the reactions of ^{12}C with ^{239}Pu and ^{238}U leading to ^{244}Cf and ^{245}Cf. More recently, considerable attention has been devoted to the production of actinides and possible superheavy elements by bombardment of ^{238}U and other heavy targets with very heavy ions (^{48}Ca, ^{86}Kr, ^{136}Xe, ^{238}U). However, no comprehensive measurements have been made of actinide yields between target and compound nucleus for systems involving heavy actinide targets and neutron-rich lighter heavy ions such as ^{18}O or ^{22}Ne. In the current work we have used radiochemical separation techniques to isolate and measure yields of isotopes of Bk through No produced in ^{18}O bombardments of ^{248}Cm. One of the most dramatic results is that isotopes of all these elements are formed in relatively high yields compared to those observed for bombardment with ^{86}Kr, ^{136}Xe, or ^{238}U ions. In on-line experiments we have previously detected[2] and measured the properties of a 1.5-sec spontaneous fission activity that is probably ^{259}Fm, the most neutron-rich nuclide known, from bombardment of ^{248}Cm with ^{18}O ions. In order to assess the importance of the extra pair of neutrons in ^{18}O, we have also measured yields of the same elements for bombardment of ^{248}Cm with ^{16}O.

In these experiments a target of $^{248}CmF_3$ containing 924 μg/cm^2 of ^{248}Cm was bombarded with 95-MeV ^{18}O and ^{16}O ions. The recoiling products were caught in a 2 mg/cm^2 gold foil which was subsequently dissolved for radiochemical processing. After preliminary processing, the individual actinides were separated by elution from a cation exchange resin column with hot alpha-ammonium isobutyrate. (The overall chemical yield was 80%.) The resulting actinide fractions were assayed by standard fission counting, and alpha and gamma spectrometry. The yields determined for the ^{18}O and ^{16}O bombardments of ^{248}Cm are shown in Fig. 1. They were calculated assuming all recoiling actinides escaped from the target (6.5 mm diam.) and were caught in the gold catcher foil (19.5 mm diam) which was about 3 mm from the target.

Comparison of the results for ^{18}O with those for ^{16}O show that the maxima of the

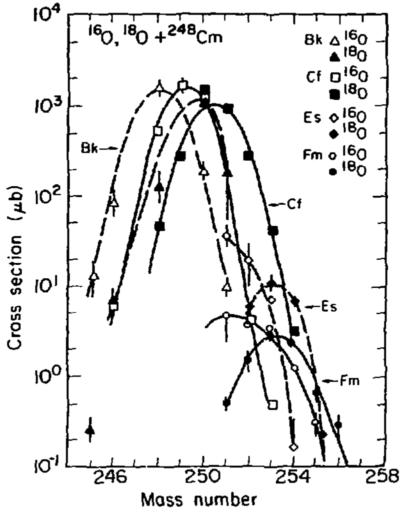

Fig. 1. Yields of the heavy actinides from 95-MeV bombardments of ^{248}Cm with ^{16}O and ^{18}O.
(XBL 811-3579)

mass-yield curves for each element are shifted to the neutron-rich side by about 2 mass units for ^{18}O relative to ^{16}O, reflecting the neutron excess of the projectile. The yield curves also appear to be rather symmetric and do not drop off sharply on the neutron-rich side. The peak yields are relatively large, ranging from a few mb for the Bk and Cf to a few μb for Fm. This is to be compared with peak yields of about a mb to a few tenths of a μb, for example, in the ^{136}Xe bombardment of ^{248}Cm. In general, the maxima of the yield curves are smaller for the ^{18}O than for the ^{16}O bombardments, but the yields of neutron-rich products are much higher. These "transfer-type" reactions may offer a method for making new neutron-rich isotopes for study that have not previously been available to us. We also propose to similarly study reactions with ^{20}Ne and ^{22}Ne and compare the results with predictions based on various mechanisms such as transfer, deep inelastic, and incomplete fusion reactions.

Footnotes and References

*Chemistry-Nuclear Chemistry Division, Los Alamos Scientific Laboratory, Los Alamos, NM 87545.

1. R. L. Hahn et al., Phys. Rev. C 10, 1889, (1974).

2. D. C. Hoffman et al., LBL Nuclear Science Division Annual Report for 1979, LBL-9711.

ADDITIONAL EVIDENCE FOR THE PRODUCTION OF ^{259}Fm IN THE BOMBARDMENT OF ^{248}Cm with ^{18}O

D. C. Hoffman,* D. Lee, A. Ghiorso, M. J. Nurmia and J. M. Nitschke

We used the MG fission-fragment spectroscopy system to make more precise measurements on the 1.5-second spontaneous-fission activity that we had tentatively identified as ^{259}Fm.[1]

The activity was again produced by bombarding a 490 $\mu g/cm^2$ target of ^{248}Cm with 95-MeV (in target) ^{18}O ions from the LBL 88 Inch Cyclotron. The recoil nuclei were stopped in helium seeded with NaCl aerosol and transferred through a capillary to the MG system where they were deposited on collection foils mounted on an 80-position fiberglass wheel. The wheel was stepped every two seconds to bring the foils successivley between four pairs of solid-state detectors for the recording of coincident fission fragments.

By replacing the wheel with a new one containing 80 clean foils every 40 minutes we were able to reduce the buildup of the 2.7-hour ^{256}Fm to such a low level that its contribution in the first crystal pair during the first two seconds of observation was only 4%. No attempt was made to subtract this background from the energy spectra.

We again found the mass-yield distribution to be narrowly symmetrical. The half-life of the activity was determined to be 1.5 ± 0.1 seconds, in agreement with the value of 1.5 ± 0.2 seconds measured by Hoffman[2] for pure ^{259}Fm produced via the ^{257}Fm (t,p) reaction.

The pre-neutron-emission total kinetic energy (TKE) spectrum for 542 pairs of coincident fission fragments observed in the first detector pair is shown in Fig. 1. The average TKE was found to be 233 MeV, in close agreement with the most probable TKE of 242 MeV measured for pure ^{259}Fm[2].

The close agreement of the measured half-life and TKE with those of ^{259}Fm would of course support the identification of the activity as ^{259}Fm. However, we feel that further measurements are in order before a positive assignment is made; in particular, more information is needed about the (1.89 ± 0.88) second fission activity observed by Bemis et al[3] in bombardments of ^{249}Cf with ^{15}N and ascribed by them to a spontaneous-fission branching in the decay of ^{260}Ha.

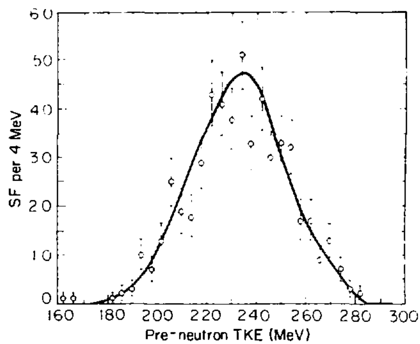

Fig. 1. The distribution of pre-neutron-emission total kinetic energies of 542 pairs of coincident fission fragments observed in the first detector pair. The average TKE is 233 MeV. (XBL 807-1547)

Footnote and References

*Chemistry-Nuclear Chemistry Division, Los Alamos Scientific Laboratory, Los Alamos, NM 87545

1. D. C. Hoffman, D. Lee, A. Ghiorso, M. J. Nurmia, J. M. Nitschke and K. Aleklett, LBL-9711 p. 66.

2. Darlene C. Hoffman, "Fission Properties of Very Heavy Actinides", IAEA 4th Symp. Phys. and Chem. of Fission, Julich, Germany, May 1979; IAEA-SM-241/B14; LBL-9126 (May 1979).

3. C. E. Bemis, Jr., P. F. Dittner, R. J. Silva, R. L. Hahn, J. R. Tarrant, L. D. Hunt, and D. C. Hensley, Phys. Rev. C16, 1146 (1977).

MAXIMUM LIKELIHOOD ANALYSIS OF NEW SHORT-LIVED SPONTANEOUS FISSION ACTIVITIES

L. P. Somerville, R. C. Eggers, M. E. Leino, J. M. Nitschke, A. Ghiorso, M. J. Nurmia

In the last annual report[1] we discussed the observation of several spontaneous fission (SF) activities with half-lives of 19 ms, 54 ms, 1.4s, and 4.8s, produced in the reactions $^{16}_{8}O$ + $^{248}_{96}Cm$, $^{18}_{8}O$ + $^{248}_{96}Cm$, $^{15}_{7}N$ + $^{249}_{97}Bk$, and $^{13}_{6}C$ + $^{249}_{97}Bk$ and detected using the recoil tape transport system. The half-lives were determined by least mean squares (LMS) analysis.

Shortcomings of half-life analysis using any of several LMS codes became apparent when dealing with few events. Therefore, a maximum likelihood (ML) computer code was written which could accommodate up to five components, in contrast to Ref. 2, which could accommodate only one variable component. This ML code makes use of the decay time t_i of each nucleus in determining the decay constants λ_j and amounts A_j of each component j; it maximizes the likelihood function

$$L = \prod_{i=1}^{n} \left(\sum_{j=1}^{m} A_j e^{-\lambda_j t_i} \Big/ \sum_{j=1}^{m} \lambda_j A_j \int e^{-\lambda_j t} dt \right)$$

where the integral extends over the time of observation. This extracts the maximum amount of information from the data.

A comparison of ML and LMS analyses of the same sets of experimental data revealed that the half-lives determined by the ML code were as much as ten per cent longer than the LMS values. Therefore, it was decided to test the ML code using computer-generated artificial data for which the half-life was fixed. Assuming a 23.3 ms half-life, 157 sets of 645 decay times with Poisson statistical fluctuations were generated. These event times were then analyzed with the ML code to determine the apparent half-life. The distribution of half-lives, as shown in Fig. 1 has a mean value of 23.3 ms which is in agreement with the 23.3 ms half-life assumed in generating the data. A similar test of 28 sets of 645 decay times plus background again showed that the ML code was able to reproduce the assumed half-life.

Having been thoroughly tested, the ML code was used to analyze the results of several experiments. Table 1 lists the half-lives of the observed SF activities in ms and the projectile energies in MeV as $T_{1/2}(E)$ determined by the ML code for experiments using the drum[3] and tape[1] systems.

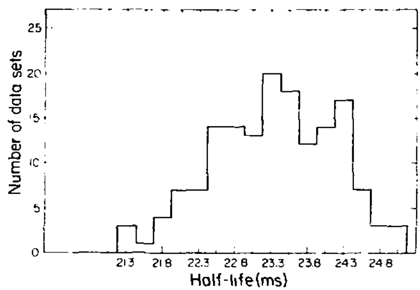

Fig. 1. Distribution of half-lives determined by the maximum likelihood code for 157 sets of 645 decay times, computer generated by assuming a 23.3 ms half-life and Poisson statistical fluctuations. (XBL 807-1389)

With the ML analysis it now appears that a 20-24 ms SF activity was produced in the reactions 78-86 MeV ^{15}N + ^{249}Bk and 92 MeV ^{16}O + ^{248}Cm; also for 88-100 MeV ^{15}N + ^{249}Bk and 109 MeV ^{18}O + ^{248}Cm a 15-17 ms SF activity was produced. However, on the basis of the available statistics we cannot distinguish between the 15-17 ms SF activity being a pure activity or the result of a small admixture of a short-lived component of ~ 5 ms with a 20-24 ms SF activity. These data alone do not allow us to make definite isotopic assignments, due to the non-specific nature of the fission process. But these results, together with the excitation function data of Refs. 1 and 3, are now not inconsistent with the possible assignment of $^{260}_{104}Rf$ to the 20-24 ms SF activity and another

Table 1

reaction	system	component 1	component 2
$^{15}N + ^{249}Bk$	drum tape	23 ± 2(78,82,86,	15 ± 4 (88,100)
$^{16}O + ^{248}Cm$	tape	21 ± 1(92)	
$^{18}O + ^{248}Cm$	tape	16.7 ± 1.5 (109),	53 ± 4 (89)

SF activity with Z < 104, (e.g., $^{261}_{103}Lr$) to the 15-17 ms SF activity. An assignment of the 50-55 ms SF activity to $^{262}_{104}Rf$ would be consistent with our data.

References

1. J. M. Nitschke et al., Nuclear Science Division Annual Report 1978-1979, LBL-9711, p. 63.

2. V. B Zlokazov, Nucl. Instr. and Meth. 151, p. 303, (1978).

3. J. M. Nitschke et al., Nucl. Phys., to be published (1981).

EXOTIC REACTIONS IN THE BOMBARDMENT OF ^{208}Pb by ^{18}O

A. Ghiorso, R. M. McFarland, M. Leino and S. Yashita

In the reaction $^{248}Cm + ^{18}O$ we have produced[1] a 1.5 sec spontaneous fission activity with a 15 nb cross section. Within experimental error it demonstrates the same characteristics, symmetric fission, total kinetic energy, and half-life, as the known[2] nuclide ^{259}Fm. If this assignment is correct it suggests the intriguing reaction mechanism in which the ^{18}O projectile transfers a ^{11}Be nucleus to the target with minimal kinetic energy loss.

To test this hypothesis we have bombarded ^{208}Pb with ^{18}O at the 88 Inch Cyclotron and sought the equivalent product, ^{219}Rn. This nuclide decays by the sequence:

$$^{219}Rn \xrightarrow[3.96\ s]{\alpha} {}^{215}Po \xrightarrow[1.78\ ms]{\alpha} {}^{211}Pb \xrightarrow[36.1\ m]{\beta^-} {}^{211}Bi \xrightarrow[2.15\ m]{\alpha}$$

The reaction recoils were stopped near the target in helium and the atoms conducted quickly into a metal sphere of 5-inch diameter with a gas flow rate of about 10 cm^3/sec. An insulated plate charged at -600 V was placed at the top of the sphere to collect the granddaugher ^{211}Pb ions generated by the alpha decay of the precursors.

Directly produced alpha activities that could interfere with the search for ^{211}Pb from ^{219}Rn were removed with both a 3-micron filter and a coaxial electrostatic precipitator in the line connecting the target chamber to the sphere. We measured the efficiency of the system by using a thin ^{223}Ra source to generate ^{219}Rn at a known rate into the target chamber, and found it to be nearly 100%. After each bombardment of 0.5 to 1 hour the collector plate was removed and analyzed for the distinctive alpha particles from ^{211}Bi in secular equilibrium with ^{211}Pb.

A small number of preliminary bombardments have been made at 110 MeV. The only alpha activity observed on the collector plate was from ^{211}Bi and decayed with about a half-hour half-life, at a rate corresponding to a cross section for ^{219}Rn of roughly 10 nb. Further bombardments are planned at different energies.

Using the same target, we have also detected ^{220}Fr, presumably made via the mechanism $^{208}Pb(^{18}O,^{6}Li)^{220}Fr$. This nuclide decays by the sequence:

$$^{220}Fr \xrightarrow[27.4\ s]{\alpha} {}^{216}At \xrightarrow[0.3\ ms]{\alpha} {}^{212}Bi \xrightarrow[60.5\ m]{\alpha(36\%)}$$

$$^{212}Bi \xrightarrow{\beta^-\ (64\%)} {}^{212}Po \xrightarrow{\alpha\ 0.3\mu s}$$

The experiments were set up to milk alpha recoils from the decaying ^{220}Fr and detect the alpha radiations from the 60.5 m duo $^{212}Bi \longrightarrow {}^{212}Po$.

The francium atoms were stopped in helium loaded with NaCl aerosol and transferred via helium jet to catcher plates in vacuum. The plates were mounted on an 80-step wheel that moved one step every 28 seconds. Secondary alpha-recoil catchers were mounted next to the first ten plates following the helium jet. After one cycle of the wheel these catchers were removed and analyzed for the alpha radiations from ^{212}Bi and ^{212}Po with a set of 10 Si-Au detectors.

Only one experiment has been tried so far, but it indicates that ^{220}Fr is produced. Some 42 events from ^{212}Bi/^{212}Po decaying with a half-life of about an hour were observed in the first four secondary catchers. The amount of activity in each foil successively decreased consistent with the half-minute half-life of ^{220}Fr.

If we assume that the ^{220}Fr gas jet yield was 50% and that 50% of the alpha-recoiling daughters were collected, then the cross section for the reaction ^{208}Pb (^{18}O,^{6}Li)^{220}Fr is roughly 0.3 microbarns at 110 MeV.

We calculated optimum Q-values and optimum excitation energies for these bombardments to see if the ^{248}Cm experiments energetically favored the "^{11}Be" transfer more than the ^{208}Pb experiments did. This preliminary calculation includes only Coulomb and recoil effects on the trajectory of the system.[3]

From Table 1, no great difference between these bombardments is immediately obvious that would explain the contradictory experimental results by Q_{opt} considerations alone. More thorough calculations will be done that will include nuclear and centrifugal contributions to Q_{opt} and, more importantly, that will consider transfer amplitudes and de-excitation survival probabilities of the heavy products.

The Q_{opt} calculations for the ^{18}O + ^{208}Pb system show that at lower initial kinetic energies, around 80 MeV (c.m.s.), $-Q_{opt}$ is 43 MeV for ^{219}Rn production. This is too low to overcome the $-Q_{gg}$ of 48.1 MeV. For ^{220}Fr production, $-Q_{opt}$ is 52 MeV, higher than the $-Q_{gg}$ of 48.1 MeV. This suggests that ^{220}Fr should be produced at lower energies with ^{219}Rn beginning to show up at higher energies. Our planned measurement of the excitation functions of these reactions should shed light on these estimates.

Table 1

System	Products	E_{lab}^{inc}(expt) (MeV)	Q_{gg} (MeV)	Q_{opt} (MeV)	E^a (MeV)
^{18}O + ^{248}Cm	^{259}Fm^a + ^{7}Be	95	-42.7	-47.4	4.7
	^{260}Md ^{ab} + ^{6}Li		-44.2	-57.8	13.6
^{18}O + ^{208}Pb	^{219}Rn + ^{7}Be	110	-47.1	-53.7	6.6
	^{220}Fr + ^{6}Li		-48.1	-65.7	17.6

^{a}Droplet model[4] mass used
^{b}imaginary nucleus

References

1. D. C. Hoffman, D. Lee. A. Ghiorso, M. J. Nurmia, J. M. Nitschke, and K. Aleklett, LBL-9711, p. 66 (1980).

2. Darleane C. Hoffman, "Fission Properties of Very Heavy Actinides," IAEA 4th Symp. Phys. and Chem. of Fission, Julich, Germany, May 1979; IAEA-SM-241/B14' LBL-9126 (May 1979).

3. F. Hubert, H. Delagrange, A. Fleury, Nucl. Phys. A 228 (1974) 415-431.

4. William D. Myers, Droplet Model of Atomic Nuclei, Plenum, New York 1977.

ACTINIDE PRODUCTION FROM THE REACTION OF ^{136}Xe with ^{248}Cm

K. J. Moody, D. Lee, R. Welch, B. V. Jacak, R. M. McFarland, P. L. McGaughey, M. J. Nurmia, M. Perry, G. T. Seaborg, R. W. Lougheed,* P. A. Baisden,* and E. K. Hulet*

We have measured the production cross-sections for many of the actinide nuclides formed by the reaction of ^{136}Xe with ^{248}Cm, at a projectile energy between 865 MeV and 795 MeV (1.2 to 1.1 times the Coulomb barrier). These are plotted in Fig. 1 as a function of the product mass number. The trans-target (Z greater than 96) cross-sections for a given element show peaks in the curves at slightly lower mass numbers compared with those measured for the same element in the reaction of ^{48}Ca with ^{248}Cm.[1] An extrapolation of the sub-target (Z less than 96) cross-sections indicates that the ^{136}Xe plus ^{248}Cm reaction may provide a viable method for the production and identification of new neutron-rich Pu and Am isotopes.

This set of data was obtained from two irradiations at the SuperHILAC, where a beam of 1130 MeV ^{136}Xe was delivered to our recently constructed actinide target facility[2]. The beam was focused through a 5-mm collimator, after which it passed through a thin Havar isolation foil and a 2.6 mg/cm^2 beryllium target backing before striking a target consisting of 2.1 mg/cm^2 of ^{248}Cm, which was present as the fluoride. Recoil nuclei were collected with a conical catcher foil between the laboartory angles of 15° and 75° with respect to the beam direction. No catcher foil geometry corrections have been applied in calculating the cross-sections summarized in Fig. 1.

During the first irradiation of 18 hours an average beam current of 300 electrical nanoamperes passed through the target. The gold catcher foil was dissolved in aqua regia and the resulting solution was passed through an anion exchange column (Dowex-1 resin). The transplutonium elements were eluted from the column with concentrated HCl, while the lighter actinide elements remained on the resin. The concentrated HCl solution containing the heavy actinides was evaporated to dryness, after which the activity was dissolved in a small volume of dilute HCl and loaded onto a cation-exchange column (Dowex-50x12) at an elevated temperature. The actinides from Cf to Md were separated from each other by elution with a low pH α-hydroxyisobutyrate solution. The column was then stripped, giving a solution containing Am, Cm and Bk, which was passed through a cation-exchange column in saturated HCl to separate the actinides from lanthanide contaminants. The original anion-exchange column was stripped of the elements from Pa to Pu, which were further processed to remove any fission products. The chemical fractions containing Cf to Md were counted to detect alpha and spontaneous fission activities, using a pulse-height analyzer, for a period of over one-half year with Si surface-barrier detectors. The other fractions were counted to detect gamma-ray emitting activities, with Ge(Li) detectors, for up to several weeks. The production cross-sections were obtained from decay curve analysis of the observed activities.

A second irradiation of 30 minutes duration, with an average beam current of 180 electrical nanoamperes, was performed to ascertain the yield of the short-lived ^{247}Am and ^{246}Am (two isomers). The aluminum catcher foil was dissolved in concentrated NaOH, and Am was co-precipitated with $La(OH)_3$. The precipitate was dissolved in HNO_3, Am(III) was oxidized to Am(VI), and LaF_3 was precipitated to remove the lanthanides from solution. Am(VI) was then reduced to Am(III), which was co-precipitated with LaF_3 in a second step. The insoluble product was ready for counting of the gamma-ray activities within 40 minutes after the end of bombardment.

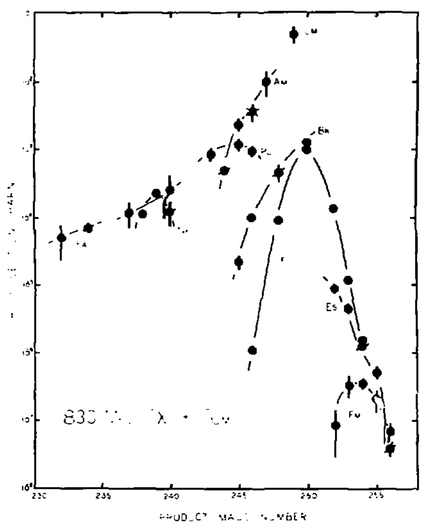

Fig. 1. Production cross-sections vs. product mass numbers from the reaction of ^{136}Xe with ^{248}Cm. (XBL 808-1558)

Comparison of the trans-target cross-sections from the reaction of ^{136}Xe and ^{248}Cm with those from the reaction of ^{48}Ca and ^{248}Cm, at an energy of 1.1 to 1.0 times the Coulomb barrier, shows that for products near the target the distributions of cross-sections as a function of mass number for a given element are very similar for the two reactions. As Z increases, the distribution for the ^{136}Xe plus ^{248}Cm reaction seems to shift to lighter mass. This shift is about one mass unit in the distribution of Fm isotopes. The peak cross-sections remain roughly equal in magnitude for the two reactions. Examinations of the cross-sections for the production of Pu and Am isotopes indicates that the cross-sections for the unknown nuclides ^{247}Pu and ^{248}Am should be on the order of tenths of millibarns and millibarns, respectively.

Footnote and References

*Lawrence Livermore Laboratory, Livermore, Ca. 94550

1. E. K. Hulet et al., Phys. Rev. Lett. 39, 385 (1977).

2. K. J. Moody, M. J. Nurmia and G. T. Seaborg, in this Annual Report.

PRODUCTION OF ^{194}At IN THE BOMBARDMENT OF ^{141}Pr WITH ^{56}Fe

S. Yashita, M. Leino,* and A. Ghiorso

The availability of rather neutron-deficient heavy projectiles such as ^{56}Fe, together with the development of a fast on-line mass separator system, enable us to produce and detect new neutron-deficient isotopes in the At region.

We bombarded a 0.6 mg/cm^2 ^{141}Pr target at the SuperHILAC with ^{56}Fe particles at energies from 243 MeV to 275 MeV. After the separation of the beam by the helium-filled SASSY mass separator magnet the fusion recoil products were focused by quadrupole magnets and passed through a pair of position sensitive counters to get time of flight information. Finally the recoil nuclei were implanted in an array of 10 silicon surface barrier detectors that were used to detect their subsequent alpha decay.

In this bombardment an unknown 7.21 MeV alpha activity with a 0.2 sec halflife was found. We searched for the possible alpha decays of daughter nuclei within 10 seconds following the detection of a 7.21 MeV alpha particle. As a result, 6.45 MeV alpha particles with a halflife of 5 ± 2 sec were found to be correlated with the 7.21 MeV alpha particles. The probability that this correlation is accidental was estimated to be less than 0.0001. Since the known nuclide ^{190}Bi (6.45 MeV alpha emitter with a 5.4 sec halflife) has the observed characteristics,[1] we assigned the 7.21 MeV alpha activity to ^{194}At, the mother of ^{190}Bi. The decay scheme is as follows:

$$^{194}\mathrm{At}\ \xrightarrow[0.2\ \mathrm{s}]{7.21\ \mathrm{MeV}\alpha}\ ^{190}\mathrm{Bi}\ \xrightarrow[5.4\ \mathrm{s}]{6.45\ \mathrm{MeV}\alpha}\ ^{186}\mathrm{Tl}$$

This assignment is further supported by the results of a calculation with the neutron evaporation code JORPLE[2] which predicts that the cross section for the reaction $^{141}Pr(^{56}Fe,3n)^{194}At$ has its maximum at 256 MeV bombarding energy. Our experimental excitation function for this new activity has a maximum at 258 MeV with 15 MeV FWHM. The cross section is of the order of 1 μb.

Footnote and References

*On leave from University of Helsinki, Finland

1. Y. Le Beyec, M. Lefort, J. Livet, N. T. Porile, A. Siivola, Phys. Rev. C9, 1091 (1974)

2. J. Alonso, Gmelins Handbuch der anorganischen Chemie, Erganzungswerk, 7b A1, II, Springer Verlag, Berlin (1974)

PRODUCTION OF ^{192}Po IN THE REACTION ^{56}FE + ^{140,142}Ce

M. Leino,* S. Yashita, and A. Ghiorso

The recoil spectrometer system SASSY at the SuperHILAC has been used to study the fusion products from the reaction $^{56}Fe + ^{140,142}Ce$. The 315 μg/cm^2 target was prepared by evaporating natural cerium onto a 2.05 mg/cm^2 Havar foil. The reaction products recoiling from the thin target were separated from the primary beam in the SASSY magnet. An array of 10 Si surface barrier detectors each of which had an active area of 12 x 27 mm^2 was used for measuring the recoil energy of the products as well as the alpha decay energies of alpha-active nuclei produced. In a set of earlier runs which have been used as comparison, the time of flight of the recoil products between two gas counters was measured also. The time of flight and the energy of the recoil products are useful in discriminating against recoil nuclei that are not complete fusion products, but still fly through SASSY. In order to measure the excitation functions for different xn products, six bombardments approximately equidistant in energy ranging from 241 MeV to 274 MeV were made.

In the measured alpha-spectra there was a continuous background, probably produced by (n,α)-reactions and recoiling (filling gas) He-nuclei, which are below the threshold to produce a signal in the gas counters. This background is created when the beam is on. In the final analysis only alpha events outside the beam pulses were accepted, and the resulting alpha-spectra were practically background-free. The FWHM of the alpha peaks was approximately 50 keV. The halflife of an alpha activity was determined in the following way: For each alpha particle of a given energy the recoil event in the same detector that had the expected recoil energy (and velocity, if measured) and that preceded it and was closest in time to the alpha particle was chosen as its probable emitter. Thus the average counting rate in each detector determines an upper limit for the halflife that can be measured. The distortions in the decay curves caused by the choice of a wrong recoil nucleus as the emitter of the alpha particle have been corrected in determining the halflives in this work. Since the daughters of the light Po isotopes produced by alpha decay have small alpha decay branches (3.3 or less) it has not been possible to observe mother-daughter or longer delay chains. The assignment of the observed activities is based on the measured excitation functions and on half-life and alpha energy predictions and systematics.

In this work the previously known isotopes $^{193-196}$Po were observed. In addition about 1000 alpha decays from an activity assigned to ^{192}Po were measured. Assuming a 10% efficiency for the observation of the alpha decay of a fusion product in SASSY, the peak production cross section for ^{192}Po in the reaction ^{56}Fe + ^{140}Ce → ^{192}Po + 4n is of the order of 10 μb. The measured alpha energy is 7.17 ± 0.02 MeV and the halflife is 34 ± 3 ms. Of the mass tables published in Ref. 1 the systematics of Liran and Zeldes seem to reproduce the experimental trend of the alpha energies of the light Po nuclei most closely. The prediction of Liran and Zeldes for the alpha energy of ^{192}Po is 7.45 MeV, but from the discrepancy between the predicted and experimental alpha energies for neighboring Po isotopes it can be estimated that this value is too high by ~ 200-230 keV. The extrapolation of the alpha halflife systematics of known light Po isotopes to ^{192}Po gives a halflife of the order of 50 ms. The Taagepera-Nurmia prediction is 30 ms. The alpha energy measured for ^{192}Po in this work differs significantly from the value of 7.12 MeV published previously.[2]

Footnote and References

*On leave from University of Helsink, Finland

1. S. Maripuu (Ed.) Atomic Data and Nucl. Data Table 17, Nos. 5-6 (1976).

2. S. Della Negra, B. Lagarde, and Y. Le Beyec, J. de Phys. Lett. 38, 393 (1977).

CHARGED PARTICLE EMISSION FROM ^{194}Hg COMPOUND NUCLEI: ENERGY AND SPIN DEPENDENCE OF FISSION-EVAPORATION COMPETITION

M. Rajagopalan,* D. Logan,† J. W. Ball,† M. Kaplan,† H. Delagrange,* M. F. Rivet,* J. M. Alexander,* L. C. Vaz,* and M. S. Zisman

Reactions between complex nuclei often give rise to intermediate transition systems with very high spins and excitation energies. For lighter projectile-target combinations this is evidenced by statistically equilibrated compound nuclei. Here the cross section measurements of evaporative H/He emission, fission, and fusion residues make possible the improvement of our understanding of nuclear de-excitation and the testing of equilibrium theory. To this end twelve reactions, indicated in Table 1, were studied. All lead to the compound system ^{194}Hg, over the excitation energy range of 57 to 195 MeV. The ^{12}C, ^{19}F and 125 MeV ^{20}Ne beams were supplied by the 88 Inch Cyclotron and the remaining beams by the SuperHILAC. Fission and evaporation residues were detected by a gas ionization chamber and H/He by solid state telescopes (45 μm, 500 μm, 5 mm Si detectors). Coincidences were also measured between fission and H/He.

In all cases the evaporative component of H/He emission was indicated by center of mass angular distributions which showed backward angle peaking. Morever, there were several factors suggesting that evaporation occurred prior to scission. For example, with the lighter projectile systems the coincidence measurements set an upper limit of 5% on the fraction of H/He in coincidence with fission. Also, for these and the remaining systems there were three additional points: (1) The shapes of the singles spectra were much narrower than those expected from fission fragment evaporation. (2) The high ^{4}He to ^{1}H ratio (≥ 0.6) indicated unrealistically high spins of fission parentage. (3) The coincident H/He energy spectra did not exhibit the kinematic shifts expected of evaporation from the moving fission fragments.

Table 1. Experimental Results for ^{194}Hg Compound Nuclei

	The Reaction Systems											
Beam	^{12}C	^{12}C	^{20}Ne	^{40}Ar	^{12}C	^{19}F	^{40}Ar	^{12}C	^{19}F	^{40}Ar	^{20}Ne	^{40}Ar
Target	^{182}W	^{182}W	^{174}Yb	^{154}Sm	^{182}W	^{175}Lu	^{154}Sm	^{182}W	^{175}Lu	^{154}Sm	^{174}Yb	^{154}Sm
E_{lab} (MeV)	77	106	125	196	121	135	221	167	186	272	252	348
E* (MeV)[a]	57	82	88	88	90	90	100	142	142	141	194	195
	Cross Sections[b] (mb), ^{4}He/^{1}H Ratio, ℓ_{cr} and ℓ_{ER}											
^{1}H	-	204	116	35[†]	266	214	73.5[†]	544	490	242	1109	703
^{2}H	-	17	6.0	2.0[†]	74	25	6.7	65	87	31.4	189	108
^{3}H	-	9	2.6	1.09[†]	11	19	2.9	37	51	15.6	164	66
^{4}He	31	126	73	37	176	152	77	387	354	232	984	624
ER	545	475	291	94	458	351	86	539	317	79	225	126
Fission	23	330	663	~500	607	780	754	861	1056	919	985	1439
Fusion	568	805	954	594	1063	1131	840	1400	1370	998	1210	1563
^{4}He/^{1}H	-	0.61	0.64	0.67	0.6[illegible]	0.71	1.05	0.71	0.72	0.96	0.83	0.89
ℓ_{cr}	25.5	36	53	66	45	39	83	65	76	101	85	142
ℓ_{ER}	25	27	39	26	29	32	26	37	38	28	36	39
	Cumulative Decay Fractions[c]											
^{1}H	-	0.25	0.12	0.091	0.25	0.19	0.087	0.36	0.36	0.26	0.90	0.45
^{2}H	-	0.034	0.006	0.005	0.02	0.022	0.008	0.04	0.063	0.03	0.16	0.07
^{3}H	-	0.011	0.003	0.002	0.01	0.009	0.003	0.02	0.037	0.016	0.09	0.04
^{4}He	0.055	0.15	0.076	0.062	0.17	0.13	0.092	0.26	0.26	0.23	0.81	0.40
ER	0.96	0.59	0.305	0.16	0.43	0.31	0.10	0.38	0.23	0.08	0.186	0.08
Fission	0.04	0.41	0.695	0.84	0.57	0.69	0.90	0.62	0.77	0.92	0.81	0.92

[†]Upper limit.

[a]Q-values were taken from A. H. Wapstra and N. B. Gove, Nucl. Data 9, 265 (1971).

[b]Cross sections for ^{1}H, ^{2}H, ^{3}H, and ^{4}He emission have been integrated for the evaporative component only as described in the text.

[c]$CDF_i = \sigma_i/\sigma_{cf}$.

The identity of fission products was universally unambiguous at angles near 90° in the center of mass and cross sections were estimated as $d\sigma/d\Omega_{c.m.}(90°) \times 2\pi^2$ with the assumption that the angular distribution goes as $1/\sin\theta$. The identity of the fusion residues, however, suffered in most systems from possible contributions from incomplete fusion paths.[1,2] Because of detector energy thresholds this was mainly true for the systems involving the heavier, more energetic projectiles.

Shown in Table 1 are the cross sections and cumulative decay fractions for the systems indicated. The latter quantities were calculated as the ratio of the emission cross section in question to that of the complete fusion cross section. Also listed are the critical angular momenta, computed under the sharp cutoff model, for fusion (ℓ_{crit}) and for evaporation residue survival (ℓ_{er}). Not listed here, but illustrated in Fig. 1, are cumulative alpha decay fractions for intermediate regions of spin spanning the range between ℓ_{crit} values from different entrance channels, but with the same excitation energy.[3]

Figure 1 illustrates the behavior of ^{4}He emission and evaporation residue (ER) survival as a function of excitation energy and average spin. As is evident, the probability for He emission (and H also) increase rapidly with E* while decreasing slowly with spin. This is true even for spins at or greater than that at which the liquid drop model predicts a zero fission barrier (~80ħ).

Shown in Fig. 2 is the behavior of ℓ_{er} ($\sigma_{ER}/\pi\lambda^2$) as a function of E* and ℓ_{crit} for the present system as well as several others reported in the literature.[4] To a first approximation, the statistical Boltzmann model predicts that ℓ_{er} should remain equal to ℓ_{crit} until near the point at which the fission barrier approaches the neutron separation energy and thereafter level off as the barrier continues to decrease. However, what is observed for all systems above is that there appears to be a distinct secondary rise at large ℓ_{crit} and/or E* values.

It is certainly clear that part or all of this trend may be accounted for by extensive pre-equilibrium pathways to the ER products. However there is also a strong suggestion that the surprisingly large H/He emission is directly responsible for the fusion survival even at spins for which the fission barrier approaches zero. In either case, to retain the validity of the statistical model at high E* and/or J the existing framework must be adjusted to allow for *both avenues. While great flexibility is possible by incorporating energy- and exit-channel-dependent level densities, it is possible that the large calculated number of decay channels for fission may be irreconcilable with the experimental observations of large H/He evaporation probability at high E* and J. These results may thus be reflecting an evolution of competition between evaporation and fission away from pure phase space models at lower energies to mechanisms that call for the inclusion of reaction dynamics.

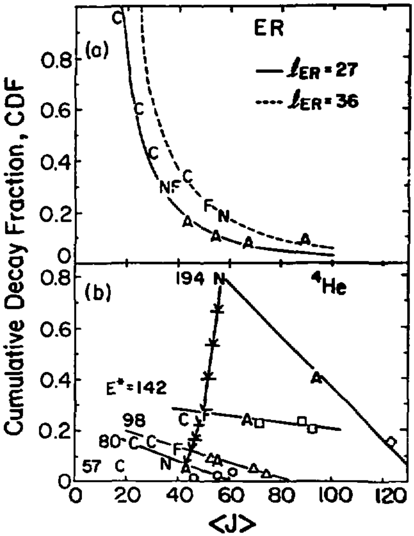

Fig. 1. Cumulative decay fractions for evaporation residues (a) and ^{4}He (b) vs average spin. The letters represent points from Table 1 from the various reactions as shown in Fig. 2. The high-spin zones are shown as: O, 80 MeV; Δ, 98 MeV; □, 142 MeV; ◊, 194 MeV. The nearly vertical arrows for ^{4}He crudely represent evaporation probabilities for each separate step in the evaporation cascade. For ^{194}Hg*, E* = 194 MeV, J = 56, one might guess for the first four evaporation steps that $\Delta J \approx 2$ and $\Delta E^* \approx 12$ for the neutron emission that is expected to dominate. Therefore the summed ^{4}He evaporation probability is ≈0.81 - 0.25 = 0.56 or for each individual step $P_\alpha \approx 0.14$. (XBL 807-10817)

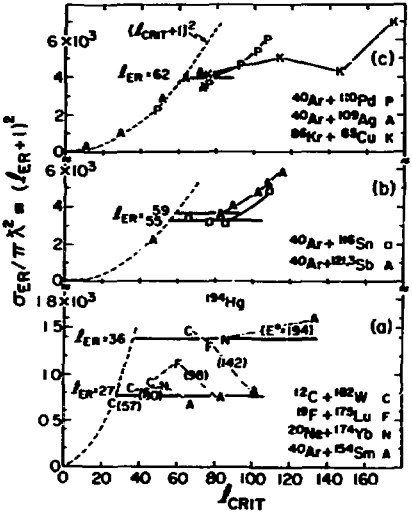

Fig. 2. The dimensionless evaporation residue cross section $\sigma_{ER}/\pi\lambda^2$ vs ℓ_{crit} for several reactions as indicated. (a) Data from this work. Excitation energies are noted for reactions leading to ^{194}Hg*. (b) and (c) Data from Ref. 4. (XBL 807-10818)

Footnotes and References

*State University of New York at Stony Brook, Stony Brook, NY 11794

†Carnegie-Mellon University, Pittsburgh, PA 15213

1. H. Delagrange, D. Logan, M. F. Rivet, M. Rajagopalan, J. M. Alexander, M. S. Zisman, M. Kaplan, and J. W. Ball, Phys. Rev. Lett. 43, 1490 (1979).

2. D. Logan, H. Delagrange, M. F. Rivet, M. Rajagopalan, J. M. Alexander, M. Kaplan, M. S. Zisman and E. Duek, Phys. Rev. C 22, 1080 (1980).

3. See for example, R. C. Reedy, M. J. Fluss, G. F. Herzog, L. Kowalski, and J. M. Miller, Phys. Rev. 188, 1771 (1969); A. M. Zebelman, L. Kowalski, J. M. Miller, K. Beg, Y. Eyal, G. Yaffe, A. Kandil and D. Logan, Phys. Rev. C 10, 200 (1974).

4. B. Tamain, C. Ngô, J. Peter, and F. Hanappe, Nucl. Phys. A252, 187 (1975); H. Gauvin, D. Guerreau, Y. LeBeyec, M. Lefort, F. Plasil, and X. Tarrago, Phys. Lett. 58B, 163 (1975); H. C. Britt, B. H. Erkkila, R. H. Stokes, H. H. Gutbrod, F. Plasil, R. L. Ferguson, and M. Blann, Phys. Rev. C 13, 1483 (1976); S. Della Negra, H. Gauvin, H. Jungclas, Y. LeBeyec, and M. Lefort, Z. Physik A282, 65 (1977).

COMPARISON OF SPECTRA FOR DEEP-INELASTIC AND COMPOUND NUCLEUS REACTIONS*

R. J. McDonald, G. J. Wozniak, A. J. Pacheco,† C. C. Hsu,‡ D. J. Morrissey, L. G. Sobotka, L. G. Moretto
C. Schuck,§ S. Shih,‖ H. Kluge,¶ F. S. Stephens and R. M. Diamond

Recent studies of the continuum γ-ray spectra following compound nucleus (CN) formation have been valuable in understanding nuclear structure at high spin. One naturally asks whether this information may be applied to other energy and angular momentum regimes, for example, deep inelastic (DI) reactions.

Important characteristics of continuum γ-ray spectra from rotational nuclei formed in the CN reaction are the following: a "bump" at about 1.0 MeV formed by the stretched E2 yrast and yrast-like transitions, where the high-energy edge is observed to move to higher energies as spin increases, and an isotropic "statistical tail" extending to several MeV. The "bump" structure is quite evident for rotational nuclei, but becomes less pronounced for products near closed shells.

Figure 1(a) illustrates the general features of in-plane and out-of-place γ-ray spectra from the DI reaction ^{165}Ho + ^{165}Ho at 8.5 MeV/A. The spectral shapes are similar to those observed in CN reactions and display the characteristic "E2 bump" at about 0.6-1.2 MeV. A comparison of these two spectra shows that the bump is more pronounced in-plane where the angular distribution for stretched E2 transitions peaks. Also evident is the statistical tail, extending to several MeV, and isotropic within experimental uncertainties.

In-plane γ-ray spectra, normalized so that the integral of each curve is equal to the average number of γ-rays emitted, $\langle M_\gamma \rangle$, are shown in Fig. 1(b) for several Q-value regions. The upper edge of the E2 bump moves to higher energy as Q increases through the quasi-elastic (QE) region (~ 0-150 MeV) and stabilizes in the DI region (~ 150 to 400 MeV). This effect, having the same spectral shapes for the regions 148<Q<191 MeV and 233<Q<276 MeV, indicates that the spin transfer is saturating. γ-multiplicity data (not shown) verifies this effect. The upper edge of the E2 bump moves from about 0.7 MeV to 2.0 MeV as Q changes from zero to 150 MeV. Over this same range of Q, $\langle M_\gamma \rangle$, changes from ~ 5 to 30. This is consistent with the findings for rotational nuclei whre E ∝ I.

The statistical tail has nearly the same slope for each spectrum. One can estimate the number of statistical transitions in each spectrum by fitting a function:

$$F(E_\gamma) \propto E_\gamma^2 EXP(-E_\gamma/T)$$

where T is an effective nuclear temperature, and is taken here as 0.6 MeV. Upon doing this, we obtain a somewhat varying number of statistical transitions as a function of Q bin, going from 0.9 to 2.1 to 3.3 to 3.3 for the four Q regions shown.

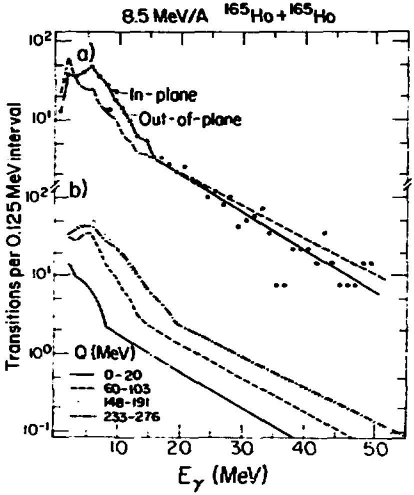

Fig. 1 (a) In- and out-of-plane γ-ray pulse-height spectra associated with reaction products having a Q ≈ -140 MeV. (b) In-plane γ-ray spectra for several Q-value bins.
(XBL 806-1194a)

In summary, the general characteristics of the continuum γ-ray spectra for rotational nuclei formed by DI reactions are similar to those formed by CN reactions. This similarity opens the door to significant new experiments in DI reactions using the same techniques that have proven so valuable for CN reactions.

Footnotes

*Condensed, in part, from LBL-11057, G. J. Wozniak, et al., Phys. Rev. Lett. 45, 1081, (1980)

Permanent addresses:

†Comision Nacional de Energia Atomica, Argentina

‡Institute of Atomic Energy, Beijing, China

§C. S. N. S. M., Orsay, France

‖Shanghai Institute of Nuclear research, China

¶Hahn-Meitner Institute, Berlin, Germany

SYNTHESIS OF HEAVY AND SUPER HEAVY ELEMENTS IN THE DEEPLY INELASTIC COLLISION OF ^{238}U WITH ^{248}Cm

J. Michael Nitschke, W. Bruchle,[*] H. Gaggeler,[*] J.V. Kratz,[*] M. Schadel,[*] K. Summerer,[*]
G. Wirth,[*] E. K. Hulet,[†] R. W. Lougheed,[†] A. Ghiorso, R. L. Hahn,[‡] F. L. Ferguson,[‡]
R. Stakemann,[§] N. Trautmann,[§] and G. Herrmann[§]

This is a preliminary report about an attempt to produce super heavy elements (SHE) and to study the yield of actinides in deeply inelastic collisions (DIC) of ^{238}U with ^{248}Cm.

Cm metal targets 4 to 7 mg/cm^2 thick were bombarded with ^{238}U ions from the Unilac, Darmstadt (West Germany). The target thickness was sufficient to degrade the beam energy from 7.5 MeV/A to below the interaction barrier. An unexpected experimental difficulty was encountered when the targets failed at total integrated beam currents of about $5 \cdot 10^{14}$ U ions, a factor 100 below the expected value. Nevertheless two experiments were carried out as planned albeit with reduced sensitivity: target recoils were stopped in (1) copper catchers and chemically separated, and (2) in Kr gas and analyzed for volatile, noble SHE's.

The results for the heaviest actinides observed in the chemistry experiment are shown in Fig. 1 together with previous results from ^{48}Ca (Ref. 1) and ^{136}Xe (Ref. 2) bombardments of ^{248}Cm targets and ^{238}U + ^{238}U (Ref. 3) for comparison. SHE's were not observed in either experiment with a cross section limit of less than 1 nb for half lives between 1 and 100 days. Cross section predictions by Riedel et al., using a diffusion model are of the same order of magnitude.

Several observations can be made with regard to the data shown in Fig. 1:

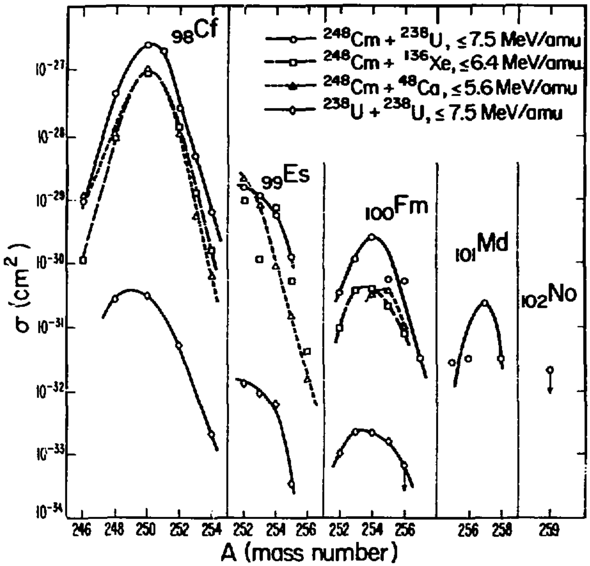

Fig. 1. Cross sections for the formation of the heaviest actinides in the reaction ^{238}U + ^{248} Cm at ≤ 7.5 MeV/A. Other reactions for comparison. The curves are drawn to guide the eye.

(XBL 808-1738)

(1) The cross sections for the formation of the heaviest actinides are about 3 orders of magnitude higher in the ^{238}U bombardment of a ^{248}Cm target compared to a ^{238}U target. This is obviously due to the fact that the nuclear diffusion is strongly dependent on ΔZ.

(2) An intercomparison of different projectiles on the same ^{248}Cm target however shows much smaller effects: The peak cross sections are only a factor 3 higher for ^{238}U compared to ^{48}Ca and ^{136}Xe projectiles. In the case of Es actually no difference in cross sections between the three ions can be found within the experimental erros. A slight shift in the centroid of the mass distribution can be observed in the ^{238}U case, which could be caused by a lower excitation energy of the products due to the heavier reaction partner and/or the larger N/Z ratio of the ^{238}U projectile.

(3) From the point of view of producing neutron rich unknown isotopes of the heaviest elements, the centroid shift is disappointingly small in particular for Fm where the most neutron rich distribution is actually obtained with ^{48}Ca + ^{248}Cm and not with ^{238}U + ^{248}Cm.

(4) The U and Cm data shown in Fig. 1 are compatible with the following assumptions: a) The heavy fragments are formed in statistical equilibrium, and b) the average excitation energy is about 45 MeV corresponding to the evaporation of about four neutrons.

(5) In this picture the centroid for the No mass distribution should be around A = 259.4 and preliminary calculations show a peak cross section of about $3 \cdot 10^{-33}$ cm^2. A similar calculation gives $5 \cdot 10^{-34}$ cm^2 for ^{287}114.

If therefore a one hundred fold increase in beam integral/sensitivity can be obtained in the future a reasonable chance still exists for the production of SHE's.

Footnotes and References

*GSI, Darmstadt (Germany)

† Lawrence Livermore National Laboratory

‡ Oak Ridge National Laboratory

§ University of Maiz (Germany)

1. E. K. Hulet, et al., Phys. Rev. Lett. 39, 385 (1977).

2. K. J. Moody, this annual report.

3. M. Schädel, et al., Phys. Rev. Lett. 41, 469 (1978).

CHARGE DISTRIBUTIONS FOR THE ^{86}Kr + ^{139}La SYSTEM*

P. Dyer,[†] M. P. Webb,[‡] R. J. Puigh,[§] R. Vandenbosch,[‖] T. D. Thomas,[¶] and M. S. Zisman

The Kr + La cross sections at 6 to 8 MeV/A exhibit interesting features[1,2] that indicate reaction mechanisms intermediate between those for lighter systems, where fusion is important, and those for heavier systems, where the Coulomb barrier is so high that little interpenetration of the projectile and target ever occurs. The picture of the Kr + La reaction that has evolved is one in which high-partial-wave projectiles are scattered to relatively large angles, interacting little with the target. Projectiles of smaller impact parameters, on the other hand, interact for increasingly longer times, with increasing overlap of nuclear matter; the combined complex rotates toward more forward angles, with possible rotation past 0°.

In a previous paper,[2] we have presented differential cross sections as a function of angle and energy loss, integrated over all reaction product nuclear charges. In this paper we present the Z-dependence of the cross sections, in order to study the mass transfer mechanism, and in particular to study the correlation between energy loss and mass transfer. One of the primary interests in this work is to study the widths of the Z distributions vs energy loss, as a function of scattering angle and particularly as a function of bombarding energy. Distributions in Z were generated from two-dimensional Q-value vs Z data by integrating over Q-value bins 25 MeV wide. An example of these distributions for 31° at 610 MeV, is given in Fig. 1.

An important mechanism for energy dissipation in peripheral collisions of heavy ions is nucleon exchange. If the excitation energies of the nuclei are modest so that the nucleon mean free path is comparable to the dimension of the system, then the energy transfer associated with exchange can be treated as a one-body interaction in which the exchanged nucleon's share of the relative kinetic energy of the two ions at the time of exchange is converted into excitation energy. Although Fermi motion and Pauli blocking are neglected in the simplest form of the exchange model, Randrup[3] has recently extended the model to include both of these effects.

If we compare our data with the extended exchange model, we would expect the rate of energy loss per exchange to vary as $(\frac{m}{\mu} E_f E_{rel})^{1/2}$, where E_f is the Fermi energy and E_{rel} is the available kinetic energy at the time of exchange. Our data are plotted in Fig. 2 as a function of this quantity, with E_f = 40 MeV.

The full and dashed curves give the absolute slopes expected from the extended exchange model with $N = \frac{A}{Z}\sigma_Z^2$ and with $N = \left[\frac{A}{Z}\right]^2 \sigma_Z^2$. We note that with this new model the data for the two bombarding energies lie on the same curve, and that the slope of the curve is consistent with the model of $N \approx \frac{A}{Z}\sigma_Z^2$. The agreement between experiment and theory suggests that the major mechanism for energy dissipation is in fact nucleon exchange. This conclusion is in contrast to that of previous studies[4] in which the effect of the exclusion principle was not taken into account.

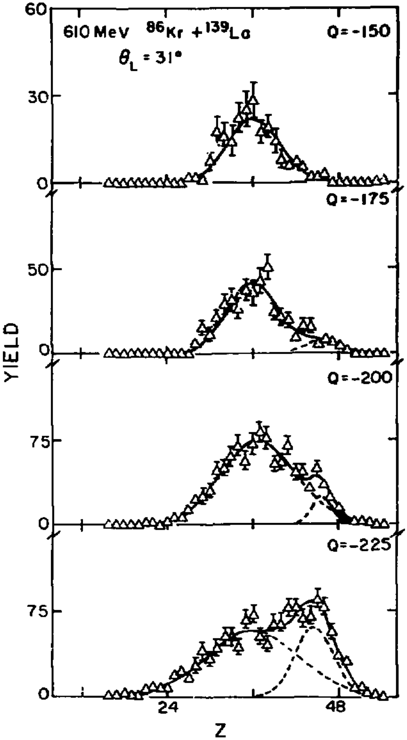

Fig. 1. Charge distributions for different energy losses at θ_L = 31° and E_L = 610 MeV. (XBL 808-1554)

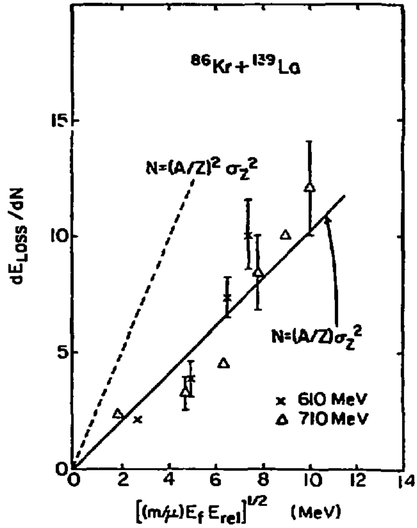

Fig. 2. Dependence of the rate of energy loss per exchange as a function of the square root of the product of the relative available energy per nucleon and the Fermi energy, E_f = 40 MeV. The full and dashed curves give the expected behavior from the exchange model for two assumptions about the relation between the number of exchanged particles and the charge distribution variances. The absolute value of the ordinate is for the assumption $N = (A/Z)\sigma_Z^2$. Rather than replotting all the experimental data points for the assumption $N = (A/Z)^2 \sigma_Z^2$, the theoretical prediction has been scaled appropriately. (XBL 808-1555)

Footnotes and References

*Condensed from Phys. Rev. C 22, 1509 (1980)

†Michigan State University, East Lansing, MI 48824

‡Los Alamos Scientific Laboratory, Los Alamos, NM 87545

§Hanford Engineering Development Laboratory, Richland, WA 99352

|| University of Washington, Seattle, WA 98195

¶ Oregon State University, Corvallis, OR 97331

1. M. P. Webb, R. Vandenbosch, and T. D. Thomas, Phys Lett. 62B, 407 (1976).

2. R. Vandenbosch, M. P. Webb, P. Dyer, R. J. Puigh, R. Weisfield, T. D. Thomas, and M. S. Zisman, Phys. Rev C 17, 1672 (1978).

3. J. Randrup, Nucl. Phys. A327, 490 (1979).

4. W. U. Schröder, J. R. Huizenga, J. R. Birkelund, K. L. Wolf, and V. E. Viola, Phys. Lett. 71B, 283 (1977); W. U. Schröder and J. R. Huizenga, Ann. Rev. Nucl. Sci 27, 465 (1977).

FAST PARTICLE EMISSION IN THE DEEP INELASTIC REACTION $^{nat}Cu + ^{20}Ne$ AT 12.6 MeV/NUCLEON*

R. P. Schmitt,[†] G. J. Wozniak, G. U. Rattazzi, G. J. Mathews,[†] R. Regimbart,[§] and L. G. Moretto

Fast protons (1-2.4 times the beam velocity) have been observed from the deep-inelastic reaction $^{nat}Cu + ^{20}Ne$ at 12.6 MeV/A. Similar proton spectral shapes are seen in both singles and coincidence. The most energetic protons are associated with partially relaxed processes rather than the most peripheral reactions. The angular correlations exhibit a strong peak near 0° for proton energies greater than 15 MeV. This correlation can be explained by evaporation calculations that take account of the steep forward-peaked angular distribution of the projectile-like fragments and evaporation-recoil effects.

In Fig. 1 proton lab energy spectra are shown for two Z-bins (θ_{PT} = +14°). We have attempted to understand these spectral shapes in terms of equilibrium evaporation[1] and have assumed that after the deep-inelastic collision the excited fragments undergo sequential decay. For the measured lab angle, atomic number and mean kinetic energy of the projectile-like fragment, the total excitation energy of both fragments was calculated from two-body kinematics. Assuming that the average excitation energy divides according to the fragment masses, the proton yield was then calculated in the moving frame using simple evaporation theory.[1] This yield was then transformed into the lab frame and the contributions from projectile and target emission were summed. The calculated spectra are in reasonable agreement with the data up to about 30 MeV (see dashed curves in Fig. 1). Since the high energy portions of the calculated spectra are due to emission from the projectile-like fragment, the failure of the calculations in this region can be attributed to a deficiency in the excitation energy of the projectile-like fragment. Trivially, increasing its share of the excitation energy would increase the yield of high-energy protons but would also simultaneously destroy the agreement with the angular distibutions.

This difficulty can be overcome by considering the thermal fluctuations[2] in the division of the excitation energy, E*, between the fragments which have been neglected so far. To evaluate this effect, we have calculated energy spectra for various divisions of E* and have folded them with a Gaussian probability distribution

$$P(E_1^*) \propto \exp[-(E_1^*-E_{1,eq}^*)^2/2\sigma^2] \quad .$$

On purely statistical grounds, a value for σ of 10 MeV is predicted from the expression $\sigma^2 = 2T^3a_1a_2/(a_1 + a_2)$, where T is the temperature of the intermediate complex and a_1 and a_2 are the level density parameters of the two fragments (see Ref. 2 for a derivation). While the calculations with (solid lines) and without (dashed lines) fluctuations are essentially identical at low energies (see Fig. 1), the incorporation of fluctuations produces a dramatic increase in the number of high energy protons. Including fluctuations in the calculations clearly reproduces the experimental proton energy spectra.

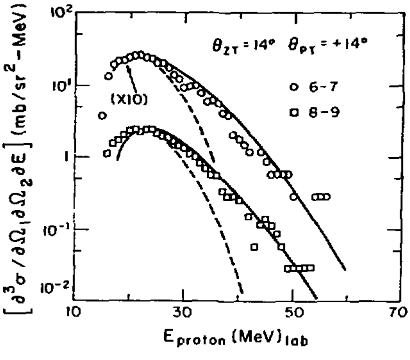

Fig. 1. Proton-energy spectra detected in a colinear geometry with Z = 6-7 (circles) and Z = 8-9 (squares). The curves are the predicted spectral shapes from a simple evaporation model with σ = 10 MeV (solid lines) and with σ = 0 (dashed lines) (XBL 806-1322)

Footnotes and References

*Condensed from LBL-9512

†Present address: Cyclotron Institute and Department of Chemistry, Texas A & M University, College Station, TX 77843.

‡Present address: W. K. Kellogg Radiation Laboratory, 106-38, California Institute of Technology, Pasadena, CA 91125.

§Present address: Laboratories de Physique Corpusculaire, Universite de Caen, 1400 Caen, France.

1. V. Weisskopf, Phys. Rev. 52, (1937) 295.

2. L. G. Moretto, Lawrence Berkeley Laboratory Report No. LBL-9130 (1979), Proceedings of the Varenna Conference, Varenna, Italy, July 9-25, 1979.

THE REACTION OF ^{20}Ne WITH ^{181}Ta at 50 MeV/A

D. J. Morrissey, G. J. Wozniak, L. W. Richardson, C. C. Hsu, R. J. McDonald and L. G. Moretto

As part of a systematic study of angular momentum transfer in heavy-ion reactions[1] we report here some results for the ^{181}Ta(^{20}Ne,Y)X system at 50 MeV/A. These data represent the high-energy end of a study that spans the region from a few to a few tens of MeV per nucleon.

A ~ 50 MeV/A ^{20}Ne beam was extracted from the Bevalac and delivered to the LESL scattering chamber. After interaction in a 100-mg/cm^2 tantalum target, projectile-like products were identified in either of two identical Si-telescopes. These telescopes consisted of a 250-μm Si surface barrier (ΔE) followed by two 5-mm Li-drifted Si detectors (E and E-reject). All light products, except protons and alphas, stopped in the first two elements of the telescopes. Prompt gamma rays and their time distribution were measured in coincidence with any valid telescope event in an array of eight 3 x 3-in. (NaI(Tl) detectors. The NaI(Tl) detectors were placed outside the scattering chamber, at 45° out-of-plane to the telescopes.

The projectile-like products were measured from 8° to 24° in the lab system. This covered the angular region from just behind the classical grazing angle, $\theta_g \approx 6°$, to the point where only Z = 1 and 2 products were observed at a low rate. In Fig. 1 we show the Wilczynski diagram for oxygen products. Even though there is a

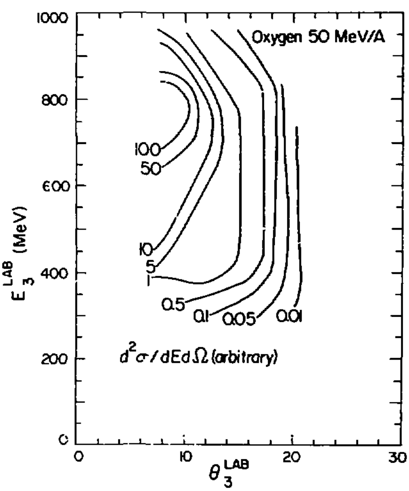

Fig. 1. A Wilczynski diagram is shown for the oxygen products. (XBL 808-1553)

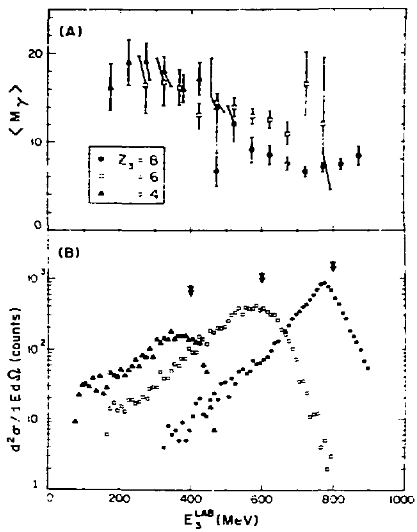

Fig. 2. The energy spectra and the average gamma-ray multiplicity as a function of particle energy are shown for the even Z products in (B) and (A), respectively. (XBL 808-1549)

relatively high threshold for detecting the oxygens (~ 200 MeV) one can see that the cross section is dominated by a peak slightly below the projectile velocity. Additional measurements inside Θ_g are desirable to determine if the lower energy oxygen products result from orbiting through 0°.

The measured values of the average gamma-ray multiplicity $\langle M_\gamma \rangle$ and the corresponding energy spectra at 8° are shown in Fig. 2 for the even Z products. Two features of the $\langle M_\gamma \rangle$ distributions are immediately apparent: (a) the values of the multiplicity are rather low, never exceeding ~ 20 and (b) the slope of the multiplicity with energy loss for each exit channel is rather small. The observations indicate that the transfer of orbital angular momentum into intrinsic spin and then into gamma-ray multiplicity is not characterized by only two large fragments in th exit channel. There are two obvious stages where this breakdown may be occurring. If the target-like residue is not able to hold the excitation energy and angular momentum imparted to it, then sequential fission would convert intrinsic spin back into orbital motion. Similarly, if the projectile undergoes fragmentation without transfer-induced transport of angular momentum, then the initial orbital motion would be contained in the orbital motion of projectile fragments. Further experiments in which we plan to differentiate between these two processes are anticipated in the next operating period.

Reference

1. Cf. L. W. Richardson et al, in this annual report.

EVIDENCE FOR THE ONSET OF PROJECTILE FRAGMENTATION IN PERIPHERAL COLLISIONS OF ^{20}Ne + ^{181}Ta

L. W. Richardson, G. J. Wozniak, D. J. Morrissey
C. C. Hsu and L. G. Moretto

The evolution with energy of heavy ion reactions in the bombarding energy range of 5 to 20 MeV/A has recently become a subject of considerable investigation. Several theories predict an onset of fragmentation-like phenomena at 15 to 20 MeV/A.[1] In an effort to gain an understanding of the reaction mechanism in this region we have undertaken a study of the energy dependence of the angular momentum transfer.

We have measured the continuum gamma ray multiplicity $\langle M_\gamma \rangle$ for peripheral collisions of ^{20}Ne + ^{181}Ta over a wide range of projectile energies. The intrinsic angular momentum of the fragments may be extracted for this system from the $\langle M_\gamma \rangle$ data since the heavy fragments produced in this reaction are good rotational nuclei known to decay predominantly through stretched quadrupole (E2) γ-ray cascades. Furthermore due to the large mass asymmetry of the system almost all of the angular momentum will reside in the heavy fragment.

The events of interest are those where the γ-rays are in coincidence with the projectile-like fragments which are moving at near beam velocity. For these events the source of momentum transfer to the target and hence $\langle M_\gamma \rangle$ must come from the interaction of the missing portion of the projectile with the target. Figure 1 shows $\langle M_\gamma \rangle$ for near beam velocity fragments (which correspond closely to the peak in the differential cross section) at four bombarding energies 7.6, 9.9, 16.7, and 21.9 MeV/A. We see for example at 7.6 MeV/A a linear increase in the angular momentum with captured mass as expected for these massive transfer events.[2] The solid lines are computed from semiclassical matching conditions leading to the constraint on the angular momentum transfer $\Delta\ell$,

$$\Delta\ell = mvR/\hbar \text{ hence } \langle M_\gamma \rangle = mvR/2\hbar$$

where $\langle M_\gamma \rangle$ is the average γ-ray mulitiplicity for the collision of two nuclei at relative velocity v leading to a transfer of mass m from one to another at radius R, which we take to be the half density matter radius of the residual heavy nucleus.

We see from Fig. 1 that for bombarding energies up to 10 MeV/A, $\langle M_\gamma \rangle$ and thus the angular momentum transfer is indeed proportional to the mass and increases linearly with the velocity. Above 10 MeV/A the angular momentum no longer increases with velocity but decreases slightly. A possible explanation for this change in the dependence of $\langle M_\gamma \rangle$ might be a loss of transferred spin to orbital motion via sequential fission of the target-like fragment. However, sequential fission is not very likely over the range of spin and excitation energy involved and one is forced to consider an alternative mechanism.

We interpret the change in the dependence of $\langle M_\gamma \rangle$ as evidence for a change in the reaction mechanism from one similar to massive transfer to projectile fragmentation. As indicated by Harvey[3] this may be thought of in terms of a simple model of limiting angular momentum. The dashed lines in Fig. 1 indicate the critical angular momentum ℓ_{crit} for each exit channel calculated from the semi-empirical formula of Wilczynski.[4] We see from the figure that for bombarding energies below 10 MeV/A mass transfer

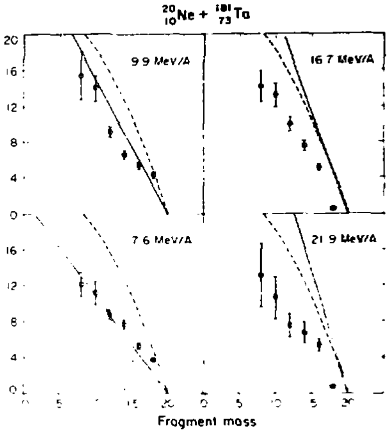

Fig. 1. $\langle M_\gamma \rangle$ as a function of mass for near beam velocity fragments. (XBL 807-1556)

leads to final states below ℓ_{crit}. Above 17 MeV/A mass transfer leads to unbound states above ℓ_{crit}, in which case none of the projectile is captured. For these fragmentation types of events one might indeed expect $\langle M_\gamma \rangle$ to decrease with increasing energy since the angular momentum transfer here may be considered to arise from an impulsive force and hence must decrease in a manner which is inversely proportional to the velocity.

References

1. K. W. McVoy and M. C. Nemes, Z. Physik A295, 1977 (1980). K. Siwek-Wilczynska, et al., Phys. Rev. Lett. 42 1599 (1979).

2. K. A. Geoffroy, et al., Phys. Rev. Lett. 43 1303 (1979).

3. B. G. Harvey, Notas de Fisica 3 (1) 99 (1980).

4. J. Wilczynski, Nucl. Phys. A216, 386 (1973).

LIGHT PARTICLE EMISSION AS A PROBE OF THE ROTATIONAL DEGREES OF FREEDOM IN DEEP-INELASTIC COLLISIONS

L. G. Sobotka, C. C. Hsu, G. J. Wozniak, G. U. Rattazzi, R. J. McDonald, A. J. Pacheco and L. G. Moretto

A promising method for the study of the transfer of orbital angular momentum into the intrinsic spins of the product nuclei in deep inelastic collisions is the sequential emission of light particles. In a manner similar to sequential fission, the width of the out-of-plane light particle angular distribution depends on the spin of the emitter. The usefulness of this technique depends primarily on two factors, the ability of obtaining out-of-plane distibutions of particles emitted from just one of the fragments and sufficient sensitivity of the distributions to the spin of the emitter to enable accurate spin determination.

Recently R. Babinet et al.[1] have shown, for the system 280 MeV ^{40}Ar + ^{58}Ni, that by use of coincidence techniques and proper selection of the reaction system and detection angles one is able to study the out-of-plane distribution of light particles emitted from an individual fragment. For the substantially heavier system 664 MeV ^{84}Kr + ^{nat}Ag we have used the same techniques to study alpha-particle emission from the target-like fragment. We find that the contamination due to light particles emitted from the projectile-like fragment to be quite small.

The compatibility of out-of-plane light particle measurements and gamma multiplicity techniques allows one to test the sensitivity of the light particle distibutions to the spin of the emitter. In the mass region covered by the present study, the gamma mutiplicity is approximately proportional to the sum of the fragments' spin.[2] Thus the requirement of an increasing number of γ-rays to be in coincidence with the Z-α events should bias the fragments' spin distribution towards larger values. This selection should result in a greater focusing of the angular distribution into the reaction plane. The energy integrated out-of-plane α-distributions in the rest frame of the emitter are shown in the figure without (a) and with (b) the requirement of two or more coincident γ-rays. The distributions without any coincident γ-ray requirement are expressed in terms of differential multiplicity.[2] As expected the angular distributions associated with the high γ-ray multiplicity events display a larger anisotropy than those without the gamma-ray requirement. The anisotropies, quantitatively expressed by the into out-of-plane ratios, indicate the sensitivity of the α-particle distributions to the spin of the emitting nucleus. Also seen in this figure is a significant sharpening of the

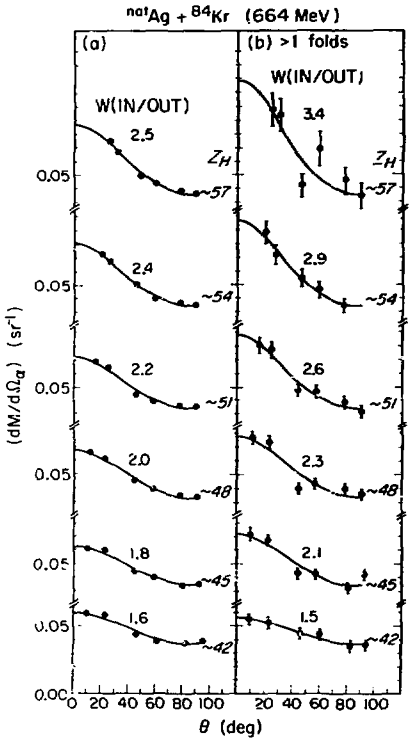

Fig. 1. Alpha-particle angular distibutions for several Z-bins as a function of out-of-plane angle. The Z bins are 3 Z-values wide and are indicated by the median Z-value. In section a) there is no coincident γ-ray requirement while in b) there are 2 or more coincident γrays. The curves in section b) are normalized at 90° to those in a) for the same Z bin. (XBL 807-3459)

angular distributions as the size of the emitter increases. This is an indication of the dependence of the fragments' spin on the mass asymmetry of the exit channel.

References

1. R. Babinet, B. Cauvin, J. Girard, J. M. Alexander, T. H. Chiang, J. Galin, B. Gatty, D. Guerreau, and X. Tarrago, Z. Physik A 295, 153 (1980).
2. M. Lefort and C. Ngô, Riv. Nuovo Cimento, 2, 1 (1979), and references therein.

EVIDENCE FOR RIGID ROTATION AND LARGE DEFORMATIONS IN THE DEEP-INELASTIC REACTION 664 MeV ^{84}Kr + ^{nat}Ag*

L. G. Sobotka, C. C. Hsu, G. J. Wozniak, G. U. Rattazzi, R. J. McDonald, A. J. Pacheco and L. G. Moretto

A prominent feature of deep-inelastic reactions is the conversion of orbital angular momentum into the intrinsic spins of the two-product nuclei. We have simultaneously measured both the gamma-ray multiplicity, M_γ, and the sequential emission of alpha particles from one of the fragments to investigate this process. Since the out-of-plane angular distributions can yield the spin of an individual fragment and M_γ provides information on the sum of the

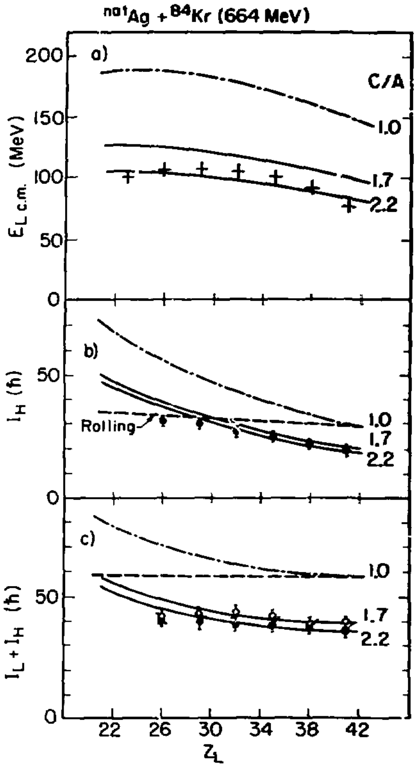

Fig. 1 (a). Center of mass fragment energies after evaporation corrections as a function of the charge of the light fragment. Horizontal bars indicate the uncertainty in the primary charge (before evaporation) of the light fragment. Solid lines are calculations for two spheroids in contact and are labeled by the ratio of axes. The broken line is for spheres.

(b) Spin of the heavy fragment extracted from the out-of-plane distributions. Calculations for rolling and rigid rotation of spheroids are indicated.

(c) Sum of the spins of the deep-inelastic fragments as determined by out-of-plane α-distributions (closed) and M_γ (open). (XBL 807-3458)

spins of both fragments, the combination is a powerful tool for investigating the partitioning of angular momentum within the dinuclear complex as well as a cross check on both methods.

A solid state telescope was used to detect the Kr-like fragment, while an out-of-plane arc with four light particle telescopes was positioned along the recoil direction to detect alpha particles evaporated from the target-like fragment. Seven NaI detectors above the reaction plane were used to obtain M_γ data. Using two-body kinematics, heavy-ion α-particle coincident events were reconstructed and transformed into the rest frame of the undetected Ag-like emitter. The resulting out-of-plane distributions exhibit large anisotropies as the size of the emitter increases. These data are used to extract the fragment spin by means of a statistical model.[1]

The fragment kinetic energies were used to estimate the deformation of the dinuclear complex at the time of scission. If one compares the data to a calculation including both the coulomb and centrifugal terms in a spheroid-spheroid model, part a of figure, a ratio of axes of ~ 2 is indicated. The spins extracted from the α-distributions, part b, show the first clear evidence for rigid rotation in this mass region and corroborate the claim of large deformations. In the third part of the figure the sum of the spins extracted from both the M_γ data and the α-distibutions is shown. The agreement is quite good, thus adding credibility to the picture of the deep-inelastic complex as two rigidly rotating substantially deformed spheroids.

<u>Footnote and Reference</u>

*Condensed from LBL-11148.

1. L. G. Moretto et al. LBL-10805 (to be published).

THE RISE AND FALL OF THE SPIN ALIGNMENT IN DEEP-INELASTIC REACTIONS*

G. J. Wozniak, R. J. McDonald, A. J. Pacheco,[†] C. C. Hsu,[‡]
D. J. Morrissey, L. G. Sobotka, L. G. Moretto
and
S. Shih,[§] C. Schück,[|] R. M. Diamond, H. Kluge,[¶] F. S. Stephens

Both the magnitude and alignment of transferred angular momentum in the reaction ^{165}Ho + ^{165}Ho at 8.5 MeV/A have been measured as a function of Q-value via continuum γ-ray multiplicity and anisotropy techniques. This symmetric system was chosen since (1) large amounts of angular momentum can be transferred to fragment spin, (2) Ho nuclei are good rotors and thus emit γ-spectra enriched in stretched E2 transitions, and (3) symmetry in the entrance channel allows us to study spin transfer and alignment over a broad range of Q-values.

Data are shown in Fig. 1. Throughout the quasi-elastic region (-100 MeV < Q < 0), both the spin transfer (circles) and the anisotropy (squares) increase. The anisotropy peaks before the spin transfer saturates and then declines to near unity at large Q-values.

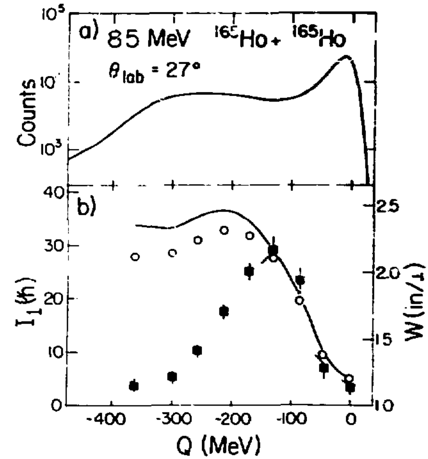

Fig. 1. Fragment spin (circles) deduced from γ-multiplicity. Ratio of in-plane/⊥ γ-ray yields (anisotropy) (squares) for the region 0.6 MeV < E_γ < 1.2 MeV. (XBL 806-1214a)

We interpret these data according to the equilibrium statistical model[1] of Moretto and Schmitt which postulates a primary depolarization mechanism caused by thermal excitation of angular-momentum-bearing collective modes. Figure 2 shows a solid line (curve 1) for the model calculation compared to the data. To give a feeling for the importance of various contributions, the same calculation is shown with no corrections for neutron evaporation (curve 2), no statistical transitions (curve 3), and no primary thermal depolarization (curve 4). A comparison clearly shows that the most important effect is the thermally-induced misalignment, indicating that the decrease of alignment is inherent to the deep-inelastic process itself.

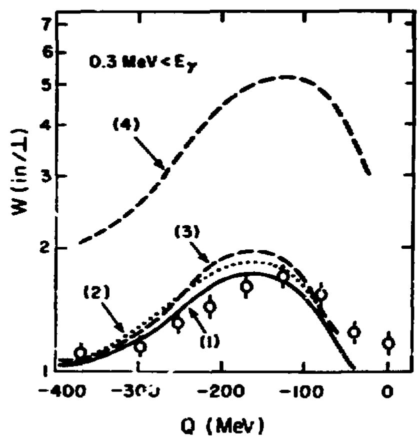

Fig. 2. Anisotropy data (circles) for E_γ > 0.3 MeV compared to stages of the model calculation. (XBL 806-1193a)

This gives rise to the following picture of angular momentum transfer and spin alignment in the deep-inelastic reaction process: in the quasi-elastic region, the transferred spin increases rapidly with Q-value whereas the thermally misaligned component increases more slowly. Thus, the aligned component dominates and the transferred angular momentum is nearly perpendicular to the reaction plane, giving a large anisotropy. However, across the deep inelastic region, the transferred spin saturates while the thermal components increase to become an ever larger fraction of the total angular momentum. Thus, the alignment decreases and the anisotropy plummets.

Footnotes and References

*Condensed from LBL-11057, G. J. Wozniak et al., Phys. Rev. Lett. 45, 1081, (1980)

†Comision Nacional De Energia Atomica, Argentina

‡Institute of Atomic Energy, Beijing, China.

§Shanghai Institute of Nuclear Research, China.

‖C. S. N. S. M., Orsay, France.

¶Hahn-Meitner Institute, Berlin, Germany.

1. L. G. Moretto and R. P. Schmitt, Phys. Rev C21 204 (1980).

AN EXCITATION FUNCTION STUDY OF THE CONTINUUM γ-RAY MULTIPLICITY IN HEAVY ION REACTIONS FROM 7 TO 22 MeV/A

L. W. Richardson, G. J. Wozniak, D. J. Morrissey
C. C. Hsu and L. G. Moretto

Over the last decade a considerable body of knowledge concerning nuclear reaction mechanisms in heavy ion collisons has developed.[1] However, relatively little is known about the energy dependence of such mechanisms.

For bombarding energies below 10 MeV/A the number of γ-rays emitted in heavy ion reactions has been shown to correlate strongly with transferred angular momentum.[2] We have investigated the dependence of the γ-ray multiplicity $\langle M_\gamma \rangle$ and of the energy and charge transfer in peripheral collisions of ^{20}Ne + ^{181}Ta from 7 to 22 MeV/A.

Table 1 shows the ratio of the projectile kinetic energy to the Coulomb barrier and the maximum angular momentum ℓ_{max} available in the entrance channel for the bombarding energies investigated.

Table 1

E_{lab} MeV	E/B	ℓ_{max}
152	1.79	83
198	2.33	110
333	3.98	169
438	5.23	203

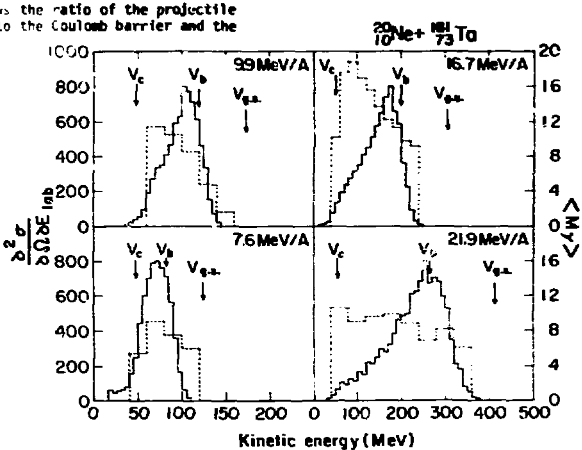

Fig. 1. $\frac{\partial^2\sigma}{\partial\Omega\partial E}$ in arbitrary units (solid lines) and $\langle M_\gamma \rangle$ (dashed lines) as a function of the lab energy for the carbon isotopes. (XBL 808-1700A)

At the higher bombarding energies we see that there is available a very large amount of energy and angular momentum that may be transferred to the reaction fragments. In such a violent collision it may certainly be possible to achieve the limit of excitation energy and angular momentum at which the target nucleus may survive.

The energy spectra of the carbon isotopes at near grazing angles for the four bombarding energies are shown in Fig. 1. The lab energy V_p corresponding to a final fragment velocity equal to the initial projectile velocity, the lab energy V_c corresponding to final fragments with the exit channel Coulomb energy, and the lab energy $V_{g.s.}$ corresponding to the ground state energy of a reaction leading to a two-body final state are indicated.

As can be observed, the energy spectra are typically broad, bell shaped and dominated by the quasi-elastic component at all bombarding energies for near grazing angles. The differential cross section has a maximum at near beam velocity and extends down to the Coulomb energy.

The γ-ray multiplicity $\langle M_\gamma \rangle$ (uncorrected for particle emission) at each bombarding energy is also shown in Fig. 1. $\langle M_\gamma \rangle$ increases through the quasi-elastic region with decreasing fragment energy (or increasing two-body total kinetic energy loss, TKEL). The maximum $\langle M_\gamma \rangle$ value is observed to change little with bombarding energy and moves to higher exit channel energies with increasing projectile kinetic energy.

Further work is in progress to understand the varying degrees of importance of mass transfer and particle emission (both equilibrium and non-equilibrium) on the angular momentum transfer as a function of projectile kinetic energy.

Footnotes and References

1. D. K. Scott, LBL-7727.

2. R. Regimbart, et al., Phys. Rev. Lett. 41, 1355 (1978)

A COMPARISON OF THE ALIGNMENT PARAMETER P_{zz} FROM GAMMA ANISOTROPY AND SEQUENTIAL FISSION MEASUREMENTS

A. J. Pacheco,* R. J. McDonald, G. J. Wozniak, and L. G. Moretto

The magnitude and alignment of transferred angular momentum in deep-inelastic (DI) collisions provide useful information which aids in understanding the reaction mechanism. Angular distributions of γ-rays, sequential fission fragments, or light charged particles have proven to be useful techniques in determining spin and alignment. These all include measurement of fragment decay following the primary reaction, and thus require extraction of the primary reaction misalignment from secondary data. Agreement (or lack thereof) among these methods is a subject of current concern.

Using continuum γ-ray multiplicity and anisotropy techniques, we have extracted the fragment spin and its alignment from the reaction $^{165}Ho + {}^{165}Ho$ at 8.5 MeV/A (Ref. 1). Alignment is described by the parameter P_{zz}, defined as:

$$P_{zz} = \frac{3\langle I_z^2\rangle}{2\langle I^2\rangle} - 1/2$$

where I_z is the aligned component of the spin I and $\langle I_z^2\rangle$ is its mean squared value. We note that P_{zz} cannot be measured directly, but must be extracted from the data via some model. We utilize a statistical equilibrium theory (Ref. 2) for the case of two equal touching spheres. The model predicts a distribution function given by:

$$P(I_x,I_y,I_z) = \mathrm{EXP} - \frac{I_x^2}{2\sigma_x^2} + \frac{I_y^2}{2\sigma_y^2} + \frac{(I - \langle I_z\rangle)^2}{2\sigma_z^2}$$

and

$$\sigma_x^2 \approx \sigma_y^2 \approx \sigma_z^2 \doteq \sigma^2 = \mathcal{I}\, T$$

where $\mathcal{I}$ is the moment of inertia for one of the two spheres and T is the nuclear temperature. P_{zz} becomes:

$$P_{zz} = \frac{2\langle I_z\rangle^2 - \sigma_x^2 - \sigma_y^2 + 2\sigma_z^2}{2(\langle I_z\rangle^2 + \sigma_x^2 + \sigma_y^2 + \sigma_z^2)}$$

where σ_x^2, σ_y^2 and σ_z^2 are the standard deviations in the x, y, and z components of the spin I. In extracting an "experimental" P_{zz}, we adjusted σ^2 to fit the anisotropy data rather than using its theoretical value. The aligned component $\langle I_z\rangle$ is calculated under the assumption that the spin I (extracted from the γ-ray multiplicity) is obtained from:

$$\langle I\rangle = \int I\, P(I_x,I_y,I_z)\, dI_x\, dI_y\, dI_z$$

Finally, since the information carried by the γ-rays applies to the state of the fragments after neutron emission, we have corrected our data to expected values prior to neutron emission (Ref 3). In this way we have extracted an "experimental" P_{zz} from our data (circles) as shown in Fig. 1.

Results from the angular distribution of sequential fission fragments from the experiment U + Kr (Ref. 4) were derived assuming a distribution in which $\sigma_y^2 = 0$, i.e., considering only fluctuations in a plane perpendicular to the recoil direction (Ref. 4). We note, here again, the model dependency of "experimental" P_{zz} data. We have transformed this data, retaining the same $\sigma^2/\langle I_z\rangle^2$, into new points to include all three sigmas (triangles). These systems have approximately the same total mass, but the entrance channel mass asymmetry differs significantly. In spite of this difference, the two sets of data are very similar and show about the same degree of alignment. Also, a model calculation (Ref. 2) for the $^{165}Ho + ^{165}Ho$ data (solid line) using $\sigma^2 = \mathcal{I}T$ is a reasonable fit to both sets of data. From this we conclude that both reactions are yielding comparable values for P_{zz}.

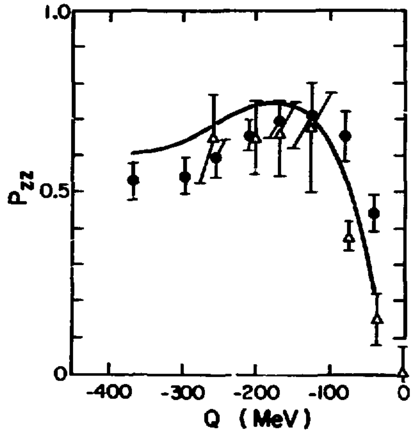

Fig. 1. Extracted P_{zz} for $^{165}Ho + ^{165}Ho$ (circles) and U + Kr (triangles) compared to a model calculation (solid line). See text for details. (XBL 808-1712)

Footnotes and References

*Permanent address: Comisión Nacional de Energia Atomica, Argentina.

1. G. J. Wozniak et al., Phys. Rev. Lett. 45, 1081 (1980).

2. L. G. Moretto and R. P. Schmitt. Phys. Rev. C21, 204 (1980)

3. S. K. Blau and L. G. Moretto. LBL-10926 (to be published)

4. R. J. Puigh et al. Phys. Lett. 86B, 24 (1979)

C. RELATIVISTIC HEAVY IONS

1. Projectile and Target Fragmentation

EMISSION OF HIGH-ENERGY GAMMA RAYS FROM RELATIVISTIC HEAVY-ION COLLISIONS

M. P. Budiansky, S. P. Ahlen,* G. Tarle,* P. B. Price*

There are several possible sources of high-energy (E > 10 MeV) gamma rays from relativistic, heavy-ion collisions; very little is known about their relative production rates. We are particularly interested in the following sources: (1) Bremsstrahlung: Our calculations indicate that the amount of bremsstrahlung emitted is a sensitive function of the dynamics of the collision. (2) Photons from π^0 decay: This is the main source of photons in the energy range of interest. (3) Δ(1236) decay: This resonance decays via Nγ about 0.6% of the time. The resulting photons, peaked around 260 MeV, may be visible above the background produced by π^0 decays.

In the past year we have designed and built a gamma-ray detector for use at the Bevalac. A preliminary model was tested at the LLL Electron Linac in July 1979, and construction of a revised version was complete in April 1980. (See Fig. 1.)

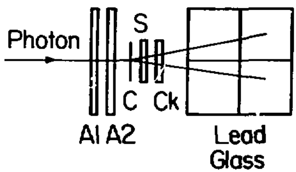

Fig. 1. Schematic diagram of gamma-ray detector. (XBL 808-1665)

By using state-of-the-art phototubes with high quantum efficiency and excellent light collection, we have achieved good energy resolution. The problem of neutron rejection was given special consideration in the design. A photon from a collision first passes through A1 and A2, which are anti-coincidence scintillator paddles to reject charged particles. The photon then interacts in converter C, a thin lead sheet, to produce an electron-positron pair. The electron and positron produce signals in S, a scintillator, and Ck, a plastic Cerenkov detector, and then deposit their energy in approximately 13 radiation lengths of lead glass. Neutron rejection is provided by analyzing the signals in S and Ck: in order to accept an event we require signals in these detectors that correspond to two relativistic, singly-charged particles. Analysis of the shower development in the lead-glass blocks provides further neutron rejection. Not shown are the target, and two detectors in the beam path that form a central-collision trigger.

In June 1980, we measured gamma-ray spectra from collisions of ^{20}Ne on ^{208}Pb, ^{40}Ar on ^{208}Pb, and ^{40}Ar on ^{40}Ca. Figure 2 shows the distribution of events in the S-Ck plane for one of our runs; we can cleanly separate the desired pair-conversion events. When this cut is applied to the raw data, a peak is readily apparent at a position that roughly corresponds to the energy of the π^0 decay peak. Further analysis, and any conclusions about bremsstrahlung or Δ decays, must await the results of a later calibration run at the LLL Linac.

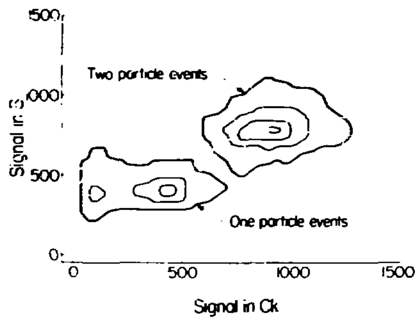

Fig. 2. S vs Ck event distribution. Contours are drawn at 25%, 50%, 75%, and 100% of peak. (XBL 808-1666)

Footnote

*Also at Space Sciences Laboratory.

PION PRODUCTION AND CHARGED-PARTICLE MULTIPLICITY SELECTION IN RELATIVISTIC NUCLEAR COLLISIONS*

K. L. Wolf,[†] H. H. Gutbrod, W. G. Meyer, A. M. Poskanzer, A. Sandoval, R. Stock, J. Gosset,[‡] C. H. King, G. King, Nguyen Van Sen,[§] and G. D. Westfall

Spectrum of positive pions with energies of 15-95 MeV were measured for high energy proton, ^{4}He, ^{20}Ne, and ^{40}Ar bombardments on targets of ^{27}Al, ^{40}Ca, ^{107,109}Ag, ^{197}Au, and ^{238}U. A Si-Ge range telescope was used to identify charged pions by dE/dx and stopped π^+ were tagged with the subsequent muon decay. In all, results for fourteen target-projectile combinations are presented to study the dependence of pion emission patterns on the bombarding energy (from 240 MeV/nucleon to 2.1 GeV/nucleon) and on the target and the projectile masses. In addition, associated charged-particle multiplicities were measured in an 80-paddle array of plastic scintillators, and used to make impact parameter restrictions on the pion-inclusive data.

Broad structures occur in the π^+ spectra for ^{20}Ne- and ^{40}Ar- induced reactions at the highest bombarding energies. Examples in Fig. 1 are of contours of constant cross section (1/p) $d^2\sigma/d\ell dE$ as a function of perpendicular pion momentum and rapidity y for 1.05 and 2.1 GeV/nucleon ^{20}Ne + ^{238}U, selected on high charged-particle multiplicity, i.e., central and near-central collisions. Many features of the π^+ emission patterns can be explained in terms of the decay of isobars produced in nucleon-nucleon collisions, along with Coulomb repulsion from the spectator and participant matter. The results of more quantitative cross section comparisons of light projectile (p,α) with heavy-ion π^+ production are explained in terms of isobar-nucleon interactions in excited nuclear matter.

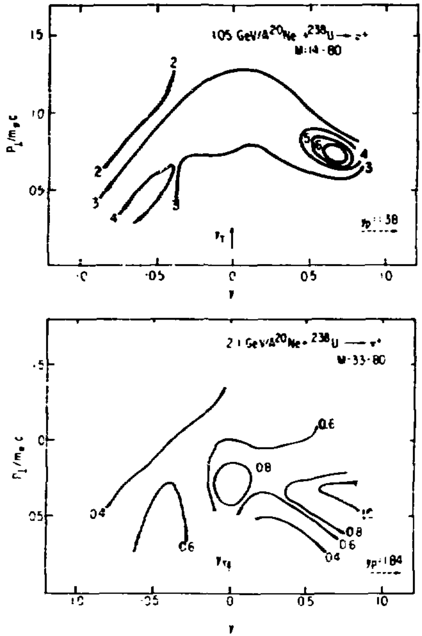

Fig. 1. (XBL 808-11330)

Footnotes

*Work performed under the auspices of the Office of Basic Energy Sciences, Division of Nuclear Physics, U.S. Department of Energy and by the Bundesminsterium fur Forschung and Technologie, West Germany.

† Present address: Argonne National Laboratory, Argonne, Illinois 60439.

‡ Present address: DPhN/ME, CEN Saclay, 91190 Gif-sur-Yvette, France.

§ Present address: ISN, 38044 Grenoble, France.

PROTON TUNGSTEN REACTIONS AT 400 GeV*

J. Cincheza,† J. Cohen,† A. Marin,† T. Visky,† E. Friedlander, A. J. Herz,‡
B. Jakobsson,§ B. Lindkvist,|| I. Otterlund,|| E. Stenlund,|| and B. Andersson||

We present results from studies of p-W reactions in thin tungsten wires embedded in emulsion by means of a new method for introducing well-defined targets into nuclear emulsions. The wires, mounted on a square frame, were introduced in the median plane between one 300 μm nuclear K5 emulsion pellicle and one 300 μm emulsion on glass by laminating the two emulsions using a lamination solution consisting of a mixture of ethyl alcohol and water (Fig. 1). The emulsions were irradiated with 400 GeV protons at FNAL. The beam was parallel to the emulsion surface and perpendicular to the wires. In all we have studied 470 p-W events. The results show that:

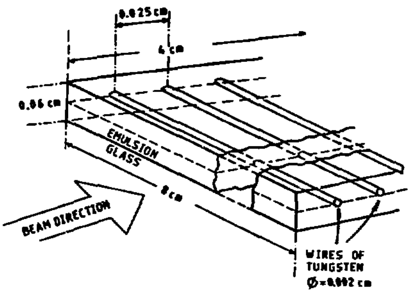

Fig. 1. Geometry of the wire-loaded emulsion plate. (XBL 808-10919)

1) The mean multiplicities of black, grey and shower track particles in p-W reactions are $\langle N_b \rangle = 11.5 \pm 0.4$, $\langle N_g \rangle = 5.2 \pm 0.2$, $\langle n_s \rangle = 20.0 \pm 0.6$.

2) The scaled multiplicity distribution in p-W reactions deviates from that observed in p-p reactions.

3) The mean number of grey prong particles (recoiling protons) is proportional to $A^{2/3}$.

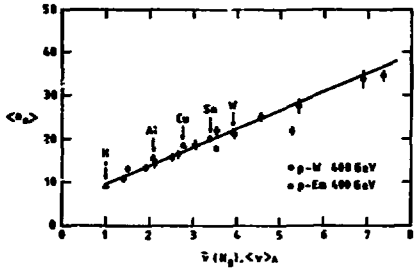

Fig. 2. Mean pion multiplicity vs. number of encounters $\tilde{\nu}(N_g)$ for emulsion and W nuclei, and $\langle \nu \rangle$, the calculated number of effective target nucleons. (XBL 808-10917)

4) The mean number of evaporated particles (black particles) for a given number of recoiling protons is A-dependent.

5) The N_g distribution provides strong evidence that N_g is a measure of the number of collisions inside the nucleus.

5) The relationship between $\langle n_s \rangle$ and $\langle N_h \rangle$ is A dependent.

7) The pion production mainly depends on the longitudinal thickness of nuclear matter (i.e., the number of encounters, ν) and not on the target mass itself (Fig. 2).

Footnotes

*Condensed from Nuclear Physics B, 158, 280, 1979.

†Central Institute for Physics, Bucharest, Roumania

‡CERN, Geneva, Switzerland

§NORDITA, Copenhagen, Denmark

||University of Lund, Lund, Sweden

LOW-ENERGY PION PRODUCTION WITH 800 MeV/N 20Ne*

J. Chiba,† K. Nakai,† I. Tanihata,‡ S. Nagamiya, H. Bowman, J. Ingersoll, and J. O. Rasmussen

Doubly differential cross sections for production of positive pions (20 MeV ≤ T_π^{Lab} ≤ 100 MeV) in bombardment of ^{20}Ne on NaF, Cu and Pb targets at 800 MeV/N have been measured with a range telescope. (See Fig. 1.) The results showed that the angular distribution of low-energy pions in the nucleon-nucleon center of mass $T_\pi^{c.m.}$ ≤ 50 MeV) isotropic, even 90° peaking at ~ 15 MeV c.m. The intermediate-energy pions (50 ≤ $T_\pi^{c.m.}$ ≤ 300 MeV) were forward and backward peaked, reflecting the individual nucleon-nucleon process in the isobar model of production.

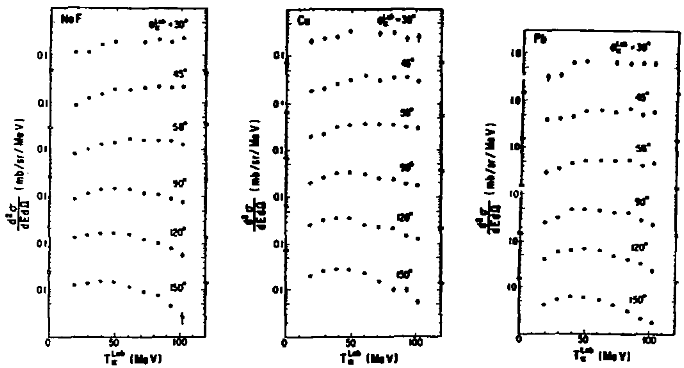

Fig. 1. Doubly differential cross sections for positive pion production with the 800 MeV/N ^{20}Ne beam on (a) NaF, (b) Cu, and (c) Pb targets, respectively. The errors are only statistical ones. (XBL 7812-14102)

Footnotes and Reference

*Condensed from LBL-8699 and Ref. 1.

†Department of Physics, University of Tokyo, Tokyo, Japan

‡Laboratory for Nuclear Studies, Osaka University, Osaka, Japan

1. J. Chiba, K. Nakai, I. Tanihata, S. Nagamija, H. Bowman, J. Ingersoll, and J. O. Rasmussen, Phys. Rev. C, 20 (4), pp. 1332-1339 (October 1979).

LOW-ENERGY PION PRODUCTION AT ZERO DEGREES IN NUCLEUS-NUCLEUS COLLISIONS*

J. A. Bistirlich, H. R. Bowman, K. M. Crowe, K. A. Frankel, O. Hashimoto,† J. G. Ingersoll, J. Jansen, M. Koike,† C. J. Martoff, J. Miller,‡ D. L. Murphy, J. Peter,§ J. O. Rasmussen, J. P. Sullivan, W. A. Zajc, W. Benenson,‖ G. M. Crawley,‖ E. Kashy,‖ J. A. Nolen, Jr.,‖ J. Quebert,¶ M. Sasao,** and T. Ward††

As part of a study of low energy charged pion production in collisions of nuclei with energies around the free nucleon pion production threshold (290 MeV per nucleon bombarding energy), a large ratio of inclusive π^- to π^+ cross sections has been observed for pions with the velocity near that of the incident projectile (i.e., 60 MeV pions for a 400 MeV per nucleon beam). Isospin symmetry suggests that that the π^- and π^+ ratio should be unity for isospin-symmetric nuclei. However, Coulomb interactions between pions and fragments of the projectile result in a large excess of negative pions with velocities near that of the projectile.[1,2]

Data from an early version of the 180 degree magnetic spectrometer used to collect the data are shown in Fig. 1, which plots invariant cross section versus pion kinetic energy in the lab for various neon beam energies incident on NaF, Cu, and U targets. An improved version of this spectrometer, which used two multi-wire proportional counters (MWPC's) inside the magnet, was used to expand, verify and improve the original set of data. The peak in the inclusive π^- cross section has now been observed for neon beam energies from 140 MeV/nucleon, which is well below the free nucleon pion production threshold, up to 670 MeV/nucleon. The peak has also been observed with a 557 MeV/nucleon Argon beam. The peak in the π^- cross section is, in general, sharpest for heavier beams and lighter targets, which strongly suggests that it is associated with spectator fragments.

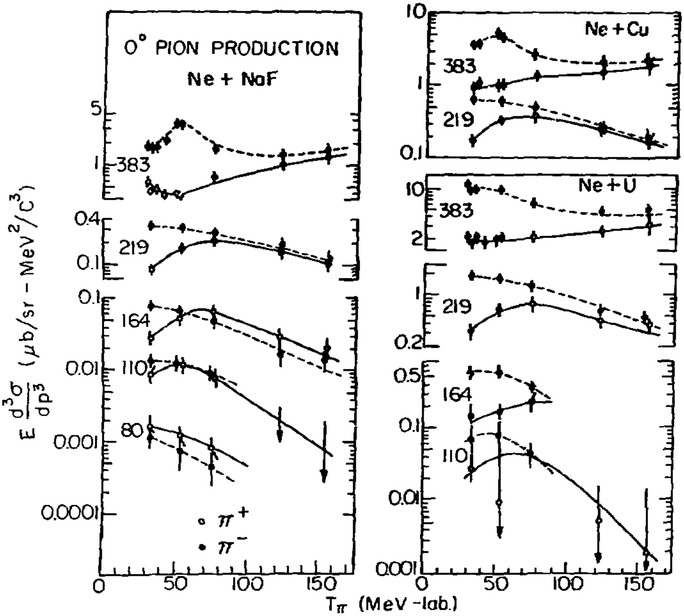

Fig. 1. (XBL 808-5736)

Footnotes and References

*Partially condensed from Phys. Rev. Lett. 43, 683 (1979), with effective in-target beam energies corrected from 125 to 80 MeV per nucleon, 150 to 110, 200 to 164, 250 to 219, and 400 to 383. cf. Errata, Phys. Rev. Lett. 44, 54 (1980).

†Institute for Nuclear Study, Tanashi, Tokyo, Japan, and LBL.

‡Dept. of Physics, Boston University, Boston, MA 02215.

§Institute de Physique Nucleaire, Orsay, France.

‖Cyclotron Laboratory and Physics Dept., Michigan State University, East Lansing, MI 48824.

¶Centre d'Etudes Nucleaires de Bordeaux I, France.

**Physics Dept., Osaka University, Toyonaka, Osaka, Japan, and LBL.

††Indiana University Cyclotron Facility, Bloomington, IN 47401.

1. G. Bertsch, Nature 283 (1980) 280.

2. M. Gyulassy and S. K. Kauffmann, Lawrence Berkeley Laboratory Report LBL-10279 (1980).

LOW-ENERGY PION PRODUCTION IN HIGH-ENERGY NUCLEUS-NUCLEUS COLLISIONS*

K. Nakai,† J. Chiba,† I. Tanihata,‡ M. Sasao,‡ H. Bowman, S. Nagamiya, and J. O. Rasmussen

Doubly differential cross sections for production of pions with 400-MeV/N ^{20}Ne on C, NaF, Cu and Pb have been measured for a range of 20 MeV < T_π^{LAB} < 100 MeV and 30° < θ_π^{LAB} < 150°. The results are compared with previous data with 800-MeV/N ^{20}Ne (see Fig. 1). The broad maximum at $\theta_\pi^{c.m.}$ = 90° in the center-of-mass angular distribution of low-energy pions observed at 800 MeV/N is not seen at the present energy. Neither was such a maximum at the central-rapidity region observed in (p + nucleus) reactions at E_p = 730 MeV. The 90° maximum seems to be a phenomenon specific to nucleus-nucleus collisions around 1 GeV/N, where the multiplicity of Δ formation is high and multiple-Δ interactions could influence the pion production. See also Wolf et al.[2]

Recently, the existence of deeply bound Δ-Δ (dibaryon) states has been shown theoretically[4] and experimentally.[5] If such multiple-Δ bound states were formed, the energies of pions from their decay should be lower than those from single-Δ decay and this could help explain the low energy central bump at 90° c.m.

Footnotes and References

*Condensed from LBL-8699 and Ref. 1.

†Department of Physics, University of Tokyo, Tokyo, Japan

‡Laboratory for Nuclear Studies, Osaka University, Toyonaka, Japan

1. K. Nakai, J. Chiba, I. Tanihata, M. Sasao, H. Bowman, S. Nagamiya, and J. O. Rasmussen, Phys. Rev. C, 20 (6) pp 2210-2218 (1979).

2. K. L. Wolf, H. H. Gutbrod, W. G. Meyer, A. M. Poskanzer, A. Sandoval, R. Stock, J. Gossett, C. H. King, G. King, Nguyen Van Sen, and G. D. Westfall, Phys. Rev. Lett. 22, 1448 (1979).

3. D. R. F. Cochran, P. N. Dean, P. A. M. Gram, E. A. Knapp, E. R. Martin, D. E. Nagle, P. B. Perkins, W. J. Schlaer, H. A. Thiessen, and E. D. Theriot, Phys. Rev. D. 6, 3085 (1972).

4. T. Kamae and T. Fujita, Phys. Rev. Lett. 38, 471 (1977).

5. T. Kamae, I. Arai, T. Fujii, H. Ikeda, N. Kajiura, S. Kawabata, K. Nakamura, I. Ogawa, T. Takada, and Y. Watase, Phys. Rev. Lett. 38, 468 (1977).

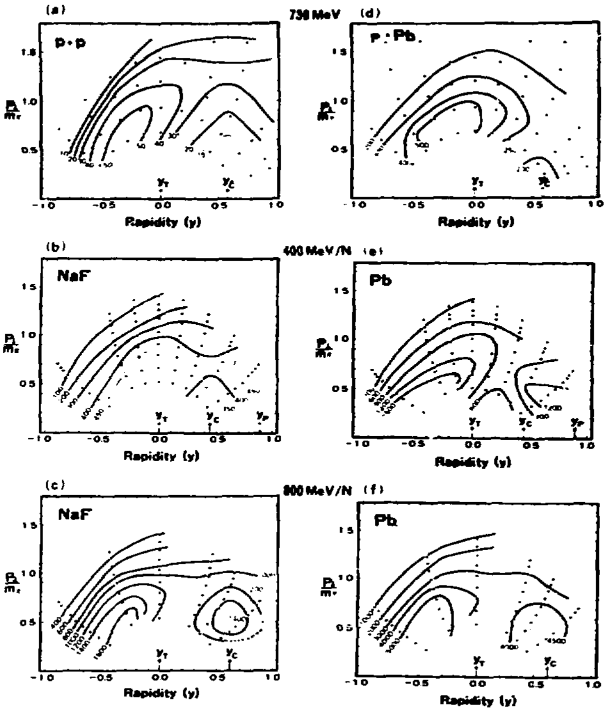

Fig. 1. Contour plots of Lorentz-invariant cross sections in $p_\perp$ (transverse momentum) and y (rapidity) plane for (a) p + p at 730 MeV[3], (b) ^{20}Ne + NaF at 400 MeV/N, (c) ^{20}Ne + NaF at 800 MeV/N, (d) p + Pb at 730 MeV[3], (e) ^{20}Ne + Pb at 400 MeV/N, (f) ^{20}Ne + Pb at 800 MeV/N. The numbers written along contour lines are the Lorentz-invariant cross sections in units of mb sr^{-1} GeV^{-2}c. The dots indicate observed points.

CALCULATION OF MUON FINAL-STATE PROBABILITIES AFTER MUON-INDUCED FISSION*

Z. Y. Ma,† X. Z. Wu,† G. S. Zhang,† Y. C. Cho,†
Y. S. Wang,‡ J. H. Chiou,‡ S. T. Sen,‡ F. C. Yang,‡ and J. O. Rasmussen

Following some muon-induced fission processes, the μ^- survives in final states bound to one of the fission fragments. Because the μ^- lifetime depends inversely on the mass of the binding nucleus, it is possible to determine the probability of μ^- being bound to the heavy fragment, the light fragment, or ejected into the continuum.

The final-state probabilities for the muon are associated with fission dynamics. If the motion of the nuclear system past the saddle point is infinitely slow, that is, by very viscous flow, the muon would always stay at the lowest energy level up to the scission point. Past the scission point the nuclear system is accelerated by the Coulomb force modified by the nuclear force and shape distortion at first, and the muon can be excited to the higher orbital and have a non-vanishing probability of ending up bound to the light fragment. On the other hand, if the motion of the nuclear system is not slow from saddle point to scission, that is, the motion is not so viscous, there should be already some fraction of muon excited-state population, even before scission. Thus, for non-viscous flow the greater percentage of muon binding to the light fragment should be obtained.

We felt it worthwhile to make new theoretical calculations[1], going beyond Ref. 2 in that we would examine extended charge distributions as well as point charges, study alternative forms of variational wave functions, and run a few cases with different conditions for fission asymmetry and nuclear viscosity form saddle to scission.

We use the method of perturbed stationary states (PSS) for the problem of the μ^- in the field of moving nuclear charges. We neglect the muon mass compared to the nuclear masses; that is, the separation motion of the nuclear centers is assumed not to be influenced by the muon motion.

In our two-state case we get two coupled time-dependent Schrödinger equations

$$\dot{a}_u(t) = -a_g(t)\,\langle\psi_u(t)\,|\tfrac{\partial}{\partial t}|\,\psi_g(t)\rangle \exp\left\{\frac{i}{\hbar}\int_0^t\left[E_u(t') - E_g(t')\right]dt'\right\} \quad (1a)$$

$$\dot{a}_g(t) = -a_u(t)\,\langle\psi_g(t)\,|\tfrac{\partial}{\partial t}|\,\psi_u(t)\rangle \exp\left\{\frac{i}{h}\int_0^t\left[E_g(t') - E_u(t')\right]dt'\right\} \quad (1b)$$

Using the modified Euler method we have integrated these equations on the NOVA 840 computer of the Atomic Energy Research Institute in Beijing.

To match the final fission kinetic energy of 170 MeV we choose the scission point of 17.6 fm as the starting distance. As for the excitation probability during the penetration of the fission barrier, we investigated two cases,

$|a_u|^2 = 0$ and $|a_u|^2 \neq 0$. For the latter case we assumed that from the saddle point to the scission point the separation speed of the two parts of the fissioning nucleus is uniform with (a) $v = 10^9$ cm/s or (b) $v = 3 \times 10^8$ cm/s. At the scission point of 18 fm the excitation probability is about 0.0015 for case (a), 0.00017 for case (b) and the kinetic energy at 18 fm is ~ 29.8 MeV for the former, ~ 2.68 MeV for the latter. The influence on the final excitation probability for case (b) can be neglected.

Fig. 1 shows the final excitation probability is ~ 0.06 for the case with $|a_u|^2 = 0$, $E_0 = 1$ MeV at 17.6 fm and ~ 0.08 for the case with $|a_u|^2 = 0.0015$, $E_0 = 29.8$ MeV at 18 fm. These results are close to the experimental estimate.

We wish to represent our foregoing calculations in a simple functional dependence on fission-charge asymmetry. Thus, for uranium ($Z_i = 92$) we have tested and found to be accurate the following expression:

$$P_\mu(Z) = \left\{1 + \exp[-b(Z^2 - (92 - Z)^2)]\right\}^{-1} = \left\{1 + \exp[b'(46 - Z)]\right\}^{-1} \quad (2)$$

The weighted sum over the fission yield curve is so nearly equal to the result for $Z_L = 40$, $Z_H = 52$ that we may use $Z_L = 40$, $Z_H = 52$ calculations to be representative of the full folded distribution.

It is satisfying to see that these simple calculations are in qualitative agreement with the experimental result of ~ 0.08 fractional attachment [3] to the light fragment and 0.92 to the heavy.

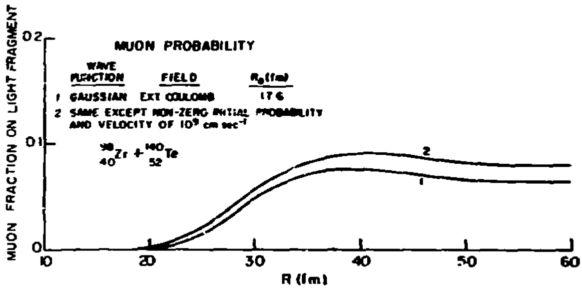

Fig. 1. Probability curves for more realistic viscous descent from saddle to scission point for fissioning system.
(XBL 799-7112)

Footnotes and References

*Condensed from LBL-9689 and Ref. 1.

†Atomic Energy Research Institute, Beijing, China

‡Fudan University, Shanghai, China

1. Z. Y. Ma, X. Z. Wu, G. S. Zhang, Y. C. Cho, Y. S. Wang, J. H. Chiou, S. T. Sen, F. C. Yang, and J. O. Rasmussen, Nuclear Physics A 348, 446 (1980). See also Chinese Journal of Nucl. Phys. 2, 107 (1980) (in Chinese).

2. P. Olanders, S. G. Nilsson and P. Moller, Phys. Lett. B90, 193 (1980).

3. S. Polikanov, Int. Atomic Energy Agency preprint IAEA-SM/23-E1 (1979).

PION PRODUCTION WITH HEAVY IONS*

Rubin H. Landau† and John O. Rasmussen

This paper[1] gives an informal review of pion production by heavy ions under the following headings: Introduction, Experimental Overview, Multiplicities, Single-particle Spectra, Cascade Calculations and Pion Interferometry in Relativistic Heavy-ion Collisions.

The promise and complexities of pions as probes of heavy ion collision dynamics are discussed for this new and developing field.

Footnotes and Reference

*Condensed from Ref. 1.

†Oregon State University, Corvallis, Oregon.

1. R. H. Landau and J. O. Rasmussen, Comments Nucl. Part. Phys. 9, pp. 1-14 (1979).

EVIDENCE FOR NONTHERMAL PION PRODUCTION IN THE CENTRAL INTERACTIONS OF Ar ON KCl AT 1.8 GeV/A

R. E. Renfordt,[*] J. W. Harris,[†] J. P. Brannigan, J. V. Geaga, H. Pugh, L. J. Rosenberg, A. Sandoval,[†] L. S. Schroeder, R. Stock[†] and K. L. Wolf[†]

The pions have in the participant-spectator models in contrast to other reaction products an unambiguous origin, namely the participants. The reaction dynamics are sensitive to the number of energies of the produced pions, which can significantly reduce the total available energy. It is necessary for models predicting single particle inclusive nucleon spectra to describe the pion production correctly. In the fireball-like models they arise from thermal production and the decay of isobars in thermal and chemical equilibrium with π^-'s, nucleons and nuclear fragments, giving an isotropic and thermal distribution in the center of mass for equal projectile and target mass systems.

As part of our streamer chamber study of the energy dependence of multipion production,[1] we have measured and reconstructed π^-'s produced in the central interactions of Ar on KCl at 1.8 GeV/A.

Preliminary results of the reconstruction of 3600 π^-'s show a nonisotropic distribution with forward-backward peaking in the c.m. frame, possibly a remnant of the $\Delta(3,3)$ decay pattern (Fig. 1). The cross section in the forward-backward cone is 39% higher than around 90° in the c.m. In order to extract a temperature of the region, where the π^-'s are produced, a thermal distribution ($E \cdot \exp(-E/T)$) has been fitted to the data, separately for π^-'s emitted in a forward-backward cone and a cone around 90°. The result is: T≈ 92 MeV summed over all emission angles, T≈ 98 MeV for the forward-backward cone and T≈ 86 MeV for 90° emission. The assumed thermal distribution fits the data quite well.

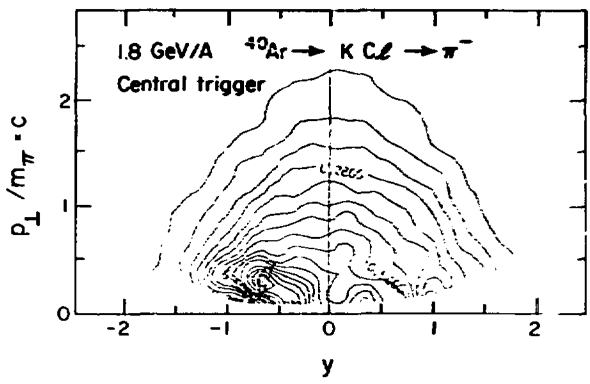

Fig. 1. Rapidity plot of π^- produced in 2600 central interactions of Ar on KCl at 1.8 GeV/A. (XBL 808-1713)

In Fig. 2 the total energy flux in the c.m. system going into π^- production is shown. The rather linear relationship with the π^- multiplicity can be reproduced by assuming an average kinetic energy of 140 MeV per π^- in the c.m. frame. Further calculations will show whether this is compatible with an independent particle model or whether coherent processes in the highly pressurized matter must be assumed.

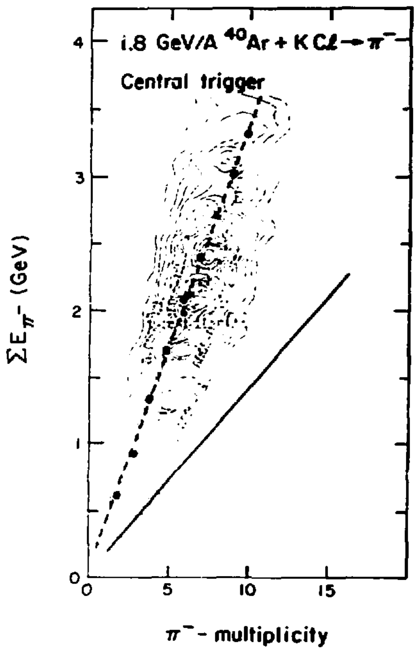

Fig. 2. π^- multiplicity vs. total center-of-mass energy going into π^-'s. The lower line corresponds to zero kinetic energy, the upper line to 187 MeV/π^- in the c.m.-frame.
(XBL 808-1714)

Footnotes and Reference

*University of Marburg, West Germany

†GSI, Darmstadt, West Germany

‡Now at Argonne National Laboratory, Argonne, IL 60440

1. J. P. Brannigan et al., in this annual report.

ENERGY DEPENDENCE OF MULTI-PION PRODUCTION IN HIGH-ENERGY NUCLEUS-NUCLEUS COLLISIONS

R. Stock,* A. Sandoval,* R. E. Renfordt,* H. E. Stelzer,* J. W. Harris, J. P. Brannigan J. V. Geaga, L. J. Rosenberg, L. S. Schroeder, and K. L. Wolf†

There is considerable interest in studying pion production and its energy dependence in A-A collisions. For example, pion multiplicity distributions provide essential information to test and constrain thermal and cascade model calculations. Recent hydrodynamic models predict an increase in the pion yield at the onset of phase transition in the dense interaction region.[1]

Using the LBL streamer chamber facility, we have systematically studied π^- production and accompanying nuclear disintegration in the interaction of ^{40}Ar and KCl for bombarding energies from 0.4-1.8 GeV/A. Data were taken in both the inelastic and a central trigger modes.

*Figure 1 shows a contour plot of the reac*tion cross section as a function of the π^-

multiplicity (n_{π^-}) and the total multiplicity (n_{tot}) for the inelastic trigger mode at 1.8 GeV/A. The reaction products are confined to a smooth distribution along a ridge with no discernible signature of anomalous pion production. For high multiplicities, the interaction approaches the total disintegration limit corresponding to the maximum number of observable charges. These features are also observed for lower bombarding energies.

The excitation function for the central trigger is shown in Fig. 2. The mean π^- multiplicity increases linearly once the bombarding energy is reasonably above pion production threshold. No marked discontinuities are observed in this dependence. Thermal models are found to overpredict the observed pion yields by about a factor of 2.

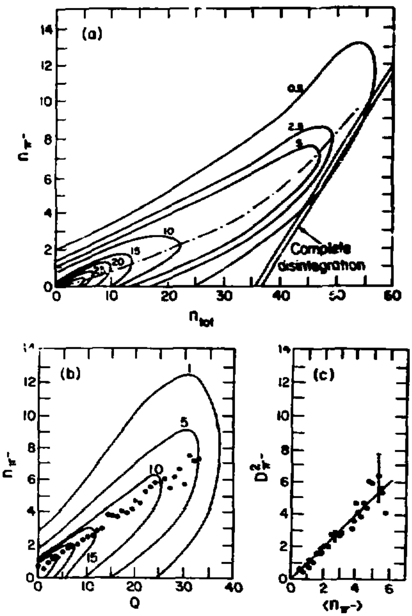

Fig. 1. Topology of reaction products for Ar and KCl in the inelastic trigger mode at 1.8 GeV/A. Solid lines are contours of constant cross section (mb). Dash-dotted line corresponds to the $\langle n_{\pi^-} \rangle$ as a function of the total multiplicity. (XBL 804-703A)

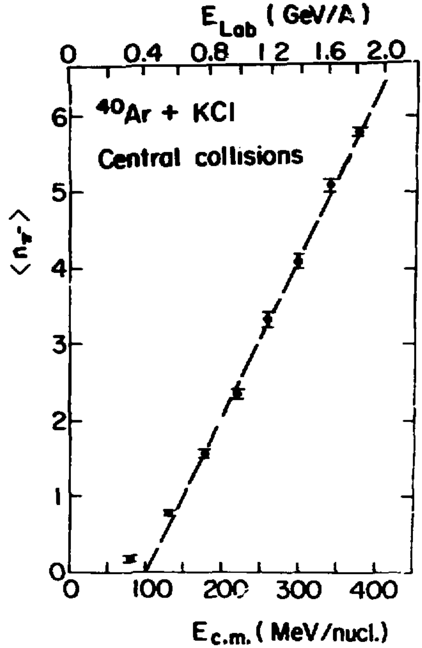

Fig. 2. Center of mass energy dependence of the mean π^- multiplicity for central collisions. (XBL 804-701)

Footnotes and Reference

*Gesellschaft für Schwerionenforschung, Darmstadt, West Germany

†Argonne National Laboratory, Argonne, Illinois 60439

1. H. Stocker, J. Maruhn, and W. Greiner, Z. Physik A286, 121 (1978) and Phys. Lett. 81B, 303 (1979).

INCLUSIVE KAON PRODUCTION IN HIGH-ENERGY NUCLEAR COLLISIONS*

S. Schnetzer, G. Shapiro, H. Steiner, I. Tanihata,†
M.-C. Lemaire,‡ R. Lombard,§ E. Moeller,‖ and S. Nagamiya

Inclusive K^+ production cross sections have been measured at angles from 15° to 80° in collisions of p (2.1 GeV/nucleon) + (NaF and Pb), d (2.1 GeV/nucleon) + (NaF and Pb), and Ne (2.1 GeV/nucleon) + (C, NaF, KCl, Cu, and Pb).

The motivation of the experiment came from the fact that the K^+ meson has a relatively small cross section for scattering on nucleons (about 10 mb), and that it is very slightly absorbed by nucleons because of its + strangeness. Therefore, we expect the observed kaon spectra to reflect more directly the initial stage of the interaction, whereas the pi-meson production reflects both initial and final stages.

We used a magnetic spectrometer. It was triggered by a Pb glass Cerenkov counter behind the spectrometer in which the Cerekov light was produced by the muon from K^+ decay. Since the yield of K^+ was about 10^{-3} of those of protons and pions, a lucite Cereknov counter was installed to veto pions. In addition, an on-line computer cut (we call it the MBD cut) was applied to reduce proton events from the main trigger.

A typical example of the spectrum is shown in Fig. 1 where invariant cross sections, (E/p^2) $(d^2\sigma/d\Omega dp)$, are plotted as a function of laboratory momentum. Using such data we studied the target-mass dependence of the yield. At forward angles the yield is roughly proportional to A_T^α, where A_T is the target mass and $\alpha \simeq 0.8$. Whereas at large angles α was ~ 1.2.

The main concern is whether or not the K^+ production is enhanced from what is normally expected. Here the word "normal" means the production cross sections calculated from non-exotic theories with reasonably convincing assumptions. A calculation by Randrup and Ko,[1] which is one such theory, predicts within a factor of 2-3 the forward yields, while the data at large angles (80°) are significantly smaller than this calculation. Randrup[2] recently modified his calculation by allowing the kaon to be scattered once (for Ne + NaF system) before detection. This modified calculation predicts reasonably well the slopes of the data. The absolute yields, however, are under predicted by a factor of ~ 2. Likewise a thermal model[3] predicts well the slopes but gives too much yield by a factor of ~ 40.

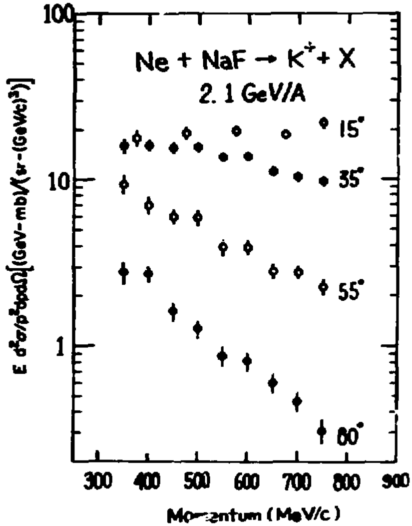

Fig. 1. (XBL 812-7908)

Footnotes and References

*Work supported by the Nuclear Science Division of the U.S. Department of Energy and INS-LBL Collaboration Program.

†On leave from INS, University of Tokyo, Tanashi-shi, Tokyo, Japan.

‡Present address: DPhN/ME, CEN de Saclay, 91190 Gif-sur-Yvette, France.

§On leave from DPhN/ME, CEN de Saclay, 91190 Gif-sur-Yvette, France.

‖Visitor from the Freie Universitat Berlin, Berlin, West Germany.

1. J. Randrup and C. M. Ko, Nucl. Phys. A343, 519 (1980).

2. J. Randrup, Phys. Lett. (in press).

3. F. Asai, H. Sato and M. Sano, Phys. Lett. 98B, 19 (1981).

STRANGE PARTICLE PRODUCTION IN CENTRAL COLLISIONS OF Ar ON KCl at 1.8 GeV/A

A. Sandoval,[*] J. P. Brannigan, A. Dacal,[†] J. Gosset, J. W. Harris,[*]
H. G. Pugh, R. E. Renfordt,[‡] L. S. Schroeder, R. Stock,[*] H. Stroebele[*] and K. Wolf[§]

The threshold for strange particle production (Λ, Σ, K) lies below the 1.8 GeV/A bombarding energy at which we have studied the central collisions of Ar on KCl. The study of the strange particle production is a unique probe of the high-energy nucleus-nucleus interactions. The high production threshold due to associated production (Λ+ K) and (Σ+ K) leads, at Bevalac energies, to their production most probably only in the first stage of the collision, before a large energy degradation has set in. In contrast to pions and isobars, they cannot be reabsorbed, due to strangeness conservation, making them a more primordial probe. Their production free NN interactions involves the strage quark-antiquark production from the vacuum. It is conceivable that this vertex is modified in a high-density high-temperature nuclear medium, making it very interesting to compare their production cross sections in different systems.

In our streamer chamber study of central collisions of equal mass systems, we are sensitive to the charged decay of neutral strange particles $K^0 \rightarrow \pi^+\pi^-$, Λ $p\pi^-$ as well as to γ conversions, $\gamma \rightarrow e^+e^-$, all of which produce secondary vertices (vees) in the fiducial volume. In order to study the strange particle production with relativistic heavy ions, a special scan of the central collision run of ^{40}Ar on KCl at 1.8 GeV/A was done to identify all the vees. The tracks were measured and reconstructed in three views; using the TVGP program, momentum vectors were obtained which were used to do a 3-constraint fit to the decay kinematics in order to identify the decaying particles. In the majority of the cases there was only one possible mass assignment that gave a small χ^2. We found that 73% of the vees were gammas which converted mostly on the high-Z material of the central electrode; 4% were identified as kaons and 23% as Λs. In Fig. 1 the resulting invariant masses of the strange particle decays are shown for the assumption that the vee corresponds to a $p\pi^-$ or a $\pi^+\pi^-$ pair. The arrows show the lines along which the Λs and K^0s should lie. For the events corresponding to a Λ mass, the momenta obtained are shown in Fig. 2 as a scatter plot in the center of mass p vs p plane. Surprisingly the Λs lie outside the region of maximum momentum in the N + N $\rightarrow$ N + Λ + K reaction, which corres-

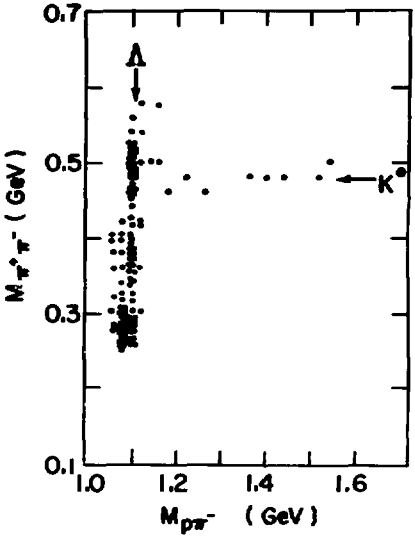

Fig. 1. Scatter plot of the reconstructed invariant masses of the charged decay of neutral strange particles produced in the central collisions of ^{40}AR + KCl at 1.8 GeV/A bombarding energy. For each event invariant masses are obtained assuming it is a $p\pi^-$ (Λ) or a $\pi^+\pi^-$(K^0) pair. The labeled arrows correspond to the lines along which Λs and K^0s would lie. Identified γs and events that converted in the central wire mesh are excluded.
(XBL 804-753)

ponds to a circle with p = 300 MeV/c radius around the c.m. Effects of fermi-motion might boost them out by 200 MeV/c more but not enough to explain the high c.m. momenta we observe.

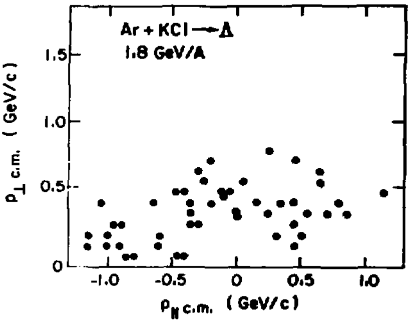

Fig. 2 Center of mass $p_\parallel$ vs $p_\perp$ scatter plot of the Λs produced in the central collisions of ^{40}Ar on KCl at 1.8 GeV/A. (XBL 804-754)

Footnotes

*Gesellschaft für Schwerionenforschung, Darmstadt, West Germany

§Present address: IFUNAM, Mexico 20 D.F.

†Present address: ANL, Argonne, IL 60440

‡University of Marburg, West Germany

NEUTRON EMISSION IN RELATIVISTIC NUCLEAR COLLISIONS*

J. D. Stevenson†

Charged particle emission in relativistic heavy ion collisions has been extensively studied in the last few years. Measurements of neutron emission have, however, only recently been made.[1] These measurements show that neutron and proton energy spectra for ~ 400 MeV/nucleon ^{20}Ne + U are substantially different[1]. The neutron to proton ratio, R,

$$R = \frac{d^2\sigma(n)}{d\Omega dE} \quad \frac{d^2\sigma(p)}{d\Omega dE}$$

decreases with increasing fragment energy. It varies from $R \approx 4$ at 20 MeV to $R \simeq 0.3$ at 600 MeV at all laboratory angles.

Recently I presented a cascade model of relativistic heavy ion collisions that accounts successfully for charged particle measurements.[2] I have found that this same model *accounts for the fragment energy dependence* of R. My model, which is parameter-free, assumes that the heavy ion collision proceeds in two steps.[2] First there is a cascade treated as a succession of free nucleon-nucleon elastic scatterings. Then in the final state some of the scattered nucleons coalesce to form light nuclei. This second stage uses the coalescence model[3] of Gutbrod et al. Using the coalescence model the proton and neutron spectra can be corrected to the time before coalescence took place. The precoalescence neutron spectrum is given by

$$\frac{d^2\sigma(n')}{d\Omega dE} = \frac{d^2\sigma(n)}{d\Omega dE} + \sum (A-Z)\, \frac{d^2\sigma(Z,A)}{d\Omega dE}$$

The sum is over all isotopes, but only H and He isotopes contribute significantly. It is important to note that Eq. 2 involves experimentally determined quantities only, no parameters. Using Eq. 2 and an analogous equation for protons it is possible to calculate the neutron to proton ratio before coalescence takes place, R'. Figure 1 compares the experimentally determined values of R' with those calculated from my cascade model. My cascade reproduces fairly well the fragment energy dependence of R'.

Much of the predicted energy dependence of *R' is due to the ~15% lower beam energy of the* neutron measurement. However, my cascade predicts that if both measurements were at exactly E_{beam} = 400 MeV/nucleon R' would fall from R' = 1.5 at 300 MeV to R' = 1.2 at 400 MeV. This is due to incomplete equilibration of the projectile-target system. Thus refined measurements of *the neutron to proton ratio R'* may provide a sensitive test of equilibration in heavy ion collisions.

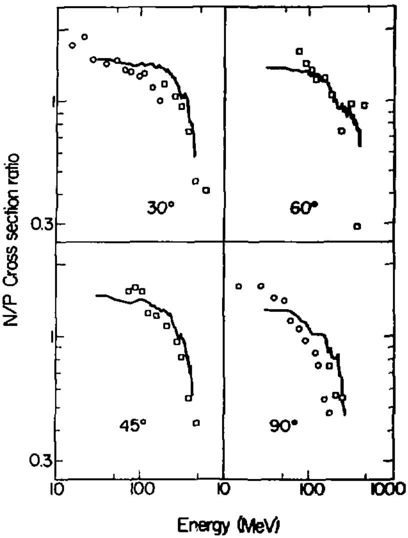

Fig. 1. Neutron to proton ratio before coalescence, R', versus energy. Triangles are based on proton data of Ref. 4. Squares are based on proton data of Ref. 5. The solid line is calculated from the cascade model discussed in the text. (XBL 807-1682)

Footnotes and References

*Condensed from a paper in preparation.

†Also at Space Sciences Laboratory

1. W. Schimmerling, J. W. Kast, D. Orthendahl, R. Madey, R. A. Cecil, B. D. Anderson, and A. R. Baldwin, Phys. Rev. Lett. 43, 1985 (1979).

2. J. D. Stevenson, Phys. Rev. Lett. 41, 1702 (1978).

3. H. H. Gutbrod, A. Sandoval, P. J. Johansen, A. M. Poskanzer, J. Gossett, W. G. Meyer, G. D. Westfall, and R. Stock, Phys. Rev. Lett. 37, 667 (1976).

4. A. Sandoval, H. H. Gutbrod, W. G. Meyer, R. Stock, Ch. Lukner, A. M. Poskanzer, J. Gosset, J.-C. Jourdain, C. H. King, G. King, Nguyen Van Sen, G. D. Westfall, and K. L. Wolf, Phys. Rev. C21, 1321 (1980).

5. M.-C. Lemaire, S. Nagamiya, O. Chamberlain, G. Shapiro, S. Schnetzer, H. Steiner, and I. Tanihata, private communication.

MEAN FREE PATH OF PROTONS INSIDE THE NUCLEUS AT E_p = 800 MeV DETERMINED FROM TWO-PROTON CORRELATIONS IN pA COLLISIONS*

I. Tanihata,† S. Nagamiya, S. Schnetzer, and H. Steiner

Inclusive proton spectra and two-proton correlations have been measured in collisions of 800 MeV protons on C, NaF, KCl, Cu, and Pb targets. A magnetic spectrometer was used to measure the inclusive spectra at laboratory angles from 10° to 60° for proton momenta between 0.5 and 2.0 GeV/C. When the spectrometer was set at θ = 40°, two-proton coincidences were measured with one proton detected by the spectrometer and the other proton detected by one of two plastic counter telescopes placed at (θ, ϕ) = (40°, 180°) and (40°, 90°), where the spectrometer was located at ϕ = 0°.

In inclusive proton spectra, strong peaks associated with pp or pn quasi-elastic scatterings (QES) were observed at small angles (15° and 30°), whereas at large angles (40° and 60°) no structures were seen in the momentum spectra. In two-proton coincidences, a peak due to pp QES clearly appeared in the proton momentum spectrum at 40° when the other proton was detected with the telescope at ϕ = 180° (in-plane two-proton coincidence); however, no structures were still seen in the spectrum when the coincidence was taken with the ϕ = 90° telescope (out-of-plane coincidence).

Figure 1 shows the target-mass dependences of the yields at the peak regions of QES. Inclusive yields, shown at the top, increase monotonically as a function of the target mass, while the in-plane coincidence yields, shown at the bottom, have a maximum value at the target

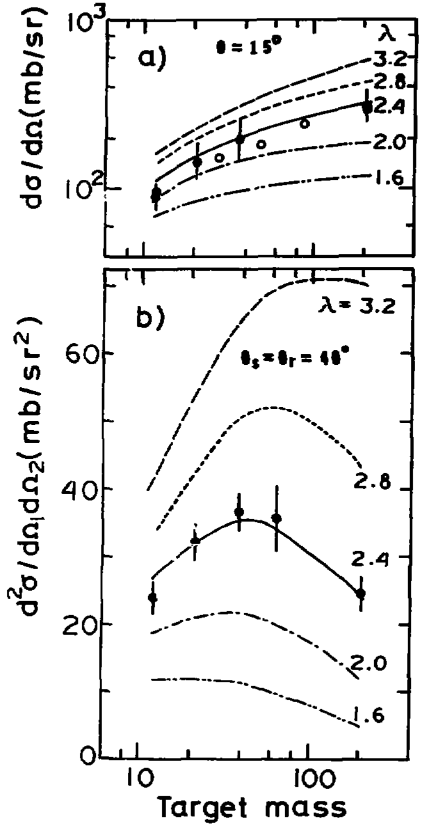

Fig. 1. Target-mass dependence of the single-proton QES cross section (a) and the two-proton QES cross section (b). Best fits are obtained for the mean free path λ = 2.4 fm.
(XBL 8012-13626)

mass around 40-50. As we increase the target mass, the probability of having pp QES increases, but at the same time, the probability of rescatterings after the pp QES also increases. In the present measurements the spectrometer and the in-plane telescope covered very limited kinematical regions, such that, if either proton from pp QES was rescattered inside the target nucleus, it would not be detected. The probability of detecting in-plane coincidence could, therefore, be lower for heavier-mass targets, due to such rescattering effects.

By parameterizing the rescattering effect before and after the pp QES by the mean free path λ, we fitted the observed target mass dependence. When we take $\lambda = 2.4 \pm 0.5$ fm for protons at 800 MeV, then the data are very well reproduced, as seen in the figure. This value is about 1.6 times larger than the value expected from the free nucleon-nucleon collisions.

Footnotes

*Abstract submitted to International Nucl. Physics Conference, Berkeley, 1980.

†On leave from INS, University of Tokyo, Tanashi-shi, Tokyo, Japan.

THE CORRELATION OF TWO PROTONS AT SMALL RELATIVE MOMENTA FROM COLLISIONS OF ^{40}Ar AND KCl AT 1.8 GeV/A

J. B. Carroll,* K. Ganezer,* G. Igo,* Y. Miake, T. A. Mulera, J. Oostens,* A. L. Sagle, V. Perez-Mendez, I. Tanihata, D. Woodard,† and F. Zarbakhsh

We have measured the correlation between two protons that are emitted at small relative momenta from collisions of 1.8 GeV/nucleon ^{40}Ar projectiles on a KCl target. We were motivated in part by the theoretical work of S. Koonin[1] who suggested that the correlation function is sensitive to the spatial (r) and temporal (τ) extent of the interaction region in relativistic heavy ion collisions. Our immediate goal is to experimentally test the feasibility of using the correlation function as a technique for measuring sizes and lifetimes. We then wish to employ this technique in conjunction with a high multiplicity trigger to measure the size and lifetime of the compound system or "fireball"[2] that may be formed in the Ar-KCl center of mass.

Measurements have been made when the average momentum of the two protons corresponds to the beam rapidity Y_B(P/Z = 2.4 GeV/c and θ_{Lab} = 6°) and the mid-rapidity $Y_B/2$(P/Z = 1.0 GeV/c and θ = 13.45°). Protons travelling at Y_B are thought to come from the projectile remnant while protons travelling at $Y_B/2$ are associated with the "fireball". By studying the correlation function, R, in these two rapidity regions, we hope to measure the relative sizes of the fireball and the projectile remnant.

The two protons are detected in a magnetic spectrometer which is instrumented with plastic scintillation counters (S), multiwire proportional chambers (MWPC) and a 24-element scintillator hodoscope (H). We have also sampled the multiplicity of high P_t fragments with an array of multiplicity counters (MU) that surround the target.

The correlation function R is formally defined from the relation

$$\frac{d^2\sigma}{d\vec{P}_1 d\vec{P}_2} = \frac{1}{\sigma_T}\frac{\langle n(n-1)\rangle}{\langle n\rangle^2}\frac{d\sigma}{d\vec{P}_1}\frac{d\sigma}{d\vec{P}_2}(1+R)$$

where $\frac{d^2\sigma}{d\vec{P}_1 d\vec{P}_2}$ is the two particle inclusive differential cross-section, $\frac{d\sigma}{d\vec{P}_1}$ is the single particle inclusive differential cross-section, σ_T is the total inclusive cross-section for observing a proton, and $\langle n\rangle$ and $\langle n(n-1)\rangle$ are the first and second moments of the proton multiplicity distribution.

Preliminary results for the correlation function using single proton mixing are shown in Fig. 1. The symbols (o) represent data at $Y_B/2$

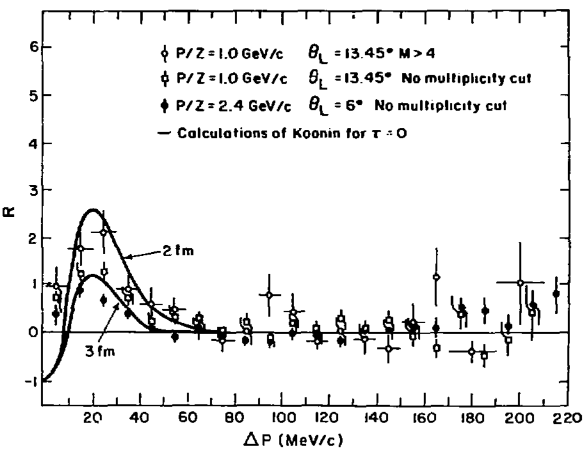

Fig. 1. (XBL 8011-2409)

for which a multiplicity of five or more was required in the trigger for both the two proton and single proton data. The symbols (X) represent data at $Y_B/2$ with no multiplicity requirement. The symbols (•) represent data near Y_B with no multiplicity requirement. The curves are S. Koonin's calculations of R for r equal to 2 and 3 fm when $\tau = 0$.

Even at this early stage in the analysis, it is possible to draw some tentative conclusions. The agreement between the shape of the data and Koonin's predictions seems quite good. The sizes obtained by comparing our data to Koonin's $\tau = 0$ calculations represent upper limits because a finite lifetime reduces the peak in the correlation function. The sizes we extract for the three different settings shown in Figure 1 are 2.2, 2.9, and 3.5 fm for data at $Y_B/2$ ($M > 4$), $Y_B/2$ ($M \geq 0$), and Y_B ($M \geq 0$), respectively. Since Koonin used Gaussian distributions it is necessary to multiply these sizes by 1.5 to compare them to the RMS values of sharp sphere distributions.

The upper limit for the size of projectile remnant is 5.5 fm which is larger than 4.1 fm, the radius of ^{40}Ar. This larger apparent size could be caused by a finite lifetime ($\tau \approx 7 \times 10^{-23}$). On the other hand, this type of experiment is sensitive to the region of the final hadronic interaction between the protons and the rest of the nuclear medium. If the projectile remnant is expanding and these last interactions occur when the density is lower than normal nuclear density, one might expect to measure a size that is larger than that of the original projectile.

The size of the source at $Y_B/2$ appears to be smaller than at Y_B. It is possible that at so high a bombarding energy only a small portion of the participant region (the geometrical overlap between the projectile and the target) are actually stopped in the center of mass. This can be checked by measuring R at lower bombarding energies.

In the near future we hope to extract lifetimes as well as sizes by fitting our data to the predictions of Koonin's model. We also plan to see whether cascade calculations[3] suggest any correlation between relative momentum and the size of the interaction region which might explain the small size we measure at $Y_B/2$.

Footnotes and References

*Physics Department, University of California, Los Angeles, CA

†California State University, Hayward, CA

1. S. Koonin, Phys. Lett. 70B (1977) 43.

2. J. Gosset et al., Phys. Rev. C16 (1977) 629.

3. J. Cugnon, T. Mizutani, and J. Vandermeulen, Cal. Tech. preprint MAP10 (Feb. 1980).

OBSERVATION OF HIGH MOMENTUM PROTONS FROM LIMITING TARGET FRAGMENTATION*

J. V. Geaga, S. A. Chessin, J. Y. Grossiord,† J. W. Harris, D. L. Hendrie, L. S. Schroeder, R. N. Treuhaft, and K. Van Bibber‡

Inclusive distributions of protons produced at 180° have been measured in the momentum range $0.3 \leq p \leq 1.0$ GeV/c. Proton, alpha, carbon, and argon beams in the range of kinetic energies $0.4 \leq T \leq 2.1$ GeV/n (4.89 GeV for protons) were incident on C, Al, Cu, Sn, and Pb targets.

The energy dependence of the proton-induced cross sections is shown in Fig. 1. Results from other measurements at 90 MeV, 600 MeV, 7.72 GeV, and 400 GeV have been included. The data indicate limiting behavior of the distributions in the range of momenta $0.4 \leq p \leq 1.0$ GeV/c starting between 1.0 and 2.0 GeV. Results with other targets and also with heavier projectiles are similar.

The dependence of the proton production cross sections on projectile mass for a carbon target at an incident energy of 1.05 GeV/n is shown in Fig. 2. The shapes of the proton spectra in the momentum range 0.4 p 1.0 GeV/c are seen to be roughly independent of projectile mass. Plotted on the same figure (in the projectile rest frame) are data from Papp[1] for C + C → p(2.5°) at 1.05 GeV/n. Recent theoretical investigations[2] show that the internal momentum distributions in nuclei can be approximated by two overlapping Gaussians when short-range correlations are included. The low momentum Gaussian is dominated by the single particle characteristics of the momentum distributions and the second Gaussian emerges when short-range correlations are considered. Specifically, these investigations propose that the higher momentum components in nuclei arise predominantly from short-range correlations. The solid line shown in Fig. 2 is a double Gaussian parametrization of the C + C → p data. If the internal momentum distributions are indeed correctly specified by the models, then one is led to conjecture that the shapes of the

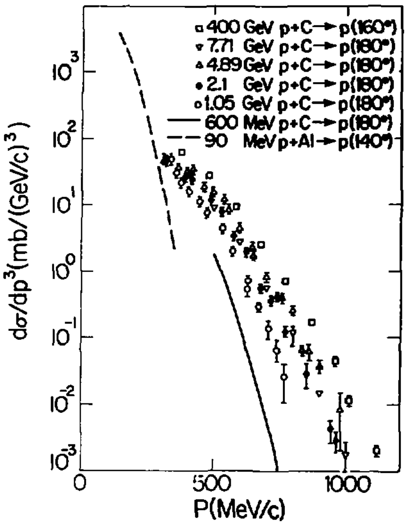

Fig. 1. (XBL 7912-13375)

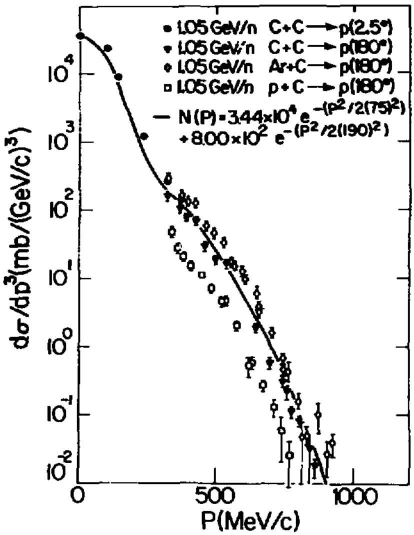

Fig. 2. (XBL 7912-13374

measured distributions in the momentum region $0.4 \le p \le 1.0$ GeV/c are a consquence of the presence of nuclear correlations.

In conclusion, we find that the data span a transition region wherein the inclusive distributions of protons in the momentum range $0.4 \le p \le 1.0$ GeV/c are found to exhibit limiting behavior. Recent theoretical work[3] also indicates that at higher energies, backward spectra in the same momentum region are mainly composed of spectator nucleons from the breakup of correlated pairs in the nucleus. The data, together with recent theoretical descriptions of internal momentum distributions in nuclei and reaction mechanisms involving correlated nucleons, strongly suggest that the limiting shapes of the measured spectra are related to the presence of correlations in the nucleus.

Footnotes and References

*Condensed from LBL-10265

†Present address: Institut de Physique Nucleaire de Lyon, France.

‡Department of Physics, Stanford University.

1. J. Papp, LBL-3633, Berkeley (1975), Ph.D. thesis (unpublished).

2. J. G. Zabolitsky and W. Ey, Phys. Lett. 76B, 527 (1978). O. Bohigas and S. Stringari, Preprint ORSAY IPNO/TH 79-59 (1979). J. W. van Orden et al., Preprint U. of Md. TR 80-046 (1979).

3. L. L. Frankfurt and M. I. Strikman, Phys. Lett. 83B, 407 (1979). T. Yukawa and S. Furui, Phys. Rev. C20, 2316 (1979).

THE AGE OF THE COSMIC RAYS*

D. E. Greiner and M. E. Wiedenbeck†

The age of the cosmic rays is one of the key parameters required in order to model processes of cosmic ray acceleration and propagation. This age, combined with the observed cosmic ray flux, establishes the power output required from the cosmic ray sources and influences the efficiency required of acceleration mechanisms. It also has direct bearing on the questions of how strongly the cosmic rays are confined in the propagation volume and of the mean density of interstellar gas in that volume.

Measurements of the abundance of long-lived radioactive isotopes in the galactic cosmic rays provide an excellent probe of this lifetime and ^{10}Be ($T_{1/2}$ = 1.6 x 10^6 years in the laboratory) is the best candidate for this measurement. The fact that the fraction of the cosmic ray beryllium expected to be ^{10}Be, even in the absence of ^{10}Be decay, is small (~ 0.1 to 0.2) makes this measurement difficult. Even the most recent isotopic composition experiments have had to rely on peak fitting techniques to derive the ^{10}Be abundance, in many cases without even the benefit of an accelerator calibration of the peak shapes. Balloon-borne experiments have suffered from the additional difficulty that ^{10}Be produced in the overlying atmosphere by fragmentation of heavier species contaminates the desired signal from galactic ^{10}Be, contributing as much as half of the observed abundance.

We have made a measurement of the isotopic composition of galactic cosmic ray beryllium which overcomes these problems. Our measurement, made with the U.C. Berkeley HKH experiment[1] aboard the ISEE-3 spacecraft, has for the first time achieved complete separation of the cosmic ray beryllium isotopes. This measurement covers the energy interval ~ 60 to 185 MeV/amu. Figure 1 shows a cross-sectional view of the detector system. Mass determinations are made on an event-by-event basis for cosmic rays stopping in the detector system employing energy loss signals from up to nine Si(Li) detectors and a trajectory measurement obtained from six drift chambers.

Figure 1 shows the distribution of masses calculated for the 345 beryllium events included in this analysis. The three well-resolved peaks correspond to ^7Be (which decays by electron capture in the laboratory but is fully stripped and therefore stable at cosmic ray energies), ^9Be and ^{10}Be. The average mass resolution for these data is σ_M = 0.15 amu, a factor of two better than achieved in any previous measurement of cosmic ray beryllium.

For the interpretation of our observations we have adopted a standard model in which cosmic ray propagation is assumed (1) to occur in a homogeneous medium subsequent to acceleration, and (2) to be characterized by an exponential distribution of potential pathlengths. In addition, cosmic rays are assumed to undergo solar modulation in penetrating to the earth's orbit.

For this analysis we obtain the number density of atoms of interstellar gas in the cosmic ray confinement volume as 0.3 ± 0.1/cm^3. This density, combined with the escape mean-free path of 5.5 g/cm^2 used in the calculation, can be used to calculate the "cosmic ray age," that is, the mean escape time from the confinement volume. For β = 1 particles we obtain $\tau_{esc} = (8.0^{+4.0}_{-2.4}) \times 10^6$ yr. These uncertainties in n_H and τ_{esc} are due to measurement errors alone.

We thank Fred Bieser, Hank Crawford, Harry Heckman and Peter Lindstrom for contributions to this experiment.

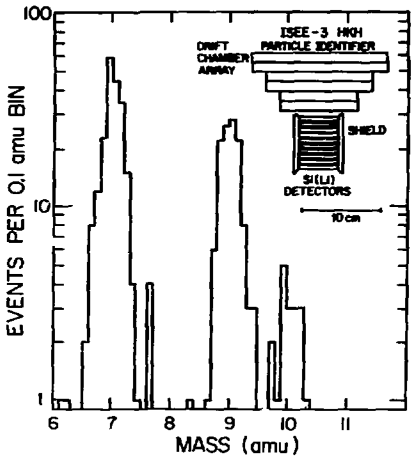

Fig. 1. Histogram of the masses calculated for the 345 beryllium events (60-185 MeV/amu). Inset shows cross sectional view of the U.C. Berkeley HKH detector system on ISEE-3.
(XBL 804-9157)

Footnotes and Reference

*Abstracted from a contribution to the Astrophysical Journal (Letters), August, 1980.

†Space Sciences Laboratory, University of California, Berkeley, CA 94720.

1. D. E. Greiner, F. S. Bieser, and H. H. Heckman, IEEE Trans. on Geoscience Electronics 16, 163 (1978).

DISCOVERY OF NEW NEUTRON RICH ISOTOPES ^{20}Ca and ^{27}F

J. D. Stevenson* and P. B. Price*

Techniques to produce extremely neutron-rich isotopes include proton-induced fragmentation of heavy nuclei, deep inelastic heavy ion reactions, and most recently, fragmentation of relativistic heavy ions.

We present results of a search for new neutron-rich isotopes produced by fragmenting 210 MeV/amu ^{48}Ca nuclei. These results include the first proof of particle stability of ^{20}C and ^{27}F. In addition we have confirmed previous reports of particle stability of ^{19}C, ^{22}N, ^{24}O, and ^{26}F.

Projectile fragments are characterized by having very small transverse momenta, $\sigma(P_\perp) \simeq$ 150 MeV/c. The longitudinal momentum is strongly peaked at the beam momentum-per-nucleon with $\sigma(P_{\parallel}) \simeq$ 150 MeV/c. Thus in the laboratory the fragments form a beam diverging only ~ 1° from the beam direction.

Our experimental procedure[1] involved deflecting the "beam" of fragments with the Bevalac Beam-40 0° spectrometer and stopping them in a stack of Lexan plastic track detectors. Later the detectors were processed and ~ 10^4 tracks were located. The end of range of each particle was determined in three dimensions. This provided simultaneous measurements of range and magnetic deflection of particles. In addition the charge was measured at the end of range. Typical beam intensity was ~10^7 ^{48}Ca ions/sec. The target was 0.89 g/cm^2 Be.

Figure 1 shows the data accumulated over a 40 hr run for carbon, nitrogen, oxygen, and fluorine nuclei. The mass resolution is $\sigma_m \simeq$ 0.23 for carbon to $\sigma_m \simeq 0.34$ at fluorine. The ratio of peak heights does not reflect the relative yields of isotopes. There is clear evidence for the first observation of ^{20}C and ^{27}F. In addition ^{22}N and ^{26}F, which have been observed only once before,[2] are confirmed. The statistical signficance of possible peaks at ^{21}C, ^{23}N, and ^{25}O is being considered.

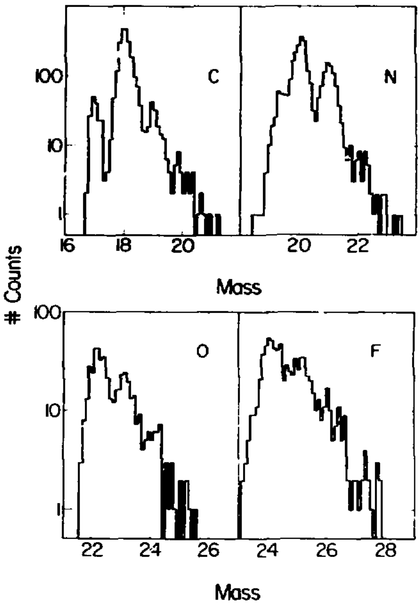

Fig. 1. Mass histograms for carbon, nitrogen, oxygen, and fluorine fragments from 210 MeV/nucleon ^{48}Ca projectiles. The isotopes ^{20}C and ^{27}F are clearly observed.

(XBL 807-1390)

Footnote and References

*Also at Space Sciences Laboratory

1. J. D. Stevenson, P. B. Price, and M. P. Budiansky, Nucl. Instr. and Meth. 171, 93 (1980).

2. G. D. Westfall, T. J. M. Symons, D. E. Greiner, H. H. Heckman, P. J. Lindstrom, J. Mahoney, A. C. Shotter, and D. K. Scott, Phys. Rev. Lett. 43, 1859 (1979).

EVIDENCE FOR ANOMALOUS NUCLEI AMONG RELATIVISTIC PROJECTILE FRAGMENTS FROM HEAVY ION COLLISIONS AT BEVALAC ENERGIES*

E. M. Friedlander, R. W. Gimpel, H. H. Heckman, Y. J. Karant, B. Judek,[†] and E. Ganssauge[‡]

Evidence for anomalously short reaction mean free paths (mfp) of projectile fragments (PF) from high energy heavy ion collisions has been persistently reported in cosmic ray studies since 1954; however, because of limited statistics, these results have not gained recognition. To overcome this limitation, we have performed two independent similar experiments with beams from the LBL Bevalac.

Two stacks of Ilford G5 nuclear research emulsion pellicles were exposed to relativistic heavy ion beams parallel to the emulsion surfaces (2.1 GeV/nucleon ^{16}O and 1.88 GeV/nucleon ^{56}Fe).

Interactions, defined as events showing emission of at least one target- or projectile-related track, were collected by scanning along the tracks of beam nuclei. Relativistic tracks of charge $Z \geq 3$, with velocity approximately equal to the beam, emitted from all generations of the extra-nuclear cascade within a 100 mr forward cone were followed until they either interacted or left the stack.

Our results, based upon 1470 events, can be summarized as follows:

1) Over the first few cm after emerging from a nuclear interaction (~ 10g/cm^2 of matter traversed or ~ 10^{-11} s proper time) the PF's exhibit significantly shorter mfp's than those derived from "normal" beams of the same charge Z;

2) at larger distances from the emission point, the mfp's revert to "normality" in the above sense;

3) the data are incompatible with a homogeneous lowering of the mfp and require the presence among PF's of at least one component with an unexpectedly high reaction cross section.

In the energy range 0.2-2.1 GeV/nucleon, the mean free path λ of beam nuclei, $2 \leq Z \leq 26$, can be parameterized as $\lambda(Z) = \Lambda Z^{-b}$, where $\Lambda = \Lambda_{beam} = (30.4 \pm 1.6)$ cm and $b = 0.44 \pm 0.02$. We investigated the dependence of Λ on distance D after emission of a projectile fragment and obtain for $D \leq 2.5$ and > 2.5 cm estimates for Λ (displayed at the bottom of Table 1) which differ by 3.4 S. D.

We display in Table 1 charge-grouped estimates for λ which illustrate that this effect is present in all charges of PF's. The probability $P_D(<F_D)$ where $F_D = \lambda^*(D < 2.5 \text{ cm})/\lambda^*(D > 2.5 \text{ cm})$ should be uniformly distributed between 0 and 1 for all charges Z. We obtain the mean $\bar{P}_D = 0.323 \pm 0.053$, which is 3.4 S.D. from the expected value of 1/2. This result is independent of any assumption about the functional dependence of λ upon Z, and indicates that within the first few cm after PF emission, λ is significantly less than at larger distances.

Let us assume as a first approximation that, in addition to normal nuclei, there is a fraction a of "anomalous" PF's with a constant "short" mfp $\lambda_a \ll \lambda$, leaving a fraction 1-a that behaves "normally" as confirmed by our observations at larger distances after emission. We have made estimates of a and λ_a by χ^2 minimization from our data and obtain $a^* \approx 6\%$, $\lambda_a^* \approx$ 2.5 cm. Assuming (sic!) that $\bar{\lambda}(Z)$ can be extrapolated to $\lambda_a \approx 2.5$ cm, this corresponds to a preposterous $Z \approx 300$.

We are not aware of explanations within the framework of conventional nuclear physics for the results of this experiment.

Table 1. Weighted estimates for the mean free path λ and the parameter Λ at different distances D from the origins of PF's for grouped charges. Expected values assuming $\lambda(Z) = \Lambda Z^{-b}$ are given in the last column.

Z	$\lambda^*(D \leq 2.5$ cm) (cm)	$\lambda^*(D > 2.5$ cm) (cm)	$\langle\lambda\rangle$ (cm)
3-8	12.4 ± 0.7	14.0 ± 0.5	14.6
9-16	8.3 ± 0.7	11.6 ± 1.0	10.6
17-26	6.0 ± 0 6	8.0 ± 0.8	8.4
	Λ^*(D 2.5 cm) (cm)	$\Lambda^*(D > 2.5$ cm) (cm)	$\langle\Lambda\rangle$ (cm)
3-26	25.0 1.1	30.0 1.0	30.4

Footnotes

*Condensed from LBL-11136, and Phys. Rev. Lett. 45, 1084 (1980)

†Division of Physics, National Research Council, Ottawa K1A 0R6, Canada

‡On leave from Fachbereich Physik, Philipps Universtat, Marburg, West Germany

TARGET FRAGMENT ENERGIES AND MOMENTA IN THE REACTION OF 4.8 GeV 12C and 5.0 GeV 20Ne WITH 238U

W. Loveland,* Cheng Luo,† P. L. McGaughey, D. J. Morrissey and G. T. Seaborg

The study of the fragmentation of a ^{238}U target nucleus by relativistic heavy ion (RHI) projectiles has revealed many new and interesting phenomena particularly in regard to the yields of the survivors of deep spallation processes (with $A_{fragment} > 150$). To better understand these phenomena, we measured the target fragment energies and momenta for two such reactions (4.8 GeV ^{12}C + ^{238}U and 5.0 GeV ^{20}Ne + ^{238}U) using the thick target-thick catcher recoil technique. Details of the experimental techniques and data analysis have been described previously.[1]

A portion of the results of these studies for the reaction of 4.8 GeV ^{12}C + ^{238}U is shown in Fig. 1. Here the fraction of target fragments recoiling forward from the target relative to the fraction recoiling backward (F/B) along with the target fragment energies is shown as a function of the product mass number A and the displacement ($Z - Z_A$) of the fragment atomic number, Z, from the non-integral Z corresponding to the center of the valley of β-stability, Z_A. In this figure one sees evidence of the occurrence of several different processes.

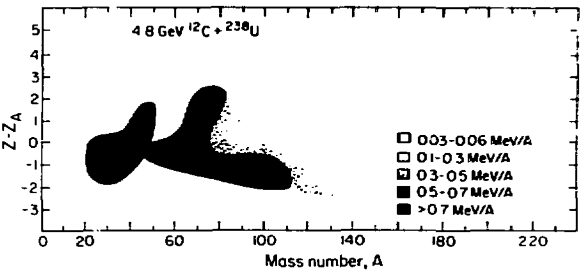

Fig. 1. A contour plot of the fragment kinetic energies <E> and F/B ratios as a function of the fragment mass number A and the position of the fragment relative to the center of the valley of β-stability, $Z-Z_A$. (XBL 809-1869)

The lightest fragments (A < 40) are characterized by high kinetic energies and large values of F/B which is consistent with their production in a "fragmentation" mechanism. The heaviest fragments (A > 150) are neutron-deficient, show very large values of F/B and very low fragment kinetic energies. Undoubtedly, these products are the result of deep spallation of ^{238}U nuclei. The intermediate mass products ($80 \leq A \leq 140$) are a complex mixture of fission and deep spallation products. The most n-rich products ($90 \leq A \leq 110$) are mostly fission fragments (F/B ~ 1, high kinetic energies). The mass and atomic numbers of these products and their kinetic energies are consistent with their formation in the fission of a species with A ~ 210, Z ~ 85 with some slight admixture of deep spallation products. Their kinetic energies are too low to be consistent with the fission of uranium-like species, a phenomenon similar to that observed in such high energy induced reactions as photon-induced fission where fission occurs primarily at the end of the evaporation chains involved in de-excitation of the primary target fragments.

The group of fragments with $40 \leq A \leq 70$ represents an interesting class of events. Their kinetic energies are relatively high and the values of F/B are also larger ($2 \leq F/B \leq 3$). One possible explanation of the origin of these events is that they represent the products of the fission of a species with A ~ 120-130. Their kinetic energies are completely consistent with this idea and their F/B ratios would indicate their formation in a non-peripheral collision. The other part of this scenario would be the large group of neutron-deficient products with $120 \leq A \leq 140$ which represent the nonfissioning survivors of the precursors of the $40 \leq A \leq 60$ events.

In Fig. 2, we show a comparison between measured and calculated values of the longitudinal velocity $\beta_{\parallel}$ ($= v_{\parallel}/c$) imparted to the fragment in the first step of the projectile-target interaction for the 4.8 GeV ^{12}C + ^{238}U reaction. The calculations of $\beta_{\parallel}$ were made using the intranuclear cascade model of Yariv and Fraenkel[3] and the firestreak model.[4] The measured values of $\beta_{\parallel}$ selected for use in Fig. 2 are for neutron deficient species. This selection was made to emphasize deep spallation reactions and to de-emphasize fission, i.e., to select products from collisions with significant projectile-target overlap. As one can see from examining Fig. 2, the cascade model grossly overestimates the values of $\beta_{\parallel}$ for all fragments with A < 209 with the firestreak model predictions also in gross disagreement with the experimental data. This situation may be analogous to the overestimates of the deep spallation product momenta in proton-nucleus collisions by cascade calculations.[5] Crespo, Cumming, and Alexander[5] speculated that the primary spallation products might emit fragments such as ^{24}Na thus reducing the spallation product momenta and providing a natural mechanism for producing the high momenta associated with these light fragments. The mechanism is reasonable given the calculated excitation energies (firestreak model) of the precursors of the A = 160-190 fragments which range in energy from 595 to 380 MeV, respectively.

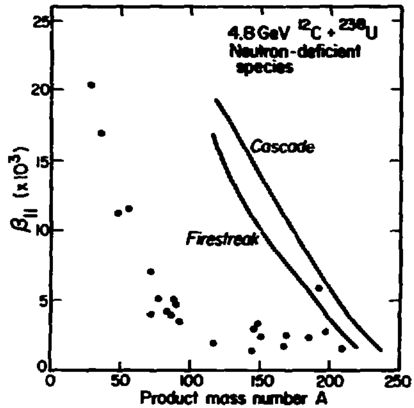

Fig. 2. A comparison of the calculated and measured values of $\beta_{\parallel}$. (XBL 806-1743)

Footnotes and References

*Permanent address: Dept. of Chemistry, Oregon State University, Corvallis, OR 97331.

†Permanent address: Atomic Energy Research Institute, Beijing, People's Republic of China.

1. W. Loveland, D. J. Morrissey, K. Aleklett, G. T. Seaborg, S. B. Kaufman, E. P. Steinberg, B. D. Wilkins, J. B. Cumming, P. E. Haustein, and H. C. Hseuh, Phys. Rev. C 23, 253 (1981).

2. B. D. Wilkins, S. F. Kaufman, E. P. Steinberg, J. A. Urbon, and D. J. Henderson, Phys. Rev. Lett. 43, 1080 (1979).

3. Y. Yariv and Z. Fraenkel, Phys. Rev. C20, 2227 (1979).

4. W. D. Myers, Nucl. Phys. A296, 117 (1978); J. Gosset, J. I. Kapusta, and G. D. Westfall, Phys. Rev. C18, 844 (1978).

5. V. P. Crespo, J. B. Cumming, and J. M. Alexander, Phys. Rev. C2, 1777 (1970).

TARGET RESIDUE RECOIL PROPERTIES IN THE INTERACTION OF 8.0 GeV ^{20}Ne with ^{181}Ta*

W. Loveland,[†] D. J. Morrissey, K. Aleklett,[‡] G. T. Seaborg,
S. B. Kaufman,[§] E. P. Steinberg,[§] B. D. Wilkins,[§] J. B. Cumming,[||] P. E. Haustein,[||] and H. C. Hseuh[||]

We report the results of an interlaboratory study of the target fragment momenta and energies from the reaction of 8.0 GeV ^{20}Ne with ^{181}Ta. We found that the fragment kinetic properties are considerably different than those found in the reaction of 25 GeV ^{12}C + ^{181}Ta and, furthermore, the specific product forward momenta observed in the reaction of 8 GeV ^{20}Ne + ^{181}Ta exceed those in relativistic proton induced reactions with heavy targets.

The experimental technique used to measure the target fragment recoil properties was the thick target-thick catcher technique. Independent foil stacks from each of the participating laboratories were irradiated simultaneously and the product radioactivities assayed by off-line γ-ray spectroscopy. The results of these measurements are presented as the fractions of each radionuclide which recoiled out of a target into the forward and backward directions, F and B, respectively. The forward to backward ratios, F/B, for various target fragments are shown in Fig. 1 along with data from similar proton induced reactions. (All data are the weighted averages of the measurements of the different laboratories which, in general, agreed within experimental uncertainty.) The results were transformed into kinematic quantities using the simple two step vector model of high energy nuclear reactions. In this model, each target fragment kinematic property is decomposed into two components, one resulting from an initial fast projectile, target interaction (the "abrasion step" of the abrasion-ablation model) and another resulting from the slow de-excitation of the excited primary fragment (the ablation step).

The general variation of F/B values with product mass shown in Fig. 1 is similar to that observed in the interaction of relativistic protons ($1 \leq E_p \leq 300$ GeV) with heavy targets. *However*, a *detailed comparison* of the F/B values measured in this work for the reaction of 8 GeV ^{20}Ne with similar values from proton-induced reactions reveals that, while the trend of F/B with product mass A is similar for all systems, the product F/B values for the 8 GeV ^{20}Ne + ^{181}Ta reaction exceed any equivalent values for the other reactions. From these F/B values (and the forward velocity or angular distributions they represent) we can conclude that limiting fragmentation (with respect to kinetic properties) has not been attained in the interaction of 8 GeV ^{20}Ne with ^{181}Ta. This conclusion is based upon the non-equivalence of

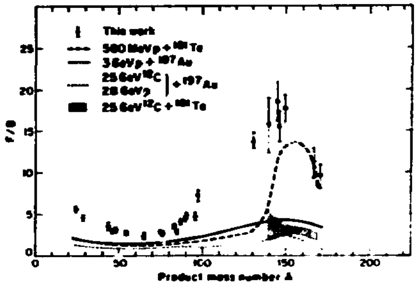

Fig. 1. Comparison of target fragment F/B ratios for various relativistic proton and heavy ion reactions with ^{181}Ta and ^{197}Au.
(XBL 801-71)

the F/B values for the reaction of 8 GeV ^{20}Ne with ^{181}Ta (this work), 25 GeV ^{12}C with ^{181}Ta[1] and 25 GeV ^{12}C with ^{197}Au.[2]

It is instructive to compare the momenta imparted to selected target fragments in the ablation phase (or second step) of the reaction since variation of this property with changes of projectile type and energy can reveal the extent to which the ablation phase of the reaction mechanism is influenced by the abrasion process which occurs during the initial projectile-target interaction. Figure 2 shows a plot of <P>, the component of the target fragment momenta due to the ablation phase of the reaction versus A for the spallation of Ta by 8 GeV ^{20}Ne and by protons of 0.45, 0.58, and 19 GeV.

For the 8 GeV ^{20}Ne induced reaction a steady increase in <P> is observed as one moves from near-target products to those that have resulted from the removal of ~ 50 nucleons from ^{181}Ta. This increase in <P> goes approximately as $\sqrt{\Delta A}$, and is indicative of sequential, step-wise momentum "kicks" being imparted, in a random walk fashion, to the ablating target fragment. The general pattern based on these results for Ta and those for Au targets is that the ablation phase of reactions leading to products with $\Delta A \lesssim 50$ is essentially energy and projectile invariant.

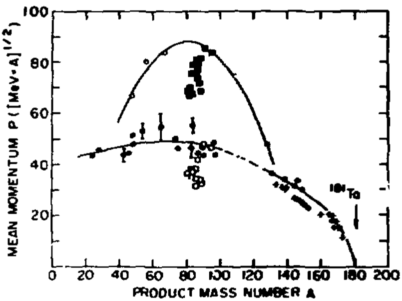

Fig. 2. Dependence of fragment momentum on product mass for the interaction of ^{20}Ne ions and protons with Ta. Data points are for: 8 GeV ^{20}Ne, the present work; 0.45 GeV ^{1}H, o, ref. 7; 0.58 GeV ^{1}H■, ref. 10; and 19 GeV ^{1}H, +, ■, also ref. 10. The solid curve through the filled circles for A > 130 is given by $P = 5.15\sqrt{\Delta A}$ where $\Delta A = 181 - A$. The uppermost curve is a parabola through the open circles.

(XBL 805-970)

Footnotes and References

*Condensed from Phys. Rev. C 23, 253 (1981).

†Permanent Address: Department of Chemistry, Oregon State University, Corvallis, OR 97331

‡Permanent Address: Studsvik Scientific Research Laboratory, Nykoping, Sweden

§Chemistry Division, Argonne National Laboratory, Argonne, IL 60439

Chemistry Department, Brookhaven National Laboratory, Upton, NY 11973

1. W. Loveland, D. J. Morrissey, and G. T. Seaborg, Oregon State University Report RLO-2227-TA35-1; D. J. Morrissey, W. Loveland, and G. T. Seaborg, Z. Physik A289, 123 (1978).

2. S. B. Kaufman, E. P. Steinberg, and B. D. Wilkins, Phys. Rev. Lett. 41, 1359 (1978).

3. N. T. Porile and N. Sugarman, Phys. Rev. 107, 1410 (1957).

4. B. Neidhart and K. Bachmann, J. Inorg. Nucl. Chem. 34, 423 (1972); U. Trabitzsch and K. Bachmann, Radiochemical Acta, 16, 129 (1974).

THE ENERGY DEPENDENCE OF ^{209}Bi FRAGMENTATION IN RELATIVISTIC NUCLEAR COLLISIONS

K. Aleklett,* D. J. Morrissey, W. Loveland,† P. L. McGaughey, and G. T. Seaborg

An ambiguous point in the description of relativistic heavy ion (RHI) reactions is the amount of excitation energy deposited in the spectator fragments by the interaction. Various models of the fast interaction generate primary fragments with varying amounts of excitation which after de-excitation reproduce the experimental results for light nuclei. Although direct measurements of this excitation energy are difficult, one can follow the trend of primary fragment excitation through some relatively simple experiments. Excitation energy in a high mass (but relatively non-fissionable) nucleus at low angular momentum is carried off mostly by evaporated neutrons. Thus, if the primary fragment cross section distributions are governed by geometry, then differences in the N/Z ratio of final residues of RHI reactions as a function of bombarding energy (same projectile and high mass target) will represent differences in the excitation energy.

Following this idea, we report the variation of the production of gold isotopes from three RHI reactions with ^{209}Bi. In these experiments, bismuth metal foils surrounded with Mylar catchers were irradiated with beams of 4.8 GeV (0.40 GeV/A) ^{12}C, 8.0 GeV (0.40 GeV/A) ^{20}Ne, and 25.2 GeV (2.1 GeV/A) ^{12}C ions from the LBL Bevalac facility. The target fragmentation products stopped in the target or catcher foils, and the induced radioactivities were measured by direct gamma ray spectroscopy and by gamma ray spectroscopy of a chemically separated gold fraction.[1] The gamma ray emitting nuclei were identified using standard techniques[2] and the production cross sections were calculated for those activities observed in the unseparated foils.

The measured cumulative yield cross sections (which include contributions from nuclei produced by radioactive decay) were corrected for this decay feeding by an iterative fitting of Gaussian distributions to the decay-corrected (and independent yield) cross sections. The resulting calculated and measured independent yield cross sections $\sigma(Z/A)$ are shown in Fig. 1. The yield of ^{194}Au is depressed relative to the other nuclidic yields in all the reactions for reasons that are not clear.

Cursory inspection of Fig. 1 shows that the distributions of Au fragments are very similar for the three reactions studied in this work. A more detailed examination of the data shows that there is a slight (≲ 1 amu) shift of the distribution centroids toward larger A values as the projectile energy increases. Thus, although the incident projectile energy changes by over 20 GeV, the excitation energy imparted to target fragments changes by less than 10 MeV.

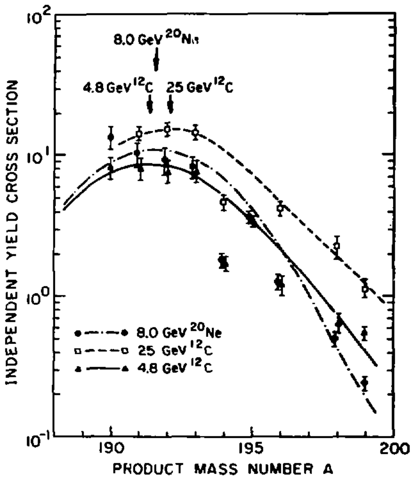

Fig. 1. The isotopic production cross sections for gold products from the reaction of 4.8 and 25.2 GeV ^{12}C and 8.0 GeV, ^{20}Ne with ^{209}Bi are shown. The lines represent the best Gaussian fit to each distribution with the arrows showing the distribution centroids. (XBL 807-10700)

We are left with the question of whether this apparent saturation in energy transfer is predicted by current models of fragmentation reactions. One highly developed model of such collision which makes predictions about the fragmentation products is the intranuclear cascade model of Yariv and Fraenkel.[3] The results of the calculations of the position of the centroid of the gold isotopic distributions using this model are in approximate agreement with the results of our study but predict values of the distribution centroids which are systematically more neutron deficient (~ 1-2 amu) than our data. Thus, the experimentally observed limiting fragmentation behavior of high mass nuclei is predicted by this model of relativistic nucleus-nucleus collisions.

What universal feature of RHI reactions is responsible for this behavior? In this case involving very peripheral collisions (impact parameter b ~ 9 fm > R_{Bi} ≃ 7.0 fm), it is simply a matter that the predicted changes in experimental distributions are very small compared to the sensitivity of the experimental measurement. Unfortunately, selection of events involving more central events suffer from the fact that such events integrate more fully the primary reaction processes through the subsequent de-excitation of the primary fragments. We conclude that the observation of limiting fragmentation behavior in yield distributions can be produced by a variety of effects, none of which are connected to the central issue of transfer of projectile kinetic energy into internal excitation.

Footnotes and References

*Permanent Address: Studsvik Scientific Research Laboratory, Nykoping, Sweden

†Permanent Address: Department of Chemistry, Oregon State University, Corvallis, OR 97331

1. The bismuth metal foils were dissolved in conc. HCL-conc. HNO_3 (1:2) with carriers. After dissolution, excess NO_2 was driven off, the solution was cooled and diluted with water. The Au was extracted twice into ether, washed twice with 1.5 M HCl and plated on Pt. This procedure required approximately 25 minutes.

2. D. J. Morrissey, D. Lee, R. J. Otto and G. T. Seaborg, Nucl. Inst. Methods, 158, 499 (1979).

3. Y. Yariv and Z. Fraenkel, Phys. Rev., C20, 2227 (1979).

EMISSION PATTERNS IN CENTRAL AND PERIPHERAL RELATIVISTIC HEAVY-ION COLLISIONS*

R. Stock, H. H. Gutbrod, W. G. Meyer, A. M. Poskanzer, A. Sandoval, J. Gosset, C. H. King, G. King, Ch. Lukner, Nguyen Van Sen, G. D. Westfall, and K. L. Wolf

Proton emission in relativistic nuclear collisions is examined for events of low and high multiplicity, corresponding to large and small impact parameters. Presented here are the first results on the multiplicity-selected proton spectra ($12 \leq E \leq 210$ MeV) as measured in a solid-state detector telescope. The data are selected for both high and low associated multiplicity as recorded in an array of plastic scintillator detectors located with approximate azimuthal symmetry for $10° \leq \theta_{lab} < 80°$. The array is sensitive to charged particles above a lower energy cutoff corresponding to 15 MeV for pions and 25 MeV for protons. The details of the experimental arrangement have been described elsewhere.[1]

The overall effect of high versus low multiplicity selection on the proton emission pattern is illustrated in Fig. 1 showing contour diagrams of the invariant cross section in the plane of transverse momentum and rapidity. The contour lines are constructed by a smooth interpolation of multiplicity selected spectra obtained at 30° (20° for some cases) to 150° in steps of 20°. They are superimposed for high and low multiplicity selections.

The typical cases chosen here to illustrate the effects found in the data are ^{20}Ne + U at 393 MeV/u and ^{40}Ar + Ca at 1.04 GeV/u. The most important observations from a comparison of these pattens are as follows:

(i) For the heavy-target cases (^{20}Ne and ^{40}Ar on Ag to U) central collisions exhibit a universal trend of the contour lines centering approximately near zero (target) rapidity. The shape of the contour line is roughly semicircular about rapidities ranging from 0 to about 0.2, the case illustrated here, indicating a continuous shift in apparent longitudinal source velocities as shown by the dashed line. This implies that there is no unique source for proton emission. The bulk of the proton cross section appears neither at fireball rapidities, which are at $y = 0.33$ for impact parameters smaller than $0.5b_{max}$ in this case, nor at the corresponding nucleon-nucleon center-of-mass rapidity $1/2(y_p + y_t) = 0.45$.

(ii) The peripheral-collision contour lines are primarily determined by the incident energy. Their shapes are almost insensitive to the choice of target and projectile, with source velocities rapidly shifting from the target domain to the mid-rapidity domain for increasing $p_\perp$.

(iii) Unlike the heavy-target cases, the central collisions of equal-size nuclei, such as ^{40}Ar + Ca and ^{20}Ne + ^{27}Al, exhibit contour lines dominated by the decay of mid-rapdity source for the bulk of the observed cross section. Note that the contours for high multiplicity in ^{40}Ar + Ca shift towards high rapidities [$(1/2\ (y_p + y_t) = 0.67$ in this case] even faster than the corresponding low-multiplicity contours, contrary to the trend exhibited by Ne + U.

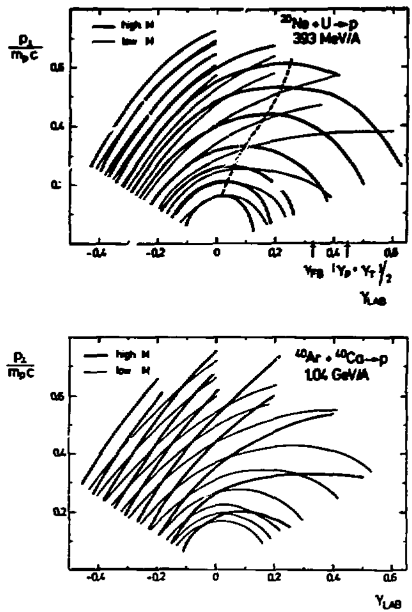

Fig. 1. Contour diagrams of invariant proton cross section for peripheral (thin line) and central (thick lines) collisions, in the plane of transverse momentum (in units of $p_\perp/m_pc$) and rapidity $y = 1/2\ \ln[(E + p_\parallel)/(E - p_\parallel)]$. Five lines are drawn for each decade of invariant cross section. The cases illustrated are ^{20}Ne + U at 393 MeV/A (top) and ^{40}Ar + ^{40}Ca at 1.04 GeV/A (bottom). (XBL 808-10889)

Footnote and Reference

*Collaboration of Lawrence Berkeley Laboratory, Gesellschaft fur Schwerionenforschung, Darmstadt, and Universitat Marburg, W. Germany, and Argonne National Laboratory.

1. A. Sandoval, H. H. Gutbrod, W. G. Meyer, A. M. Poskanzer, R. Stock, J. Gosset, J. C. Jourdain, C. H. King, G. King, Ch. Lukner, Nguyen Van Sen, G. D. Westfall, and K. L. Wolf, Phys. Rev. C 21, 1321 (1980).

COULOMB DISSOCIATION OF ^{18}O

D. L. Olson,* B. L. Berman,* D. E. Greiner, H. H. Heckman, P. J. Lindstrom, G. D. Westfall, and H. J. Crawford*

Measurement of fragmentation cross sections have been made with 1.7 GeV/nucleon ^{18}O projectiles incident upon targets of Be, C, Al, Ti, Cu, Sn, W, Pt, and U at the Bevalac. The differential cross sections (in momentum) were measured for fragments with rigidity $4.79 \leq R \leq 6.28$ GV. These cross sections were fitted with a Gaussian form in parallel momentum to give total cross sections in fifteen fragmentation channels from ^6Li to ^{18}F.

The Coulomb dissocation process can be described as the interaction between the projectile nucleus and the nuclear-Coulomb field of the target.[1,2] Given the theoretical form of the virtual photon spectrum and the measured photodissociation cross sections for $^{18}O(\gamma,n)^{17}O$, $^{18}O(\gamma,2n)^{16}O$ and $^{18}O(\gamma,p)^{17}N$[3] the calculated Coulomb idssociation cross sections for these reactions are of the form

$$\sigma_C(T,F) = Z_T^2 S(F,b_{min}), \quad (1)$$

where T and F denote target and fragment, respectively, and b_{min} is the minimum impact parameter for the process.

In this experiment we measured cross sections in which both nuclear and Coulomb processes contribute. Our analysis has taken the observed cross sections to be

$$\sigma(T,F) = \sigma_{nuc}(T,F) + \sigma_C(T,F) \quad , \quad (2)$$

where $\sigma_{nuc}(T,F)$ is assumed to satisfy factorization according to

$$\sigma_{nuc}(T,F) = \gamma_T \gamma^F \quad (3)$$

the factors γ_T and γ^F depending on, respectively, the target and fragment only. The form of Eq. 2 neglects interference between nuclear and Coulomb processes which is expected to be less than 10%.

A large set of the cross sections with no Coulomb component were analyzed for factorability. This produced the individual γ_T and γ^F factors and showed the factorization hypo- thesis to be valid to $\pm 5\%$.

Figure 1 shows the dependence of the target factor, γ_T, on target mass, A_T. The curve is from fitting the indicated form of γ_T where the value -0.9 is derived from the fit. The points plotted for ^{17}O, ^{16}O, and ^{17}N are the ratio

$$"\gamma_T" = \frac{\sigma(T,F)}{\gamma^F}$$

which would have followed the line if there had been no Coulomb contribution. The departure from the line indicates the strong dependence on Z_{target}. The scale is proportional to the cross section for each fragment and comparison of the open points to the line shows the relative sizes of Coulomb and nuclear cross sections.

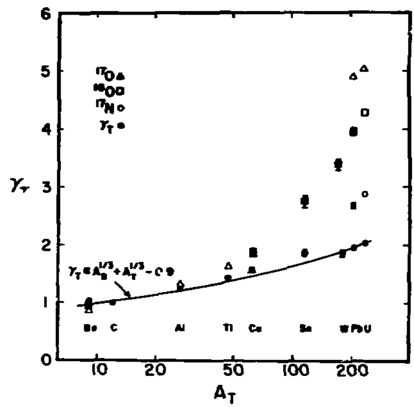

Fig. 1. Target factor vs. target mass. $\gamma_T = \langle \frac{\sigma(T,F)}{\gamma^F} \rangle_F$; for ^{17}O, ^{16}O, ^{17}N, the effective target factor is $"\gamma_T" = \frac{\sigma(T,F)}{\gamma^F}$.

(XBL 808-10918)

Table 1. Coulomb dissociation cross sections.

Fragment	Target	σ_C(mb)	Calculated cross sections	
			JPE1	WW
(a)				
^{17}O	Ti	8.66 ± 2.74	13.4	12.5
	Pb	136.04 ± 2.90	132.0	135.0
	U	140.83 ± 4.11	162.0	167.0
^{16}O	Ti	6.34 ± 2.54	5.78	5.41
	Cu	9.0 ± 3.5	9.42	8.97
	Sn	27.5 ± 4.0	24.0	23.7
	W	50.0 ± 4.3	46.1	46.8
	Pb	65.16 ± 2.32	53.9	55.2
	U	74.27 ± 1.74	66.1	68.1
^{17}N	Ti	-.45 ± 1.01	2.87	2.41
	Pb	20.23 ± 1.82	23.3	23.8
	U	25.10 ± 1.55	28.5	29.2
(b)				
^{16}N	Ti	3.0 ± 2.2		
	Pb	8.0 ± 4.5		
	U	10.8 ± 5.1		
^{14}C	Ti	8.8 ± 1.1		
	Pb	33.7 ± 4.0		
	U	35.1 ± 2.7		
^{13}C	Ti	-1.6 ± 1.5		
	Pb	21.9 ± 2.4		
	U	17.6 ± 2.6		

The experimental values of σ_C, using Eq. 2, are shown in Table 1. Part (a) shows the fragments for which theoretical predictions can be calculated. The column JPE1 is calculated with E1 virtual photon spectrum of Jäckle and Pilkuhn with the parameter b_{min} being 1/2 fm larger than the sum of the 50% charge density radii of the target and projectile. The column WW is calculated with the virtual photon spectrum of Weiszäcker-Williams in Ref. 2 but with b_{min} that is 3 fm larger than that used for JPE1 values. Part (b) shows the cross sections in fragmentation channels for which the appropriate photodissociation cross sections have not been measured and calculated predictions are impossible. The cross sections in these channels are reasonable, however.

In this experiment we can't distinguish between the two photon theories in a fashion that is independent of b_{min}. The theory of Jäckle and Pilkuhn yields a value of b_{min} that appears to be physically more reasonable. Because the calculated Coulomb dissociation cross section increases for decreasing b_{min}, the observation that the ^{16}O cross sections are relatively larger than for either ^{17}O or ^{17}N when compared to the theory, suggests that the nuclear two-neutron loss process occurs at a smaller impact parameter than the one-nucleon loss process. By fitting b_{min} to these three channels individually, we find the ^{16}O channel to have an impact parameter that is 2 fm smaller than either the ^{17}O or ^{17}N channels.

Overall, the principal conclusion of this experiment is that the enhancement of the fragmentation cross sections, appropriate to the photonuclear reaction channels of ^{18}O, for high-charge targets, is well described by the process of Coulomb dissociation.

Footnotes and References

*Lawrence Livermore Laboratory, Livermore, CA 94550

†Space Sciences Laboratory, Berkeley, CA 94720

1. T. Jäckle and H. Pilkuhn, Nucl. Phys. A247, 521 (1975).

2. J. D. Jackson, Classical Electrodynamics, Wiley, NY, second edition, p. 719 (1975).

3. J. G. Woodworth, K. G. McNeill, J. W. Jury, R. A. Alvarez, B. L. Berman, D. D. Faul, and P. Meyer, Phys. Rev. C19, 1667 (1979).

2. Central Collisions

STREAMER CHAMBER RESULTS ON THE MECHANISM FOR PRODUCTION OF HIGH MOMENTUM PARTICLES IN THE BACKWARD DIRECTION IN RELATIVISTIC NUCLEAR COLLISIONS

J. W. Harris,* A. Sandoval,* H. E. Stelzer,* R. Stock,* J. Brannigan, J. V. Geaga, L. S. Schroeder, and R. N. Treuhaft

There exists considerable long-standing controversy on the origin of particles with high momentum in the backward direction. Since production of nucleons beyond 90° in the laboratory is kinematically forbidden in free nucleon-nucleon interactions, particle emission in this region is of particular interest. Single hard-scattering combined with internal Fermi motion, multiple scattering cascades, and intranuclear correlations are a few of the most notable backward particle production mechanisms that have been proposed. Inclusive proton momentum density distributions accumulated from recent projectile and target fragmentation experiments in conjunction with theoretical predictions suggest the presence of short-range correlations in the nucleus as an important mechanism.[1]

In the interest of obtaining more-complete event information on the production mechanisms associated with backward particle emission, the exclusive charge-particle production accompanying backward particle emission was studied in the streamer chamber at the Bevalac. The streamer chamber was triggered on a charged-particle with $p \gtrsim 250$ MeV/c at $\theta_{Lab} > 90°$. Approximately 10,000 events were photographed in the bombardment of C, KCl, and BaI_2 targets with 2.1 GeV protons. The mean positively-charged particle multiplicites associated with a backward trigger particle from these targets were observed to be $\langle M_+ \rangle = 4.7 \pm 0.1$, 6.7 ± 0.2, and 8.0 ± 0.2 respectively. Particle trajectories were measured and reconstructed using the Three View Geometry Program (TVGP).

A kinematic analysis of two-prong events (an 8.7% subset of all events) in $p + {}^{12}C$ interactions was initiated to determine the contribution of two specific mechanisms to the backward particle spectrum: (1) single hard scattering with coherent recoil of the residual nucleus $[p + {}^{12}C \rightarrow p + p + {}^{11}B]$[2,3] and (2) scattering from two correlated nucleons in the nucleus $[p + (pn) \rightarrow p + p + n]$. The fraction of two-prong events that lie within one standard deviation of satisfying the kinematics for the hard scattering mechanism is 0.015 ± 0.015. The fraction of events satisfying the kinematics for scattering from a pair of nucleons is considerably higher: 0.275 ± 0.063. These results are not sufficient to determine the reaction mechanism uniquely since the kinematics are not unique to these processes. However, they are highly suggestive of the presence of correlations in the nucleus and their importance in backward particle production.

The production of the $\Delta(3,3)$ isobar in the reaction $p + p \rightarrow n + \Delta^{++}$ (1232) accounts for a major fraction of the pp total cross section at energies from 1-2 GeV.[4] Therefore, the effects of the subsequent decay $[\Delta^{++} \rightarrow p + \pi^+]$ and/or absorption $[\Delta^{++} + n \rightarrow p + p]$ of isobars on the backward particle spectra must be considered. If isobar production is an important mechanism, a back-to-back (180°) correlation between the proton and π^+ in the Δ^{++} decay frame and between the two protons in the $(\Delta^{++} + n)$ absorption frame is expected as illustrated in Fig. 1. This correlation may be preserved in the laboratory system due to the dominance of low momentum transfer in the production cross

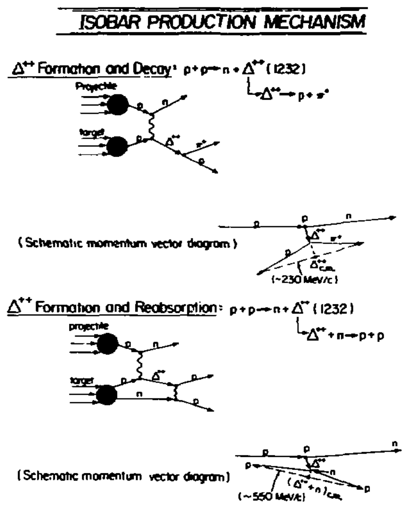

Fig. 1. $pp \rightarrow n\Delta^{++}(1232)$ isobar production mechanism: (top) diagram for $\Delta(3,3)$ isobar formation and decay; (bottom) diagram for $\Delta(3,3)$ isobar formation and reabsorption. Associated schematic momentum vector diagrams in the laboratory system are also displayed for each case. (XBL 809-2017)

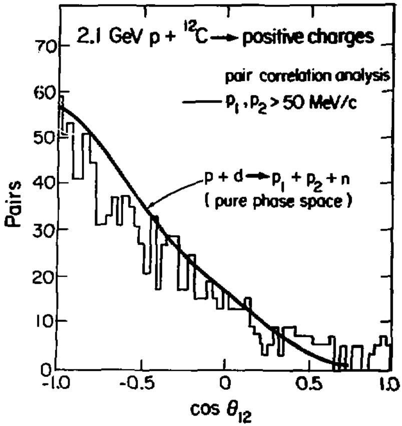

Fig. 2. Correlation between all pairs of positively-charged particles in each event as a function of the cosine of the angle between the particles (histogram) where one particle of each pair is emitted at $\theta_{lab} > 90°$. The curve represents results of a phase space calculation for 2.1 GeV p + d → p + p + n. (XBL 809-2054)

section of the Δ^{++} isobar. As displayed in Fig. 2, a 180° correlation between the angles of positively-charged particles is observed in the analysis of all p + ^{12}C events providing evidence for $\Delta(3,3)$ isobar production as an important mechanism for production of high momentum particles in the backward direction. However, such a correlation is also predicted by a [p + d → p + p + n] pure phase space calculation represented by the curve in Fig. 2. These results may reflect the concept that the Δ^{++} production and reabsorption process schematized in Fig. 1 and the p + d → p + p + n process are in fact intimately related and are important to the production of high momentum particles in the backward direction.

Footnote and References

*Gesellschaft fur Schwerionenforschung, Darmstadt, W. Germany.

1. J. V. Geaga, S. A. Chessin, J. Y. Grossiord, J. W. Harris, D. L. Hendrie, L. S. Schroeder, R. T. Treuhaft and K. Van Bibber, Phys. Rev. Lett. 45 (1980) 1993.

2. R. D. Amado and R. M. Woloshyn, Phys. Rev. Lett. 36 (1976) 1435.

3. S. Frankel, Phys. Rev. Lett. 38 (1977) 1338.

4. O. Benary, L. R. Price and G. Alexander, University of California Radiation Laboratory Report No. LBL-20000 NN (August 1970).

CORRELATIONS OF CHARGED PARTICLE MULTIPLICITY PATTERNS AND HEAVY FRAGMENTS FROM RELATIVISTIC NUCLEAR COLLISIONS*

A. Baden, M. Freedman, H. H. Gutbrod, I. J. Henderson, S. Kaufman, K. Karadjev,[†] M. R. Maier, V. Manko,[†] J. Peter,[‡] H. G. Ritter, E. P. Steinberg, H. Stelzer, A. I. Warwick, F. Weik, H. Wieman, B. D. Wilkins[§]

In a recent Bevelac experiment completed in May 19..., a rather comprehensive measurement of the properties of emitted charged fragments and the associated spray of fast charged particles has been achieved. The purpose of the experiment is to investigate effects seen (a) in an earlier Bevelac experiment[1] where correlations were measured between light fragments and their associated fast charged spray, and (b) in a previous series of measurements with proton projectiles made at the ZGS,[2] where coincident fragements were observed.

We have measured multiparticle correlations. Heavy slow fragments are identified as to their mass and energy in a double-arm TOF apparatus consisting of two position-sensitive avalanche detectors[3] and two arrays of silicon detectors. Light fragments were identified by Z in four ΔE-E ionization chamber telescopes. The layout of these detectors is shown in Fig. 1. In addition fast charged particles were detected in a multiplicity array of 80 scintillator paddles,[1] each of which provided a pulse-height spectrum. The forward angles between 2° and 9° are covered by the Plastic Wall.[4] This provides pattern information, momentum measurement and Z identification of the fast charged particles in this forward cone.

The experiment examines specifically (a) the collisions leading to binary emission of fragments, (b) the light fragment production in very violent collisions which seems to be dependent only on the total incident energy rather than on the velocity or the mass of the projectile, and (c) the observed perpendicular momentum, "sidekick,"[1] of heavy target residues (probably in semiperipheral collisions) and the possible deflection of the projectile matter.

Recent experiments at the ZGS[2] have provided evidence of an exciting new phenomenon. The experiments measured the energies, masses (by time of flight), and correlation angles of coincident heavy fragments emitted near 90° to the beam in 2.2 to 11.5 GeV proton bombardment of uranium. The analysis of the results has established that the fragment-fragment correlation is very nearly collinear and that binary breakup frequently occurs when the total fragment mass is as low as one-quarter that of the target. The missing mass is probably emitted as a large number of light nuclei or particles. In addition, the total kinetic energy for such events is higher than predicted for a statistical fission process.

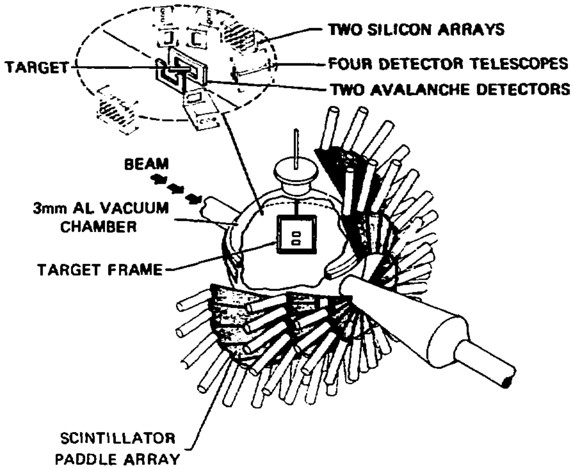

Fig. 1. Exploded view of the layout of the detectors within the chamber. (XBL 808-1691a)

In this work the binary events have been observed from reactions induced by both proton of associated fast charged particles has been measured. An investigation of this multiplicity pattern will be of great value in characterizing the nature of the reaction mechanism.

Information on the momentum of the light charged particles detected in the Plastic Wall will yield momentum correlations between the fragments and the spray, and momentum reconstruction will be possible for selected events. These data will yield the transverse momentum transfer and elucidate the mechanism by which the kinetic energy dissipation in the collision is diverted from thermalization into the collective sidekick observed in the previous studies.[1]

Footnotes and References

*Collaboration of Lawrence Berkeley Laboratory, Argonne National Laboratory, and Gesellschaft für Schwerionenforschung, Darmstadt.

†Visitors from Kurchatov Institute of Atomic Energy, Moscow.

‡Visitor from I.P.N., 91406 Orsay, France.

§Argonne National Laboratory.

1. W. G. Meyer, et al, LBL-9151 and Phys. Rev. C, to be published.

2. B. D. Wilkins, et al., Phys. Rev. Lett. 43 (1979) 1080.

3. H. Stelzer, in this annual report.

4. A. Baden et al., in this annual report.

D. ISOTOPES PROJECT

ISOTOPES*

C. Michael Lederer

Ordinary matter consists of the 286 isotopes of 83 elements that are stable or long-lived compared to the age of the earth. For most polyisotopic elements, the relative abundances of the isotopes are remarkably constant. Isotopes are usually assayed by mass spectrometry.

Of many isotope-separation methods that have been develped, two (electromagnetic and thermal diffusion) are used commonly to produce small quantities of many isotopes for research purposes, and two others (the GS chemical-exchange process for hydrogen, gaseous diffusion for uranium) are used on an industrial scale. The large-scale use of gas centrifuges for uranium is imminent, and laser separation methods appear promising for uranium, deuterium, and expanded-scale production of research materials.

In addition to the applications of ^{235}U and deuterium in nuclear energy, separated isotopes serve as chemical tracers and as targets or beam particles in radioisotope production and nuclear research. Isotope effects on chemical equilibria and reaction rates are well understood; kinetic effects provide a useful tool for the study of reaction mechanisms. Isotopic substitution in living systems has yielded new knowledge in the biological sciences, as has the study of natural isotopic abundance variations in the geosciences.

Footnote

*Abstract of a review article to be published in Encyclopedia of Chemical Technology, 3rd ed., edited by David Eckroth, John Wiley and Sons, New York (1981). The article includes 6 tables, 5 figures, and 95 references. A longer version, from which the published article was condensed, is contained in LBL-10124.

NUCLEAR STRUCTURE DATABASE*

R. B. Firestone and E. Browne

The seventh edition of the Table of Isotopes[1] contains evaluated radioactive decay and nuclear reaction data for all known nuclides as of 1977. This data exists in an LBL computer file that was designed for the production of level-scheme plots and was not suitable as a database for horizontal compilations and systematic studies of nuclear properties. We have restructured this file by removing the references and non-data plotting instructions. The new file has been modified to greatly improve the ease and speed of data searches and represents the most complete and up-to-date collection of nuclear data currently available.

An initial search of the database was performed to create a file of all levels with measured half-lives and their associated deexcitations. This file was then utilized to extract the known Weisskopf enhancements for the lowest lying $2^+ \rightarrow 0^+$ transitions in even-even nuclei. These results are presented in Table 1 where the systematic trends of small enhancements near closed shells and large collective enhancements (of order A) in the deformed regions are clearly demonstrated. We intend to use the database for a systematic study of γ-ray transition selection rules, and, in the future, to expand the content of this database and promote its general use.

Table 1. E2 Weisskopf enchancements for the $2_1^+ \rightarrow 0_1^+$ transitions in even-even nuclei, Z = 2-50. Closed shells are indicated by ***.

N \ Z	2	4	6	8	10	12	14	16	18	20	22	24	26	28	30	32	34	36	38	40	42	44	46	48	50
2	*	*	*	*	*	*	*	*	*	*	*	*	*	*	*	*	*	*	*	*	*	*	*	*	*
4	*		9	*						*				*											*
6	*	8	5	*						*				*											*
8	*	*	*	4	18	*	*	*	*	*	*	*	*	*	*	*	*	*	*	*	*	*	*	*	*
10	*			3	22	17				*				*											*
12	*			1	12	20	7			*				*											*
14	*			*	6	13	13	16		*				*											*
16	*			*		13	8	9	15	*				*											*
18	*			*			8	7	10	*				*											*
20	*	*	*	*	*	*	*	3	4	2	18	*	*	*	*	*	*	*	*	*	*	*	*	*	*
22	*			*					10	10	14			*											*
24	*			*					8	10	23	25		*											*
26	*			*						3	14	19		*											*
28	*	*	*	*	*	*	*	*	*	2	6	11	8	6	*	*	*	*	*	*	*	*	*	*	*
30	*			*						*	13	14	16	10											*
32	*			*						*			13	13											*
34	*			*						*				12	22										*
36	*			*						*				8	18										*
38	*			*						*				*	15	21	19								*
40	*			*						*				*	19	25	40	58							*
42	*			*						*				*		34	44	56	41						*
44	*			*						*				*		27	33	39							*
46	*			*						*				*			24	19	27						*
48	*			*						*				*			17	15	10						*
50	*	*	*	*	*	*	*	*	*	*	*	*	*	*	*	*	*	*	7	5	*	*	*	*	*
52	*			*						*				*						6	15	21			*
54	*			*						*				*						[illegible]	20	30			*
56	*			*						*				*						[illegible]	21	41			*
58	*			*						*				*							37	1	57	46	*
60	*			*						*				*						62	76	[illegible]	49	52	*
62	*			*						*				*						9	73		[illegible]	27	16
64	*			*						*				*							[illegible]	62	57	11	15
66	*			*						*				*								[illegible]		[illegible]	11
68	*			*						*				*									21	[illegible]	11
70	*			*						*				*									13		[illegible]
72	*			*						*				*											11
74	*			*						*				*											9
76	*			*						*				*											*
78	*			*						*				*											*
80	*			*						*				*											*
82	*	*	*	*	*	*	*	*	*	*	*	*	*	*	*	*	*	*	*	*	*	*	*	*	*

Table I, continued. Z = 52-100.

N \ Z	52	54	56	58	60	62	64	66	68	70	72	74	76	78	80	82	84	86	88	90	92	94	96	98	100
60																*									
62																*									
64																*									
66		50														*									
68	[illegible]	[illegible]														*									
70	17	48	[illegible]													*									
72	31	41	[illegible]	[illegible]												*									
74	25	35	61	75												*									
76	[illegible]	45	36	72												*									
78	15	22	33													*									
80			19													*									
82	*	*	25	12	19	11	*	*	*	*	*	*	*	*	*	*	*	*	*	*	*	*	*	*	*
84				21	23											*									
86			[illegible]		32	11										*									
88			49	38	56	57	60		68	73						*									
90			57	79	116	141	159	149	110	90						*									
92				[illegible]		175	156	174	167	147						*									
94					[illegible]		147	193	200	[illegible]	126					*									
96							199	199	213	[illegible]	153					*									
98								208	209	205	[illegible]					*									
100									210	202	148					*									
102									207	[illegible]	149					*									
104										201	187				[illegible]	*									
106										179	157	147	126	125	44	*									
108											154	134	99	94		*									
110												118	97	93		*									
112												111	76	79		*									
114													73	62		*									
116													62	46	41	*									
118														45	30	*									
120														29	27	*									
122															19	*									
124															13	3									
126	*	*	*	*	*	*	*	*	*	*	*	*	*	*	*	*	*	*	*	*	*	*	*	*	*
128																*									
130																*									
132																*									
134																*		45	111						
136																*		59	94	[illegible]					
138																*			123	169	223				
140																*			144	194	234				
142																*				201	234				
144																*				182	250	265			
146																*					271	294			
148																*						296	333		
150																*						292	324		
152																*							323		
154																*								357	
156																*									

Footnote and Reference

*Condensed from LBL-11089

1. Table of Isotopes, 7th edition: C. M. Lederer and V. S. Shirley, editors; E. Browne, J. M. Dairiki, and R. E. Doebler, principal authors; A. A. Shihab-Eldin, L. J. Jardine, J. K. Tuli, and A. B. Buyrn, authors, John Wiley and Sons, Inc., New York (1978).

THE FEASIBILITY OF PRODUCING ^{11}C, ^{13}N, ^{15}O and ^{18}F WITH HEAVY ION-BEAMS*

R. B. Firestone, M. R. Betlach,[†] J. M. Tiedje,[†] M. K. Firestone[‡]

The short-lived tracer ^{13}N has proven uniquely useful in our studies of biological nitrogen transformations.[1,2] With the closing of the Michigan State University cyclotron there is no longer a suitable facility for these ^{13}N experiments. We therefore investigated the possibility of producing ^{13}N with heavy-ion beams such as those available at the LBL 88 Inch Cyclotron. Useful sources of ^{11}C, ^{15}O, and ^{18}F could also be produced with these beams.

We performed ALICE particle-evaporation code calculations[3] to predict the various isotope yields from 15-MeV p, 75-MeV ^{3}He, and 300-MeV ^{12}C beams incident on natural H_2O targets. These calculations, summarized in Table 1, indicate that substantial quantities of ^{11}C, ^{13}N, ^{15}O, and ^{18}F are produced with heavier beams. We previously used the 15-MeV p beam because it produces nearly pure sources of ^{13}N containing only small ^{18}F impurities. The experimental yields of both ^{13}N and ^{18}F were predicted well with the ALICE calculations. To test the heavy-ion calculations we bombarded a natural H_2O sample with a 75-MeV ^{3}He beam. The resultant activity was analyzed by half-life and by high pressure liquid chromatography (HPLC). The yield of ^{13}N and ^{18}F again agreed well with the ALICE calculations; the ^{15}O yield was too low; and no ^{11}C was observed. This disparity in the ^{15}O and ^{11}C results may arise because these species are produced largely in the gaseous state while the experimental system was not gas tight. To purify a ^{13}N source we acidified it, evaporated it to dryness, reconstituted the source with 0.001 N NaOH, again evaporated it to dryness and finally reconstituted it with H_2O. An HPLC analysis of the raw and purified sources is shown in Fig. 1. After this treatment only $^{13}NO_3^-$ remained (plus ^{18}F which was not detectable by HPLC) suggesting that heavy-ion beam should be useful for ^{13}N production.

A wide variety of beam at the LBL 88 Inch Cyclotron should be useful for tracer production. Since natural H_2O is a target of choice, sources can be produced in the beam dumps without interfering with simultaneous nuclear physics experiments.

Table 1. Calculated and experimental isotope yields for various beams on H_2O targets.

			Yield (mCi/μA per 10 min)[a]				
			15-Mev p		75-MeV ^{3}He		300-MeV ^{12}C
Isotope	t 1/2 (m)	E_B	Experiment	Theory[b]	Experiment	Theory[b]	Theory[b]
^{13}N	9.96	1.20	20	31	96	81	26
^{11}C	20.4	0.96	0	0	< 1[c]	51	8.2
^{15}O	2.03	1.73	0	0	67	384	109
^{18}F	109.8	0.63	0.2	0.1	12	5.5	4.2

[a]Assuming beam stops in the target.

[b]Calculated using the ALICE compound nuclear particle evaporation code (Reference 3).

[c]None observed.

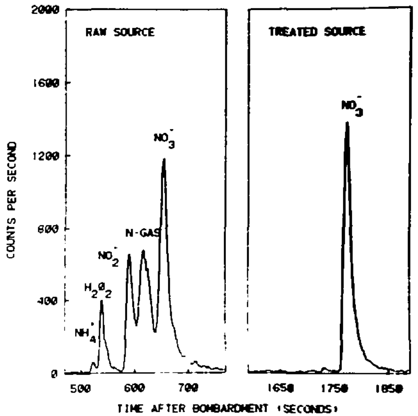

Fig. 1. (XBL 804-9287)

Footnotes and References

*Condensed from LBL-10919.

†Departments of Microbiology and of Crop and Soil Sciences, Michigan State University, East Lansing, MI 48824.

‡Department of Soils and Plant Nutrition, University of California, Berkeley, CA 94720

1. J. M. Tiedje, R. B. Firestone, M. K. Firestone, M. R. Betlach, M. S. Smith and W. H. Caskey, Soil Sci. Soc. Amer. J. 43, 709 (1979).

2. M. K. Firestone, M. S. Smith, R. B. Firestone, and J. M. Tiedje, Soil Sci. Soc. Amer. J. 43, 1140 (1979).

3. M. Blann and F. Plasil, ALICE: A Nuclear Evaporation Code, U. S. Atomic Energy Commission Report COO-3494-10, 1973.

II. THEORY OF NUCLEAR COLLISIONS

A. NONRELATIVISTIC

THE DYNAMICS OF NUCLEAR COALESCENCE OR RESEPARATION *

W. J. Swiatecki

A qualititative theory of the macroscopic dynamics of sub-sonic nucleus-nucleus collisions is presented. Attention is focused on three degrees of freedom: asymmetry, fragment separation, and neck size. The physical ingredients are a macroscopic (liquid-drop) potential energy, a macroscopic dissipation (in the form of the wall- and wall-plus-window formulae) and a simplified treatment of the inertial force. These ingredients are distilled into algebraic equations of motion that can often be solved in closed form. The applications include the calculation of the normal modes of motion around the saddle-point shapes, and the division of nuclear reactions into: a) dinucleus (deep-inelastic) reactions, b) mononucleus or composite nucleus (quasi-fission) reactions, and c) compound-nucleus reactions. Static and dynamic scaling rules are deduced for comparing different reactions in a systematic way, an example being the following: "For two dinuclear systems with the same value of the effective fissility defined by

$$\left(\frac{Z^2}{A}\right)_{eff} \equiv \frac{4Z_1Z_2}{A_1^{1/3}A_2^{1/3}(A_1^{1/3} + A_2^{1/3})} ,$$

the dynamical time evolutions resulting from head-on collisions should be approximately similar, provided lengths are measured in units of the reduced radius $\bar{R}$ $(\equiv R_1R_2/(R_1 + R_2))$ and times in units of $\rho \bar{v} \bar{R}^2/\gamma$." (Here ρ is the mass density of nuclei, $\bar{v}$ is the mean nucleonic speed and γ is the nuclear surface-energy coefficient.)

Estimates are given for the critical curve in the space of target and projectile mass above which deep-inelastic reactions ought to make their appearance. The extra push over the interaction barrier needed to make two nuclei form a composite nucleus or else to fuse into a compound nucleus is also estimated (Fig. 1).

The dynamics of dozens of (head-on) collisions have been followed in the three-dimensional configuration space of asymmetry, fragment-separation and neck-opening. The predictions of the theory, in the full range of asymmetries and injection velocites, are being compared with experiment. Extension to noncentral collisions is under way.

Footnote

*Condensation of LBL-10911, to be published in Physica Scripta, 1981.

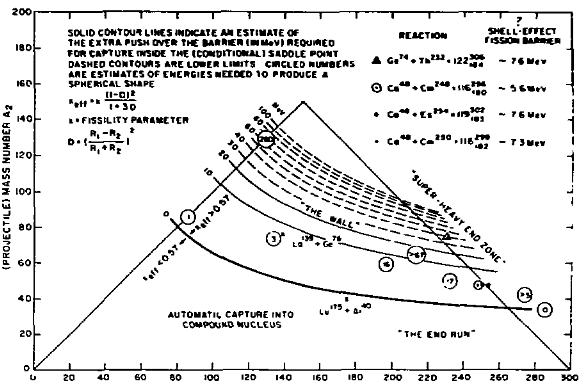

Fig. 1. The extra push over the interacton barrier (in a head-on collision) needed for fusion into a composite nucleus (lines and dashed lines) and into a compound nucleus (circled numbers). (XBL 806-1201)

EFFECT OF PAULI BLOCKING ON EXCHANGE AND DISSIPATION MECHANISMS OPERATING IN HEAVY-ION REACTIONS*

W. U. Schroder,† J. R. Birkelund,† J. R. Huizenga,† W. W. Wilcke, and J. Randrup

Although considerable progress has been made during recent years in understanding the mechanisms operating in damped nuclear reactions, several of the most characteristic features of these processes have so far escaped a consistent theoretical description. This is particularly true of the experimental well-established correlations,[1] between energy dissipation and nucleon exchange. Experimental evidence is in accord with the assumption of successive *exchange of single nucleons proceeding simultaneously* with dissipation of relative kinetic energy in many small steps. We have examined available data in order to expose the systematic properties of dissipation and exchange mechanisms associated with damped nuclear reactions. It is shown that these features cannot be understood on purely classical ground but find a natural explanation when the fermion nature of the exchanged nucleons is taken into account.

A quantal model[2] is applied attributing energy dissipation to the stochastic exchange of nucleons between two Fermi-Dirac gases in relative motion, a description expected to be relevant for the modest excitations attained in the *damped reactions under consideration.* The model expresses the rate of change of the projectile mass number A and the energy dissipation rate as

$$dA/dt = F_A N'(\epsilon_F), \quad dE_{loss}/dt = \langle\omega^2\rangle_F N'(\epsilon_F). \tag{1}$$

Here $N'(\epsilon_F) = \partial N(\epsilon_F)/\partial\tau_F$ is the differential current of nucleons exchanged between the gases calculated with neglect of the Pauli blocking effect. This form factor governs the overall intensity of the interaction and depends delicately on the details of the interaction zone. The quantity ω is the amount of intrinsic excitation produced by the exchange of a nucleon and the brackets denote an average over the orbitals in the Fermi surface, the only ones participating. The two quantites in Eq. (1) can both be represented in terms of one-body operators and may, therefore, be calculated without taking explicit account of the Pauli exclusion principle.

This, however, is not true for the particle-number dispersion σ_A^2, a quantity depending explicitly on the correlations present, such as those imposed by the Fermi-Dirac statistics of the nucleons. The rate of growth of σ_A^2 is, in this model, equal to the total rate of actual exchanges, as *long as the system has not evolved too far* towards equilibrium. It is given by

$$d\sigma_A^2/dt = 2\tau^* N'(\epsilon_F). \tag{2}$$

Here, $\tau^* = \langle\omega/2 \coth(\omega/2\tau)\rangle_F$ is a measure of the energy interval around the Fermi level contributing to exchange processes. In the limit $|\omega| \ll \tau$, it approaches the nuclear temperature τ, whereas in the case $|\omega| \gg \tau$, $\tau^* \simeq 1/2 \langle|\omega|\rangle_F$ may be considerably larger than τ, because of a larger relative displacement of the two Fermi spheres. In any case, the appearance of τ^* in Eq. (2) ensures that proper account is taken of the quantum statistics at all temperatures.

It is possible to make simple idealized estimates of the correlation between the energy loss and the number dispersion. Quantitative results have been obtained from dynamical calculations of collisions trajectories in a coordinate space including the fragment-mass and -charge asymmetries.

Typical results of the calculations (full curves) are compared to experiment in Fig. 1. The dashed curves represent the dynamical calculations in the classical limit. The Pauli principle is essential to the good agreement between data and the quantal model.

In summary, the good agreement between data *and model predictions found in general demonstrates* that energy dissipation in damped reactions can be consistently understood in terms of the nucleon exchange mechanism in which the Pauli exclusion principle plays a crucial role.

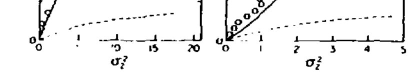

Fig. 1. Comparison of model predictions for the correlation $E_{loss}(\sigma_Z^2)$ with data for the reactions $^{209}Bi + ^{136}Xe$ (left) and $^{209}Bi + ^{56}Fe$ (right). The dashed curves represent the classical limits of the full calculations (full curves). (XBL 808-11029)

Footnotes and References

*Condensed from Phys. Rev. Lett. 44, 308 (1980), LBL-10529.

[†]Departments of Chemistry and Physics, University of Rochester, Rochester, NY 14627.

1. W. U. Schröder and J. R. Huizenga, Ann. Rev. Nucl. Sci. 27, 465 (1977).

2. J. Randrup, Nucl. Phys. A307 (1979), and A327, 490 (1979).

QUANTAL DYNAMICS OF CHARGE EQUILIBRATION IN DAMPED NUCLEAR COLLISIONS*

E. S. Hernandez,[†] W. D. Myers, J. Randrup, and B. Remaud[‡]

In quasi-elastic and deep-inelastic nuclear reactions charge equilibration appears to occur quite rapidly. This rapid movement of protons in one direction and neutrons in the other can be viewed as a collective mode associated with isovector-type hydrodynamical flow in the dinucleus analogous to the Steinwedel-Jensen description of the giant dipole resonance (GDR) in ordinary nuclei. Since we find that the characteristic energy of such a mode is typically much larger than the nuclear temperatures encountered, the fluctuations in the charge asymmetry degree of freedom are expected to come mainly from zero-point motion.

Such a description of the charge asymmetry mode has already been applied with some success by Swiatecki and Blann to charge and mass distributions seen in fission,[1] and more recently to heavy-ion reactions by Moretto,[2] by Berlanger et al.,[3] and by Hofmann, Gregoire, Lucas and Ngo.[4,5] However, as pointed out by Nifenecker et al.,[6] it is essential to consider the time dependence of the shape of the system in order to correctly establish the connection between the GDR-like collective motion and the width of the charge distibution which is experimentally observed.

Roughly speaking, the inertia associated with the charge asymmetry degree of freedom is inversely proportional to the size of the neck connecting the two colliding nuclei. Trajectory calculations predict that the pinch-off takes place sufficiently rapidly that the width of the charge distribution is "frozen in" by the increasing inertia.

In order to describe the division of charge between the two partners, for a given mass asymmetry, we use the isospin component of the projectile-like nucleus T = (N-Z)/2. The potential-energy surface of the dinucleus varies rather gently in the A-direction while the strong symmetry energy makes it much steeper in the T-direction. Furthermore, the dynamical evolution along the mass asymmetry proceeds relatively slowly and can often be entirely neglected.

In Fig. 1 the calculated results are compared with the experimental data of Ref. 3. The upper portion of the figure shows the mean charge <Z> and the lower portion shows the width Γ of the final charge distribution at a fixed mass partition; both quantites are plotted as functions of the total center-of-mass kinetic energy loss E* which is approximately the same as the induced intrinsic excitation in the fragments.

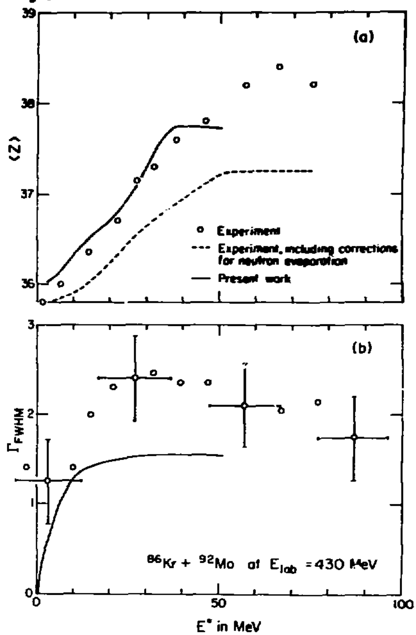

Fig. 1. (XBL 779-2954)

The primary experimental data are shown as the open dots on the upper portion of the figure and the dashed curve results after correction for neutron evaporation has been made. The calculated values are given by a solid curve.

The present calculations give a quick rise of Γ with E*, followed by a broad maximum. The maximum occurs at around E* = 35 MeV in agreement with the data but it is not as pronounced. The overall magnitude of the calculated curve is seen to fall somewhat below the experimental data. We are encouraged by the fact that these predictions are consistent with the observations. This is especially significant since all the coefficients entering in the various formulas are either fundamental nuclear constants or have been otherwise fixed beforehand so that there are no adjustable parameters.

Footnotes and References

*Condensed from LBL-9761, Nucl. Phys. A (in press)

†Permanent address: Departmento de Fisica, Facultad de Ciencias Exactas y Naturales, 1428 Buenos Aires, Argentina.

‡Permanent address: Institue de Physique, Universite de Nantes, 2 rue de la Houssiniere, 44072 Nantes, France.

1. W. J. Swiatecki and H. M. Blann, unpublished notes (1961); W. J. Swiatecki, lecture at Princeton University, 7 March 1961

2. L. G. Moretto, J. Sventek and G. Mantzouranis, Phys. Rev. Lett. 42 (1979) 563.

3. M. Berlanger, A. Gobbi, F. Hanappe, U. Lynen, C. Ngo, A. Olmi, H. Sann, H. Stelzer, H. Richel, and M. F. Rivet, Proc. Int. Workshop on Gross Properties of Nuclei and Nuclear Excitations VII, Hirschegg, Austria, Jan. 1979; also Z. Phys. A291 (1979) 133.

4. C. Gregoire, R. Lucus, C. Ngo and H. Hoffman, Proc. IVth Balaton Conf. on Nucl. Phys., Keszthely, Hungary, June 1979.

5. H. Hofmann, C. Gregoire, R. Lucas and C. Ngo., preprint DPh-N/MF/79/22, CEN, Saclay, July 1979.

6. H. Nifenecker, J. Blachot, J. P. Bocquet, R. Brissot, J. Crancon, C. Hamelin, G. Mariolopolous and Ch. Ristori, preprint Centre d'Etudes Nucleaires, Grenoble, July 1979.

AN ADIABATICITY CRITERION FOR COLLECTIVE MOTION*

G. Mantzouranis, W. D. Myers and J. Randrup

In studies of the charge equilibration process in strongly damped nuclear collisions, we have found that the width of the charge distribution of the projectile-like fragment is "frozen in" when the neck between the two nascent fragments decreases rapidly just before separation.[1]

Our approach was to view the charge equilibration process as one aspect of the collective motion of neutrons against protons in the composite system formed by the colliding nuclei. Thus, we were mainly concerned with the ground state motion in the giant dipole resonance (GDR) degree of freedom for the dinuclear complex. To determine the width of the charge distibution we resorted to a numerical calculation that followed the time-dependent GDR as the collision took place. The results of the calculations corresponded closely with the observed values.

In order to eliminate the need for numerical calculations and make the approach more generally available we are developing an empirical method for calculating the dispersion in a collective coordinate that is "frozen in" when the inertial mass increases rapidly. For the systems of interest (nuclear collisions and fission) the mass is inversely proportional to the size of the opening between the two halves of the system. Consequently we can focus our attention on a collective coordinate whose associated mass $m \propto b^{-1}(t)$ where b decreases linearly with time. The equation of motion for the width of the distribution σ is

$$\ddot{\sigma} - (\dot{b}/b)\dot{\sigma} + kb\sigma = (\hbar^2/4)b^2\sigma^{-3} \qquad (1)$$

where k is the stiffness parameter for the GDR. This parameter changes very little during the collision so it can be fixed at its scission value. Examination of Eq. (1) suggests that the quantity

$$C = \frac{3}{4}\frac{(\dot{b}/b)^2}{kb} - 1 \qquad (2)$$

is critical for determining whether the system is able to adiabaticly follow the time variation of b or whether the process becomes nonadiabatic. The figure shows how this quantity can be used in practice to avoid the need for numerical calculations.

In the upper part of Fig. 1 we have plotted (as heavy straight lines) the adiabatic value of the fourth power of the full width at half maximum Γ^4 (where $\Gamma = 2.355\sigma$) for four different values of $\dot{b}$ (-0.002, -0.008, -0.014,

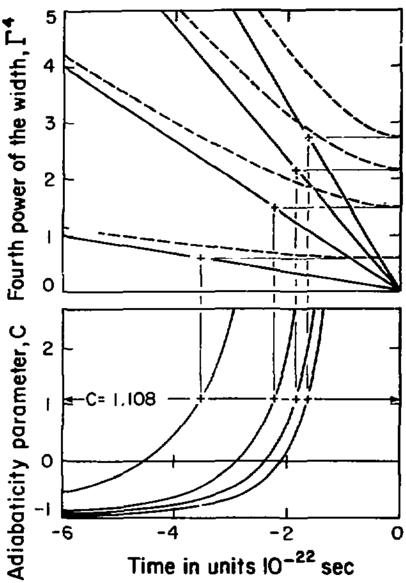

Fig. 1. Curves used to determine the value of the critical quantity C which can then be used to estimate the final value of the width Γ. (XBL 807-1637)

-0.020) that bracket the range of physically interesting values. The heavy dashed lines are numerically calculated values of $\Gamma^4(t)$ obtained from solving Eq. (1) with k = 4 MeV. When the final "freeze-out" value of $\Gamma^4(t)$ is projected back to the adiabatic curves, one can determine the time at which the adiabatic value of Γ was the same as the final value. If this time is projected down to the lower part of the figure, we find that the critical quantity C has approximately the same value in each case of 1.108. This result allows us to estimate Γ_{final} since we know that

$$\Gamma^4_{adiabatic} = (2.355)^4 \frac{\hbar^2}{4k} b \qquad (3)$$

Footnote and Reference

*Condensed from LBL-11542, Phys. Lett. 98B (1981)

1. E. S. Hernandez, W. D. Myers, J. Randrup and B. Remaud, "Quantal Dynamics of Charge Equilibration in Damped Nuclear Collisions," LBL-9761 (October 1979), to be published.

ANGULAR DISTRIBUTIONS OF SEQUENTIALLY EMITTED PARTICLES AND GAMMA RAYS FROM NEARLY ALIGNED NUCLEI FROM DEEP INELASTIC COLLISIONS

L. G. Moretto, S. Blau, and A. Pacheco

Thermal fluctuations in deep inelastic collisions can produce an angular momentum misalignment in the resulting fragments. A statistical analysis of the problem leads to the following distribution in the three angular momentum components for asymmetric system[1]:

$$P(\underset{\sim}{I}) \propto \exp-\left(\frac{I_x^2}{2\sigma_x^2} + \frac{I_y^2}{2\sigma_y^2} + \frac{(I_z - \bar{I}_z)^2}{2\sigma_z^2}\right)$$

where $\sigma_z^2 = \sigma_y^2 = \frac{6}{7}\mathscr{I}T$, $\sigma_x^2 = \frac{6}{5}\mathscr{I}T$, is the temperature of the intermediate couples and $\mathscr{I}$ is the moment of inertia of one of the two fragments.

If one of the fragments either fissions or under-goes particle decay, the angular distribution of the emitted particles is

$$w(\theta\phi) = \frac{1}{S}\left[\frac{I^2_{min}}{A_{min}} \exp(-A_{min}) - \frac{I^2_{max}}{A_{max}} \exp(-A_{max})\right]$$

where $A_{max(min)} = I^2_{max(min)}\left[\frac{\cos^2\theta}{2S^2} - \beta\right]$; $\beta = \frac{\hbar^2}{2T}\left[\frac{1}{\mathscr{I}_\parallel} - \frac{1}{\mathscr{I}_\perp}\right]$;

$$S^2(\theta,\phi) = K_0^2 + (\sigma_x^2\cos^2\phi + \sigma_y^2\sin^2\phi)\sin^2\theta + \sigma_z^2\cos^2\theta;$$

$$K_0^2 = \frac{1}{\hbar^2}\left[\frac{1}{\mathcal{I}_\parallel} - \frac{1}{\mathcal{I}_\perp}\right]^{-1} T \quad ;$$

and $\mathcal{I}_\parallel$, $\mathcal{I}_\perp$, $\mathcal{I}_n$ are the parallel and perpendicular moments of inertia of the critical shape (saddle point) and of the residual nucleus after neutron emission respectively.

Similarly for the stretched emission of gamma rays we have the following angular distribution (we set $\sigma_x^2 = \sigma_y^2 = \sigma_z^2$):

$$W(\theta)_{E1} = \frac{3}{4}[1 + \cos^2\theta + \beta^2(1 - D(\beta))(1 - 3\cos^2\theta)]$$

$$W(\theta)_{E2} = \frac{5}{4}\,[1 - \cos^4\theta$$

$$-2\beta^2\left\{3\sin^2\theta\,\cos^2\theta - 2\cos^4\theta - \frac{3}{4}D(\beta)\right.$$

$$\left.(\sin^2\theta - 4\cos^2\theta)\sin^2\theta\right\}$$

$$-3\beta^4\left\{4\cos^4\theta + \frac{3}{2}\sin^4\theta - 12\sin^2\theta\,\cos^2\theta\right\}(1 - D(\beta))]$$

where $\beta = \frac{\sigma}{I_z}$ and $D(\beta) = \sqrt{2}\beta F(1/\sqrt{2}\beta)$ and $F(x)$ is the Dawson integral:

$$F(x) = e^{-x}\int_0^x e^{t^2}dt$$

These formulae provide a most direct tool to extract information on the fragment spin misalignment from angular distribution.

Reference

1. L. B. Moretto and R. P. Schmitt, Phys. Rev. C 21, 204, 1980. LBL-10805.

EFFECTS OF PARTICLE EVAPORATION ON THE ANGULAR MOMENTUM OF THE EMITTING NUCLEUS FOR DEEP INELASTIC AND COMPOUND NUCLEAR REACTIONS*

S. K. Blau and L. G. Moretto

Gamma multiplicity measurements[1] and angular distributions of photons, light particles and fission fragments[2] provide information about the magnitude and alignment of the angular momentum transferred during deep inelastic processes. None of these data, though, many be interpreted properly without including a correction for the effects of particle emission on the angular momentum of the residual nucleus. We endeavor to provide analytical formulae to show how such corrections can be made.

We assume that the evaporation process is controlled by a critical shape[3] (emitter/ejectile complex) consisting of residual nucleus and emitted particle in contact with each other. In our model the ejectile removes angular momentum equal to the orbital angular momentum of the ejectile/emitter complex, i.e., it carries no intrinsic spin. We assume that the probability of emission at a given colatitude, θ, is proportional to the Boltzmann factor $\exp(-E_{rot}(\theta)/T)$. We find that the average angular momentum removed by an ejectile is:

$$\langle I_{ejct}\rangle = I(1 - F - (1 - F^2)g(Z)/2F$$

$$+ (1 - F^2)^2\, h(Z)/8F^3, \qquad (1)$$

where

$$F = J/(J + \mu R^2),$$

$$Z = I/\sqrt{2}K_0$$

$$g(Z) = (\mathrm{erf}(Z)/\sqrt{\pi}/2 -$$

$$Z\exp(-Z^2)/\sqrt{\pi})/Z^2\,\mathrm{exp}(Z)), \text{ and}$$

$$h(Z) = (3\sqrt{\pi}\,\mathrm{erf}(Z)/4 - 3Z\exp(-Z^2)/2 -$$

$$-3Z\exp(-Z^2))/(\sqrt{\pi}Z^4\,\mathrm{erf}(Z)).$$

The functions $g(Z)$ and $h(Z)$ may be expanded in powers of Z. Their expansion to second order in Z yields:

$$g(Z) \simeq 1/3 - 4Z^2/45$$
$$h(Z) \simeq 1/5 - 4Z^2/45.$$

Substitution of these approximations for the analytical expressions in Eq. 1 and the formulae that follow introduces an error of $\lesssim$ 3%.

In order to calculate the dispersion in the angular momention of the residual nucleus due to emission of an ejectile, we may assume that for a given colatitude, θ, ejectiles are emitted isotropically. If we estimate $\langle p^2\rangle = 3mT$

where m is the ejectile's mass and T is the nuclear temperature we find:

$$\sigma_x^2 = \sigma_y^2 = \frac{I\,(1-F)^2}{2}\left[(g^2(Z) - h(Z)\right] + \frac{mr^2T}{2}$$

$$(1 + g(Z)), \qquad (2)$$

$$\sigma_z^2 = I^2(1-F)^2\,(h(Z) - g^2(Z)) + mr^2T$$

$$(1 - g(Z)), \qquad (3)$$

where x and y are two orthogonal directions in the reaction plane and the z direction is perpendicular to the reaction plane.

We also calculate the dispersion in the angular momentum of the residual nucleus with a model in which the velocity of emitted ejectiles follows the Maxwell velocity distribution weighted by a factor, $v_\perp$, the velocity of the ejectile perpendicular to the surface at the point of evaporation. The results are essentially identical with those of the isotropic model given in equations 2 and 3.

For non-fissioning compound nuclei we choose the x' axis to be the beam axis. The y' and z' axes are orthogonal axes perpendicular to the beam axis. The components of the dispersion of the angular momentum of the compound nucleus after evaporation of an ejectile may be expressed in terms of σ_x^2, σ_y^2 and σ_z^2:

$$\sigma_{x'}^2 = \sigma_x^2 = \sigma_y^2 \qquad (4)$$

$$\sigma_{y''}^2 = \sigma_z^2,\ (\sigma_y^2 + \sigma_z^2)/2. \qquad (5)$$

Footnote and References

*Condensed from LBL-10926

1. M. Lefort and C. Ngo, Riv. Nuovo Cimento. 12, 1 (1979) and references therein.

2. L. G. Moretto, S. Blau, and A. Pacheco, LBL Report No. 10805 (to be published).

3. L. G. Moretto, Nucl. Phys. A 247, 211 (1975).

HIGH-MULTIPOLE ISOVECTOR MODES AND CHARGE FLUCTUATIONS IN HEAVY ION REACTIONS*

L. G. Moretto, C. R. Albiston and G. Mantzouranis

The isobaric charge distribution of fragments in deep-inelastic scattering provides information regarding the thermal and quantal fluctuations of axial component of the E1 mode associated with the intermediate complex.[1] There have been allegedly contradictory findings of small and large charge fluctuations at large and small mass asymmetries, respectively.

To elucidate the role played by mass asymmetry and the higher-order isovector modes, we propose a simple model in which the intermediate complex is approximated by a cylinder split into two parts, and study its axial modes.

Using the Steinwedel-Jense hydrodynamical model, we obtain the mode frequencies $\omega_n = k_n u$, where u is the isospin sound velocity and $k_n = (\pi/2a)n$, the wavenumber of the nth mode, is given by te boundary conditions of the mode wave functions on the cylinder. The potential energy as a function of the charge excess of one of the fragments yields the stiffness constant

$$c_n = \pi^2\, X\left(\frac{A}{Z^2}\right)\frac{n^2}{\sin^2[n\pi Q]}$$

where X is the liquid drop symmetry energy coefficient and Q is the degree of symmetry.

In the limit of low temperature, the partial charge widths are given by

$$\sigma_n^2 = \hbar\omega_n/2c_n$$
$$= \sigma_1^2(\text{symmetry})\,\sin^2[n\pi Q]/n$$

and are plotted in Fig. 1. The contribution of the higher modes is comparable to that of the lowest one, and the partial widths of all the modes depend strongly on Q. At complete asymmetry (Q = 0), all widths vanish.

The total charge width

$$\sigma^2 = \sigma_1^2(\text{symmetry})\sum_n \frac{\sin^2[n\pi Q]}{n}$$

diverges logarithmically; however, the finite size of the nucleon sets an upper limit on n.

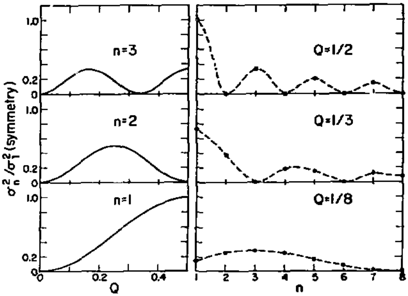

Fig. 1. The square of the normalized partial width is plotted (a) against the degree of symmetry at fixed n, and (b) against n at a fixed degree of symmetry. (XBL 7910-4421)

Footnote and Reference

*Condensed from LBL-9896, Phy. Rev. Lett. 44, 924 (1980).

1. L. G. Moretto, J. Sventek, G. Mantzouranis, Phys. Rev. Lett. 42, 563 (1979).

MANIFESTATIONS OF EXCITATION ENERGY FLUCTUATIONS IN DEEP INELASTIC COLLISIONS

D. J. Morrissey and L. G. Moretto

The equilibration of excitation energy between the partners in deep inelastic collisions has to occur on a very short time scale. This fast equilibration is required by observations that the mean number of evaporated neutrons from reaction products is indicative of a splitting of the total dissipated energy in proportion to the fragment masses[1,2] over the whole range of dissipated energy, even for very small energy loss (i.e., the shortest collision times). Thus, the thermalization time must be shorter than the shortest interaction times so that the fragments always remain in themal equilibrium. A further check of statistical equilibrium can be made by observing fluctuations in the sharing of the excitation energy between the two fragments. This distribution of excitation energy, E, is proportational to the level densities[3]:

$$P(x)dx \propto \rho_1(x)\rho_2(E - x)dx \quad (1)$$

For small excursions about the mean, E_0^*, the distributions is approximately Gaussian:

$$P(x)dx \propto e^{-(E_0^* - x)^2/2\sigma^2}\, dx \quad (2)$$

where σ^2 is a function of the temperature and the level density parameters:

$$\sigma^2 = 2T^3 \frac{a_1 a_2}{a_1 + a_2} \quad (3)$$

For the symmetric system $A_1 = A_2 = 100$ with $E = 100$ MeV we obtain ($a = A/8$), $E_0^* = 50$ MeV, and $\sigma = 10$ MeV.

We have explored two avenues through which the fluctuations could manifest themselves, neutron energy spectra and evaporated neutron number. We have found these two observables complementary in that fluctuations have a large effect on the neutron energy spectra only when the mass asymmetry is large and fluctuations introduce a covariance in the number of evaporated neutrons that is prominent for equal mass fragments.

Figure 1 shows the neutron energy spectrum expected from the light partner (20:180 mass split). The constant temperature neutron spectrum was calculated as:

$$P(\varepsilon_\nu, T) = \frac{\varepsilon}{T^2} e^{-\varepsilon/T} \quad (4)$$

The neutron spectrum for a fluctuating excitation energy was calculated by numerical folding of Eq. 1 with Eq. 4. The increase in the probability of emitting a high-energy neutron is very dramatic.

The covariance of the number of emitted neutrons from reaction partners was investigated with a simple Monte Carlo code. The division of

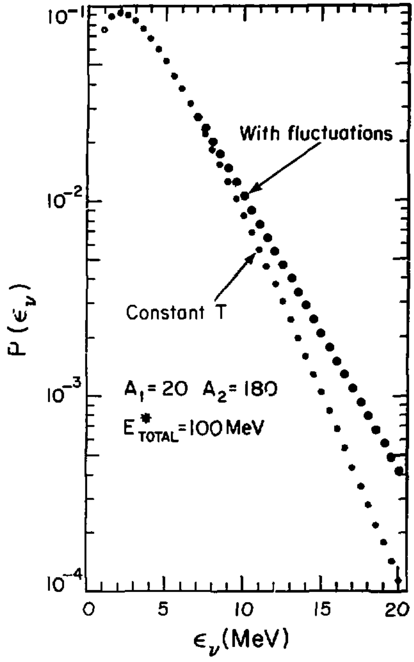

Fig. 1. The calculated neutron energy spectra from the light partner with and without fluctuations are shown. (XBL 808-1551)

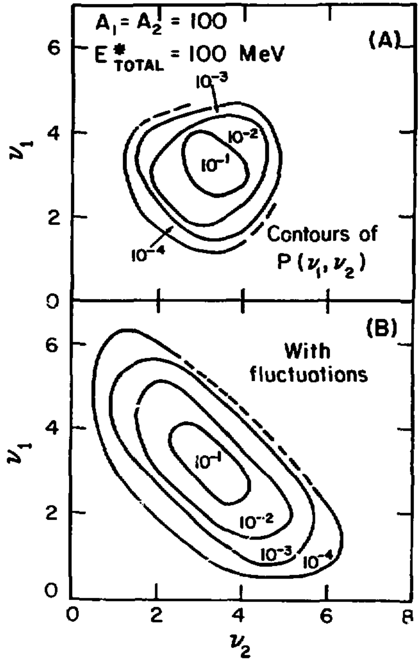

Fig. 2. The correlation of the number of neutrons emitted from symmetric fragments is shown for discrete excitation energy division in (A) and with fluctuations in (B). (XBL 808-1552)

the excitation energy was either fixed or picked at random in proportion to Eq. 1. Then the two fragments were allowed to emit neutrons until the nuclei had cooled to less than (B_ν + 2T'), where B_ν is the liquid drop neutron binding energy and T' is the temperature after emission of the previous neutron. The probability contours for emission of ν_1 neutrons from fragment 1 and ν_2 neutrons from fragment 2 are shown in Figs. 2(A) and (B). Again, a dramatic change can be seen when we turn on the fluctuations (Fig. 2 (B)). Experiments along these lines should therefore be very useful in establishing if thermal equilibrium is really attained.

References

1. B. Cauvin et al., Nucl. Phys. A301, 511 (1977).

2. Y. Eyal et al., phys. Rev. Lett. 41, 625 (1978).

3. L. G. Moretto, Proc. Varenna Conf., Varenna, Italy, July 9-25, 1979 (in press) and LBL-9130.

ANGULAR MOMENTUM FRACTIONATION PRODUCED BY AN ℓ-DEPENDENT POTENTIAL ENERGY*

C. R. Albiston and L. G. Moretto

The gamma-ray multiplicity associated with deep-inelastic collisions provides information about the spin of the product fragments. For nonequilibrated systems, the variation of the multiplicity with mass asymmetry may shed light on the time dependence of the angular momentum transfer.

We present experimental evidence for angular momentum fractionation caused by an ℓ-dependent potential energy, and we explain it using a simple model. The gamma-ray multiplicity for 340-MeV ^{40}Ar + ^{159}Tb at 50° in the lab[1] (Fig. 1) drops sharply with decreasing fragment charge, or increasing mass asymmetry, in contrast to the multiplicity measured for Ne + Ag, Ar + Y, Kr + Ag, and Kr + Ho.

A possible explanation is suggested by Fig. 2. For low ℓ waves, the potential at the injection point slopes downward with increasing mass asymmetry, whereas it slopes upward for high ℓ waves, barring their diffusion. Consequently, the fragments of lower charge are preferentially populated by lower ℓ waves and smaller gamma-ray multiplicities.

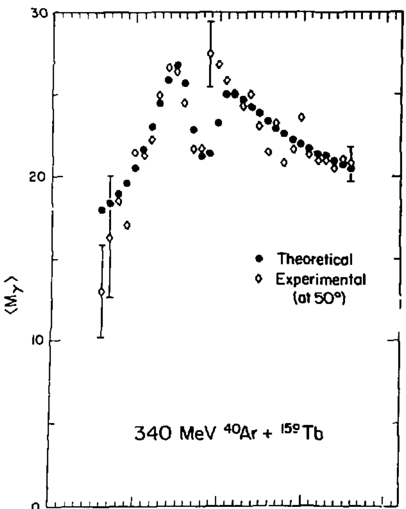

Fig. 1. Gamma-ray multiplicities as a function of fragment charge with representative error bars on the experimental results. (XBL 804-4135)

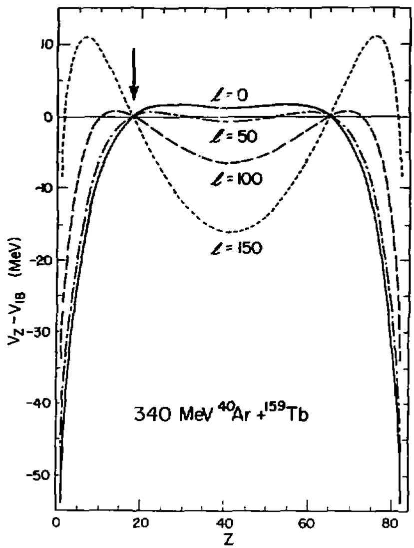

Fig. 2. Potential energy as a function of fragment charge for representative ℓ waves. The arrow indicates the entrance-channel asymmetry, or injection point, for this reaction. (XBL 804-4136)

A simple diffusion model can describe this effect more quantatively. The asymmetry potentials are approximated by inverted parabolas, each peaking at $A = A_{max}$, and whose curvature increases with ℓ: $V_\ell = (1/2)c_\ell(Z - Z_{max})^2$. In this case, the Fokker-Planck equation describing the time dependence of the population along the asymmetry coordinate has an analytical solution:

$$\phi(h,\ell) = c_\ell^{1/2}(2\pi T[1 - \exp(-2c_\ell t_\ell/K)]^{-1/2}$$

$$\exp\left\{\frac{-c_\ell[\,h - h_0\exp(-c_\ell t_\ell/K)]^2}{2T[1 - \exp(-2c_\ell t_\ell/K)]}\right\}$$

where t is the interaction time, K is the friction coefficient, and $h = h_0$ at the injection point.

Simple ansatze are made for the dependence on ℓ of the interaction time and the curvature of the potential. The multiplicity is given by half of the the first moment of the fragment spin with respect to the distribution $\phi(h,\ell)$; the results are shown in Fig. 1. This calculation is not intended to fit the data quantitatively; rather, it serves to demonstrate that the difference in the potential energies of the various ℓ waves must be accounted for.

Footnote and Reference

*Condensed from LBL-10664.

1. M. Lutolf et al., Nucl. Sci. Div. Annual Report 1978-1979, LBL 9711, p. 67.

A TIME-DEPENDENT HARTREE-FOCK STUDY OF HIGH-ENERGY RESONANCE INDUCED BY HEAVY-ION COLLISION

H. Flocard and M. S. Weiss*

Recent heavy-ion experiments measuring, with high-resolution, cross sections as a function of excitation energy, have shown that superimposed on the previously known quasi-elastic peak and deep inelastic broad bump, there existed well-defined structures.[1] The exact nature of these structures is still far from being elucidated, but one natural explanation would be that they correspond to high lying resonances. It was therefore tempting to see whether such resonances could be predicted by a time-dependent Hartree-Fock calculation (TDHF). We first chose the starting point of our calculation so as to reproduce the experimental condition, namely a $^{40}Ca + ^{40}Ca$ at an energy E_{lab} = 400 MeV and an impact parameter leading to a quasi-grazing collision (L = 100 ħ). Once the collision was completed, we stopped each fragment so it did not fly out of the box in which the calculation was performed. We then let the two outgoing fragments evolve in time in their c.m. frame, and we recorded the time evolution of their multipole moments.

In a second state we analyze this time evolution and try to detect if it contains high frequency vibrational modes. A first observation is that the motion of all moments is highly dominated by nonlinear phenomena. A direct Fourier transform shows the major peaks occuring in the 0-3 MeV range which, in view of the total time over which the motion is recorded (2 x 10^{-21}s), cannot be considered as significant (a 2-MeV mode performs only one vibration in 2 x 10^{-21}s). However, some structures are evident at high energy. Their analysis is made difficult by the background noise generated by the Fourier transform performed on a finite time interval. In order to study the high energies it is necessary to filter out the low-energy modes and the ensuing high frequency background that they artificially generate. Indeed, subtracting from the calculated curve its smooth part obtained by convolution with a Gaussian shows clearly the existence of underlying vibrations whose energy can be slowly extracted. A more detailed analysis of which frequencies are excited, in which multipole moment, is now needed in order to assign each frequency to a specific shape vibration of the nuclei. An investigation as to whether the rather large number of vibrations seen in our calculation corresponds to independent modes or whether they can be sorted into families of frequencies multiple of a given number, thus indicating a nonlinear vibration, is presently underway.

Footnote and Reference

*Lawrence Livermore National Laboratory, Livermore, CA 94580.

1. N. Frascaria et al., Phys. Rev. Lett. 39, 918 (1977) and ORSAY Preprint IPNO PAN-79-19 (1979).

APPLICATION OF THE IMAGINARY TIME STEP METHOD TO THE SOLUTION OF THE STATIC HARTREE-FOCK PROBLEM

K. T. R. Davies,* H. Flocard, S. Krieger† and M. S. Weiss‡

The Hartree-Fock (HF) method appears over the years as one of the most powerful methods available to study nuclear structure. However, it entails the solution of nonlinear equations for which no mathematical analysis is yet available. One must therefore rely on empiricism to find schemes, necessarily of iterative nature, which ensure a convergence toward the HF solution. One such scheme was developed in the forties and used extensively in the sixties by several groups to study nuclear structure properties. It involves the expansion of the single particle wave function on a given basis followed by a construction of the HF Hamiltonian h in the variational space. Subsequent diagonalizations of the HF Hamiltonian provide the wave functions for the next approximations of the HF Hamiltonian. With minor improvements this method has proven quite successful in all the cases in which it could be implemented. The crucial limitation of the method is the size N of the variational space which must not exceed N ~ 100 for the calculation to remain manageable. For the description of complicated shapes like those appearing in heavy-ion collisions of fission processes this limitation appears too restrictive. In addition, the diagonalization of the Hamiltonian matrix at each interation provides un-useful information on high lying (and very likely unphysical) states. The imaginary time method that we propose studies only those states that contribute to the Hartree-Fock solution (unless information on specified unoccupied states is also desired). It also allows the handling of large variational spaces. For example, calculations have been performed for spaces of dimension N = 2000. The iterative procedure goes as follows. Starting from an initial guess of the useful single particle wave functions, we generate the HF Hamiltonian matrix h and the wave functions at the next iteration by the transformation

$$\psi_i^{(n+1)} = \exp\left(-\frac{\lambda h^{(n)}}{\hbar}\,\psi_i^{(n)}\right) . \qquad (1)$$

In the proceeding formula i stands for the single particle index, (n) labels the iteration, and λ is a parameter of the method that happens to be homogeneous to an imaginary time step. Before moving to the next iteration, the $\psi_i^{(n+1)}$ must first be orthogonalized, since the transformation (1) is not unitary. Practically, the exponential in formula (1) can be replaced by a few terms' expansion so that transformation (1) amounts to successive multiplications by $h^{(n)}$. Since in many cases the matrix $h^{(n)}$ is sparse, the storage and calculation problem is greatly reduced. The method has been successfully applied for several calculations for the study of either fission or nuclear molecular states. We plan now to apply it to study the changes in nuclear shapes induced by high values of the angular momentum like those achieved by a heavy-ion collision.

Footnotes

*Oak Ridge National Laboratory, P.O. Box X, Oak Ridge, TN 37830
†Department of Physics, University of Illinois at Chicago Circle, Box 4348, Chicago IL 60680
‡Lawrence Livermore Laboratory, University of California, Livermore, CA 94550

B. RELATIVISTIC

TARGET FRAGMENTATION CALCULATIONS WITH THE NUCLEAR FIRESTREAK MODEL

P. L. McGaughey, D. J. Morrissey, and G. T. Seaborg

Previous calculations of the fragmentation of heavy targets, induced by beams of relativistic heavy-ions, have been performed under the formalisms of the nuclear fireball model[1] and the intra-nuclear cascade (INC) model.[2] These models represent two limiting views of the mechanism of interaction of nuclei colliding at relativistic velocities. The INC model pictures the interaction as consisting of the uncorrelated collisions of individual nucleons within the two nuclei, while the fireball model assumes that the interaction is localized to the overlap region, with the non-overlapping regions being unaffected. Both systematics require a two step reaction: during the first step the struck target nucleus fragments into highly excited remnants, and in the latter step the remnants de-excite by statistical emission of particles and by fission.

Unfortunately, the fireball model calculation is much inferior to that of the INC model, for it severely underestimates the excitation energy deposited in the fragment during the abrasion step and cannot predict angular and linear momentum transfer at all, both of which are calculated by the use of the INC model. In order to retain the collective nature of the interaction and to eliminate the unrealistic clean-cut assumptions of the fireball model, we have extended the firestreak model of Myers[3] to include the calculation of the residual masses, excitation energies, and linear and angular momenta of the primary target remnants that are produced in these reactions. Under this newer formalism, the two colliding nuclei have diffuse nuclear surfaces that are generated by folding a short-range (Yukawa) function into the conventional sharp-sphere density distribution. It is assumed that during the collision the interaction is localized to the overlap region, where co-linear tubes of nuclear matter from the projectile and target undergo completely inelastic collisions. A transparency function, which is based upon the total free nucleon-nucleon cross sections, is included to prevent collisions from occuring between tubes containing an insufficient density of nucleons. Once two tubes have collided, they fuse and equilibrate their kinetic and thermal energies. If the resulting kinetic energy of the fused tubes is less than its binding energy to the target, then it is captured and contributes directly to the target fragment's excitation energy, mass, and momenta, which are all explicitly conserved during the interaction. The de-excitation step of the reaction is handled in identical fashion to that of the other models.

In Fig. 1, the results of some of the calculations of the fast collision step are given for the reaction of 400 MeV/A $^{20}Ne + ^{238}U$, as calculated by the three models. The INC computer code was executed using an eight step density distribution for the two nuclei, with the inclusion of Fermi motion of the nucleons, and the allowance of meson production. The fireball code used took neutron skin effects into account for the target nucleus. The firestreak calculation was performed including Pauli-principle blocking in the target. The latter two computations both used a giant dipole resonance model to obtain the initial charge distributions of the residual nuclei. The de-excitation phase of each calculation was performed using a standard Monte Carlo statistical evaporation code, which had been modified to include fission competition for all target fragments. The three final mass distibutions,

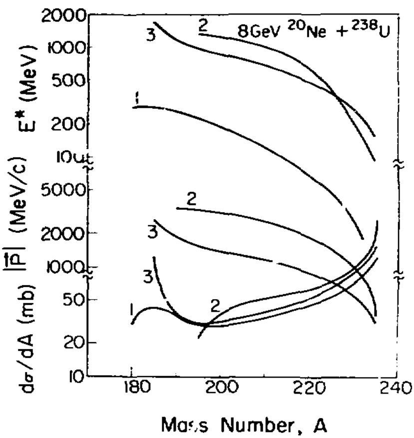

Fig. 1. Excitation energies, recoil momenta, and masses of target fragments produced during the primary interaction of 8.0 GeV $^{20}Ne + ^{238}U$, as calculated by the fireball (1), intra-nuclear cascade (2), and firestreak (3) models. (XBL 808-1675)

as calculated by this code, are given in Fig. 2, together with the experimentally measured distribution.[4]

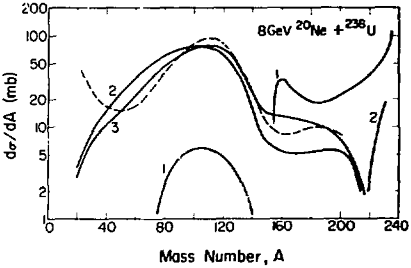

Fig. 2. Calculated mass-yield distributions of the target residues after de-excitation, labeled as in Fig. 1. The dashed line is the experimental data, as reported in reference 4. (XBL 808-1676)

Several conclusions are immediately suggested by an inspection of Figs. 1 and 2. As mentioned previously, the fireball model is clearly deficient, in that the predicted excitation energy transfer is far too low. This results in the generation of mass distributions with heavy mass yields which are far in excess of those actually observed. The similarity between the excitation energies, the momenta, and the mass distributions predicted by the firestreak and the INC models is very striking, with the INC model predicting generally higher energy transfer and less mass removal during the fast part of the collision. It is somewhat surprising that two such divergent collision mechanisms give nearly the same results. This suggests that although the interaction may well be collective in nature, this collectivity does not manifest itself in these experimental observables. Indeed, the shape of final mass distribution seems to be more sensitive to the choice of the statistical evaporation model parameters than to the differences between the firestreak and INC model predictions. Nevertheless, the firestreak has two apparent advantages over the INC model, for overall it produces the better fit to the experimental mass distribution for target residues formed from the interaction of 8 GeV ^{20}Ne + ^{238}U, and because it requires less than one-tenth of the computer time to perform the same calculation.

References

1. D. J. Morrissey, W. R. Marsh, R. J. Otto, W. Loveland, and G. T. Seaborg, Phys. Rev. C 18, 1267 (1978).

2. Y. Yariv and Z. Fraenkel, Phys. Rev. C 20, 2227 (1979).

3. W. D. Myers, Nucl. Phys. A 296, 177 (1978).

4. P. L. McGaughey, D. J. Morrissey, W. D. Loveland, and G. T. Seaborg, Nuclear Science Div. Annual Report 1978-1979, LBL-9711, p. 92.

TWO-PARTICLE CORRELATIONS IN HIGH-ENERGY NUCLEAR COLLISIONS

Jörn Knoll* and Jørgen Randrup

We discuss the correlations of two particles (proton-proton, proton-pion) in high-energy nuclear reactions by means of the linear-cascade model (rows on rows).[1,2] It describes the observed cross sections in terms of contributions arising from dynamically independent groups of interacting nucleons. In addition to a correlated part where both observed particles aise from the same group of nucelons, there is also a signficant background contribution from the particles originating from two independent groups. The construction of the one and two particle spectral functions by means of a Monte Carlo simulation method allows the inclusion of various dynamical effects, such as the production of delta isobars or precritical scattering.

The presently available data[3] express the amount of correlation by a ratio R of the in-plane to out-of-plane coincidence cross sections registered in a tag counter and spectrometer. Our initial studies indicate that not only the height of the quasi-elastic peak, but also its position in momentum space may be sensitive to the background term and to correlations arising from the sharing of energy and momentum among more than two particles.

For proton induced reactions (p,2p) only one participant cluster exists per event. Therefore the background term vanishes, thus enhancing the quasi-elastic peak such that it can be directly studied in the coincidence cross section.

The calculated coincidence spectra are found to be in close agreement with the data[3] for light systems. The observed shadowing effects in heavy sustem, however, are beyond the scope of this simple model.

Footnote and References

*Heisenberg fellow (Germany), from Sept. 1, 1980: Gesellschaft fur Schwerionenforschung (GSI), D-6100 Darmstadt, West Germany.

1. J. Hüfner and J. Knoll, Nucl. Phys. A290 (1977) 460; J. Knoll and J. Randrup, Nucl. Phys. A324 (1979) 445; J. Randrup, Phys. Lett. 76B (1978) 547.

2. J. Knoll, Phys. Rev. C 20 (1979) 509. J. Randrup, Nucl. Phys. A316 (1979) 509.

3. S. Nagamiya et al., J. Phys. Soc. Japan 44, Suppl. (1979) 378, and I. Tanihata et al., to be published.

STATISTICAL MODEL FOR INTERMEDIATE-ENERGY NUCLEAR COLLISIONS*

J. Randrup and S. E. Koonin[1]

We have developed a statistical model for multi-fragment final states in nuclear collisions with bombarding energies $E/A < 200$ MeV. A portion of the system formed with energy per nucleon ϵ and isospin polarization $I = (N-Z)/A$ is assumed to decay according to the available non-relativistic phase-space. The conservation of energy, nucleon number, and charge is most conveniently imposed by considering the grand canonical ensemble and introducing appropriate Lagrange multipliers. This results in a "fragment gas" at nuclear density ρ_0/X, where $\rho_0 = 0.17$ fm^{-3} is the nucleon density of ordinary nuclei and X is a parameter of order unity. The ground and all known particle-stable excited states of fragments with $A \leq 16$ are included explicity in the internal fragment partition functions, while those for $A > 16$ are approximated in a Fermi-gas model. For given values of ϵ, I, and X, we calculate the temperature and the fragment mass and charge distributions.

The figures show some instructive results: the temperature $\tilde{\tau}$ for a given ϵ (Fig. 1) is always greater than that of free nucleons ($= 2/3\epsilon$) because composite fragments effectively eliminate some translational degrees of freedom. The ratio of produced free neutrons to free protons (Fig. 2) increases dramatically

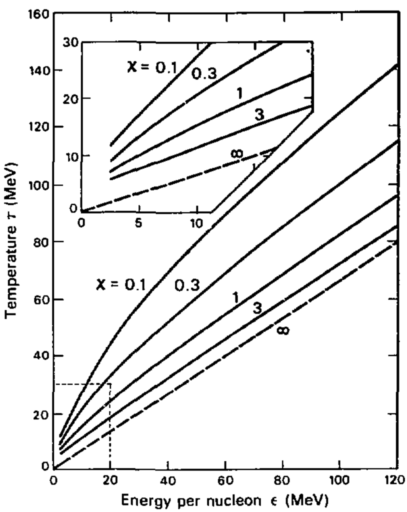

Fig. 1. (XBL 803-533)

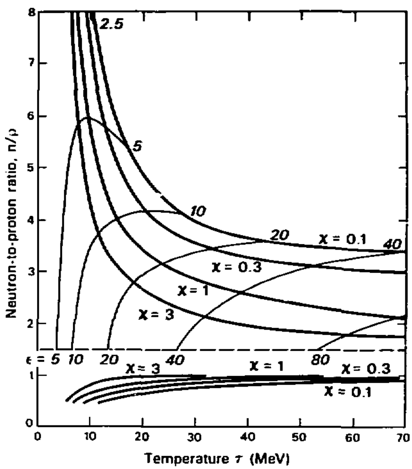

Fig. 2. (XBL 803-534)

with I, since all light composite fragments have $N \simeq Z$.

Although our model has no dynamical assumptions, it can nevertheless correlate and predict many experimental observables in terms of only 3 parameters (ϵ, I, and χ), which can be determined from experiment. Any dynamical mechanisms which may be invoked to explain intermediate energy collisions can therefore be judged against these "background" predictions.

Footnotes

*Condensed from LBL-10959, Nucl. Phys. A (in press)

†W. K. Kellogg Radiation Laboratory, Cal Tech, Pasadena, CA 91125; Alfred P. Sloan Foundation Fellow, supported in part by the NSF.

FINITE PARTICLE NUMBER EFFECTS IN HIGH-ENERGY NUCLEAR COLLISIONS: IMPLICATIONS ON PION-SPECTRA*

Steffen Bohrmann and Jörn Knoll†

Recently high-energy nuclear collisions[1] have been studied by means of a statistical model.[2] It describes the observed cross sections in terms of contributions arising from dynamically independent groups of interacting nucleons, ascribing highest entropy distributions in line with the conservation laws to each group. The model has particularly elucidated the role of finite particle number effects in inclusive proton spectra.[3] In this work the model has been extended to include the production of pions. As in Fermi's statistical theory[4] the rate of pions produced out of a group of nucleons follows from the assumptions of complete equilibrium in all degrees of freedom in the system which is assumed to be confined to a given volume. Consequently and analogously to other thermo-chemical models[5] a density parameter governs the production rates. This is the only free parameter of the model. It has been chosen such as to reproduce the observed pion multiplicities at 800 MeV/A beam energy.

As a consequence of the finite number of particles involved in a heavy-ion reaction the asymptotic slopes of the one-particle spectra (protons or pions) turn out to be steeper than those calculated with models using bulk-limit distributions[5] and are in fair agreement with experimental data. Especially the dependence of the spectra on the mass of the colliding system can be explained as an effect of the respective difference in the numbers of particles involved. Furthermore, some of the scaling features of inclusive pion spectra[6] can be reproduced and seem to reflect the dominance of kinematical effects in these cases.[7] The statistical model in general proves to be superior to other models based on the equlibrium assumption in all cases where kinemetical limits are being approached, e.g. for pion production at forward angles which was recently measured up to the kinematical limit.[8]

While the pion production rates still remain to be understood, the inclusive proton- and pion-spectra reflect a great deal of features typical for equilibrized but finite systems.

Footnotes and References

*Condensed from LBL-10970. This work was supported in part by the Bundesminsterium für Forschung and Technologie, West Germany.

†Max Planck Institut für Kernphysik and Institut für Theoretische Physik der Universität, 6900 Heidelberg, West Germany.

1. S. Nagamiya et al., Phys. Lett. 81B (1979) 147 and I. Tanihata et al., Phys. Lett. 87B (1979) 349.

2. J. Knoll, Phys. Rev. C 20 (1979) 773.

3. J. Knoll, Nucl. Phys. A. 343 (1980) 511.

4. E. Fermi, Progr. of Theor. Phys. 5 (1950) 570.

5. J. I. Kapusta, Phys. Rev. C 16 (1977) 1493 and J. Gosset, J. I. Kapusta, G. D. Westfall, Phys. Rev. C 18 (1978) 844.

6. J. Papp et al., Phys. Rev. Lett. 34 (1975) 601.

7. R. H. Landau and M. Gyulassy, Phys. Rev. C 19 (1979) 149.

8. E. Aslanides et al., Phys. Rev. Lett. 43 (1979) 1466.

CLUSTER ANALYSIS OF THE INTRA-NUCLEAR CASCADE*

J. Cugnon,† J. Knoll,‡ and J. Randrup

We attempt to disentangle the apparently complicated results of an intra-nuclear cascade calculation (INC)[1] of relativisitic nuclear reactions by analyzing the cluster structure of each cascade event. The basic building bricks, the clusters, comprise those nucleons that are in intimate interaction contact. In this way we achieve a formulation of the collision problem close to those used in simplified approaches, facilitating a direct comparison with simple physical ideas.

We distinguish between gentle and violent interactions by means of a cut-off in momentum transfer, the violent collisions defining the clusters. The cut-off chosen of the order of the Fermi momentum was found to be of no dynamical relevance for each cluster's spectrum.

The main results are the following. The resulting nucleon momentum distributions pertaining to a specific cluster size do not depend on the colliding nuclei (universality). The spectral shapes in particular are found in close agreement with those calculated with the simple rows-on-rows model[2] with the limiting behavior for cluster sizes beyond eight nucleons. The largest discrepancy with simplified models appears in the size of the clusters formed. While straight-line concepts in the rows-on-rows model lead to fairly small clusters, the intranuclear cascade links many nucleons into the same cluster. The main reason for these large sizes produced in the INC was traced to the finite value of the N N interaction radius which leads to an increase in transverse communication as the size of the cluster grows. A structural analysis of these large clusters would probably reveal them as built up of several subclusters linked by only one or two interactions. In such a case the subclusters may more directly reflect the dynamical information on the process.

We see the present analysis as an aid to improve the INS. In particluar, it may reduce its complexity and hence increase the practical utility of the INS for relatively rare events such as high momentum components or multiparticle coincidences.

Footnotes and References

*Condensed from LBL-11301, Nucl. Phys. A (in press)

†Kellogg Radiation Laboratory, Caltech, Pasadena, CA 91125; on leave from University of Liege, Belgium.

‡Heisenberg fellow; from Sept. 1, 1980: Gesellschaft fur Schwerionenforschung, GSI, D-6100 Darmstadt, West Germany.

1. a) J. Cugnon, Cal Tech preprint MAP-9, Jan. 1980. b) Cugnon, T. Mizutani, J. Van Der Meullen, Cal Tech preprint MAP-10, Feb. 1980.

2. a) J. Hüfner, J. Knoll, Nucl. Phys. A290, 460 (1977). b) J. Knoll, J. Randrup, Nucl. Phys. A324, 445 (1979).

K^+ PRODUCTION IN RELATIVISTIC NUCLEAR COLLISIONS*

Che Ming Ko and Jørgen Randrup

A current Bevalac experiment measures the spectrum of charged kaons produced in relativistic nuclear collisions.[1] Although the partial cross section for kaon production is relatively small, such an experiment is of great interest because of the important new information it may provide about the nuclear collision dynamics. Positive kaons have a relatively small interaction cross section (~ 9 mb) with nucleons so that they are more likely to escape unperturbed once created. Since the threshold (~ 1.6 GeV) for their production is relatively high on the scale of presently available beam energies, the kaons are predominately produced before the initial kinetic energy is substantially degraded. They are therefore expected to be better suited as messengers of the primary, violent stage of the collision which might otherwise remain quite elusive.

Our study is based on a conventional multiple-collision picture of the nuclear reactions. In particular, we employ the approximate linear-cascade model developed by Hüfner and Knoll[2] and later extended by Knoll and Randrup.[3] This is probably quite adequate for our present exploratory study. Two baryonic states were included: the nucleon N(940) and the delta resonance $\Delta(1232)$. The baryonic cascade then involves the process $NN \rightleftharpoons N\Delta \rightleftharpoons \Delta\Delta$. Due to the Lorentz dilation factor, which is around 3, the deltas are not likely to decay until after the cascade is completed. It is therefore important to note that the pions, whether created during the primary cascade or later, are expected to have too little energy to produce any kaons in their further interactions with the nucleons. We therefore expect that the dominant source of kaons is the primary baryon-baryon collisions. Since the partial production cross section for kaons is so small we may safely employ a perturbative approach in which the dynamical feed-back effect of the kaon production on the further collision process is ignored.

The quantities needed in order to generate the kaon spectra in a nucleus-nucleus collision are the kaon spectra associated with the various types of elementary baryon-baryon collisions. Experimentally, the available information is limited to proton induced reactions at few energies. From both the available experimental information and the theoretical extrapolations based on the one-pion exchange model, we arrive at the following conclusions for the kaon spectra from the baryon-baryon collisions: 1) the angular distribution is isotropic in the center-of-mass system. 2) the momentum distribution can be parameterized by $d\sigma/dp \approx x^2(1-x)$ where $x = p/p_{max}$ is the kaon momentum measured in units of its maximum value. 3) The energy dependence of the isospin-averaged total kaon production cross section is approximately given by $\bar{\sigma}_{NN} \approx 1.33\ \bar{\sigma}_{N\Delta} \approx 2\ \bar{\sigma}_{\Delta\Delta} \approx 144\ \mu b\ p_{max}/m_K c$, where m_K is the mass of kaon.

We have calculated the differential kaon cross sections for the experimental cases of p, d, and Ne projectiles on targets ranging from NaF to Pb. The calculation yields kaon distribution which are nearly isotropic and centered near the mid-rapidity $y_c = y_{beam}/2 = 0.92$. The total inclusive kaon cross section is predicted to approximately scale as the product of the nuclear masses AB.

The predictions obtained from the multiple-collision model are significantly different from what would result in a thermal model. Such a model would predict that kaons are emitted from a source which moves with half the beam rapidity for symmetric systems but with a smaller rapidity for a light projectile incident on a heavy target. Also, the scaling behavior predicted in the multiple-collision model is not expected to hold in the thermal model. The kaons should therefore be very well suited for discriminating between the cascade-type picture and the thermal picture.

The initial Fermi motion of the nucleus is instrumental in broadening the kaon distribution over a wide domain in rapidity space and thus leads to kaons at considerably larger laboratory angles than that could result in a proton-proton collision. It is thus conceivable that the kaons may be used to probe the intrinsic momentum distribution of the nucleons; this might be a particularly powerful method at beam energies below the nucleon-nucleon kaon production threshold where the kaons would be produced exclusively due to the Fermi motion.

Footnote and References

*Condensed from LBL-10530; Nucl. Phys. A 343 (1980) 519.

1. S. Schnetzer et al., Bevalac Experiment No. 471H

2. J. Hüfner and J. Knoll, Nucl. Phys. A270 (1977) 460

3. J. Knoll and J. Randrup, Nucl. Phys. A324 (1979) 445

A MODEL FOR PION ABSORPTION IN NUCLEI*

Che Ming Ko and Steffen Bohrmann†

Recently, detailed experimental studies of the pion absorption process in nuclei for pion energies in the region of the Δ resonance have been carried out.[1] The general features of these data suggest that the energy and the momentum brought in by the pion are equally shared among several nucleons the number of which ranges between 3 and 6 depending on the target mass. The inclusive spectra of these nucleons are structureless and monotonically decreasing with increasing nucleon energy. In analogy to the statistical model of high-energy nuclear reactions[2] we suggest that the nucleons sharing the pion-energy and momentum are these lined up in a "row" extending in beam direction at the impact parameter of the pion. Energy and momentum are completely randomized among these nucleons, i.e., their available phase space is occupied uniformly. The resulting proton spectra agree very well with the measured data (see Fig. 1; data are from Ref. 1).

The mean number of nucleons in a row is governed by the cross section given to this row. It can be adjusted to give the observed value for a fixed target. This same value of the cross section (40 mb) reproduces the observed mean number of participating nucleons for any target (Fig. 2 (c)). Taking into account the slightly varying probability for absorbing a pion with the number of nucleons in a row gives almost exactly the observed integrated proton yields except for the lightest target, which may be due to completely neglecting the two-nucleon-absorption process in our model (Fig. 2 (a)). Finally, the ratio of the integrated proton yield following the absorption of a π^+ to the yield after the absorption of a π^- is as well reproduced (Fig. 2 (b)).

The success of our simple model supports the assumption that energy and momentum of the incoming pion are equally shared among the nucleons in a row. The model, however, does not deal with the dynamical details of the process, which may be very involved because of the large number of participating particles. Further research perhaps may clarify this question.

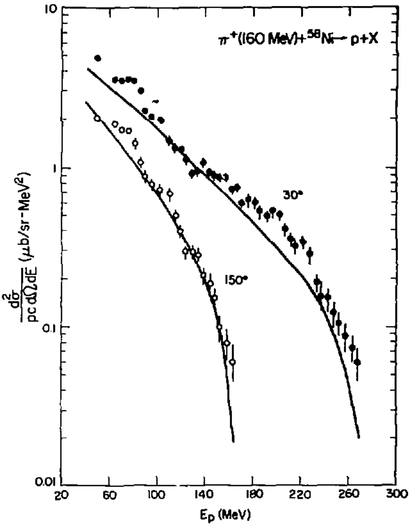

Fig. 1. Inclusive proton spectra after pion absorption. Data are from Ref. 1. (XBL 806-1324)

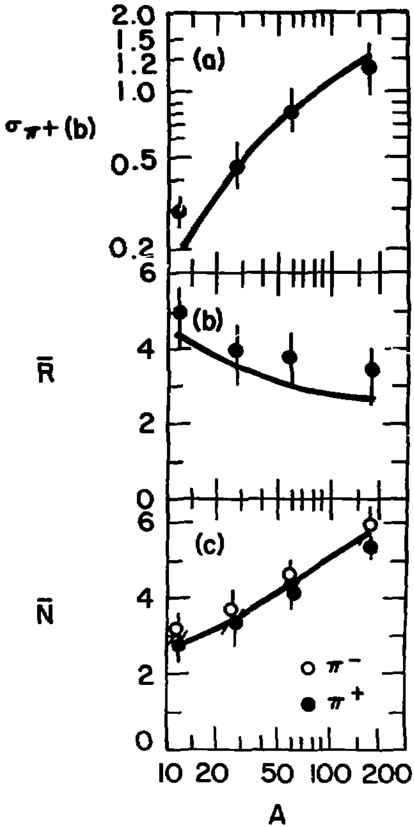

Fig. 2. Data are from Ref. 1: (a) Total proton yield after the absorption of a π^+ on various targets (^{12}C, ^{27}Al, ^{58}Ni, ^{181}Ta). (b) Ratio of the proton yield after π^+-absorption to the yield after π^--absorption as a function of the target mass. (c) Mean number of nucleons sharing the energy and momentum of the pion as a function of the target mass. (XBL 806-1323)

Footnotes and References

*Condensed from LBL-11041.

†On leave of absence from Institut für Theoretische Physik der Universität, 6900 Heidelberg, West Germany. Work supported in part by Bundesministerium für Forschung und Technologie, West Germany.

1. R. D. McKeown, S. J. Sanders, J. P. Schiffer, H. E. Jackson, M. Paul, J. R. Specht, E. J. Stephenson, R. P. Redwine, and R. E. Segel, Phys. Rev. Lett. 44, 1033 (1980).

2. J. Knoll, Phys. Rev. C20, 773 (1979).

RELATIVISTIC NUCLEAR COLLISIONS: THEORY*

Miklos Gyulassy

Recent theoretical developments in relativistic (0.5-2.0 GeV/nucleon) nuclear collisions are reviewed. The statistical model, hydrodynamic model, classical equation of motion calculations, billiard ball dynamics, and intranuclear cascade models are discussed in detail.

We have learned a tremendous amount about the basic reaction mechanism. The roles of geometry, phase space, and kinematics have been shown to dominate many of the gross features of the data. However, initial state interactions (Fermi motion) and final state interactions (composite production, Coulomb fields, and nuclear shadowing) often lead to complicated distortions of the particle spectra. We have learned that finite mean free path effects cannot be ignored in any reaction studied so far. The spectra show clear non-equilibrium effects.

The significant non-equilibrium component even in near central Ne + U collisions virtually rules out a 1-fluid hydrodynamic description of such data. Since hydrodynamics is the only direct link between data and the nuclear equation of state $W(\rho,T)$, the prospects of determining W from data do not seem promising. The problem is not that we are looking at the wrong observable (central triggered proton inclusive cross sections), but rather that hydrodynamics does not take into account finite mean free paths and binding that seem essential from the data.

On the other hand, we saw that the high momentum components of inclusive spectra are very insensitive to dynamical details of the compression phase. Thus, we cannot hope to learn about high density nuclear matter from such data either.

It must be emphasized though that we do not have a complete understanding of the reaction mechanism. Many detailed features of the data such as the π^+ bump at $y = y_{cm}$, $p_\perp \approx 0.5$ m_π are only partially understood. The low energy $E < 50$ MeV, Ne + U→ p data are also not well understood. In these cases, we still have to sort out the complex interplay of the many elements of the reaction mechanism.

Footnote

*Condensed from LBL-11040.

TEST OF SQUARE LAW FOR DEUTERON FORMATION IN RELATIVISTIC NUCLEAR COLLISIONS*

C. C. Noack,† M. Gyulassy, and S. K. Kauffmann

One of the striking features of nuclear collisions in the 0.2-2.0 GeV/nucleon range is the copious production of light composite fragments. The first attempt at understanding light composite production was in terms of the coalescence model of Ref. 1. Since the probability that a nucleon is found in a coalescence volume is proportional to the invariant proton inclusive cross section: $\sigma_1(p) = \omega d\sigma_1^3/dp_1^3$, a simple power law is predicted for the inclusive cross section of a fragment with A nucleons,

$$\sigma_A(p) \equiv \omega_A \frac{d^3\sigma_A}{d^3p_A} \propto (\sigma_1(p))^A \quad , \qquad (1)$$

where ω_A and p_A are the energy-momentum per nucleon of fragment A. For deuterons, Eq. (1) just states that the deutron yield should be proportional to the square of the proton yield.

Since extensive new data for a large variety of projectile and target combinations at various energies have become available,[2] it is now possible to test the square law over a much broader domain of reactions. These data[2] test the square law in high density regions of momentum space, where in terms of the coalescence model,[1] the probability of finding two or more nucleons in a coalescence volume approaches unity.

To generalize the coalescence model to make it more appropriate for the high density region, we suggest the modification

$$\sigma_A(p) \propto \sigma_1(p)\ (\sigma_{ch}(p))^{A-1}, \qquad (2)$$

where $\sigma_{ch}(p)$ is the "primordial" proton distribution, which we obtain by summary over proton, deuteron, triton, etc., data.

We have calculated a certain type of "best fit" to the proportionality constants in Eqs. 1 and 2 for the special case of deuterons

$$R := \sigma_d(\underset{\sim}{p})/\sigma_1^2(\underset{\sim}{p}) \quad (3)$$

$$R' := \sigma_d(p)/(\sigma_T(\underset{\sim}{p})\sigma_{ch}(\underset{\sim}{p})) \quad (4)$$

with R and R' forced to be independent of $\underset{\sim}{p}$ ("best" constants) but not of the type of collision partners or beam energy.

The straight lines in Fig. 1(a) correspond to a proton square law, (Eq. 1). The straight lines in Fig. 1(b) correspond to the generalized square law of Eq. 2. On this log-log plot we see remarkable adherence to both laws within a factor of 2. This form of plotting σ_p^2 vs σ_d emphasizes that the approximate law works within a factor of 2 over three or four decades of cross section!

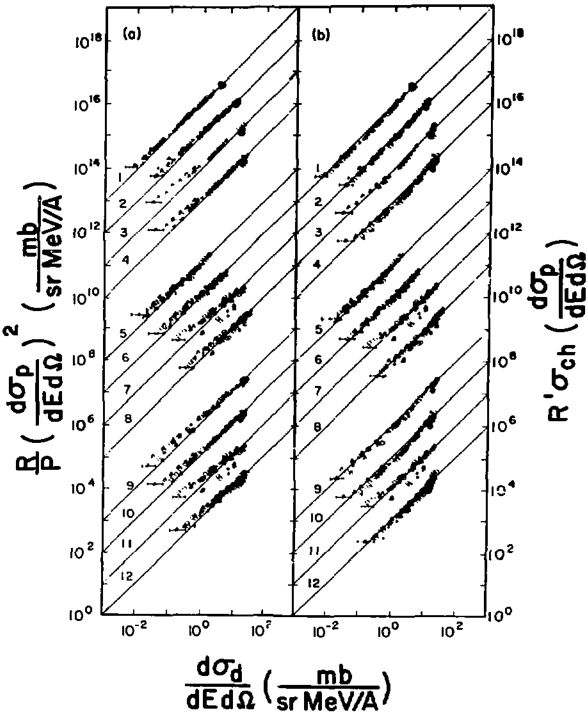

Fig. 1. (a) Plot of $R(\underset{\sim}{p})\sigma_p^2$ vs $(\underset{\sim}{p})\sigma$. Typical experimental error bars are indicated. The data have been shifted by factors of 10^n to separate the reactions. The straight lines correspond to the "square law." (b) Plot of $(\underset{\sim}{p})R'\sigma_p\sigma_{ch}$ vs $\underset{\sim}{p}\ \sigma_d$ for the same reactions as in (a). Straight lines correspond to the generalized square law of Eq. 2.
(XBL 804-9221)

Footnotes and References

*Condensed from LBL-11053.

†Universitat Bremen, 280D Bremen 33, West Germany.

1. H. H. Gutbrod, A. Sandoval, P. J. Johansen, A. M. Poskanzer, J. Gosset, W. G. Meyer, G. D. Westfall, and R. Stock, Phys. Rev. Lett. 37 (1976) 667.

2. A. Sandoval, H. H. Gutbrod, W. G. Meyer, A. M. Poskanzer, R. Stock, J. Gosset, J. C. Jourdain, C. H. King, Ch. Lukner, Nguyen Van Sen, G. D. Westfall, and K. L. Wolf, Phys. Rev. C 21, (1980) 132.

COULOMB EFFECTS IN RELATIVISTIC NUCLEAR COLLISIONS*

M. Gyulassy and S. K. Kauffmann

Recent data on nuclear collisions in the 1 GeV/nucleon range have revealed unusual angular and momentum magnitude distributions[1] of single particle fragments such as $\pi^{\pm}$, p, n. While it is tempting to attribute those unusual features to nuclear compression effects, it has become increasingly clear[2] that Coulomb final state interactions in nuclear collisions are complex and have to be understood before any conclusions on the role of nuclear compressions can be reached. We have derived simple analytical formulas to calculate Coulomb distortions, and we apply them to the analysis of recent data.

We aim to supplement and extend previous works by deriving analytical formulas that clearly reveal the structure and form of Coulomb distortions in nuclear collisions. Our basic approach is to use first order relativistic perturbation theory which readily yields an expression for Coulomb distortions for an arbitrary space-time dependent charge current. In particular, effects due to finite nuclear sizes, expanding fireballs and multiple charged fragments, are easily calculated. To overcome some of the limitations of perturbation theory, we recast our results in a non-perturbative (Gamow factor) form.

We found it noteworthy that a simple classical calculation already reveals the essential qualitative features of Coulomb final state interactions. It shows the single particle inclusive cross sections for $\pm$ charged particles to be of the form

$$\sigma_{\mp}(\underset{\sim}{k}) = \sigma_0(\underset{\sim}{k} \mp \delta \underset{\sim}{p}(\underset{\sim}{k}))\, D(\underset{\sim}{k}), \qquad (1)$$

where $\sigma_0(k)$ is the corresponding single particle neutral inclusive cross section. $D(\underset{\sim}{k})$ is a Coulomb phase space distortion factor, which tends to suppress positively charged particles relative to neutrals, and is important for momenta $\underset{\sim}{k}$ close to those of any surviving nuclear fragments having sizeable charges,[1] while $\delta p(k)$ is a Coulomb impulse that acts to enhance positively charged particles relative to neutrals, and is important for momenta $\underset{\sim}{k}$ where $\sigma_0(k)$ is falling steeply with increasing $|\underset{\sim}{k}|$.[2] We have kept the form of Eq. 1, but, using perturbation theory, the Gamow factors, and thermal averages as guides, we have modified the classical analytical results for $D(\underset{\sim}{k})$ and $\delta p(\underset{\sim}{k})$ to approximately incorporate relativity, quantum effects, and the thermal expansion of the nuclear fireball. For our first calculations with Eq. 1, we have chosen to keep the formulas entirely analytical by using the fireball model for $\sigma_0(\underset{\sim}{k})$.

For the π^-/π^+ at $\theta_{lab} = 0$, the Coulomb phase space distortion factor $D(k)$ produces sharp peaks at pion rapidities equal to those of the projectile and target spectators, as shown in Fig. 1. Note that the projectile and target spectators differ a bit in rapidity from the beam and target, due to the friction of the collision. This friction also slightly heats the spectators, preventing infinitely high Coulomb peaks. In Fig. 1(a) the data apparently reveal the projectile spectator Coulomb peak.[1] In Fig. 1(b), the data show the π^-/π^+ ratio going perceptibility below unity at high pion rapidities--apparently confirming the Coulomb impulse effect.

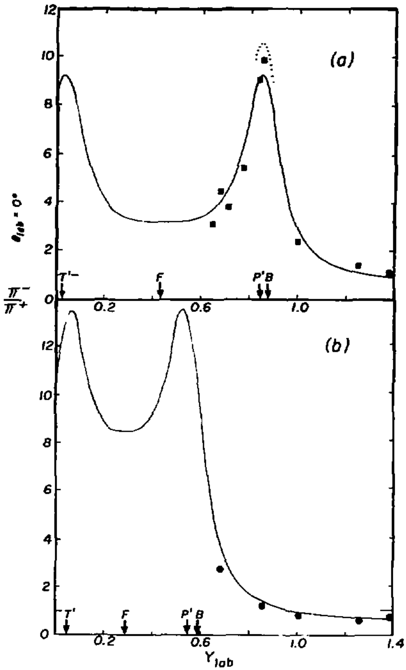

Fig. 1. The π^-/π^+ ratio at $\theta_{lab} = 0°$ as a function of rapidity y_{lab}. The reaction[1] is Ne + NaF $\rightarrow \pi^{\pm}$ at (a) 383 MeV/nucleon (square points) and (b) 164 MeV/nucleons (solid dots). Solid curve shows Coulomb distorted fireball model results. Dotted segment in (a) shows sensitivity of results to 20% reduction of initial radii. (XBL 802-8094)

We have obtained similar results to Ref. 2 on pion focusing for π^+ yields at $\theta_{c.m.} = 90°$ using our analytic formulas. The role of Coulomb effects on the n/p ratio were also calculated.

Footnote and References

*Condensed from LBL-10279.

1. W. Benenson et. al., Phys. Rev. Lett. 43 (1979) 683; and Errata, Phys. Rev. Lett. 44 (1980) 54.

2. K. G. Libbrecht and S. E. Koonin, Phys. Rev. Lett. 43 (1979) 1581.

QUARK CONFINEMENT IN A CYCLIC SYMMETRIC FIELD THEORY MODEL

Herbert M. Fluck

When the production of a single quark is impossible due to confinement, one thinks about studying quark matter that might be simpler. However producing quark matter in equilibrium will be experimentally even harder than producing nuclear fusion at a steady rate. Therefore the curiosity to study the properties of quark matter has to wait for some time. So we study the region in-between, but as usual the middle is more difficult than the extremes and so the investigation of the structure of the nucleons and their resonances, as well as the interaction between them -- from the point of view of quarks -- is faced with the formidable complexity of QCD (SU(3)) calculations. For example the field equations describing the proton in terms of three quarks and one gluon field contain as many degrees of freedom as the field equations for a carbon nucleus made of 13 nucleons and a pion and ρ-meson field.

I seek an alternative theory of strong interactions that will have all essential properties of QCD and be simpler. This is a Z(3)-symmetric field theory of scalar particles and fermions. Z(3) is a discrete abelian group, that takes a special place between continuous abelian groups like U(1) and nonabelian groups like SU(3). The model is defined in physical Minkowsky space but the results presented are obtained in the 1 + 1 dimension space-time continuum only, where closed form solutions are possible.

The action for the model is:

$$S(\psi_1,\psi_2,\phi_1,\phi_2) = \int dt dx \, [1/2|\partial_\mu\phi_1|^2 + 1/2|\partial_\mu\phi_2|^2 - \lambda(\phi_1^2+\phi_2^2)^2 + \nu(\phi_1^3 - 3\phi_1\phi_2^2) + \mu(\phi_1^2+\phi_2^2) + \gamma + i\bar\psi_1\gamma_\mu\overleftrightarrow{\partial}_\mu\psi_1 - m\bar\psi_1\psi_1 + i\bar\psi_2\gamma_\mu\overleftrightarrow{\partial}_\mu\psi_2 - m\bar\psi_2\psi_2 + g(\bar\psi_1\psi_1 - \bar\psi_2\psi_2)\phi_1 - g(\bar\psi_1\psi_2 + \bar\psi_2\psi_1)\phi_2] \quad (1)$$

First I find soliton solutions that tunnel between the three vacuum states of the scalar field system.[1] Then the wave equations of the fermions coupled to the solitons have a solution that is equivalent in effect to confined individual fields in a color singlet state ($E_F = 1/2g\phi_V$):[2]

$$\psi_1(t,x) = N \begin{pmatrix} 1 \\ \exp(-i5\pi/6) \end{pmatrix} \exp(-iE_F t - H(x)) \quad (2)$$

$$\psi_2(t,x) = i\sigma_3\psi_1(t,x) \quad ,$$

where σ_3 is the third Pauli matrix and H(x) a positive definite function:

$$H(x) = g(2\lambda)^{-1/2} \ln[\cosh((3\lambda/2)^{1/2}\phi_V(x - x_0))]. \quad (3)$$

An example of the energy spectrum of the model is shown in Fig. 2.

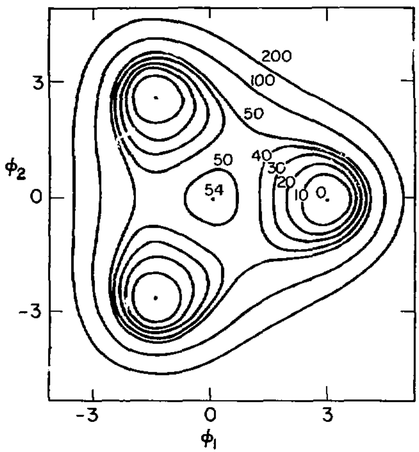

Fig. 1. Equipotential lines for the self-interaction potential of the scalar fields. The three minima vacuum states are clearly seen.

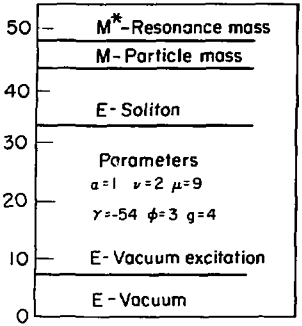

Fig. 2. Energy spectrum (arbitrary units) for the same set of coupling constants that give Fig. 1.

References

1. H. M. Ruck, Nucl. Phys. B167, 320 (1980).

2. H. M. Ruck, Proceedings of the IX International Colloquium on Group Theoretical Methods in Physics, Cocoyoc, Mexico, 1980, Springer Verlag, Oct.-Nov. 1980.

HYPER-STRANGE HADRONIC MATTER

Norman K. Glendenning

In a recent letter, Chin and Kerman[1] have suggested the possible production of long-lived hyper-strange multi-quark object in high-energy nuclear collisions. They studied the stability of quark matter as a function of the fraction of strange quarks. Based on the currently popular values of the MIT bag constants they found that the energy per baryon of infinite matter becomes a minimum for a ratio of strangeness to baryon number of approximately 2. This minimum lies above the energy of free nucleons so that an object made of this matter is only metastable, its decay still characterized by the weak decay lifetime of strange baryons.

In this note, we investigate whether a hyperstrange hadronic object also possess a metastable state and would have a lower or higher energy than the corresponding quark object. We do this by means of a straightforward extension of relativistic field theory of matter solved in the mean field approximation.[2] In this theory the nucleons are coupled to scalar and vector mesons. The meson fields are approximated by their mean values, which are related to the scalar and baryon densities $\bar{\psi}\psi$ and $\psi^{+}\psi$. The nucleon field then obeys a Dirac-like equation in which the nucleon mass is shifted by the scalar field and the energy eigenvalues by the vector field. The ratio of coupling constants to masses of the mesons are two parameters which are adjusted to reproduce the saturation properties of infinite nuclear matter. To this system we now add the $\Lambda(1116)$, $\Sigma(1193)$ and $\Xi(1318)$ fields, each of which is coupled to the mesons. The strength of this coupling is not well established. Universal coupling is somewhat suggested for the coupling of these octet baryons to the mesons. On the other hand we can look to hyper-nuclei for evidence. A coupling of the Λ to the fields that is 1/3 less than for the nucleon in light nuclei produces the correct binding energy. Therefore we consider two possibilities, 1) universal coupling, or 2) $g^{\Lambda,\Sigma,\Xi} = 1/3g^{N}$ for both the scalar and vector coupling.

In Fig. 1 the binding energy per baryon, $(\varepsilon/\rho - m_N)$, of the two phases, quark and hadron, are compared as a function of strangness fraction. For the hadron phase, results for the two hyperon coupling constants are shown.

We conclude that no metastable state exists for hyper-strange objects in the hadronic phase in contrast to the quark phase.

One reservation can be mentioned. Both estimates of energy are extrapolations in different models of nature. The parameters of the bag model are optimized with respect to a few hadron masses and have no known connection to larger objects. The parameters of the hadronic matter model are determined by properties of nuclear matter and Λ-nuclei, and extrapolated away from these conditions.

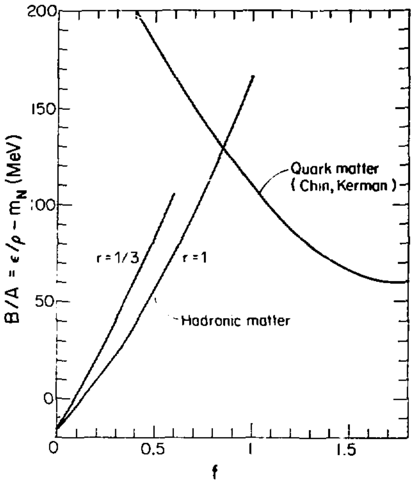

Fig. 1. Binding of hyper-strange matter in the hadronic and quark phase are compared as a function of strangeness fraction per baryon. In the hadronic phase, results for two hyperon coupling constants are shown. (XBL 808-1663)

References

1. S. A. Chin and A. K. Kerman, Phys. Rev. Letters 43 (1979) 1292.

2. a) M. H. Johnson and E. Teller, Phys. Rev. 98 (1955) 783, b) H. P. Duerr, Phys. Rev. 103 (1956) 369, c) J. D. Walecka, Ann Phys. 83 (1974) 491, d) S. A. Chin, Ann Phys. 108 (1977) 301.

PION CONDENSATION IN A RELATIVISTIC FIELD THEORY CONSISTENT WITH BULK PROPERTIES OF NUCLEAR MATTER*

B. Banerjee,† N. K. Glendenning, and M. Gyulassy

Pion condensation has not previously been investigated in a theory that accounts for the known bulk properties of nuclear matter, its saturation energy and density and compressibility. We have formulated and solved self-consistently, in the mean field approximation, a relativistic field theory that possesses a condensate solution and reproduces the correct bulk properties of nuclear matter.

Up to moderate density, the internal quark structure of the nucleons can be ignored. In this case the nuclear forces can be represented by the exchange of mesons in the various spin, isospin channels. In order of these quantum numbers these meson fields are

$$\sigma(J = 0^+, I = 0), \quad \omega_\mu(1^-, 0),$$

$$\pi(0^-, 1), \quad \rho_\mu(1^-, 1) \ldots$$

and they are Yukawa coupled to the 8-component nucleon field through the interaction Lagrangian

$$\mathcal{L}_{int} = g_\sigma \sigma \bar{\psi}\psi - g_\omega \omega^\mu \bar{\psi}\gamma_\mu\psi - g_\pi(\partial^\mu \pi) \cdot (\bar{\psi}\gamma_5\gamma_\mu \tau\psi)$$

$$- g_\rho \rho^\mu \cdot (1/2\bar{\psi}\gamma_\mu \underset{\sim}{\tau}\psi + \underset{\sim}{\pi} \times \partial_\mu \pi) \ldots .$$

We show how to incorporate the effects of short-range correlations, the Δ-resonance, and finite-size form factors into a renormalized coupling constant, g_π, by establishing a relationship with the propagator approach at the condensation theshold. The coupling is essentially independent of density over the range considered. The theory is solved in its relativistically covariant form of a general class of space-time dependent pion condensates. By making a local isospin gauge transformation on the nucleon fields, the solution to the Dirac equation can be obtained algebraically. Two cases are studied, corresponding to parameters of the Lagrangian, which in both cases yield *identical saturation properties and differ only* in their softness at higher density. This latitude was introduced to represent our ignorance of the equation of state away from the saturation point. Only one of these possessed a condensate solution for pion-nucleon coupling constant at the value of the renormalized coupling. This was the case where the equation of state was softer at higher density. Even in this case the condensate energy was very small, not exceeding 3 MeV for density up to $3\rho_0$ (see Fig. 1). This is in sharp contrast with other studies based on the chiral σ-model.[1] Since the normal state of the σ-model does not possess the saturation properties of nuclear matter,[2] we believe that our estimate is more reliable. Thus self-consistency and compatibility with bulk nuclear properties are strong constraints on the existence, persistence and magnitude of the condensate phase. Despite the small condensate energy in our theory, the corresponding amplitude of the spin-isospin density is very significant, being about $\rho/2$, as seen in Fig. 2. We conclude that a pion condensate is

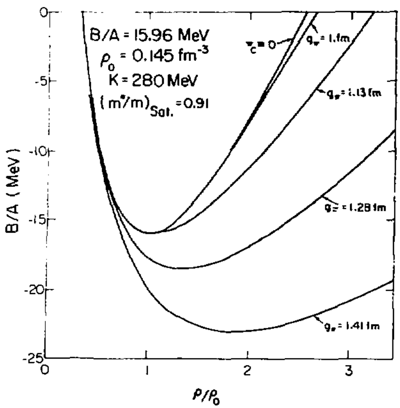

Fig. 1. Showing the "normal" state labeled $\pi_C = 0$ and pion condensed states labeled with g_π. The vacuum value of g_π is 1.40 fm, but the renormalized value is 1.0 fm, for which condensate energy is very small.

(XBL 805-837)

compatible with the known bulk properties of nuclear matter, but that its contribution to the energy is very small although there may be rather large amplitude spin-isospin waves.

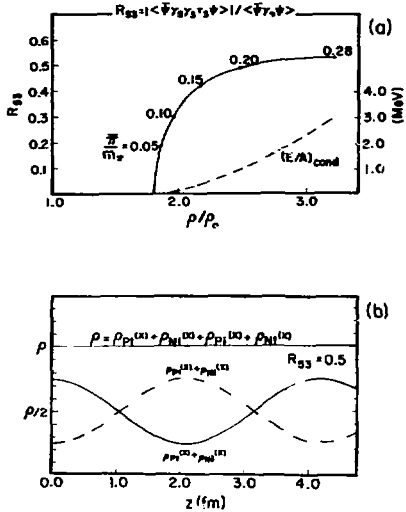

Fig. 2. In (a) the amplitude R_{53} of the spin-isospin density oscillations in units of the baryon density. Also indicated are values of the condensate field and the condensate energy. Part (b) illustrates magnitude of the spin-isospin oscillations for R_{53} = 0.5 as a function of coordinate parallel to condensate momentum $\underset{\sim}{k}$. p↑ means proton with spin up.

Footnotes and References

*Condensed from LBL-10979.

†Permanent address: Tata Insitute of Fundamental Research, Bombay, India.

1. H. J. Perner, K. Yazaki, P. Bouche, M. Rho, Nucl. Phys. A329 (1979) 491.

2. A. K. Kerman and L. D. Miller, Proc. 2nd High-Energy Heavy-Ion Summer Study, LBL-3875 (1974) p. 73.

PION CONE .NSATION AT FINITE TEMPERATURE

N. K. Glendenning and A. Lumbroso*

In a related work, pion condensation in zero temperature matter was investigated in a relativistic field theory.[1] Unlike earlier work on the subject, the theory was constrained to possess the known saturation properties of nuclear matter. Here we investigate matter in the same theory at finite temperature. Of course finite temperatures are interesting because pion condensation is believed to be an important mechanism involved in the cooling of neutron stars. Morever, nuclear collisions at high energy, if they produce dense matter, certainly produce it at finite temperature.

The meson fields considered are the chargeless scalar and vector mesons σ and ω and the pseudoscalar isovector pion field. The first two are Yukawa coupled to the 8-component nucleon field, and the pions are vector coupled to the axial vector isospin current of the nucleons. The field equations are solved for the mean values of the fields, evaluated for finite temperature medium.

Our results are surprising. Contrary to common expectation, the pion condensed state is not quenched as the temperature is increased but persists to as high a temperature as makes sense to consider in this model of nature. (The limit of validity is reached when higher baryon resonances are appreciably populated,[2] or when matter undergoes a phase transition to quark matter.[3])

In Fig. 1 we show the normal and pion condensed equations of state as a function of density for three temperatures. It is true that the critical condensate density increases with temperature (dotted line). However, the equation of state is dramatically softened by the condensate as the temperature is increased. Therefore, the hydrodynamical flow of hot dense matter will be strongly influenced by the transition to a condensate phase. Moreover, a subsequent phase transition to quark matter may be facilitated by this softening of the equation of state because, for a given energy and density, the temperature of the matter is considerably higher in the condensed than in the normal state.

These results are somewhat encouraging as concerns the d .ection of a condensed phase in relativistic nuclear collisions, although the lifetime of the high-density region is much shorter than the disassembly time of the collision complex, which fact may permit final state interactions to obscure the effects of the softened equation of state on the flow.

However, there is another feature with possibly important consequences. As is well known, the pion condensate corresponds to a specific alignment of spin and isospin, an isospin lattice, having an orientation in space, with a wave number $k \approx 1.5\ fm^{-1}$. What has not been noted previously is that in this direction the pressure is greater than in the transverse directions. This suggests that in unbound systems in which a condensate is induced, the matter will disassemble preferentially along the direction of the condensate. To detect such jets in nuclear collisions, coincidence experiments on single events would have to be performed. In bound systems, such as nuclei in the condensed phase with temperatures up to ~ 15 MeV (see figure), or neutron stars, the differential pressure in the condensate direction would induce an elongation until the pressure is counterbalanced by the surface tension.

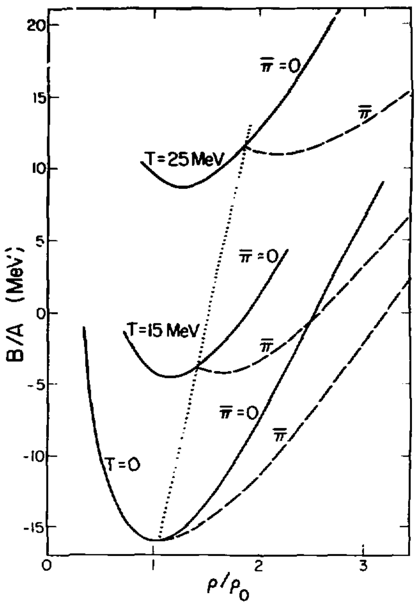

Fig. 1. Binding energy per nucleon as a function of density for two temperatures. The normal state is labeled "$\bar{\pi} = 0$" and the condensed state of $\bar{\pi}$. The renormalized pions nucleon coupling is δ_π = 1.13 fm. The energy of the condensate is minimized for wave number of the spin-isospin density oscillations, k = 1.5 fm^{-1}. The critical density as a function of temperature is indicated by dotted line.
(XBL 808-1448)

Footnote and References

*On leave from CEN, Saclay, France.

1. B. Banerjee, N. K. Glendenning, and M. Gyulassy, LBL-10572 (submitted to Phys. Lett.), LBL-10979 (submitted to Nucl. Phys.).

2. S. I. A. Garpman, N. K. Glendenning and Y. J. Karant, Nucl. Phys. A322 (1979) 382.

3. J. I. Kapusta, Nucl. Phys. B148 (1979) 461 and references therein.

PION CONDENSATION AND INSTABILITIES: CURRENT THEORY AND EXPERIMENT*

Miklos Gyulassy

In this report, current calculations of pion condensation phenomena in symmetric nuclear matter are first reviewed. The comparison between RPA and MFA methods is made with special attention given to the mean field theory of Banerjee, Glendenning and Gyulassy.[1] Those results show that in equilibrium the magnitude of the spin-isospin fluctuations in the pion condensed phase are large and insensitive to the parameters of the theory. Using this and previous[2] results, a novel calculation of the number of coherently radiated pions in nuclear collisions is made. The result of that estimate is that the degree of coherence, which could be observed by pion interferometry,[3] is very small. Subsequent analysis (to be published) taking into account the multiplicity of unstable pion modes k as well as pion absorption yields a larger number of coherently radiated pions per nucleon:

$$\left(\frac{\bar{n}_{\pi^-}}{A}\right)_{\text{coherent}} \approx 0.01\left(\frac{\gamma}{m_\pi}\right)^2 A e^{-A^{1/3}/3} , \qquad (1)$$

where $\gamma/m_\pi \approx 0.1$-0.2 is the average growth rate of the instability[2] and A is the number of participating nucleons. For $A = 100$, $\gamma = 0.2\ m_\pi$ this gives $(\bar{n}_{\pi^-}/A)_{coh} \approx 10^{-2}$ as compared to experimental value[4] of 4×10^{-2} from 1 GeV/nucleon Ar + KCl. The degree of coherence in that case would be $D \approx 1/4$. Such a degree of coherence could be observable[3] if Coulomb final state distortions are properly removed from $\pi^-\pi^-$ correlation data.

Footnote and References

*Condensed from LBL-10883.

1. B. Banerjee, N. K. Glendenning, and M. Gyulassy, LBL-10572 (April 1980).

2. M. Gyulassy, W. Greiner, Ann. Phys. 109 (1977) 485.

3. M. Gyulassy, S. K. Kauffmann, and L. W. Wilson, Phys. Rev. C20 (1979) 2267.

4. A. Sandoval et al., GSI Preprint 80-15, 1980.

BETA STABILITY OF NEUTRON MATTER

J. Boguta

The cooling of neutron stars, especially since the launch of the Einstein X-Ray Observatory, has elicited a number of suggestions explaining the high neutrino luminosity required to understand this rapid cooling. A natural explanation of this, such as the beta decay of neutrons i.e., $n \rightarrow p + e^- + \nu_e$ was ruled out, because of the difficulty in conserving momentum near the corresponding Fermi surfaces.[1] The Fermi-Dirac factor would significantly surpress such a cooling mechanism. Alternative processes such as pion condensation[2] and recently proposed beta decay of the down quark[3] $d \rightarrow u + e^- + \bar{\nu}_e$ have been suggested as a way to rapidly cool the neutron star. The pion condensate model implies that there exists a new collective mode inside neutron stars, while the quark model suggests that the interiors of the neutron stars are composed of quarks. In view of these interesting suggestions to account for the rapid neutron star cooling, another look at the beta decay of ordinary neutrons in a dense neutron start is quite appropriate. Perhaps a conventional explantion of neutron star cooling is still possible.

It is known that one has to pay the price of symmetry energy when separating neutrons from protons. It, together with Coulomb energy, plays an essential role in determining the line of beta stability in nuclei. It stands to reason that it should be considered in studying the proton concentration in beta stable neutron stars. For this purpose we study nuclear matter in a relativistic quantum field theory proposed by Walecka.[4,5]

The actual details of this model are unimportant to support our conclusions, as long as the symmetry energy of ordinary, symmetric (N = Z), nuclear matter is correctly parametrized. Figure 1 shows the proton Fermi momentum in beta equilibrium with neutrons for two values of symmetry energy. In both cases neutron stars can be cooled by beta decay.

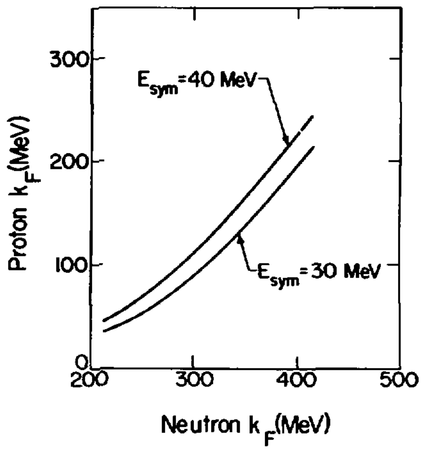

Fig. 1. (XBL 809-1996)

References

1. J. N. Bahcall and R. A. Wolf, Phys. Rev. 140B, 1445 (1965); Phys. Rev. 140B, 1452 (1965).

2. O. Maxwell, G. E. Brown, D. K. Campbell, R. F. Dashen and J. T. Manassah, Astrophys. J. 216, 77 (1977); R. F. Sawyer and A. Soni, Astrophys. J. 216, 73 (1977).

3. N. Iwamoto, Phys. Rev. Lett. 44, 1637 (1980); A. Burrows, Phys. Rev. Lett 44, 1640 (1980).

4. J. D. Walecka, Ann. Phys. 83, 491 (1974).

5. J. Boguta and A. R. Bodmer, Nucl. Phys. A292, 413 (1977).

RELATIVISTIC QUANTUM FIELD THEORY OF FINITE NUCLEI

J. Boguta

A relativistic quantum field theory of nuclear matter was proposed by Walecka,[1] in which the dominant properties of nuclear matter such as saturation and binding energy per particle are accounted for by the presence of scalar (σ) and vector (ω) meson fields. This model, conceptually, is in sharp disagreement with conventional nuclear physics approach, where a static two body force together with a non-relativistic Schrodinger equation form the basis to describe a many body system such as the nucleus. The conventional approach, after 15 years of intense cultivation, has reached such a point of sophistication that only minor modifications are possible.[2] Nonetheless, it still fails to provide a reliable phenomenological tool by which normal nuclear properties can be tied together with higher density and temperature phenomena in nculear matter. Furthermore, the whole approach might be unduly complicated. Ideally, one would like to have a complete description of nuclear physics, where the bulk properties of nuclei are directly related to the forces derived from low energy nucleon-nucleon scattering. It has been emphasized by Serber[3] and Walecka[1] and a long time ago by Teller and Johnson,[4] that nuclear structure can perhaps be easier understood by a much simpler, single body central force. After all, this is the basis of the shell model. It has been shown by Miller[5] that relativistic effects in such a mesonic central field approach are very important, in that they affect the single body kinetic energy. Thus the investigation of alternative nuclear matter models is desirable. In this note we shall explore the phenomenological consequeces of the Walecka model.

Recently Walecka and Serot[6] showed that the field equations of the Walecka model, truncated for numerical convenience, give a fair description of the charge densities in Ca^{40} and Pb^{208}. Serber has shown that a nuclear model based on a mesonic field σ, together with a hard core repulsion given by an excluded volume, gives rather good results for finite nuclei.[3] In this work we show that a careful analysis of the Walecka model, together with a better choice of parameters leads to charge distributions in Ca^{40}, Ca^{48}, Ni^{58}, Zr^{90}, Pb^{208} that are in rather good agreement with experimental data, where it is available, and in an overall agreement with the more refined non-relativistic Hartree-Fock calculations. The quality of our results in the Thomas-Fermi approximation leads us to believe that a relativistic Hartree approximation to the Walecka model will give an excellent description of spherical, closed shell nuclei.

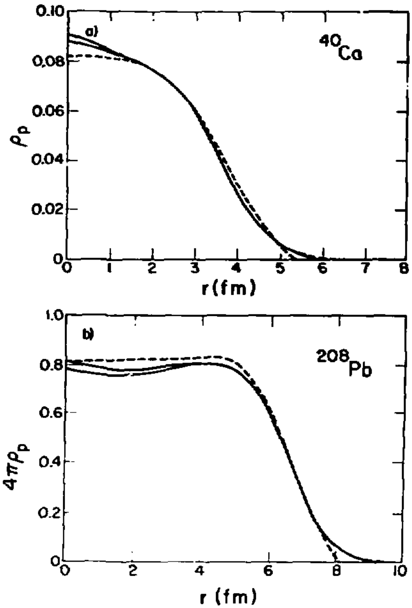

Fig. 1. (XBL 809-1991)

References

1. J. D. Walecka, Ann. of Phys. 83, 491 (1974).

2. J. Negele, Seventh Intl. Conf. on High Energy Physics and Nuclear Structure, ed. M. Lochner (Birkhauser Verlag, Basel, 1978) p. 231.

3. R. Serber, Phys. Rev. 14C, 718 (1976).

4. M. H. Johnson and E. Teller, Phys. Rev. 98, 783 (1955).

5. L. D. Miller, Phys. Rev. Lett. 28, 1281 (1972).

6. B. D. Serot and J. D. Walecka, Phys. Lett. 87B, 172 (1980).

PROPERTIES OF T ≠ 0 NUCLEI IN A RELATIVISTIC QUANTUM FIELD THEORY

J. Boguta

The knowledge of the equation of state of nuclear matter at various densities and temperatures is of considerable interest, in that it enters into the calculation of a large number of physically interesting phenomenon. Ideally such an equation of state should be calculated from a theory that is known to be reliable. Unfortunately, this is impossible to do. The next best thing is to use a theory that does reproduce known nuclear matter properties and does not violate important constraints such as relativity and the effects of the mesonic degrees of freedom at high densities. The only known way to achieve both goals is through a relativistic quantum field theory, in which it is possible, in a systematic way to compute the corrections.[1] It has been shown by Chin[2] that such a theory, in a mean field approximation, becomes more accurate with increasing density. What has not been appreciated thus far is that the model is a good phenomenological tool in studying the properties of finite nuclei.[3]

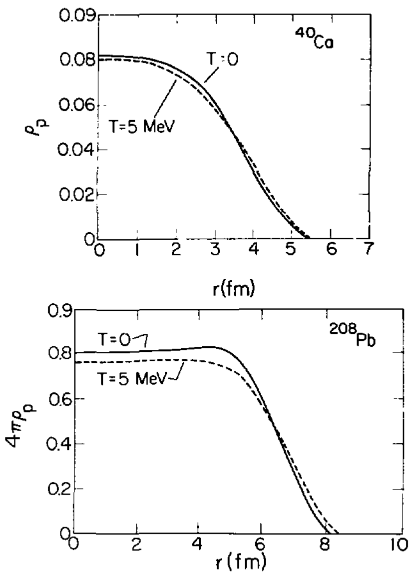

Fig. 1. (XBL 809-1985)

The interest in studying non-zero temperature ($T \leq 5$ MeV) has been stimulated by the production of highly excited nuclei. To describe these many body systems, a statistical approach seems a natural one. The very high temperature ($T \geq 50$ MeV) behavior of the Walecka model has been studied for neutron matter[4] and symmetric matter with a tower of resonances.[5] Temperature effects for the size and mass of neutron star has also been investigated.[6] There have also been a number of conventional nuclear physics calculations for the temperature properties of finite nuclei.[7] Of particular interest for us in this work will be the level density parameter a. If ΔE is the thermal excitation energy of the nucleus, then $\Delta E = aT^2$, where T is the temperature. Experimentally determined nuclear excitations can be fitted by $a \approx A/8$, where A is the mass number.[8] We find $a \approx A/9.8$.

In this work we present solutions of the Walecka model for finite nuclei at non-zero temperatures. Presently we still deal within the Thomas-Fermi approximation. This approximation is, strictly speaking, inconsistent with the boundary conditions of the problem. We made rather trivial modifications to overcome this problem. At this stage of investigation, this will serve our needs to show that the Walecka model does give a good description of the level density parameter and a reasonable description of densities in Ca^{40} and Pb^{208} for temperatures up to 5 MeV. *A consistent* calculation, involving the solution of relativistic Hartree equations will be reported later.

References

1. J. D. Walecka, Ann Phys. 83, 491 (1974).

2. S. A. Chin, Ann. Phys. 108, 491 (1977).

3. F. E. Serr and J. D. Walecka, Phys. Lett. 79B, 10 (1978); J. Boguta and J. Rafelski, Phys. Lett. 71B, 22 (1977); L. N. Savushkin, Sov. J. Nucl. Phys. 30, 340 (1979); R. Brockmann and W. Weise, Phys. Rev. 16C, 1282 (1977); B. D. Serot and J. D. Walecka, Phys. Lett. 87B, 172 (1980); J. Boguta, Relativistic Quantum Field Theory of *Finite Nuclei*, LBL preprint, *July 1980*.

4. J. D. Walecka, Phys. Lett. 59B, 109 (1975).

5. S. I. A. Garpman, N. K. Glendenning, and Y. J. Karant; Nucl. Phys. A322, 382 (1979).

6. J. Boguta, Hot and Cold Neutron Stars, LBL preprint July, 1980.

7. G. Sauer, H. Chandra, and U. Mosel; Nucl. Phys. A264, 221 (1976); U. Mosel, P.-G. Zint and K. H. Passler; Nucl. Phys. A236, 252 (1974).

8. A. Bohr and B. R. Mottelson, Nuclear Structure Vol. 1 (W. A. Benjamin, Inc. 1969, New York) p. 186.

COLOR EXCITATION AND EXOTIC NUCLEI

Y. J. Karant

Recent observations of the apparent short mean free paths of relativistic nuclear projectile fragments in emulsion suggest that these fragments are contaminated by a component with an anomalously large reaction cross section. I suggest that this effect might be due to the formation of an internally color-polarized *multi-baryon state. For this explanation to be* tenable, it must: (1) be allowed to exist, (2) be long-lived ($\tau \geq 10^{-10}$ sec), (3) have a suitable mass and be produced with a large enough probability to account for several percent of the projectile fragment flux, and (4) have a larger cross section than a normal nucleus of the same (B,Z).

By considering the color algebra of QCD, I show that (1) is satisfied and (2) and (4) are closely related problems. As contrasted with the three-valence quark system (B = 1) which has only one color singlet state, the six-valence quark system (B = 2) has two: $(3)^6 \longrightarrow 1 \otimes 1 \to 1$ and $(3)^6 \longrightarrow 8 \otimes 8 \to 1$, both of which are topological invariants. If one extends the algebra to $SU(2)_{flavor} \otimes SU(2)_{spin} \otimes SU(3)_{color} \longrightarrow SU(12)$, there are two states of interest $(N^1_{1/2})^2$ (ordinary deuteron-like state) and $(\Delta^8_{1/2})^2$ (a dibaryon of two color 8, isospin 3/2, and spin 1/2 "baryons"). In all orders, the $(\Delta^8_{1/2})^2 \not\to (N^1_{1/2})^2$ by gluon exchange (due to the flavor singlet nature of g) nor by ordinary $q\bar{q}$ (meson) exchange. Only quark tunneling permits the decay of such an object.

To restrict this tunneling probability to an acceptable level, one needs a large object with an effective barrier between the two color octet baryons. Since $8 \otimes 8$ is repulsive, one obtains a natural model in which both 8's repel but nonetheless are confined at some distance of several fm. This inner repulsion prevents a fast tun*neling decay. Point (3) is not addressed by* this model.

COULOMB EFFECTS IN A NUCLEUS-NUCLEUS CASCADE MODEL

Y. J. Karant and C. C. Noack*

There has been much interest in the effect of the Coulomb interaction on the differential cross sections in high energy nucleus-nucleus collisions. In p-p collisions, one can easily neglect such effects, since they are of order α. However, in an AA' state, they become of order $ZZ'\alpha$, which in many cases is non-neglible.

To explore this, we are working within the context of the SIMON code. SIMON is a relativistic nucleus-nucleus inter-nucleon cascade model. It uses experimental np, pp nn differential cross sections, takes partial account of Fermi motion and binding energies, and treats the cascade as developing simultaneously in both target *and projectile nuclei* (that is, it has moving-moving collisions).

There are two aspects of the problems which we ignore at the start: meson (and isobar) production and complex nuclear ejectiles. All complex fragments (A = 2 and above) must come from de-excitation of the target and projectile remnants after the cascade has stopped.

We assume that during the cascade, Coulomb forces are absent. As soon as a particle has left the cascade region (defined by having reached a point in space where the instantaneous local particle density is insufficient for it to have any further collisions), Coulomb forces are turned on. Let x be the position vector for the i^{th} particle, with velocity $c\beta$ x, and momentum p so that

$$\vec{p} = \frac{m}{\sqrt{1-\beta^2}}\,\vec{\beta}, \quad \dot{\vec{p}} = e\vec{E}$$

where $\vec{E}$ is calculated from all other A = 1 particles as though they were on straight line trajectories. However, the target and projectile remnants are placed on Coulomb trajectories under their mutual influence (ignoring the effect of the ejectiles) and are included in calculating E. Thus, we ignore magnetic and retardation effects, but do include the relativistic relation between $\vec{p}$ and $\vec{\beta}$. Detailed comparison with experiments are now under way.

Footnote

*Department of Physics, University of Bremen, West Germany.

A. SUPERHILAC AND 88 INCH CYCLOTRON

THE SUPERHILAC ON-LINE ISOTOPE SEPARATOR

J. Michael Nitschke

The on-line isotope separator (Fig. 1) as described in last year's annual report[1] has undergone a considerable transformation. A new plasma ion source and a surface ionization source were developed. The plasma source was tested off-line and has produced Kr beams with efficiencies of 22%. The transmission through the mass spectrometer is ≥90%, and a resolution of $(\frac{m}{\Delta m})$ FWHM of ~ 2000 has been obtained (Fig. 2). The operating temperature of the arc source is 2500°C so that elements with high boiling points can be separated. While the performance of the arc source has not yet been optimized, the surface ionization has been tested extensively. The operating principle of the source is as follows: recoils from a thin target transverse two heat shields and pass through an array of capillary tubes into the ionization region where they are stopped in slanted tantalum strips. They diffuse out of these strips and are surface ionized on the inner wall of the ionization chamber which is made of tungsten operating at 2900°C. The ion extraction, acceleration and mass analysis have been described previously.[1]. The purpose of the capillary array is to act as a molecular flow restriction that prevents the gaseous reaction products from back-diffusing towards the target. Thin Ta windows, which have been tried for the same purpose, fail after short periods. Isotopes of the following element have been separated so far: Na, In, Dy, Ho, Er, Tu, Fr, Ra and Ac. The efficiencies are 12%, for Fr, 3% for Ac and a few percent for the rare earth elements. The 3% efficiency of Ac was achieved for an isotope with 0.8 sec half-life (^{213}Ac); this serves as an illustration for the obtainable separation speed, which is however highly element-dependent. At present four masses can be studied simultaneoulsy in the focal plane if they decay by particle emission. γ spectra of In isotopes have been obtained by removing monoisotopic samples from the separator via a vacuum lock and off-line γ spectroscopy. Ninty percent of all on-line runs were carried out with Ne beams from the SuperHILAC operating at the rate of 2 pps parasitically to the Bevalac bio-med program.

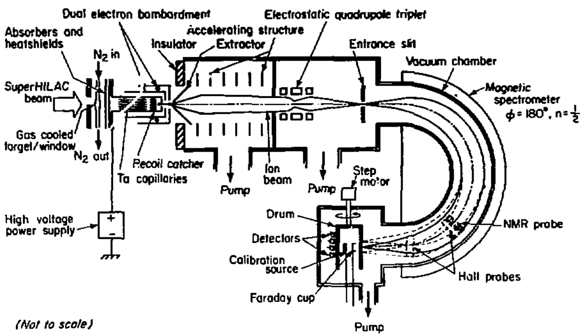

Fig. 1. Principal components of the SuperHILAC on-line isotope separator with surface ionization source. (XBL 808-1739)

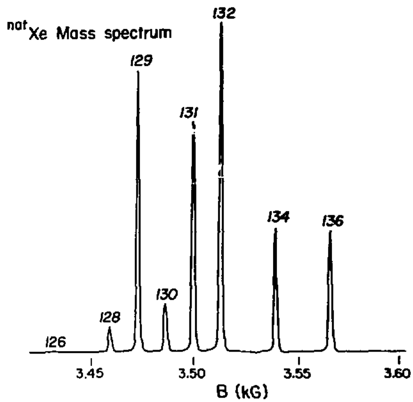

Fig. 2. ^{nat}Xe mass spectrum at the focal plane of the on-line isotope separator obtained with the plasma ion source (E_{ion} = 20 KeV, resolution: $m/\Delta m$ = 1140 FWHM). (XBL 808-1754)

Reference

1. Nuclear Science Division Annual Report 1978-1979, LBL-9711, p. 229.

IMPROVEMENTS TO THE He-JET FED ON-LINE MASS SEPARATOR RAMA

R. F. Parry, M. D. Cable, J. M. Wouters, J. Äystö,* and J. Cerny

Efforts to increase the total efficiency, reliability, and versatility of the Recoil Atom Mass Analyzer (RAMA) have resulted in several improvements. These include a target box redesign, a new version of our standard ion source that has been developed to increase the overall yield of several nuclides, and finally the addition of a process control computer to monitor and adjust various devices critical to a stable operational environment for RAMA.

The target box redesign was centered around increasing the reliability, servicing ease, and operating convenience of our multiple capillary system.[1] This was accomplished by adding several target/degrader ladders that could be set up for various multiple target-multiple capillary designs (Fig. 1). Also incorporated was a refrigeration system that supplements the previous liquid nitrogen vapor cooling that keeps the target box at a constant temperature necessary for optimal cluster formation for the He-jet transport system. The redesign has eliminated a set of rear isolation foils that previously separated the Faraday cup (at vacuum) from the target box (at ~ 1.5 atm of He). The intention is to replace the downstream cup with one located at the rear of the pressurized target box. Further development of the Faraday cup is underway because initial results produced somewhat misleading beam current readings due to secondary electron emission.

Some ion source development was necessary in order to proceed with an experiment[2] to measure the decay of ^{36}Ca because the previous source did not produce calcium in sufficient yield. The position of the arc and filament were inverted in the new source, resulting in a longer and smaller diameter plasma compared to the original source. The higher plasma density and longer interaction region resulted in a substantial increase in the ^{36}Ca and ^{37}Ca yields.

The installation of a process control computer, a ModComp MODACS III, has recently been implemented to monitor and adjust various sytem elements on RAMA. Presently the system monitors the field strength of our analyzing magnet through a link with the recently developed CERN NMR, various magnet power supplies including the Wien filter and several sextupoles, and the extraction voltage of the ion source. Our current development efforts include monitoring the total RAMA system status

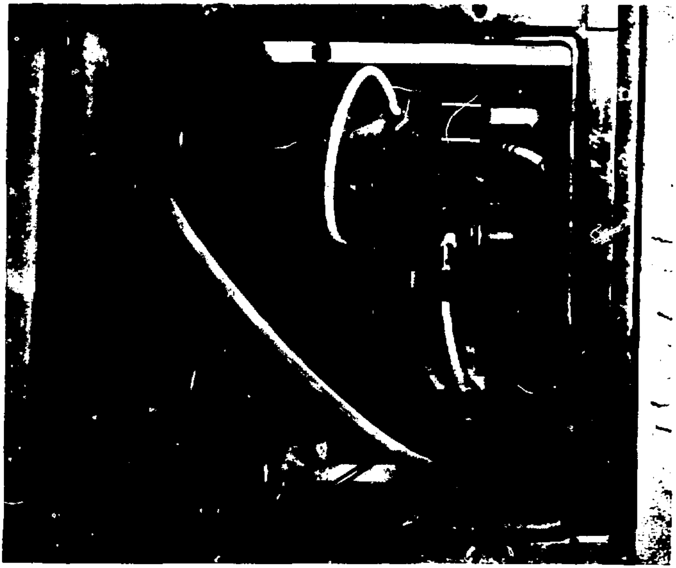

Fig. 1. The RAMA target box. (BBC 803-3384)

(valves, diffusion pumps, LN traps, etc.), complete closed loop control of the analyzing magnet, system control programming for mass changes, calibrations, etc., interactive RAMA control and monitoring, and a CPU to CPU link with the ModComp IV/25 on-line data acquisition computer at the 88 Inch Cyclotron.

Footnote and References

*Present address: University of Jyväskylä, Dept. of Physics, Nisulankatu-78, Jyväskylä-72, Finland.

1. D. M. Moltz, J. M. Wouters, J. Äystö, M. D. Cable, R. F. Parry, R. D. von Dincklage, and J. Cerny, LBL preprint LBL-9721 (in press).

2. J. Aysto, M. D. Cable, R. F. Parry, J. M. Wouters, D. M. Moltz, and J. Cerny, LBL preprint LBL-11193 (in press).

HALL PROBE CONTROLLED NUCLEAR MAGNETIC RESONANCE MAGNETOMETER

J. M. Nitschke and A. A. Wydler

The precise determination of atomic masses with the SuperHILAC on-line isotope separator depends upon the exact measurement of the ion energy and the magnetic field of the analyzing magnet. The ion energy is determined by the accelerating potential which is measured with a precision voltage divider and a 6-1/2 digit digital volt meter. The magnetic field is measured with a nuclear magnetic resonance (NMR) probe. Like all NMR probes, it has to be retuned manually whenever the magnetic field is changed (except for small variations). This is quite inconvenient in particular when the NMR is linked to a computer that calculates the mass from the NMR frequency and the ion energy. The device described here eliminates any tuning and affords a completely automatic mass determination. Figure 1 shows the principal components: The Hall probe and the NMR probe are located adjacent to each other inside the homogeneous magnetic field section of the analyzing magnet. The tuning of the NMR probe is affected by the coarse frequency control voltage. This voltage is derived from the Hall probe via the Hall probe amplifier, an active filter, and the summing amplifier Amp. II. An offset is introduced into Amp. II because the control voltage spans a range from 0 to 7 V while the magnetic field varies from 3.5 to 10.5 kG. This primary control circuit would be sufficient for tuning the NMR if its frequency were a linear function of the control voltage. But since this is not the case, a correction signal is generated in Amp. I that compares the field measured by the Hall probe with the converted NMR frequency. In addition, an error signal from the NMR and an offset voltage are added. This combined correction signal ensures perfect tracking between the field measured by the Hall probe and the NMR frequency, which amounts to an automatic tuning procedure. The function of the error signal is to lock the NMR signal to the zero crossing of the magnetic field modulation. For an ion energy of 50 keV, as used in the SuperHILAC on-line isotope separator, the masses that can be determined automatically range from 45 to 380 amu. Other mass ranges can be obtained by changing the Hall probe.

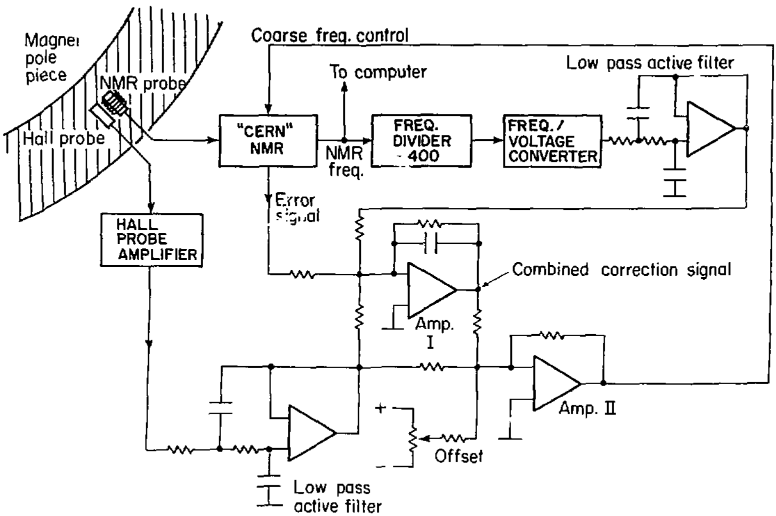

Fig. 1. Block diagram of Hall probe controlled NMR magnetometer. (XBL 808-1736)

NON-DESTRUCTIVE BEAM INTENSITY MEASUREMENT

J. M. Nitschke and J. A. Hinkson

For most experiments at heavy ion accelerators it is mandatory that the instantaneous beam intensity, the profile of the macroscopic beam pulse, and the total integrated beam current be measured. The conventional methods are to design the target as a Faraday cup that also stops the beam, or to let the beam transverse the target and catch it in a separate Faraday cup. In the case of an on-line isotope separator neither method is feasible because the beam stops in a target-ion source combination that is operated at a high voltage potential of several tens of kilovolts. We therefore developed the beam measuring system shown in Fig. 1, which relies on the charge induced by individual microscopic beam bunches as they traverse an electrostatic pickup electrode. A microscopic beam bunch at the SuperHILAC is typically 1 to 3 cm long and has a repetition frequency of 70.289 MHz. As it passes thorough the 5-cm long pick-up electrode it induces a voltage (U) that is proportional to the charge (Q) carried by the bunch and inversely proportional to the capacity (C) of the electrode, i.e., $U = Q/C$. This voltage has a fundamental frequency of 70.289 MHz and several harmonics depending on the degree of bunching or debunching of the beam. It is amplified in a preamplifier of 20 db gain and 5 MHz bandwidth and mixed down to an IF of 1 MHz. The IF amplifier has a bandwidth of about 100 KHz and a gain of 80 db; it is followed by a detection circuit, a gated integrator and a sample and hold circuit. The momentary output of the sample and hold circuit is proportional to the integrated beam intensity during one macropulse. The shape of the macropulse is displayed at the output of the detection circuit. An attenuator between the preamplifier and the mixer serves as a range switch. This device has been used successfully in many on-line runs at the SuperHILAC and is generally calibrated by comparing its output to a conventional Faraday cup in order to avoid errors due to the varying microstructure of the beam.

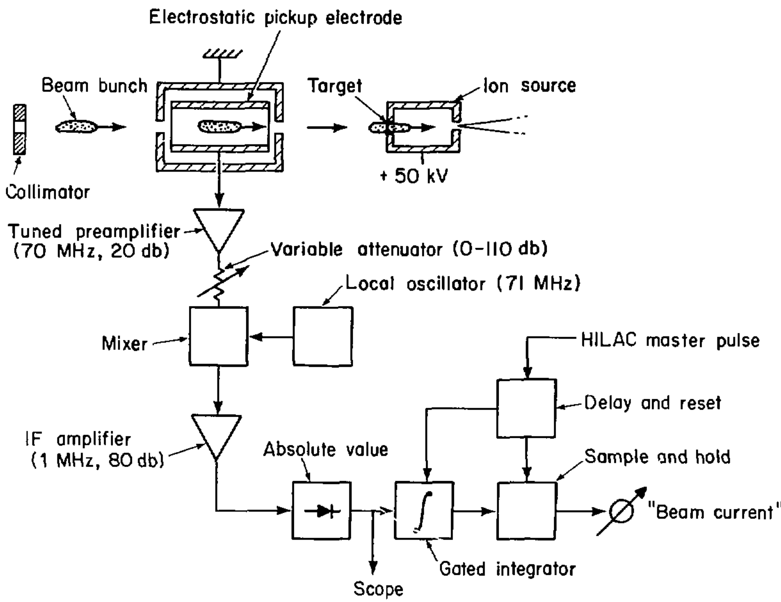

Fig. 1. (XBL 808-1737)

RECENT PROGRESS IN ION SOURCES AND PREACCELERATORS*

David J. Clark

Recent progress in ion sources is reviewed. The types of sources discussed include positive and negative proton and deuteron sources developed for conventional preaccelerators and for neutral beam applications. Positive heavy ion sources for conventional linacs and for induction linacs are included. Negative heavy ion sources are used for tandem electrostatic accelerators. Positive and negative polarized ion sources for protons and deuterons inject cyclotrons, tandems and linacs. Some recent preaccelerator designs are summarized.

Ion source development of many different types of sources has been undertaken by groups throughout the world. Groups working on each type of source generally have good communication with each other, but it is also valuable to have interaction between research groups working on different source types. For example, the development of the multiaperture sources in the ion engine field and for neutral beams offers useful computer methods and extractor designs for high current injectors for particle physics and heavy ion fusion. The techniques developed in experimental plasma physics are also valuable for ion sources. The contact ionization sources developed in plasma studies and also for ion engines are useful for negative heavy ion sources and for high current induction linac injection. Also, the magnetic bucket confinement system for plasmas is finding applications in high currrent sources for neutral beam formation. So we need a healthy interaction between various source people and with those in plasma science.

The listing and description of ion sources is such a large field that it would take a book to do it justice, such as the one by Valyi.[1] Recent reviews have been given by Osher[2] on many light and heavy ion sources, by Curtis[3] on duoplasmatrons for proton linacs, by Middleton[4] on negative heavy ion sources, by Clark[5] and Seliger[6] on sources for heavy ion fusion, by Haeberli[7] and Glavish[8] on polarized ion sources, and by Kunkel[9] on neutral beams for fusion. The present review will concentrate on sources developed for particle accelerators and sources developed for other fields which may have useful applications in particle accelerators. In such a large field of development, only a few typical examples can be chosen to illustrate recent developments in each source area.

The specific types of sources described include duoplasmatrons and duopigatrons for proton linacs, multiaperture sources for fusion plasma heating, PIG, ECR, and EBIS sources for heavy ion cyclotrons and linacs, negative ion sources for linacs, fusion injectors and electrostatic accelerators, and polarized sources.

Footnote and References

*Condensed from LBL-9619.

1. L. Valyi, Atom and Ion Sources (Wiley, New York, 1977).

2. J. E. Osher, IEEE Trans. Nucl. Sci. NS-22, 3, 1626 (1975).

3. C. D. Curtis, Proc. 1976 Proton Linear Accelerator Conf., p. 179, A.E.C.L. Canada (1976).

4. R. Middleton, Revue de Physique Appliquee 12, 10 1435 (1977).

5. D. J. Clark, IEEE Trans. Nucl. Sci NS-24, 3, 1064 (1977).

6. D. J. Clark and R. L. Seliger, Proc. Heavy Ion Fusion Workshop, ANL-79-41, p. 127 (1978).

7. W. Haeberli, Proc. Conf. on High Energy Physics with Polarized Beams and Polarized Targets, AIP No. 51, p. 269 (1979).

8. H. F. Glavish, Proc. 5th Conf. on Applications of Small Accelerators, Denton, Texas (1978).

9. W. B. Kunkel, IEEE Trans. Nucl. Sci, NS-26, 3, 4166 (1979).

OPERATION OF A HIGH-CURRENT XENON SOURCE*

Warren Chupp, Dave Clark, Robert Richter, John Staples, and Emergy Zajac

The development of heavy ion accelerator driver systems for inertial confinement fusion will also require the development of high current heavy ion sources. High current plasma arc sources have already been developed at LBL in connection with neutral beam program.[1] This paper reports the results of adapting the Ehlers type source to produce singly charged xenon ions and subsequently accelerate them to 500 kilovolts.

A multi-aperture Ehlers-type source has been constructed and operated to produce a 60 mA Xe^{+1} beam. A schematic of the multi-aperture xenon source is shown in Fig. 1. The electron current is supplied by a circular array of eight 0.02 inch diameter tungsten filaments connected in parallel. The large hemispherical anode is shaped to reduce the arc potential, favoring Xe^{1+} production. The extraction lens is a 13 hole accel-decel system with typical operation voltages of 25 and 3 kV.

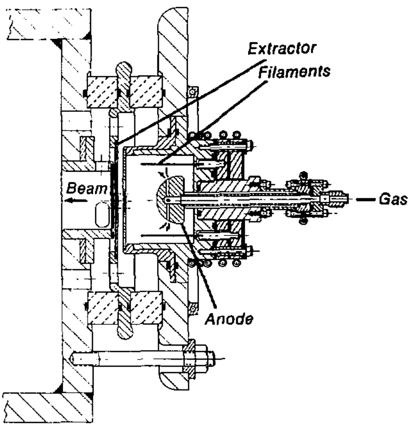

Fig. 1. The multi-aperture xenon source. (XBL 793-8705)

The low voltage test stand consists of four principle components: the xenon source including its accel-decel lens, the pumping system, a 4 inch quadrupole triplet, and a 50 degree analyzing magnet. Two Sargent-Welch turbomolecular pumps provide a pumping speed of 3000 liters/sec at the ion source, while a diffusion pump and an additional turbomolecular pump provide 1650 liters/sec pumping in the transport system. Diagnostic equipment includes several Faraday cups, a 32-wire x-y beam profile monitor, a slotted plate emittance measuring device, and two sets of x-y jaws to determine the beam size. Extraction and decel lens potentials are supplied by two unregulated supplies capable of delivering 80 kV at 10 mA dc with additional capacity to compensate for beam loading effects. The arc supply can deliver 300 volts at 50 amperes with a pulse length of 500 μsec, and the paralleled source filaments are powered by a 10 volt 150 ampere dc supply. Pulsed gas is supplied to the source by a voltage-controlled piezo-electric valve. Calculations of beam optics with space charge included showed that even 1 mA of uncompensated space charge would cause a factor of 2 loss in transmission, so the 35 mA beam in the cup was at least 97% neutralized. The fact that the experimental setting of the quadrupoles were within 15-20% of those calculated without space charge indicated that the space charge is well compensated. For a total acceleration voltage of 22.5 kV, the normalized emittance area ε_N = 0.027 $\pi \pm 10\%$ cm-mrad, for a current of 29 mA.

After initial tests on the xenon source were completed in the low voltage facility, the xenon source was installed in a 500 kV test terminal. The normalized emittance area is 0.08-0.11 π cm-mrad at 500 keV. The transmitted beam current was 35 mA in this run. Currents of up to 60 mA have been produced, but the emittance at these higher currents has not been measured. The Xe^{+1} charge state was found to be 90% of the total when operating at an arc voltage of 20 V. As is to be expected, higher arc voltages lower the Xe^{+1} percentage through the production of higher charge states.

Footnote and Reference

*Condensed from LBL-8859.

1. W. R. Baker et al., Proceedings of the Symoposium on Ion Sources and Formation of Ion Beams, BNL Conf. Report 1971.

A FAST ACCESS MODULAR TARGET SYSTEM FOR THE IRRADIATION OF ACTINIDE TARGETS WITH HIGH INTENSITY HEAVY-ION BEAMS

K. J. Moody, M. J. Nurmia and G. T. Seaborg

We have designed and built a target system for the irradiation of thin actinide targets with high intensity heavy-ion beams, for use in radiochemical experiments. The system offers quick access to short-lived activities. The modular design allows the target apparatus to be quickly disassembled and rebuilt into other configurations and used for the irradiation of other target types.

Figure 1 is an exploded view of the actinide target facility. It is enclosed in a glove box with a filtered exhaust. The beam is collimated with a graphite collimator of variable diameter, which is clamped to the water-cooled collimator housing. This housing is electrically isolated front and back by Teflon spacers so the beam current striking the collimator can be measured separately from the target. The bolts holding the system together have a 1-mm clearance all-around in the collimator housing. Rotational orientation is maintained with pins. The beam next passes through an electron suppressing magnet, a 1.8 mg/cm^2 Havar vacuum window, and the target. The target and the window are both cooled with jets of nitrogen gas with a total flow of 1500 standard liters/hour. Constant pumping on the target chamber with a rotary pump keeps the gas pressure below 100 torr. The beam is stopped in the water-cooled end-piece. The difference in temperature between the incoming and outgoing water is monitored as a measure of the beam power. The infra-red radiation from the target is monitored through a quartz window in the end-piece (not shown in Fig. 1). Infra-red and beam power signals are used to limit the beam current. The electrical signal from the end-piece and the gas-cooling jacket are summed to determine the beam flux.

Recoiling products are collected on a truncated conical foil, which the beam does not strike, shown in Fig. 1. The end-piece is put in place by pressing it against the last Teflon spacer and giving it a clockwise twist to lock it under the restraining bolts. At the end of an experiment, the system is let up to air and the end-piece is twisted off. In recent

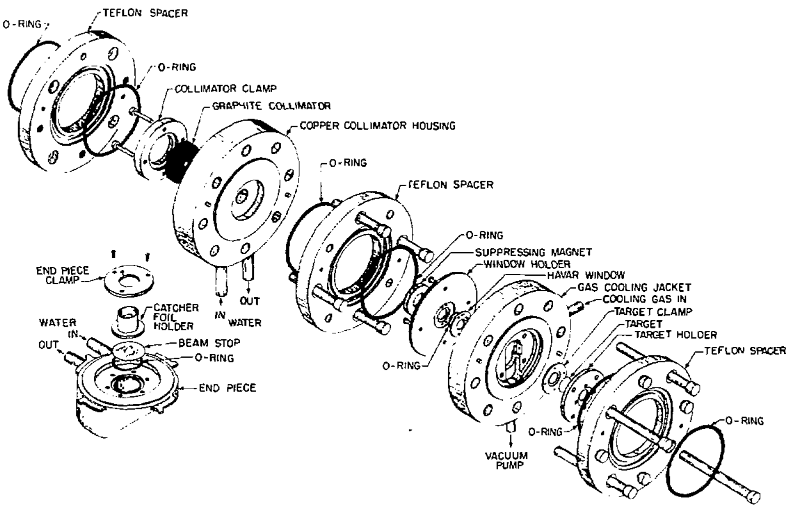

Fig. 1. Target system for the irradiation of actinide targets with high intensity heavy-ion beams. (XBL 803-503)

experiments the catcher foil was ready for transportaion within 90 seconds of the end of the irradiation.

Two tests of the target system were made with a blank target of 0.01 mm thick beryllium. In one test, a beam of 144 MeV $^{20}Ne^{7+}$ at 36 pulses/sec with an average intensity of 3.5 microamperes was delivered to the target. This beam deposits approximately two watts of heat in the vacuum window. No problems were encountered. Another test was performed with an intense beam of 100 MeV $^{12}C^{6+}$ at two pulses/sec. The beam current was gradually stepped up until the peak current was 80 electrical microamperes, at which point the water-cooled beam stop was punctured.

The system has been used in several irradiations of targets of ^{248}Cm and ^{244}Pu with beams of ^{136}Xe and ^{86}Kr at average intensities of as much as 500 electrical nanoamperes on the ^{248}Cm target and as much as 1.4 microamperes on the ^{244}Pu target. No problems have been encountered.

CALIBRATION OF A HIGH-EFFICIENCY DEUTERON TENSOR POLARIMETER

E. J. Stephenson,* R. J. Holt,† J. R. Specht,† J. D. Moses,‡ R. L. Burman,‡
G. D. Crocker,‡ J. S. Frank,‡ M. J. Leitch,‡ and R. M. Laszewski§

The polarized deuteron beam from the 88 Inch Cyclotron was used to calibrate a high-efficiency polarimeter sensitive to the deuteron t_{20} moment. This polarimeter was subsequently used at LAMPF to measure the t_{20} polarization of deuterons recoiling from elastic scattering by 142-MeV positive pions. Both three-body (Fadeev) and isobar doorway models in their present form provide a satisfactory description of the cross section for π-d elastic scattering. However, the outgoing deuteron polarization is more sensitive to many important details in the calculations. The first measurement of such a polarization was conducted with this polarimeter and reported in Ref. 1. The final result of $t_{20} = -0.23 \mp 0.15$ for $T_\pi = 140$ MeV and $\theta_\pi = 180°$ is in disagreement with all theories.

The polarimeter, shown in Fig. 1, makes use of the ^{3}He(d,p)^{4}He reaction below 15 MeV. Near 0°, both the ^{3}He(d,p)^{4}He cross section and T_{20} analyzing power are large. To give the polarimeter a large efficiency, a thick target of compressed ^{3}He (750 psi) was used. The large reaction Q-value facilitated the detection of outgoing protons, which were identified and counted with a pair of plastic scintillators. In addition, the incident deuterons were observed in a scintillator as they entered the ^{3}He gas. Thus, the polarimeter provided a direct measure of the efficiency ϵ, the ratio of proton to deuteron count rates. This efficiency is sensitive to the deuteron t_{20} moment acccording to

$$\epsilon = \epsilon_0(1 + t_{20}T_{20})$$

where ϵ_0 is the efficiency for an unpolarized deuteron beam and T_{20} is the polarimeter analyzing power.

In the π-d elastic scattering experiment, the LAMPF Low Energy Pion channel was used to deliver an energy analyzed pion beam to the target, and to separate the recoil deuterons from the pion beam and transport them to the polarimeter. The emerging deuterons were expected to cover a wide area and contain a large range of deuteron energies. So the polarimeter was constructed with a large

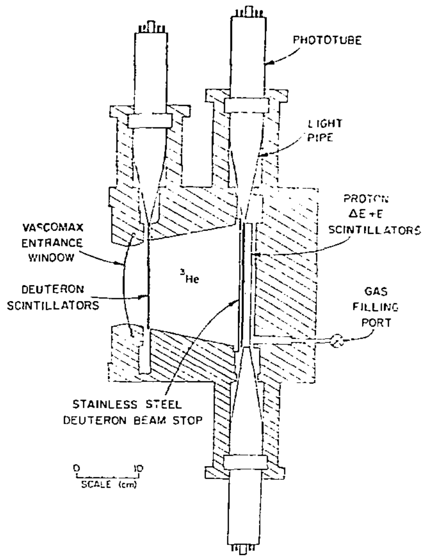

Fig. 1. Cross sectional view of the deuteron polarimeter showing the entrance window and particle detectors. (XBL 8011-12741)

entrance window (81 cm^2) and two x-y wire chambers in front to locate the incident deuteron position and angle.

To provide enough information to analyze the full distribution of recoil deuterons, the calibration was carried out at a variety of deuteron energies, entrance positions, and angles of incidence.[2] The cyclotron provided 47-MeV tensor polarized deuterons. The polarization was monitored upstream with the $^4He(d,d)^4He$ reaction.[3] To reduce the intensity, the beam was dispersed by multiple scattering and recollimated ahead of the polarimeter. Rapid spin flip was used to reduce systematic errors. Aluminum degrader foils were used to change the deuteron energy. The calibration consisted of measurements of both the unpolarized efficiency ϵ_0 and the tensor analyzing power T_{20}. It was found that the efficiency was insenstive to the position or angle of incidence of the deuteron on the polarimeter, while T_{20} rose slowly for positions near the edge of the entrance window. No sensitivity was observed to other deuteron moments. The largest sensitivity was to the deuteron energy, as shown in Fig. 2. The average efficiency and analyzing power for the distribution of deuterons observed at LAMPF was $\epsilon_0 = 1.52 \pm 0.06 \times 10^{-4}$ and $T_{20} = -0.60 \pm 0.05$, making this the most efficient deuteron polarimeter available.

In subsequent experiments, a second polarimeter of similar design will be calibrated and used to obtain an angular distribution of the recoil deuteron t_{20} moment. Segmentation of the proton counter should provide additional information on t_{22}. This second polarimeter will also be used to observe the recoil polarization from electron-deuteron scattering. This experiment should permit the first separation of the deuteron electric monopole and quadrupole formfactors.

We are indebted to H. E. Conzett, R. M. Larimer, P. von Rossen, H. Weiman, and the technical staff at Berkeley for their assistance during the calibration of the polarimeter. This work was performed under the auspices of the U. S. Department of Energy and partially supported by the National Science Foundation.

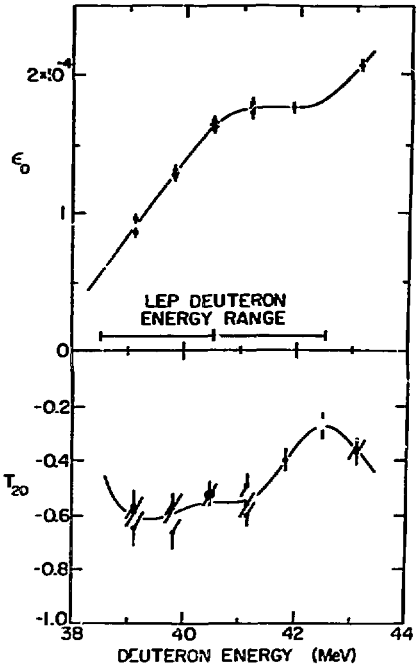

Fig. 2. Energy dependence of the polarimeter efficiency ϵ_0 and analyzing power T_{20}. The curves are a guide to the eye. The horizontal bar depicts the central energy and maximum energy spread of the recoil deuterons in the π-d experiment. (XBL 8011-12742)

Footnotes and References

*Present address: Indiana University Cyclotron Facility, Bloomington, IN 47405

†Argonne National Laboratory, Argonne, IL 60439.

‡Los Alamos Scientific Laboratory, Los Alamos, NM 87545.

§University of Illinois, Champaign-Urbana, IL 61820.

1. R. J. Holt et al., Phys. Rev. Lett. 43, 1229 (1979).

2. E. J. Stephenson et al., to be published.

3. E. J. Stephenson et al., Phys. Rev. C21 (1980).

THE EFFECTIVE SOLID ANGLE OF A RECTANGULAR COLLIMATOR FOR THE PASSAGE OF FRAGMENTS FROM BREAKUP PROJECTILES

A. C. Shotter,* A. N. Bice and Joseph Cerny

In certain experimental investigations the outgoing particles from a nuclear reaction can be excited to energies above particle breakup thresholds; these particles can then breakup, usually into two fragments. More often than not, the best way to record such events is to record the coincidence of breakup fragments in separate counters. However it is sometimes experimentally expedient to record the two fragments in the same detector system (e.g., studying ^{8}Be production by observing its two break-up α's in a single system). If the detectors system is a $\Delta E \times E$ particle telescope then these events may be identified by their special mass identification signals. If such a procedure is followed then it is important for cross section estimates to determine the effective solid angle of the collimator. For a rectangular collimator a general expression has been derived for this effective solid angle.

The breakup kinematics for the situation considered is shown in Fig. 1. The center-of-mass is denoted by V_C. The velocities of the two fragments in the center-of-mass frame are V_1, V_2, their masses m_1, m_2. The total laboratory energy of the projectile is denoted by E and the center-of-mass energy by ϵ. The collimator is assumed to be of dimensions $2a \times 2b$ and is placed a distance d from the target. The radius of the breakup sphere corresponding to V_1 ($\geq V_2$) at the collimator plane is given by

$$r = V_1 d / V_c,$$

where $r = d\left(\frac{m_2}{m_1} \cdot \frac{\epsilon}{E}\right)^{1/2}$.

If the actual solid angle subtended by the collimator is Ω then

$$\Omega_{eff} = \Omega P(a,b),$$

where

$$P(a,b) = \frac{1}{\pi\alpha\beta}\Bigg\{\beta(1+\alpha^2)\tan^{-1}\left[\frac{\beta}{(1-\alpha^2-\beta^2)^{1/2}}\right] + \alpha(1+\beta^2)\tan^{-1}\left[\frac{\alpha}{(1-\alpha^2-\beta^2)^{1/2}}\right]$$

$$+ (1-\alpha^2-\beta^2)^{1/2}\left(\frac{\alpha^2+\beta^2+2}{3}\right)$$

$$-2\alpha\beta\tan^{-1}\left[\frac{\alpha\beta}{(1-\alpha^2-\beta^2)^{1/2}}\right] - (1-\alpha^2)^{1/2}\,\frac{2+\alpha^2}{3}$$

$$-(1-\beta^2)^{1/2}\left(\frac{2+\beta^2}{3}\right) - \alpha\sin^{-1}(\alpha) -$$

$$\beta\sin^{-1}\beta + 2/3\Bigg\}$$

where $\alpha = (a/r)$, $\beta = (b/r)$, and provided $r^2 \geq a^2 + b^2$.

As a check to the accuracy of this expression, numerical calculations were also undertaken. These calculations simulated breakup events and tested whether any particular pair of breakup fragments passed through the collimator. It was assumed that the breakup fragments were isotropic with respect to the rest frame of the decaying projectile. Typically, for each P(a,b) calculated ~ 10^6 breakup events were sampled. In Fig. 2 a comparison between the results from the two methods is shown for different collimator configurations.

$$E_{LAB} = 1/2(m_1+m_2)V_c^2;\ \epsilon = 1/2 m_1 v_1^2 + 1/2 m_2 v_2^2$$

$$m_1 v_1 = m_2 v_2$$

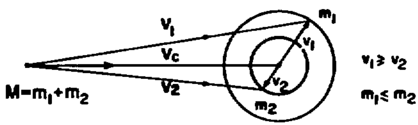

Fig. 1. Kinematic breakup cone. (XBL 807-1531)

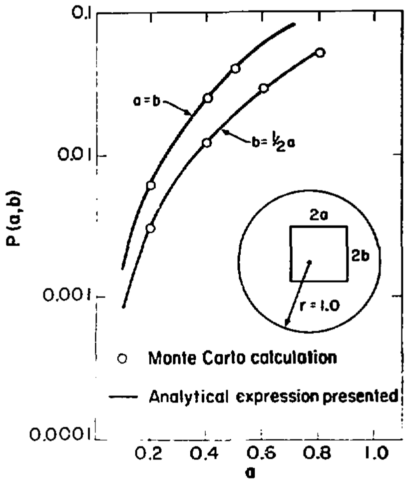

Fig. 2. The analytical function P(a,b) for a normalized breakup sphere. (XBL 807-1532)

TIME-WALK CHARACTERISTICS OF AN IMPROVED CONSTANT FRACTION DISCRIMINATOR

G J Wozniak, L W Richardson and M R Maier*

Many interesting aspects of deep-inelastic reactions can be investigated by measuring both the atomic number and mass of the reaction products. Very thin silicon detectors with exceptional uniformity ($\Delta T/T < 1\%$) are now commercially available which allow the identification of atomic numbers up to $Z \approx 40$. Furthermore, these detectors have good timing properties such that when coupled to fast electronics, signal rise times of < 2 ns and time resolutions of < 100 ps have been achieved. In order to retain this time resolution over a wide range of input signal amplitudes, the contribution form the electronics should be made sufficiently small so that off-line corrections to the data are not necessary. Commercial constant fraction discriminators (CFD) are available which have a time walk of less than 100 ps for large dynamic ranges, however, we would like to report here on a simple and much less costly alternative, which is the modification of a standard LBL-CFD[1] (21 x 1031 P-1) to make it competitive with the best commercial CFDs.

To measure the time walk of a CFD, a fixed amplitude signal from a pulser with a fast rise time (~ 1.0 ns) was fed into a 50 Ω splitter. One of the output signals was kept constant in amplitude for all the measurements and was connected directly to a reference CFD. The other output of the splitter was connected to a precision attenuator (a Wandel & Goltermann type RT-1 specially selected for low walk, i.e., < 30 ps which fed directly the second CFD with a clipping time of 1 ns. A biased time-to-amplitude converter (TAC) was started by the reference and stopped with the delayed output signal from the second CFD. The time walk of the second CFD was measured by varying the attenuation factor and measuring the centroid of the TAC peak. The time scale was calibrated with a precision delay line (0.50 ± 0.01 ns). For such a measurement it is essential that the different attenuator settings do not change the signal rise time or pulse shape.

In Fig. 1 the measured time walk is plotted

Footnote

*On leave from the Physics Department, University of Edinburgh, Edinburgh EH93JZ, United Kingdom.

versus the input signal amplitude. For the unmodified LBL-CFD, the measured time walk (triangles) is 500 ps over an input voltage range of 0.1 to 2.5 V. For the modified CFD, the time walk (circles) is substantially reduced to less than 30 ps over the same dynamic range. These results indicate that by optimizing the leading edge (LE) and zero-crossing (ZC) discriminator settings, the electronic contribution to the time resolution can be made sufficiently small such that in many situations time-walk corrections are unnecessary. Furthermore, this modification, which consists of replacing two integrated circuits (ICs) in the original circuit[1] with faster IC's, (i.e., replace the AM 685 from AMD[2] by an SP 9685 from Plessey[3]) is relatively easy and less expensive than buying a new low walk CFD.

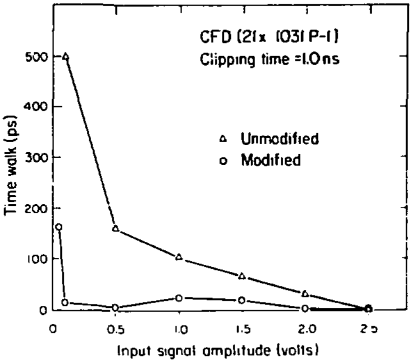

Fig. 1. Measured time walk versus input signal amplitude for the unmodified (triangles) and modified (circles) CFD. (XBL 808-1697)

In Fig. 2(a) the dependence of the walk on the LE discriminator threshold is shown. The observed time walk is a slowly varying function of the input signal amplitude above 100 mV. Below 100 mV, the time walk increases rapidly with decreasing signal amplitude and is quite sensitive to the LE discriminator setting. For a LE threshold of 5 mV (solid curve), the maximum time walk is ±100 ps for input signals varying from 50 mV to 500 mV. By increasing the LE discriminator threshold, the time walk can be reduced further if the low amplitude data can be excluded.

The dependence of the time walk on the ZC discriminator setting is shown in Fig. 2(b). Slightly better walk characteristics are observed (dashed curve) if the ZC discriminator threshold is offset (< 0 mV) to trigger in the lower half of the noise. Also, shown in Fig. 2(b) is the FWHM of the TAC peak (dotted curve) as a function of the input signal amplitude. This FWHM is constant (~ 20 ps) for input voltages above 0.3 V. Below 0.3 V the FWHM increases from 20 to 40 ps, as the noise begins to dominate the time resolution.

In summary, we have shown that an easy and inexpensive modification to a standard LBL-CFD substantially improved its time-walk characteristics. Furthermore, over the input signal amplitude range of 50 mV to 2 V, the time walk will be less than ±100 ps regardless of the ZC discriminator setting if the LE threshold is sufficiently low (≤10 mV).

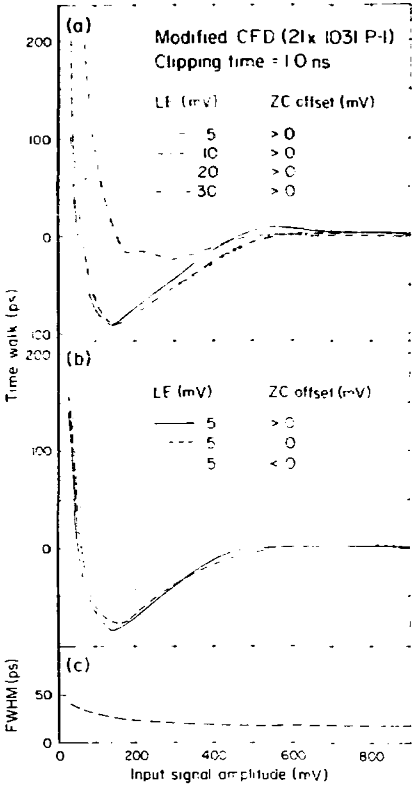

Fig. 2. Measured time walk (a) for several LE discriminator settings and (b) for several ZC discriminator settings. The electronic time resolution (FWHM) is also shown (dash-dot curve: LE = 5 mV, ZC = 0 mV).

Footnote and References

*Permanent address: University of Marburg, West Germany.

1. M. R. Maier and D. A. Landis, Nucl. Inst. and Meth. 117, (1974) 245.

2. Advanced Micro Devices, Sunnyvale, CA 94086.

3. Plessey Semiconductors, Irvine, CA 92714.

B. BEVALAC

STREAMER CHAMBER MEASUREMENTS AT THE BEVALAC

J. P. Brannigan, A. Dacal,* J. Geaga, J. W. Harris,† J. Miller, H. G. Pugh,
R. E. Renfordt,‡ L. J. Rosenberg, A. Sandoval,† L. S. Schroeder, H. E. Stelzer,† R. Stock,†
H. Strobele,† and K. L. Wolf§

In reactions of heavy ions at relativistic energies, the multiplicity of secondary particles can be very large. For example in a collision between Ar + KCl, 60 charged particles have been observed, exceeding the number of protons in the target and projectile combined. In order to extract information about possible reaction mechanisms it is desirable to detect as many of these particles as possible.

A triggered streamer chamber offers the possibility of detecting charged particles with 100% efficiency in a 4π geometry, either for an unbiased sample of events or for events selected according to some criterion imposed by the trigger conditions. The LBL streamer chamber has a sensitive volume of 126 x 59 x 40 cm^3 in a 1.32 tesla field. The primary ionization in the 90% Ne - 10% He gas mixture at S.T.P. is amplified by a factor of 10^8 by a 10 ns 700 kV pulse applied across the chamber subsequent to detection of an event by the trigger detectors. The streamers produced along each track are photographed on high-speed 35 mm film in three-view geometry. The chamber can be triggered 3 to 4 times per second, limited by the film advance mechanism and the charging time of the Marx generator. The memory time of the streamer chamber is about 2 μs.

Basic trigger modes for the streamer chamber are derived from small scintillators placed along the beam line, in particular an upstream scintillator just before the target and a downstream scintillator some distance after the target along the beam trajectory. In the "inelastic" trigger mode the pulse height from the downstream scintillator is required to differ from the pulse height for beam particles by sufficient to indicate that an interaction has occurred in the target. In the "central" trigger mode the downstream scintillator is required to have essentially no pulse, indicating that the projectile has been destroyed by the interaction. Studies of stream chamber pictures in the two modes indicate that the central triggers for Ar + KCl collisions correspond closely to the selection of head-on nuclear collisions. Other trigger modes are possible with the existing set up, and a hodoscope array presents the possibility of tagging each event with scintillator pulse heights to provide additional information for particle identification.

The pictures are scanned and measured manually. Information obtained directly from the scanning includes results on the number of negative pions produced per collision as a function

Table I.

Projectile	Target	Beam (GeV/A)	Trigger: Inelastic	Trigger: Central	Trigger: Other
Ar	KCl	0.4 - 1.82 (8 energies)	x	x	
	BaI_2	0.8	x	x	
	Pb_3O_4	0.4, 0.8		x	
^4He	KCl	1.0, 1.8	x		
	BaI_2	1.0, 1.8	x		
p	KCl	2.1	x		backward
	BaI_2	2.1	x		backward
	Pb_3O_4	2.1	x		backward
^{12}C	BaI_2	0.2			test run

verted gammas, or lambda charged decays. After measurement and reconstruction of the events in three dimensions, the particles' momenta and emission angles are extracted. The main characteristics of the reconstruction are: 4π solid angle and 100% efficiency for charged particles, lower threshold of less than 1 MeV for protons and vertex position resolution of ~ 1 mm, $\Delta p/p$ < 5%; angular resolution < 1° and limited charge resolution.

The exposures listed in Table 1 have been made and are in the process of analysis: of bombarding energy, and on the number of "vees" produced corresponding to kaons, con-

The following experiments have been approved for future running:

- Study of pion and hyperon production in equal mass systems,
- Intermediate energy (100-200 MeV/A) heavy ion reaction mechanisms, and
- Test of the streamer chamber capabilities for U beams.

These experiments are collaborations between the basic LBL/GSI group and one or more from Argonne National Laboratory, University of Arizona, University of Marburg, and University of Mexico. The University of California at Riverside (R. T. Poe et al.) also has a program using the streamer chamber.

Some modifications and improvements to the system that are in progress or under investigation are improvements in the gas mixture, stabilization of the Marx generator, use of image intensifiers, construction of external hodoscope and trigger arrays, semiautomatic reconstruction, and use of CCD cameras and image digitization.

Footnotes

*Instituto de Fisica, UNAM, Mexico

†GSI, Darmstadt, West Germany

‡Universty of Marburg, West Germany

§Now at Argonne National Laboratory, Argonne, IL 60440

A GLOW MEMORY CHAMBER FOR USE IN THE MEASUREMENT OF HIGH MULTIPLICITY EVENTS*

M. A. Elola, T. A. Mulera, V. Perez-Mendez, and P. E. Wiedenbeck

One characteristic of relativistic heavy ion collisions is the high multiplicity (50-100 secondary particles) of a "typical" event. Information regarding the multiplicity, both its magnitude and any directional information, is desirable as an indicator of the violence of the collision and in the study of such phenomena as jet formation, hydrodynamic splash or other forms of collective behavior. We have been working to develop and build a detector capable of providing such information for use as a target area detector in the Heavy Ion Spectrometer System (HISS) at the Bevalac.

Conventional wire chamber readout techniques are plagued by x-y correlation ambiguities when more than one particle is registered in the chamber. In fact, to completely resolve all such ambiguities for n particles requires the reading out of n + 1 separate coordinates. Clearly, resolution of the ambiguities involved in an event of multiplicity, say 50, by this method would be prohibitively expensive. The reading out of each separate x-y coordinate in the detector via, for example, charged coupled devices is likewise an expensive solution to the problem. In our scheme, the x-y ambiguities are resolved in an inexpensive fashion by employing the detector itself as a correlated event memory, a method first suggested by Neumann and Sherrard.[1]

The passage of a charged particle through our apparatus is used to ignite a glow discharge at the point of passage. This ignition may be achieved through the use of pulsed spark chamber techniques or by some less cataclysmic avalanche method. Once ignited, the flow discharge may maintained by a dc potential of several hundred volts for an indefinite period of time. This "memorization" of the position of the event allows the x-y correlation ambiguity to be resolved as follows. Each wire of one coordinate, say x, which registers a hit is successively interrogated by the superposition of a voltage pulse over the dc glow maintenance voltage. The wires of the y-coordinate are then examined for the transmissions of this pulse through the conductive glows. In this way, the x-y positions of the glows, and thus of the hits, are determined in an unambiguous way.

A large effort has been expended in studying the glow discharge mechanism and in prototyping glow discharge memory gaps. A "honeycomb" cell structure has been developed that gives good glow stability, multiple hit efficiency, and that prevents the ignition of spurious glows in cells neighboring the location of the desired glow. Development of a readout system to locate these glows is being carried out with the help of the Physics Instrument Systems Group.

Ignition of glow discharges may be achieved by placing a conventional spark chamber gap atop the glow memory gap. Residual ions and ultraviolet light from the spark serve to ignite a glow discharge in the cell nearest the spark.

Because of the traditional problems of long dead times and high radio frequency noise levels associated with the use of spark chambers, alternative ignition methods are being investigated. Two such methods are ignition by ultraviolet light produced in gas scintillations, and ignition by the production and multiplication of electron ion pairs in an avalanche less cataclysmic than a spark discharge, i.e., an avalanche taking place in the proportional or Geiger regime.

The final version of the multiplicity detector will surround the HISS target and will have an active area subtending as much of 4π steradians as is compatible with construction requirements.

Footnote and Reference

*Condensed from an LBL report in preparation and a paper submitted to the International Conference on Nuclear Physics, Berkeley (1980).

1. M. J. Neumann and T. H. Sherrard, IEEE NS-12, 379 (1965). An elaboration on this idea may be found in H. Kobayakawa and T. Yamaki, Int. Conf. on Instrumentation for High Energy Physics, Frascati (1973).

RESPONSE OF NaI:Tl TO RELATIVISTIC Ne, Ar, AND Fe

M. H. Salamon and S. P. Ahlen*

An exposure of a 1/2 inch thick commercial Harshaw NaI:Tl crystal scintillator to relativistic ^{20}Ne, ^{40}Ar, and ^{56}Fe ions was performed at the Bevalac. The fixed 600 MeV/amu beams were nearly continuously degradable in energy by an extremely precise, automated Pb absorber[1] upstream of the crystal. A silicon detector midstream of the absorber and crystal discriminated against ions that had undergone charge reducing nuclear interactions in the absorber. The NaI:Tl crystal's sole transparent face emitted into the interior of a light diffusion box, which by randomizing the light direction before PMT (EMI9817Q) detection effectively eliminated variation in spatial response. Calibration between runs was maintained by a ^{241}Am-doped NaI:Tl crystal permanently affixed to the light diffusion box; temperature control was maintained to minimize thermal crystal response variation (< 0.4%).

The scintillation efficiencies $dL/d\epsilon$ (ϵ = total kinetic energy) were determined by differentiation of a fitted function $L(\epsilon)$, the light output of an ion of energy ϵ entering an infinitely thick crystal, to the data $\Delta L = [L(\epsilon_{in}) - L(\epsilon_{out})]$ versus ϵ_{in}. The resulting fit is excellent, as seen in the inset in Fig. 1 (the cusp corresponds to maximum energy deposition in the crystal, as the ion stops just at the exit surface). The efficiencies thus determined are shown in the figure, along with the scintillation efficiency of cosmic ray secondary (atmospheric) muons (minially ionizing) measured separately with the same crystal-light diffusion box configuration. Thirty radiation lengths of Pb eliminated contaminating shower electrons, and a widely separated, triple detector coincidence requirement eliminated both noise and non-vertical muons.

The rough error bars on the ion data, shown at both ends of the curves, are based on magnitudes of variations resulting in $dL/d\epsilon$ from insertion of artifical normally distributed errors on top of the raw data which gives an estimate of $dL/d\epsilon$ inaccuracy, as well as on estimated inter-run calibration errors. The muon error is based on the estimated error in peak assignment in the Landau distribution collected during the muon exposure.

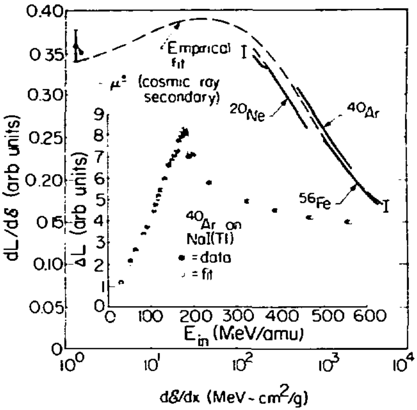

Fig. 1. (XBL 808-1701)

Compared to organic scintillators, NaI:Tl evidences a remarkable lack of dependence on track structure (radial variation of energy deposition), evidenced by the fact that the ion's $dL/d\epsilon$ nearly falls on a universal scintillation efficiency curve. The gross structure of this curve is similar to that observed for low energy data (e^-, p, α, $2 < Z < 10$).[2,3]

An empirical curve may be fit to the efficiency data that is based on mixed mono- and bi-molecular reactions occurring between uncorrelated electrons and holes and between excitons. Postulating a certain exciton production fraction, the kinetics may assume the form $dn/dt = -k_1 n - k_2 n^2$, where the first term contributes to radiation (quenching) for excitons (electrons) and the second to quenching (radiation) for excitons (electrons). The solution has the form $dL/d\varepsilon \propto (1 - \lambda) + \frac{1}{S}[a \ln(1 + \frac{\lambda}{S} S) - b \ln(1 + (\frac{1-\lambda}{b}) S)]$ where $S = d\varepsilon/dx$ ($MeV\text{-}cm^2/g$) and λ = exciton fraction. The fit shown (dashed line) is for $\lambda = 0.75$, $a = 275$, $b = 1.0$, with normalization constant 0.433.

Although the physical significance of the kinetic equation is limited, the fit it affords can be of use to those needing NaI:Tl response information in heavy ion experiments or heavy element cosmic ray experiments.

Footnote and References

*Also at Space Sciences Laboratory.

1. This automated absorber can be made available to other experimentalists at LBL. Please contact the authors.

2. R. B. Murray and A. Meyer, Phys. Rev. 122, 815 (1961).

3. J. B. Birks, The Theory and Practice of Scintillation Counting, (Pergamon Press, 1964).

A RANGE-ENERGY PROGRAM FOR RELATIVISTIC HEAVY IONS IN THE REGION 1 < E < 3000 MeV/amu*

M. H. Salamon

A computer program is now available on PSS at LBL's Computer Center that calculates stopping power (dE/dx), range, or energy using the prescription of Ahlen[1,2] which is accurate to $\leq 1\%$ in the regime of high charge Z and relativistic energies.

Starting with the well known Bethe formula for stopping power, derived quantum mechanically in the first Born approximation ($(Z\alpha/\beta) \ll 1$), several correction terms are added which maintain accuracy as Z increases past the point of validity of the Bethe expression:

(1) the Bloch correction bridges the gap between the quantum ($Z\alpha/\beta \ll 1$) Bethe and classical ($Z\alpha/\beta \gg 1$) Bohr stopping powers, giving the Bethe-Bloch formula:

(2) the Mott correction term is based on expansions of the Mott cross-section which contribute close collision stopping power terms up to Z^7;

(3) the Z^3 low velocity polarization correction terms adjust for failure of the impulse approximation made in the Bethe-Bloch treatment;

(4) the shell effect term corrects for failure of certain assumptions in stopping power derivations when the ion velocity drops below any of the atomic electronic shell velocities;

(5) the standard expression for the density effect is included;

(6) the effective charge of the projectile ion is calculated to account for electron pickup.

Above 8 MeV/amu, range-energy tables are calculated by integration for dE/dx. For E < 8 MeV/amu, the expressions for dE/dx becomes unreliable and empirical range-energy relations[3] are relied on.

The full report discusses use of the program, and the program itself is an appendix. Copies of the program may be obtained by executing the control card

LIBCOPY, EXTUSER, X, INTRO, RDEDX, RRANGE, RNERGY.

and DISPOSE-ing the file X as desired.

Footnote and References

*Condensed from LBL-10446 (1980).

1. S. P. Ahlen, Phys. Rev. A17, 1236 (1978).

2. S. P. Ahlen, Rev. Mod. Phys. 52, 121 (1980).

3. W. H. Barkas and M. J. Berger, in Studies of Penetration of Charged Particle in Matter, Natl. Acad. Sci. Publ. 1133 (1964).

MEASUREMENT OF HIGHER ORDER CORRECTIONS TO STOPPING POWER FOR RELATIVISTIC Ne, Ar, AND Fe Beams*

M. H. Salamon, S. P. Ahlen,† K. C. Crebbin, and G. Tarle†

Measurements of range of 600 MeV/amu ^{20}Ne, ^{40}Ar, and ^{56}Fe in absorbers of Al, Cu, and Pb have been made to test the accuracy of the higher order Mott, Bloch, and polarization correction terms[1,2] to the Bethe expression of stopping power.

After extraction from the accelerator and passage through a series of accurately known upstream materials, the ions were slowed to nearly stopping in each of the three primary absorbers (Al, Cu, Pb); the residual range was traversed in a stack of a few hundred thin (~ 0.03 g/cm^2) sheets of Lexan polycarbonate plastic. Subsequent chemical etching exposed stopping tracks, yielding a mean ion range. By integrating dE/dx through the complete list of stopping matter, initial (extraction) energies were calculated. These computed energies varied, depending upon which correction terms mentioned above were or were not included in the expression for dE/dx. To be compared to these calculated energies are the actual beam energies, which were determined by using the Bevalac itself as a time-of-flight device,[3] providing unparalled beam energy accuracy.

Figure 1 summarizes the results, where three sets of data, one for each absorber, are shown. The ordinate gives the percentage deviation of the integrated energies from the actual measured beam energies which determine the ordinate zero; the measured beam energy errors are represented by horizontal dashed lines. Shown are integrated energies calculated using a dE/dx expression with no correction terms added (o), with all but the Bloch term added (□), and with all the expected correction terms added (Δ). Systematic and random thickness uncertainties in the matter list contribute to the error bar. The larger error bar also includes a systematic uncertainty in the I_{adj} of the absorber.

The failure of the Bethe expression at high Z is unequivocal. Although the fully corrected dE/dx (Δ) is within errors, the fact that the absence of the Bloch term (□) provides nearly as good a fit suggests that a relativistic calculation of the Bloch term (presently a non-relativistic calculation) might yield a correction of smaller magnitude.

As Z→0, one demands that higher order corrections in Z vanish with respect to the

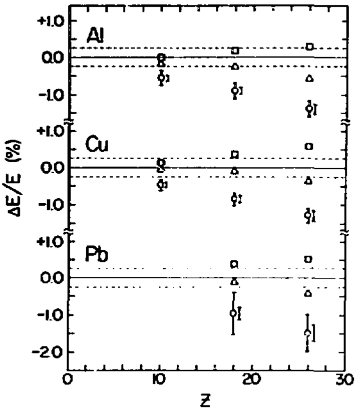

Fig. 1. Deviations of calculated (integrated) energies determined by time-of-flight methods versus ion charge, for three absorbers (Al, Cu, Pb). (XBL 806-10380)

Bethe expression, i.e., all the integrated energy points should coverge to $\Delta E/E = 0.0$ (within errors). Extrapolation confirms this, reinforcing confidence in the independent calculation of the actual beam energies.

Footnotes and References

*Condensed from paper submitted to Phys. Rev. Lett.

†Also at Space Sciences Laboratory

1. S. P. Ahlen, Phys. Rev. A17, 1236 (1978).

2. S. P. Ahlen, Rev. Mod. Phys. 52, 121 (1980).

3. K. C. Crebbin, LBL-11669 (1980).

4. M. H. Salamon, LBL-10446 (1980).

BEVALAC DATA ACQUISITION PROJECT

Chuck McParland*

The Bevalac software effort is nearing the end of its second year. This effort has produced a software system (QDA-MULTI) that is currently installed and in use on six DEC PDP-11's at the Bevatron.

Experimental software needs at the Bevatron vary greatly. To be generally useful, the system must be adaptable to experiments ranging from a weekend effort at an existing experiment facility to a year-long development of a new beam line or detector system. To this end the system attempted to meet several design goals:

1) To provide a common "core" of data acquisition programs for all PDP-11 machines in use at the Bevatron,
2) To structure the system to easily accommodate user-written, experiment specific code, and
3) To allow (i.e., require) experimenters to specify CAMAC data sources and FCNA codes to be used in reading them.

The degree to which experimenters are required to program this system varies. Many experimenters need specify nothing more than the commands required to access the proper CAMAC modules. The software for experiments of this sort can be assembled in a few hours. For these experiments, QDA-MULTI is almost a ready-to-run system.

Most Bevalac experiments, however, require the addition of experiment-specific programs. These consist of user-written analysis rountines within MULTI, special MBD data acquisition code, or user-written displays. In one instance, experimental needs have required the addition of several parallel analysis tasks that display their results through MULTI. For these applications, QDA-MULTI should be viewed as a software structure which has been only partially filled in. The "empty" routines are there to accept experiment-specific code.

Experience at the Bevatron shows this philosophy of experimenter-software involvement to be a realistic one. Future plans for 1981 include greater use of disk spooling, enhancement to MULTI, increased histrogram storage, and addition documentation to aid in user-written software.

Footnote and Bibliography

*Space Sciences Laboratory, University of California, Berkeley, CA 94720

1. Fermilab MULTI User Gude, Fermilab PN77.4, Sept. 1, 1978.

2. E. Harvey, "Data acquisition using PDP-11 and MBD branch drive at LBL," IEEE Trans. on Nucl. Sci. NS-26, 4633 (1979).

TRAJECTORY RECONSTRUCTION AT HISS

Douglas D. Tuttle

As part of the HISS facility, we are providing a complete method for trajectory reconstruction. This method requires the creation of reconstruction software and magnet mapping hardware.

The hardware portion consists of a three-component magnetic field mapper, a microprocessor-based controller and interface to the VAX. The mapper will have three Hall probes mounted mutually orthogonal to one another, one for each field component. Each Hall probe signal will be digitized and passed to the VAX via CAMAC and a PDP 11/34. The Hall probes will be moved sequentially through a sufficient number of three-space positions to define the whole magnetic field to an accuracy of ~ 1 - 3 x 10^{-4} of $|B|_{max}$. Probes and amplifiers of this accuracy are readily available. The probes will most likely require some form of temperature stabilization (~ 1-10°C). Electric motors under control of the microprocessor will move the probes to the required positions. The probe positions will be continuously sensed by linear encoders and/or a combination of shaft and linear encoders, and will be digitized and read into the controller. Software in the controller will enable measurement and buffering of ~ 256 points of data. Software for an entire field map will reside in either the 11/34 or the VAX. Complete field maps will reside on a VAX disk file.

Since the HISS facility already has an NMR system, the drift in the normalization of the field can be monitored. Also, because the required coordinates are generated in the controller, errors due to known mechanical distortions can be corrected for, e.g., gravitational "sag" and thermal expansion and contraction.

The field will be measured on a uniform grid of points that lie on the surface of a rectangular volume. The field at interior points will be obtained by solving Laplace's equation with the measured boundary conditions. Exterior points will be obtained by Taylor's series extrapolation.

There will be approximately 40,000 field measurements made, taking each approximately 1 second. Thus, 10 hours will be required to measure one map. If the entire volume were to be measured (instead of reconstructed), nearly a week would be required. Thus, reconstruction greatly reduces the mapping time.

Once the field is reconstructed a large sample of trajectories (~ 10,000) will be found by numerical integration. Trajectory reconstruction will then consist, essentially, of interpolation between these sample trajectories. Our method of using Chebychev polynomials will closely parallel a fast and efficient method developed at CERN by H. Wind.

To date, both field and trajectory reconstruction software are operational but need modifications before they are ready for general use. They are, however, ready for complete testing, including a modelling of the effects of mechanical distortions in the magnetic field mapper and drift chambers on final momentum errors. This is now being done.

In addition to these efforts, a general Monte Carlo program will be provided. Two experiments, 507 and (3?), have already been simulated with a preliminary version of this program. Results were included in the PAC presentations in Nov-Dec 1979.

The magnet mapper is still in the design phase. A time line will be established about about August 5, 1980, and a complete design will be ready about September 1, 1980.

HISS DETECTOR SYSTEMS

Hank Crawford,* Jim Carroll,* Fred Bieser,* Shoji Nagamiya and James Symons

The first five experiments at the HISS facility will be performed between March and June of 1981. These Phase I experiments require analysis of multiple particles from each event to investigate the energy transfer spectrum, the production of very high transverse momentum light and heavy fragments, the role of electromagnetic excitation in nuclear fragmentation, and the size of the interaction region in relativistic nucleus-nucleus reactions. To accomplish this program required collaboration among all the experimental groups to design and construct a set of detectors common to all experiments that could be easily reconfigured to meet the specific needs of each measurement. The system must measure the charge, mass and momentum of up to 10 fragments from each interaction

The Phase I detector system consists of three major subsystems. To measure rigidity (= P/Z) we use two large (1 x 2 m) drift chambers based on our ISEE-3 satellite drift chamber design[1] in conjunction with the HISS magnetic field. To measure charge Z we will use a 1 x 1 x 0.5 m xenon-filled ionization chamber, and sample the ionization along the fragments' path up to 50 times.[2] To measure velocity we use both a scintillator array (30 pieces, each 200 x 10 x 2 cm) for time of flight and a silica aerogel Cerenkov hodoscope.[3] In addition we will employ two position sensitive parallel plate avalanche chambers to define the incident particle vectors. With the system configured as shown in Fig. 1 we expect to attain charge resolution of ~ 0.2e at Z = 26, mass resolution of < 0.3 amu at A = 20 and momentum resolution of < 10 MeV/c for each fragment.

This system is scheduled for completion in November 1980. Fabrication of the drift chamber parts at UCLA is almost complete, with one of the large chambers ready for the winding shop. Construction of the xenon ionization chamber has begun at UCD, and test at the 88 Inch Cyclotron

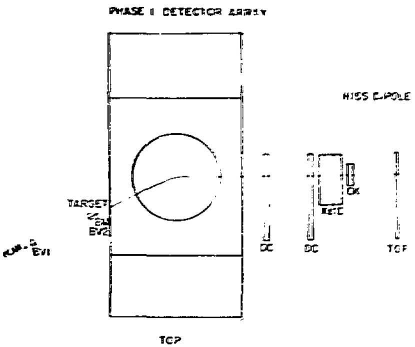

Fig. 1. (XBL 807-10739A)

are planned for the fall. The time of flight array, with a time resolution of 70 psec FWHM attained on the first sample in a 1.88 GeV/nucleon Fe beam, is being fabricated in Japan.

Footnote and References

*Space Sciences Laboratory, Berkeley, CA 94720

University of California, Los Angeles, CA 90024

1. D. E. Greiner, JF. S. Bieser, and H. H. Heckman, Proc. IEEE on Geosci. Elec. GE-16, 163 (1978).

2. M. Aderholz et al., NIM 118, 419 (1974).

3. M. Cantin et al., NIM 118 (1974).

PLASTIC WALL SCINTILLATOR DETECTOR ARRAY*

A. Baden, H. H. Gutbord, M. Maier, J. Peter,† H. G. Ritter, H. Stelzer, A. I. Warwick, F. Weik, and H. Wieman‡

An array of plastic scintillators, called the "plastic wall," has been developed for use in heavy ion reaction studies at the Bevelac. This 150-element, time-of-flight detector, shown in Fig. 1, was designed for use with the 4π solid-angle plastic ball system.[1] It will cover the most forward scattering cone (0° to 9°).

The plastic wall covers an area of 192 x 192 cm, and consists of scintillators arranged in two areas: the inner area and the outer area. The inner area is a square of 48 x 48 cm consisting of 36 individual counters each 4 cm thick. At a distance of 6 m from the target in the plastic ball, this area covers an angular region of about 0° to 2.5°. The outer region extends to 9° and consists of 60 pairs of position-sensitive scintillation detectors. The distance of 6 m corresponds to flight times varying from 24 nsec at 800 MeV/n to 65 nsec at 50 MeV/n. The width of the scintillators of 8 cm results in an angular resolution of 0.75°.

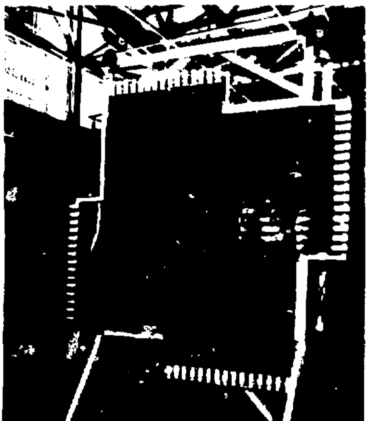

Fig. 1. Outer portion of the plastic wall scintillator detector array. (CBB 799-12302)

The purpose of the inner region of the plastic wall is to provide the information necessary to form an event trigger for both the plastic ball and the wall. This is achieved by comparing the inner wall signals with those of an upstream beam counter. The fragments are identified by their time of flight and their pulse height in the scintillators. The trigger can thus be defined by selections on fragment velocity and/or on nuclear charge in the 36 counters. A fragmentation can lead to several fragments hitting the inner regions, so a subdivision into 36 individual detectors allows us to identify the degree of fragmentation.

The purpose of the wall's outer region is to detect the reaction products or projectile fragments at angles between 2° and 9° with sufficient angular resolution and multiparticle detection capability. It is made of 60 position-sensitive double modules, each consisting of two scintillator rods with dimensions of 72 x 8 x 4 cm thick. Each scintillator of the double module is viewed by one photomultiplier at different ends (Fig. 2). The time difference between the two photomultiplier signals give the longitudinal position of the particle in the double module; the mean time gives the flight time from the upstream detector.

For high-energy charged particles the dE/dx in one or both scintillators combined with the time of flight allows us to detect Z and E/A. For energies below 1220 MeV/n, particles are stopped in the wall. Thus the velocity measurement and the E information determines the mass of the stopped particles. The double coincident dE/dx information for particles above 80 MeV/n, furthermore, allows one to discriminate against neutron and gamma response in the scintillators, which is rather important because as many neutrons as protons are expected for light projectiles at forward angles.

The outer region of the wall has already been used in an experiment to study slow target fragments in coincidence with fast charge particles.[2] Beam velocity and slower (Z = 1 and 2) particles were identified in the 2.5° to 9° cone with this detector using a variety of projectiles (P, He, C and Ne, ranging in energy from 250 to 4900 GeV/n). The time resolution obtained between scintillators in the pairs was better than 350 psec (FWHM), thus providing a longitudinal position resolution better than the 8 cm width of the scintillators. Preliminary scans of the data have shown an in-plane enhancement of light particles observed in the wall, correlated with heavy slow fragments at large angles. Also, multiple hits in the wall tend to be localized rather than spread symmetrically about the beam axis.

TOF-PLASTIC WALL

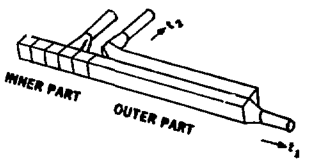

Fig. 2. Schematic view of scintillator elements from the plastic wall array. (XBL 7910-12432)

Footnotes and References

*Collaboration of Gesellschaft fur Schwerionenforuschung, Darmstadt and the University of Marburg, West Germany, and Lawrence Berkeley Laboratory.

†Visitor from I.P.N., 91406 Orsay, France.

1. A. Baden et al., in this annual report.

2. H. H. Gutbrod et al., in this annual report.

CHARGED PARTICLE IDENTIFICATION WITH MODULES OF THE PLASTIC BALL

H. H. Gutbrod, M. Maier, H. G. Ritter, A. Warwick, F. Wiek, H. Wieman and K. Wolf*

In the low energy pion line at LAMPF a set of 13 plastic ball modules (see Fig. 1) was used to measure the efficiency and particle separation capability of the plastic ball detector[1,2] for pions and protons.

Each module is a ΔE-E detector wherein the ΔE counter is a 4 mm thick CaF_2 crystal. The E counter consists of a 36 cm long plastic scintillator. Both are optically coupled and read out by one photomultiplier. ΔE and E signals are separated via pulse shape analysis. In addition to the ΔE-E identification the positive pions are detected by their delayed $\pi^+ \rightarrow \mu^+ \rightarrow e^+$ decay. This is achieved by measuring the energy of the positron and the decay time for the $\mu^+ \rightarrow e^+$ decay.

Thirteen modules out of the 815 were chosen such that the response of different module types and the effect of scattering out of particles into neighbouring modules could be measured. The individual modules were studied for geometrical effects, e.g., by injecting the beam at the center, a corner, or a triangular side.

The energy was varied between 30 and 300 MeV for pions and between 30 and 90 MeV for protons. An excellent separation between pions and protons could be obtained. The overall energy resolution is better than 5 . Most of the events in which particles scatter out of the module during the process of slowing down can be reconstructed by summing up the energy signals of neighboring modules. This procedure is especially important for obtaining a high detection efficiency for the pions, where the decay positron is usually stopped in more than one module.

Fig. 1. Plastic ball modules under test at the low energy pion channel, LAMPF. (CBB 808-9285)

Footnote and References

*Collaboration of Lawrence Berkeley Laboratory, Gesellschaft fur Schwerionenforschung, and Argonne National Laboratory.

1. M. R. Maier, H. G. Ritter, H. H. Gutbrod, IEEE Trans. NS-27, 42 (1980).

2. Bevalac Proposal 488H, Lawrence Berkeley Laboratory.

POSITION-SENSITIVE PARALLEL PLATE AVALANCHE COUNTERS

H. Stelzer* and A. Baden

For an experiment[1] at the Bevelac we have built two parallel plate avalanche counters that measured, in addition to timing, the position of the incoming particle in one direction. The spectrum of particles to be measured ranged from light particles, like Be, to heavy fragments. The two counters were placed on both sides of the target parallel to the beam direction. The reaction products from the target, after passing one of the avalanche counters, were stopped in an array of 28 silicon detectors, which measured the energy and the time-stop signal. The flight-path of this TOF telescope was only 31 cm. The impact point on the avalanche counters was measured along the beam direction and this information, together with the silicon detector that showed the stop signal, gave the interaction point on the target. The target had an angle of 15° to the beam.

The sensitive areas of the avalanche counters were 160 x 30 and 90 x 50 mm, respectively. The outer dimensions of the detector housing were 205 x 84 x 26 and 135 x 94 x 26 mm, respectively.

The construction of the counters and the position readout was done in a similar way, as described in Ref. 2. The two electrodes were made of 15 $\mu g/cm^2$ Formvar foils and glued onto epoxy frames (Fig. 1). The foils were then evaporated with 20 $\mu g/cm^2$ silver. Onto the cathode 4 mm wide strips (< 0.55 mm separation) were evaporated by means of a mask. Due to the heat sensitivity of the fragile foils, the evaporation process had to be done in about 10 steps, with cooling-down periods in between. The two electrodes were mounted exactly parallel to each other with a gap of 1.9 mm. The construction allowed an easy gas-flow through the gap.

The timing signal was taken off from the anode. The individual stripes of the cathode plane were connected to a chain of 100 Ω resistors (cf. Fig. 1). The ends of this resistor chain were connected to linear amplifiers, and the position was determined by the charge-division method. The windows of the detector housing were stretched polypropylene foils (40 $\mu g/cm^2$ thick). The total thickness of such a counter was 150 $\mu g/cm^2$ as determined by an energy-loss measurement.

The counters were operated at 6 mb isobutane at 470 V. The applied high voltage was kept relatively low. Alpha particles from a ^{252}Cf source were still detected (with reduced efficiency) and strongly ionizing particles did not develop a spark. Thus reliable operation of the counters during weeks of running time could be maintained.

The TOF-telescope was frequently calibrated with α's and fission fragments from a ^{252}Cf source. Figure 2 shows such a calibration spectrum. The α- and the fission-peaks allow a measurement of the plasma delay of silicon detectors for heavily ionizing particles. We

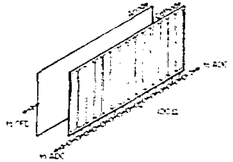

Fig. 1. Position-sensitive parallel-plate avalanche counter. (XBL 807-1684)

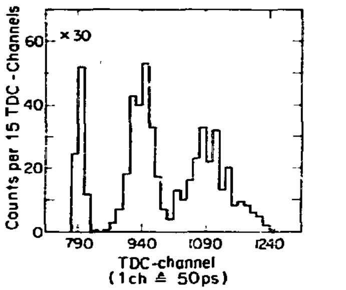

Fig. 2. TOF-spectrum of a ^{252}Cf source. The α peak (left peak) has been scaled down by 30. (XBL 807-1685)

measured a plasma delay of 1.5 ns, which is very close to the published value[3] (1.8 ns). This shows that, if at all, there is only a weak dependence of the timing output of an avalanche counter on the type of the incoming particle.

Footnote and References

*Gesellschaft fur Schwerionenforschung, Darmstadt, West Germany

1. A. Baden et al., contribution to this annual report

2. Y. Eyal, H. Stelzer. Nuc. Instr. and Methods 155 (1978) 157.

3. H. Henschel and R. Schmidt. Nucl. Instr. and Methods 151 (1978) 529.

A SIMPLIFIED CONSTANT FRACTION DISCRIMINATOR CIRCUIT FOR APPLICATION IN MULTICHANNEL DISCRIMINATORS

M. R. Maier*

The original circuit of the constant fraction discriminator[1] (CFD) has been simplified (see Fig. 1). It uses now only two integrated circuits. This version is therefore particularly suited for the constructon of multichannel CFD's. We have built two versions of the multi CFD, one quad CFD (21x414, LBL) and an octal CFD ("wall-box," GSI).

The quad CFD has all controls on the front panel, i.e., threshold, walk adjust, and dead time. Each channel has three logic outputs, two with short, clipped signals, and one which shows the dead time--these are all fast NIM negative signals. It has also an inspect output for walk adjustment purposes.

The octal CFD, because of limited front panel space, has only two outputs per channel; one produces a clipped signal, the other shows the dead time; all are fast NIM signals. There is a common threshold control and a common deadtime control for all eight channels. The walk adjustment is done internally with a gated base line restorer. In addition, the wall-box has an OR output, where all channels are OR-ed together, and a multiplicity output, which produces 100 mV with a source resistance of 50 Ω per channel fired. For the application in the plastic ball experiment, it has a linear sum output, which gives the sum of all input signals (divided by 16). On the back panel there are eight linear outputs, AC coupled emitter followers that isolate the digital logic from the analog circuitry. There are also eight additional logic outputs, with positive going MECLO signals.

These multi-CFDs use plug-ins to define the fraction, which can be easily changed. Different plug-ins can be used to reconfigure the input stages as leading edge or zero cross dis-

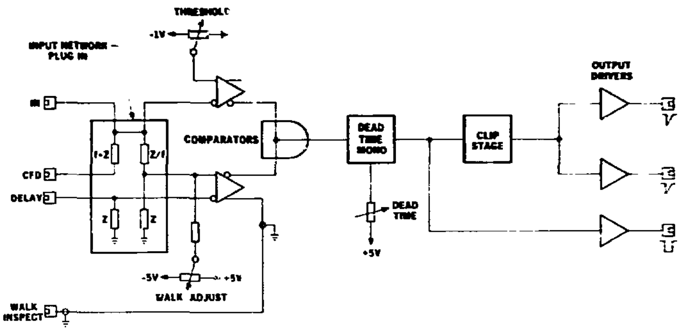

Fig. 1. Simplified constant fraction circuit. The input comparators are fast dual ECL comparator IC's; the dead time monostable and the CLIP stages are a dual ECL flipflops with proper feedback. Note the wired-AND connection on the outputs of the comparators. (XBL808-11106)

criminators. The delay for the constant fraction has to be supplied externally. The CFD delay should be equal to the pulse-rise time multiplied by (1 - fraction):

$$t_{CFD} = t_{rise}(1 - \text{fraction}).$$

The range of amplitudes at the input is -5 mV to -5 V. Minimum input pulse width is ? nsec FWHM, and the minimum rise time is 500 ps. Since we now use faster ICs than in the original circuit,[2] the walk of these units is less than 100 ps for input pulses between -50 mV and -5 V[3].

Footnote and References

*Visitor from University of Marburg, West Germany.

1. M. R. Maier, P Sperr, NIM87, p. 13.

2. M. R. Maier, D. A. Landis, NIM 117, p. 245.

3. G. F. Wozniak, L. W. Richarson, M. R. Maier, separate contribution to this annual report.

IMPROVEMENTS TO THE MULTI ON-LINE ANALYSIS SYSTEM

Friedemann Weik*

To increase the on-line analysis facility above the level provided by the MULTI system,[1] which is mostly used at the Bevalac PDP-11 computers, a parallel analyzing task (ANALTK) has been developed.

The main part of this task is a set of user-written Fortran subroutines, independent for different problems or users, which have an initialization part to define the histograms with their names and limits, and an analysis part in which the histrogramming itself is done by a call to an ASSEMBLER subroutine. The use of ASSEMBLER has been chosen to increase the speed and to reduce the necessary space. This is true for all other parts of the task too. Furthermore, to keep the command-handler of ANALTK as small as possible, it has only a CLEAR and a MOVE function. The MOVE sends a histrogram to MULTI and enables an additional activity like a display or print.

The histogramming space in ANALTK can have up to 22 k words. The synchronization for each event is done by MULTI and allows only one parallel task to have access to the data. However, by means of a priority changing control task, two to five tasks have analyzed into 420 histograms in parallel and by that means sampled the incoming data for the 489H experiment,[2] which had 455 data words per event.

Additonal changes to MULTI have been made to improve its possibilities in this kind of experiment.

To give an overview over the whole event or a selected part of it, there is now a special two-dimensional display mode, for which the y-position is the number of the word within the event, and the x-position is the value of that word (see Fig. 1). This gives something like a "footprint" of an event. The superposition of many events in such a display has recognizable structure, for example Fig. 1 shows pulser data peaked in each spectrum.

Another overview facility is a histogram for which each channel is dedicated to one word within the event and is only incremented if the value of that word lies between selected limits. By this a "noisy" detector in an array of equivalent ones shows as a peak, a nonfiring detector as a drop in the histogram.

The newest feature is a vector variable type, which points to a consecutive group of words in the integer-, real-, or data-array. By this means more than one variable can be the input to one histogram or to a two dimensional dot display. In the latter case each value of the first vector is displayed against the corresponding value of the second.

In the near future the implementation of two-dimensional histrograms in ANALTK and their display in MULTI is planned.

Footnote and References

*Gesellschaft fur Schwerionenforschung, D-6100 Darmstadt, West Germany.

1. J. F. Bartlet et al., Fermi Laboratory report PN-97.4.

2. A. Baden et al., in this annual report.

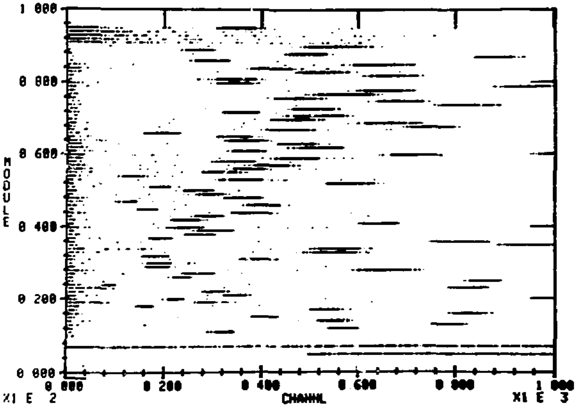

Fig. 1. Simultaneous display of pulser data in all 455 spectra produced by the detectors of Bevalac experiment 489H. (XBL 808-10939)

PART 3. APPENDICES

Thesis Abstracts

DEVELOPMENT OF THE HELIUM-JET FED ON LINE MASS SEPARATOR RAMA AND ITS APPLICATION TO STUDIES OF T_z = -2 NUCLEI*

Dennis Michael Moltz

The study of nuclei far from beta stability is hampered greatly when the nuclide of interest decays in a manner identical to that of a nuclide produced in greater yield in the same bombardment. Attempts to observe the protons associated with the decay of the A = 4n, T_z = -2 series of beta-delayed proton emitters failed because of the large number of protons arising from the strong beta-delayed proton decay of the A = 4n+1, T_z = -3/2 nuclides. One solution to this problem is through the use of an on-line mass separator. Development of the Berkeley helium-jet fed on-line mass separator RAMA is discussed as applied to studies of the A = 4n, T_z = -2 nuclides.

RAMA, an acronym for Recoil Atom Mass Analyzer, has typical efficiencies of 0 1% for ~75 elements with melting points $\leq$2000°C. This efficiency permits decay studies to be readily performed on nuclei with production cross sections >500 μb for γ-ray spectroscopy and ≳1 μb for discrete energy charged particle spectroscopy. The mass range on the normalized RAMA focal plane is ±10%. The quoted efficiency is for a mass resolution of M/ΔM ~300.

RAMA has been used to observe two members of the A = 4n, T_z = -2 series of beta-delayed proton emitters, ^{20}Mg and ^{24}Si. Observation of beta-delayed protons from a mass-separated sample of ^{20}Mg($t_{1/2}$ ~ 95 ms) establishes the mass-excess of the lowest T = 2 (0^+) state in ^{20}Na (13.42 ± 0.05 MeV), thereby completing the mass twenty isospin quintet. A similar measurement of the decay of ^{24}Si ($t_{1/2}$ ~100 ms) establishes the mass-excess of the lowest T = 2 (0^+) state in ^{24}Al (5.903 ± 0.009 MeV). The mass 24 isospin quintet is incomplete because the mass of ^{24}Si remains unknown. In both cases, excellent agreement is obtained using only the quadratic form of the isobaric multiplet mass equation (IMME).

---

*Abstract of LBL-9718 (Oct. 1979).

TRANSFER PRODUCTS FROM THE REACTIONS OF HEAVY IONS WITH HEAVY NUCLEI*

Kenneth Eugene Thomas III

Production of nuclides heavier than the target from ^{86}Kr and ^{136}Xe induced reactions with ^{181}Ta and ^{238}U has been investigated. Attempts were made to produce new neutron excessive neptunium and plutonium isotopes via the deep inelastic mechanism. No evidence was found in this work for ^{242}Np or ^{247}Pu. Estimates were made for the production of ^{242}Np, ^{247}Pu, and ^{248}Am from heavy ion reactions with uranium targets.

Comparisons of reactions of ^{86}Kr and ^{136}Xe ions with thick ^{181}Ta targets and ^{86}Ta targets and ^{86}Kr, ^{136}Xe and ^{238}U ions with thick ^{238}U targets indicate tht the "most probable" products are not dependent on the projectile. The most probable products can be predicted by the equation

$$Z-Z_{target} = 0.43\ (A-A_{target}) + 1.0.$$

The major effect of the projectile is the magnitude of the production cross-section of the heavy products. Based on these results, estimates are made of the "most probable" mass of element 114 produced from heavy ion induced reactions with ^{248}Cm and ^{254}Es targets. These estimates give the mass number of element 114 as ~ 287 if produced in heavy ion reactions with these very heavy targets.

Excitation functions of gold and bismuth isotopes arising from ^{86}Kr and ^{136}Xe induced reactions with thin ^{181}Ta targets were measured. These results indicate that the shape and location (in Z and A above the target) of the isotopic distributions are not strongly dependent on the projectile incident energy. Also, the nuclidic cross-sections are found to increase with an increase in projectile energy to a maximum at approximately 1.4-1.5 times the Coulomb barrier. Above this maximum, the nuclidic cross-section is believed to be due to fission of the heavy products caused by high excitation energy and angular momentum.

---

*Abstract of LBL-9886 (Nov. 1979).

INTERACTIONS OF 100 MeV/NUCLEON ^{40}Ar WITH URANIUM*

Kenneth Alan Frankel

Fragments produced in the interactions of 100 MeV/nucleon ^{40}Ar projectiles with a uranium target have been measured at energies from 10 to 130 MeV/nucleon at angles from 10° to 170°. Nuclei with charge $5 \leq Z \leq 10$ were observed.

The data can roughly be divided into two groups, corresponding to central and peripheral collisions. The central collision data can be fit with a thermal model that uses two recoiling sources. The source velocities are consistent with the predictions of the fireball and target explosion models, but the source temperatures inferred from the data are higher than one would expect on the basis of energy and momentum conservation. These results are similar to those obtained in previous studies at beam energies of 400 and 500 MeV/nucleon. The data also follow the pattern of the universal curve of invariant cross section vs momentum observed at higher beam energies by Price et al. The projectile fragmentation data are also fit by two thermal sources. There are indications that the observed temperatures are higher than one would expect on the basis of other projectile fragmentation studies.

The projectile fragmentation data are studied in terms of a simple friction model. Order of magnitude estimates show that the data may be consistent with the model, but further development, calculation and experimentation are necessary to check the validity of the model at this beam energy.

A preliminary investigation is made of the possibility that the projectile may pick up one or more target nucleons before its fragments. This process leads to widening of the distributions at large momentum transfers.

From this broad survey we find that much of the spectrum can be described by falling exponentials in energy in the emitting frames. We conclude that the observed spectrum is due to nonthermal sources as the temperatures derived from the slopes of the exponentials are greater than those we predict.

---

*Abstract of LBL-10980 (Dec. 1979).

Nuclear Science Division Seminars*

Aug. 6, 1979	Peter Glassel Max Planck Institut	Fission properties of very heavy nuclei nuclei produced in deep inelastic collisions.
Oct. 22, 1979	Robert Stockstad ORNL	Heavy-ion fusion at sub-barrier energies.
Oct. 15, 1970	Gary Westfall	Production of neutron-rich nuclei by fragmentation of 212-MeV/amu ^{48}Ca.
Oct. 22, 1979	Norman Glendenning	Very high energy nuclear collisions and the symptotic spectrum of hadrons.
Oct. 29, 1979	Carolyn Albiston	The effects of giant modes on charge and angular distributions in heavy-ion reactions.
Oct. 29, 1979	Rose Marie McFarland	Recoil ranges of trans-target products from ^{18}O + ^{248}Cm.
Nov. 5, 1979	D. Ceperley	Exact solutions of the many-body Schodinger equations via stochastic methods.
Nov. 12, 1979	K. Aleklett Studsvik, Sweden	Delayed neutron emission probabilities for 30 isotopes of Ga, Br, In, Sb, I, and Cs.
Nov. 19, 1979	L. D. McLerran SLAC	Explosive quark matter and the Centuaro event.
Nov. 26, 1979	John Harris	Deep inelastic scattering and particle emission in collisions of "light" heavy ions.
Nov. 30, 1979	Noriaki Lakahasi	Spin polarization and alignment in the deep inelastic heavy ion collisions.
Dec. 3, 1979	John Rasmussen	Experiences and research results on a Shanghai sabbatical.
Jan. 7, 1980	Shoji Hagamiya	Geometry and dynamics of high-energy heavy ion collisions.
Jan. 14, 1980	Erwin Friedlander	Interaction properties of projectile fragments from relativistic heavy ion collisions at Bevalac energies: An LNL-NRC collaboration.
Jan. 21, 1980	Herbert Bolotin LBL and University of Melbourne	Level spectroscopy of ^{197}Au and the core excitation model.
Jan. 28, 1980	John Sullivan	Small angle pion production in heavy ion reactions.
	Patrick L. McGaughey	Application of the nuclear fireball model to target residue production in the relativistic reaction of neon and uranium.

*Speakers are LBL staff unless otherwise indicated.

Feb. 2, 1980	E. L. Alpen	Bevalac biomedical science.
Feb. 11, 1980	Barry Berman LLNL	Coulomb dissociation of ^{18}O.
Feb. 18, 1980	Cornelius Noack LBL and University of Bremen, West Germany	Cascade calculations of high energy nuclear collisions.
Feb. 25, 1980	H. J. Mang Technishe Universitat Munchen, West Germany	Application of HFB theory to high spin states in the rare earth region.
Mar. 10, 1980	K. Johnson MIT and SLAC	The MIT bag model of hadron structure.
Mar. 24, 1980	J. Kapusta LASL	Angular momentum transfer in heavy ion reactions from 7.7 to 22.4 MeV/A.
	Michael Cable	Beta delayed proton decay of ^{36}Ca.
Apr. 7, 1980	Edward Teller LLNL	A personal view of future U.S. energy options.
Apr. 14, 1980	Ray Sawyer U.C. Santa Barbara	Some neutron star physics involving nuclear theory.
Apr. 21, 1980	J. Kratz GSI, Darmstadt West Germany	U + U reactions at GSI.
Apr. 28, 1980	Roger Parry	Math measurements of neutron deficient indium isotope.
	Gianluca Rattazzi	A study of the magnitude and direction of fragment spin orientation for the systems Xe + Au and Ho + Ho at 8.5 MeV/A.
May 5, 1980	Paul Vincent GSI, Darmstadt West Germany	Positrons and x rays from superheavy quasi atoms.
May 12, 1980	C. M. Lederer	E1 lifetimes for octopole vibrational states in the actinide region.
May 19, 1980	T. L. Khoo ANL	Feeding of very high spin yrast states.
	B. Muller University of Frankfort, West Germany	Atomic clocks for nuclear collisions.
June 2, 1980	Alden Bice	Light ion structure and reaction studies via measurement of unbound outgoing systems.
	Lee Sobotka	Light particle emission as a probe of the rotational degrees of freedom in deep inelastic reactions.
June 9, 1980	C. D. Goodman Indiana University	Intermediate energy (p,n) reactions and giant resonances.

Nuclear Theory Meetings*

Aug. 1, 1979	Klaus Reidel GSI, Darmstadt, West Germany	Relaxation phenomenon in deep inelastic scattering.
Aug. 8, 1979	R. Vinh Mau Orsay	Baryonium: Multiquark of quasi nuclear state?
Aug. 15 and	Miklos Gyulassy	Normal versus abnormal nuclear states in mean field theory.
Aug. 20, 1979	John Vergados Greece	Lepton non conserving processes in nuclei.
Aug. 22, 1979	Horst Stocker GSI	Indications for strong compression effects in nuclear collisions.
Aug. 29, 1979	Roger Barrett University of Surrey	Kaon nucleus optical potentials and the K^--p atom.
Aug. 30, 1979	Oriol Bohigas	Sum rules, fluid dynamics and giant resonances.
Sept. 5, 1979	R. Remaud LBL and Universite de Nantes	Quantal treatment of damped relaxation modes: The charge equilibrium in heavy ion reactions.
Sept. 6, 1979	Z. Paltiel MIT	A self consistant scheme for calculating energy levels, transition matrix elements, tunneling effect, etc.
Sept. 12, 1979	W. M. Howard LLNL P. Moller Lund University, Sweden	Potential energy surfaces and decay properties of neutron rich heavy elements and its astrophysical implications.
Sept. 19, 1979	Stefan Frauendorf Dresden	Quasi particle band structure above the Yrast line.
Oct. 4 and 17, 1979	Yasha Karant	Color excited nuclei.
Oct. 10, 1979	J. Speth Institut fur Kernphysik Julich	Dynamical theory of giant resonances.
Nov. 7, 1979	Hubert Flocard Orsay	Microscopic calculations of molecular resonances: Calculation of collision mass parameters from adiabatic time-dependent Hartree-Fock.
Nov. 28, 1979	Jørgan Randrup	Kaon production in relativistic nuclear collisions.
Dec. 19, 1979	E. S. Hernandez LBL and Faculty of Science, Buenos Aires	Current theories of Quantal damped motion and fluctuations.
Jan. 17, 1980	Phil Siemens Copenhagen	Evidence for quark matter in nuclear collisions.

*Speakers are LBL staff unless otherwise indicated.

Jan. 23, 1980	H. Kleinert Berlin	Semiclassical approach to large-amplitude collective nuclear excitations.
Jan. 30, 1980	Xi-jun	A. Some theoretical physics research in Shanghai. B. Pion condensates.
Feb. 22, 1980	Herbert Ruck	Fusion of quark bags.
	J. Meyer-Ter-Vehn	Unnatural parity state in nuclei and pion condensation.
Apr. 23, 1980	Yoram Alhassid Cal. Tech.	A constrained phase space approach to analysis of nuclear reaction data.

Papers Published and LBL Reports Issued 1979-80

ACUER, P. (See HILLIS, D. L., LBL-9519)

ALBISTON, C. R. (See MORETTO, L. G., LBL-9896)

ALEKLETT, K. (See LOVELAND, W., LBL-10810)

ALEONARD, M. M. (See WARD, D., No LBL number)

ALMBERGER, J., I. Hamamoto, G. Leander, and J. O. Rasmussen
Theoretical Rotational Signatures for Neutron Pickup Reaction to $(i_{13/2})^2$ Bands
No LBL number, September 1979
Phys. Letts. 90B (1980) 1

ANDREWS, H. R. (See WARD D., No LBL number)

AVERY, M. (See VAN BIBBER, K., LBL-9979)

AWES, T. C. (See WESTFALL, G. D., LBL-9926)

AYSTO, J., M. D. Cable, R. F. Parry, J. M. Wouters, D. M. Moltz, and Joseph Cerny
Decays of the $T_Z = -2$ Nuclei ^{20}Mg, ^{24}Si and ^{36}Ca
LBL-11193, June 1980
Phys. Rev. C.

AYSTO, Juha and Joseph Cerny
Current and Future Directions in the Study of Light Nuclei Employing an on-Line Mass Separator
LBL-9878, September 1979
Presented at the International Symposium on Future Directions in Studies of Nuclei from Stability, Vanderbilt University, Nashville, TN, September 10-13, 1979. J.H. Hamilton, et al. (Eds.) 257 (1980)

AYSTO, J. (See CERNY, Joseph, LBL-9876)

AYSTO, J. (See MOLTZ, D. M., LBL-9721)

BANERJEE, B., N. K. Glendenning and M. Gyulassy
Pion Condensation in a Field Theory Consistent with Bulk Properties of Nuclear Matter
LBL-10979, May 1980
Nucl. Phys.

BEMIS, C. E., Jr., (See NITSCHKE, J. M., LBL-10173)

BETLACH, M. R. (See FIRESTONE, R. B., LBL-10919)

BIESER, F. S. (See WIEDENBECK, M. E., LBL-8920)

BIRCHALL, J., W. T. H. van Oers, H. E. Conzett, P. von Rossen, R. M. Larimer, J. Watson, and R. E. Brown
Analyzing Powers of $^3He(p,p)^3He$ Elastic Scattering between 30 and 50 MeV
LBL-11121, June 1980
Presented at the 5th International Symposium on Polarization in Nuclear Physics, Santa Fe, NM, August 11-15, 1980

BIRKELUND, J. R. (See SCHRODER, W. U., LBL-10529)

BLOEMHOLF, E. (See VAN BIBBER, K., LBL-9979)

FIRESTONE, R. B., M. R. Betlach, J. M. Tiedje, and M. K. Firestone
The Feasibility of Producing ^{11}C, ^{13}N, ^{15}O, and ^{18}F with Heavy-ion Beams
LBL-10919, May 1980
Advances in Chemistry

FIRESTONE, R. B. and E. Browne
Nuclear Structure Database
LBL-11089, UC-34c, June 1980

FLOCARD, H. (See DAVIES, K. T. R., LBL-10269)

FOSSAN, D. B. (See HILLIS, D. L., LBL-9519)

FOWLER, M. (See NITSCHKE, J. M., LBL-10173)

FRAENKEL, Z. (See MORRISSEY, LBL-8964)

FRANKEL, Kenneth Alan
Interactions of 100 MeV/Nucleon ^{40}Ar with Uranium
LBL-10980, December 1979

FRIEDLANDER, E. M., R. W. Gimpel, H. H. Heckman, Y. J. Karant, B. Judek, and E. Ganssauge
Evidence for Anomalous Nuclei among Relativistic Projectile Fragments from Heavy Ion Collisions at Bevalac Energies
LBL-11136, June 1980
Phys. Rev. Lett.

FROIS, B. (See LAMONTAGNE, C. R., LBL-8555)

GANSSAUGE, E. (See FRIEDLANDER, E. M., LBL-11136)

GEAGA, J. V., S. A. Chessin, J. Y. Grossiord, J. W. Harris, D. L. Hendrie, L. S. Schroeder, R. N. Treuhaft and K. Van Bibber
Observation of High Momentum Protons from Limiting Target Fragmentation
LBL-10265, April 1980
Phys. Rev. Letts.

GEAGA, J. V. (See VAN BIBBER, K., LBL-8939)

GELBKE, C. K. (See WESTFALL, G. D., LBL-9926)

GHIORSO, A. (See HULET, E. K., LBL-9844)

GHIORSO, A. (See NITSCHKE, J. M., LBL-10173)

GIMPEL, R. W. (See FRIEDLANDER, E. M., LBL-11136)

GLENDENNING, Norman K.
Pion Condensation in a Theory Consistent with Bulk Properties of Nuclear Matter
LBL-10388, January 1980
Invited paper presented at International Workshop VIII, Hirschegg, Austria, January 14-19, 1980

GLENDENNING, N. K. (See BANERJEE, B., LBL-10572)

GLENDENNING, N. K. (See BANERJEE, B., LBL-10979)

GOLDBERG, D. A. (See ZISMAN, M. S., LBL-9405)

GOLDBERG, D. A. (See ZISMAN, M. S., LBL-10204)

GOSSET, J. (See SANDOVAL, S., LBL-8771)

GOUGH, R. A. (See MOLTZ, D. M., LBL-9476)

GREINER, D. E. (See WESTFALL, G. D., LBL-9926)

GREINER, D. E. (See WIEDENBECK, M. E., LBL-8920)

GROSSIORD, J. Y. (See GEAGA, J. V., LBL-10265)

GROSSIORD, J. Y. (See VAN BIBBER, K., LBL-8939)

GUIDRY, M. W. (See NEESE, R. E., no LBL number)

GUIDRY, M. W. (See RASMUSSEN, J. O., LBL-8540)

GUIDRY, Mike (See RASMUSSEN, no LBL number)

GUTBROD, H. H.
Search for Collective Phenomena in Relativistic Nuclear Collisions
LBL-11123, June 1980
Presented at the 1980 Institute for Nuclear Studies, Kikuchi Summer School on Nuclear Physics at High Energies (Fuji-Yoshida) July 1-4, 1980, and Conference on High Energy Nuclear Interactions and Properties of Dense Nuclear Matter (Hakone) Japan, July 7-11, 1980

GUTBROD, H. H.
Search for Extreme States in Nuclear Matter (or Looking for Collective Phenomena)
LBL-10624, March 1980
Presented at the International Conference on Extreme States in Nuclear Systems, Dresden, West Germany, February 4-9, 1980)

GUTBROD, H. H. (See MAIER, M. R., LBL-10062)

GUTBROD, H. H. (See MEYER, W. G., LBL-9151)

GUTBROD, H. H. (See SANDOVAL, S., LBL-8771)

GYULASSY, M., S. K. Kauffmann, and Lance W. Wilson
Pion Interferometry of Nuclear Collisions. I. Theory
LBL-8759, April 1979
Phys. Rev. C20 (1979) 2267

GYULASSY, Miklos
Pion Condensation and Instabilities: Current Theory and Experiment
LBL-10883, May 1980

GYULASSY, M. and S. K. Kauffmann
Coulomb Effects in Relativistic Nuclear Collisions
LBL-10279, March 1980

GYULASSY, M. (See BANERJEE, B., LBL-10572)

GYULASSY, M. (See BANERJEE, B., LBL-10979)

GYULASSY, M. (See KAUFFMANN, S. K., LBL-9011)

HABS, D. (See HILLIS, D. L., LBL-9519)

HAMAMOTO, I. (See ALMBERGER, J., no LBL number)

HAMILTON, J. H. (See RASMUSSEN, LBL-8540)

HARRIS, J. W. (See GEAGA, J. V., LBL-10265)

HAUSSER, O. (See WARD, D., no LBL number)

HAUSTEIN, P. E. (See CERNY, Joseph, LBL-9876)

HAUSTEIN, P. E. (See LOVELAND, W., LBL-10010)

HECKMAN, H. H. (See FRIEDLANDER, E. M., LBL-11136)

HECKMAN, H. H. (See WESTFALL, G. D., LBL-9926)

HECKMAN, H. H. (See WIEDENBECK, LBL-8920)

HENDRIE, D. L. (See GEAGA, J. V., LBL-10265)

HENDRIE, D. L. (See VAN BIBBER, K., LBL-8939)

HERNANDEZ, E. S.
The Role of Fluctuations in the Quantal Description of Damped Motion
LBL-10321, January 1980

HERNANDEZ, E. S. and G. Mantzouranis
Markovian and Non-Markovian Effects in Heavy-Ion Reactions at k10-200 MeV per Nucleon
LBL-9568, August 1979
Phys. Rev. C22 (1980)

HERNANDEZ, E. S., W. D. Myers, J. Randrup and B. Remaud
Quantal Dynamics of Charge Equilibration in Damped Nuclear Collisions
LBL-9761, October 1979
Nucl. Phys.

HERNANDEZ, E. S. and B. Remaud
Quantal Fluctuations and Invariant Operators for a General Time-Dependent Harmonic Oscillator
LBL-9558, August 1979
Phys. Lett. 75A (1980) 269

HERNANDEZ, E. S. (See Remaud, B., LBL-9506)

HILLIS, D. L., C. P. Roulet, F. S. Stephens, P. Aguer, C. Ellegaard, D. B. Fossan, D. Habs, H. J. Korner, H. Kluge, S. Shih, and R. M. Diamond
Super-Deformed Shapes in Rotating Nuclei
LBL-9519, October 1979
Phys. Rev. Letts.

HSEUH, H. C. (See LOVELAND, W., LBL-10010)

HULET, R. K., R. W. Lougheed, J. F. Wild, J. H. Landrum, J. M. Nitschke, and A. Ghiorso
Chloride Complexation of Element 104
LBL-9844, May 1979
J. Inorg. Nucl. Chem. 42 (1980) 79

HULET, R. K. (See NITSCHKE, J. M., LBL-10173)

HUZENGA, J. R. (See SCHRÖDER, W. U., LBL-10529)

INGERSOLL, J. (See CHIBA, J., LBL-8699)

JAHN, R. (See STAHEL, D. P., LBL-8636)

JOURDAIN, J.-C. (See SANDOVAL, A., LBL-8771)

JUDEK, B. (See FRIEDLANDER, E. M., LBL-11136)

KAPUSTA, Joseph
Mechanisms for Deuteron Production in Relativistic Nuclear Collisions
LBL-9251, June 1979
Phys. Rev. C21 (1980) 1301

KARANT, Y. J. (See FRIEDLANDER, E. M., LBL-11136)

KAUFFMANN, S. K. and M. Gyulassy
Charge-Constrained Coherent Pion States Produced in Nuclear Matter
LBL-9011, April 1979
Nucl. Phys. A333 (1980) 392

KAUFFMANN, S. K. (See GYULASSY, M., LBL-8759)

KAUFFMANN, S. K. (See GYULASSY, M., LBL-10279)

KAUFMAN, S. B. (See LOVELAND, W., LBL-10080)

KIDD, J. M. (See WESTFALL, G. D., LBL-9926)

KING, C. H. (See SANDOVAL, A., LBL-8771)

KNOLL, Jorn (See BOHRMAN, Steffen, LBL-10970)

KLUGE, H. (See HILLIS, D. L., LBL-9519)

KO, Che Ming
Evidence for Statistical Fluctuation in the Fragmentation of ^{16}O at Intermediate Energies
LBL-9985, November 1979
Phys. Rev. C21 (1980) 2672

KO, Che Ming and Steffen Bohrmann
A Model for Pion Absorption in Nuclei
LBL-11041, June 1980
Phys. Lett. B

KO, Che Ming and TA-chung
180^{o} Production of p, d, and t, and p-p Correlation in p-Nucleus Collisions
LBL-8933, March 1979
Phys. Rev. Lett. 43 (1979) 994

KO, C. M. (See RANDRUP, J., LBL-10530)

KORNER, H. J. (See HILLIS, D. L., LBL-9519)

KRIEGER, S. (See DAVIES, K. T. R., LBL-10269)

LAMONTAGNE, C. R., B. Frois, R. J. Slobodrian, H. E. Conzett, and Ch. Leemann
The p-Si Elastic Scattering in the Region of Giant Multipole Resonances
LBL-8555, December 1978
Z. Physik A - Atoms and Nuclei 295 (1980) 55

LANDAU, Rubin H. and John O. Rasmussen
Pion Production with Heavy Ions
LBL-8654, January 1979
Invited Comm. Nucl. Part.
Phys. 9 (1979) 1

LANDRUM, J. H. (See HULET, E. K., LBL-9844)

LANDRUM, J. H. (See NITSCHKE, J. M., LBL-10173)

LARIMER, R. M. (See BIRCHALL, J., LBL-11121)

LARIMER, R. M. (See STEPHENSEON, E. J.. LBL-9531)

LEANDER, G. (See ALMBERGER, J., no LBL number)

LEBER, R. E. (See NITSCHKE, J. M., LBL-10173)

LEBER, R. E. (See RASMUSSEN, J. O., LBL-8540)

LEEMANN, Ch. (See LAMONTAGNE, C. R., LBL-8555)

LEEMANN, Ch. (See STEPHENSON, E. J., LBL-9531)

LEGRAIN, R. (See RAE, W. D., LBL-11135)

LEMAIRE, M.-C.
Complex Fragment Emission in Relativistic Heavy Ion Collisions
LBL-10555, October 1979
Presented at the Colloque Fanco-Japonaise de Physique Nucleaire avec des Ions Lourds, Saclay, France, October 8-12, 1979)

LEMAIRE, M.-C. (See TANIHATA, LBL-9352)

LINDSTROM, P. J. (See WESTFALL, G. D., LBL-9926)

LINDSTROM, P. J. (See WIEDENBECK, M. E., LBL-8920)

LOUGHEED, R. W. (See HULET, E. K., LBL-9844)

LOUGHEED, R. W. (See NITSCHKE, J. M., LBL-10173)

LOVELAND, W., D. J. Morrissey, K. Aleklett, G. T. Seaborg, S. B. Kaufman, E. P. Steinberg, B. D. Wilkins, J. B. Cumming, P. E. Haustein, and H. C. Hseuh
Target Residue Recoil Properties in the Interaction of 8.0 GeV ^{20}Ne with ^{181}Ta
LBL-10010, May 1980
Phys. Rev. C

LOVELAND, W. (See MORRISSEY, D. J., LBL-8983)

LUKNER, Ch. (See MEYER, W. G., LBL-9151)

LUKNER, Ch. (See SANDOVAL, A., LBL-8771)

MA, A. Y., X. Z. Wu, G. S. Zhang, Y. C. Cho, Y. S. Wang, J. H. Chiou, S. T. Sen, C. C. Yang, and J. O. Rasmussen
Calculation of Muon Final State Probabilities after Muon-Induced Fission
LBL-9689, August 1979
Nucl. Phys.

MAHONEY, J. (See RAE, W. D., LBL-11135)

MAHONEY, J. (See WESTFALL, G. D., LBL-9926)

MAIER, M. R., H. G. Ritter, and H. H. Gutbrod
The Plastic Ball - A Multi-Detector, Large Solid Angle Spectrometer with Charged Particle Identification for the Bevalac
LBL-10062, January 1980
Presented at the Proceedings of the IEEE Transactions in Nuclear Science, San Francisco, California, October 17-20, 1979
IEEE Trans. on Nucl. Sci. NS-27 (1980) 42

MAIER, M. R. (See RICHARDSON, L. W., LBL-10146)

MANTZOURANIS, G. (See HERNANDEZ, E. S., LBL-9568)

MANTZOURANIS, G. (See MORETTO, L. G., LBL-9896)

MATHEWS, G. J., and L. G. Moretto
On Barrier Penetration in Complete-Fusion Systems
LBL-8972, March 1979
Phys. Lett. 87B (1979) 331

MATHEWS, G. J. (See SCHMITT, R. P., LBL-9512)

MATHEWS, G. J. (See SOBOTKA, L. G., LBL-8512)

McPARLAND, C. (See WESTFALL, G. D., LBL-9926)

MEYER, W. G., H. H. Gutbrod, Ch. Lukner and A. Sandoval
Correlations between Slow and Fast Fragments in
Relativistic Nuclear Collisions
LBL-9151, May 1979
Phys. Rev. C22 (1980) 179

MEYER, W. G. (See SANDOVAL, A., LBL-8771)

MOLLER, Peter (See RASMUSSEN, J. O., no LBL number)

MOLTZ, Dennis M.
Development of the Helium-Jet Fed on-Line Mass Separator
RAMA and its Application to Studies of T_z = -2 Nuclei
LBL-9718, October 1979

MOLTZ, D. M., R. A. Gough, M. S. Zisman, D. J. Vieira,
H. C. Evans and J. Cerny
Development of the Helium-Jet Fed on-Line Mass Separator
RAMA, I
LBL-9476, December 1979
Nucl. Inst. and Meth. 172 (1980) 507

MOLTZ, D. M., J. M. Wouters, J. Aysto, M. D. Cable,
R. R. Parry, R. D. von Dincklage, and J. Cerny
Development of the He-Jet Fed on-Line Mass Separator
RAMA, II
LBL-9721, December 1979
Nucl. Inst. and Meth. 172 (1980) 519

MOLTZ, D. M. (See AYSTO, J., LBL-11193)

MOLTZ, D. M. (See CERNY, Joseph, LBL-9876)

MORETTO, L. G., C. R. Albiston and G. Mantzouranis
High Multipole Isovector Modes and Charge Fluctuations
in Heavy Ion Reactions
LBL-9896, November 1979
Phys. Rev. Letts. 44 (1980) 924

MORETTO, Luciano G. and Richard P. Schmitt
Equilibrium Statistical Treatment of Angular Momenta
Associated with Collective Modes
LBL-8656, May 1979
Phys. Rev. C21 (1980) 204

MORETTO, L. G. (See MATHEWS, G. J., LBL-8972)

MORETTO, L. G. (See RICHARDSON, L. W., LBL-10146)

MORETTO, L. G. (See SCHMITT, R. P., LBL-9512)

MORETTO, L. G. (See SOBOTKA, L. G., LBL-8512)

MORRISSEY, D. J., W. Loveland, M. de Saint Simon, and
G. T. Seaborg
Target Residues from the Reaction of 8 GeV ^{20}Ne with
^{181}Ta and ^{197}Au
LBL-8983, May 1979
Phys. Rev. C21 (1980) 1783

MORRISSEY, D. J., L. F. Oliveira, J. O. Rasmussen,
G. T. Seaborg, Y. Yariv and Z. Fraenkel
Microscopic and Macroscopic Model Calculations of
Relativistic Heavy Ion Fragmentation Reactions
LBL-8964, March 1979)
Phys. Rev. Letts. 43 (1979) 1139

MORRISSEY, D. J. (See LOVELAND, W., LBL-10010)

MORRISSEY, D. J. (See NAGAMIYA, S., LBL-10461)

MURPHY, M. J. (See RAE, W. D., LBL-11135)

MYERS, William D., Jørgen Randrup, and Gary D. Westfall
Workshop on Nuclear Dynamics
LBL-10688, March 1980
Workshop on Nuclear Dynamics, Granlibakken, Tahoe City, California, 17-21 March 1980

MYERS, W. D. and W. J. Swiatecki
Droplet Model Theory of the Neutron Skin
LBL-9306, June 1979
Nucl. Phys. A336 (1980) 267

MYERS, W. D. (See HERNANDEZ, E. S., LBL-9761)

NAGAMIYA, S.
Central Nuclear Collisions: the Past and the Future
LBL-10956, May 1980
Presented at the Hakone Seminar on "High Energy Nuclear Interactins and Properties of Dense Nuclear Matter", Hakone, Japan, July 7-11, 1980

NAGAMIYA, Shoji
Topics in Relativistic Heavy-Ion Collisions
LBL-9611, August 1979
Nucl. Phys. A335 (1980) 517

NAGAMIYA, S. and D. J. Morrissey
The Geometrical Aspect of High-Energy Heavy Ion Collisions
LBL-10461, February 1980
Phys. Letts. B

NAGAMIYA, S. (See CHIBA, J., LBL-8699)

NAGAMIYA, S. (See NAKAI, K., LBL-10936)

NAGAMIYA, S. (See TANIHATA, LBL-9352)

NAKAI, K., J. Chiba, I. Tanihata, M. Sasao, H. Bowman, S. Nagamiya, and J. O. Rasmussen
Low-energy Pion Production in High-energy Nucleus-nucleus Collisons
LBL-10936, 1979
Phys. Rev. C20 (1979) 2210

NAKAI, K. (See CHIBA, J., LBL-8699)

NEESE, R. E., M. W. Guidry, R. Donangelo, and J. O. Rasmussen
Surface Structure of Deformed Nuclei by Radial and Angular Localization in Heavy Ion Scattering
No LBL number
Phys. Letts. 85B (1979) 201

NEESE, Richard (See RASMUSSEN, J. O., no LBL number)

NGUYEN, Van Sen (See SANDOVAL, A., LBL-8771)

NITSCHKE, J. M., M. Fowler, A. Ghiorso, R. E. Leber, M. J. Nurmia, L. P. Somerville, K. E. Williams, E. K. Hulet, J. H. Landrum, R. W. Lougheed, J. F. Wild, C. E. Bemis, Jr., R. J. Silva, and P. Eskola
Search for an 80-ms Spontaneous Fission Activity in Bombardments of ^{249}Bk with ^{15}N
LBL-10173, January 1980
Nucl. Phys. A.

NITSCHKE, J. M. (See HULET, E. K., LBL-9844)

NUCLEAR SCIENCE DIVISION
Nuclear Science Division Annual Report 1978-1979
LBL-9711, UC-34, March 1980

NURMIA, M. J. (See NITSCHKE, J. M., LBL-10173)

OLIVEIRA, L. F. (See MORRISSEY, LBL-8964)

PANG, W. (See VAN BIBBER, K., LBL-9979)

PARRY, R. F. (See AYSTO, J., LBL-11193)

PARRY, R. F. (See CERNY, Joseph, LBL-9876)

PARRY, R. F. (See MOLTZ, D. M., LBL-9721)

PEKER, L. K. (See RASMUSSEN, J. O., LBL-8540)

POSKANZER, A. M. (See SANDOVAL, A., LBL-8771)

PRICE, P. B. (See STEVENSON, J. D., LBL-10054)

PRUESS, K.
Amplitude for Transitions between Molecular (Two-Center) Channels
LBL-7747, June 1978
Nucl. Phys. A330 (1979) 209

RAE, W. D., R. G. Stokstad, B. G. Harvey, A. Dacal, R. LeGrain, J. Mahoney, M. J. Murphy, and T. J. M. Symons
Molecular Resonances and the Production of Fast α-Particles in the Reaction of ^{16}O with $^{12,13}C$ Nuclei
LBL-11135, June 1980
Phys. Rev. Letts.

RAMON, Ceon and Elizabeth A. Rauscher
Superluminal Transformations in Complex Minkowski Space
LBL-9752, November 1979
Foundation of Phys.

RANDRUP, J.
Multiple Nucleon Transfer in Damped Nuclear Collisions
LBL-9638, December 1979
Notes for a lecture given at the Enrico Fermi Summer School on Nuclear Physics, Varenna, Italy, July 9-21, 1979

RANDRUP, J.
Nuclear Collisions at $E/A = T_F$
LBL-9520, July 1979
Invited talk given at the "Symposium on Heavy-Ion Physics from 10 to 200 MeV/AMU," Brookhaven National Laboratory, July 16-20, 1979

RANDRUP, Jørgen
Nuclear Collisions at Several Tens of MeV per Nucleus
LBL-9902, October 1979
Notes for lectures given at the Serre-Chevallier Summer School, Serre-Chevallier, France, September 10-14, 1979

RANDRUP, J.
Nuclear Proximity Forces
LBL-9569, October 1979
Notes for a lecture given at the Enrico Fermi Summer School of Nuclear Physics at Varenna, Italy

RANDRUP, J. and C. M. Ko
Kaon Production in Relativistic Nuclear Collisions
LBL-10530, January 1980
Nucl. Phys. A343 (1980) 519

RANDRUP, J. and W. J. Swiatecki
One-Body Dissipation and Nuclear Dynamics
LBL-10495, October 1978
Ann. of Phys. 125 (1980) 193

RANDRUP, J. (See HERNANDEZ, E. S., LBL-9761)

RANDRUP, Jørgen (See MYERS, William D., LBL-10688

RANDRUP, J. (See SCHRÖDER, W. U., LBL-10529)

RASMUSSEN, J. O., M. W. Guidry, T. E. Ward, C. Castaneda, L. K. Peker, L. Leber, and J. H. Hamilton
Rotational Energy Expressions and Least-Squares Fitting of Backbenders and Similar Nuclei
LBL-8540, June 1979
Nucl. Phys. A332 (1979) 82

RASMUSSEN, John, Peter Moller, Mike Guidry, and Richard Neese
Giant Resonance Polarization Terms in the Nucleus-Nucleus Potential*
No LBL number, 1980
Nucl. Phys. A341 (1980) 149

RASMUSSEN, J. O. (See ALMBERGER, J., no LBL number)

RASMUSSEN, J. O. (See CHIBA, J., LBL-8699)

RASMUSSEN, John O. (See LANDAU, Rubin H., LBL-8654)

RASMUSSEN, J. O. (See MA, A, Y., LBL-9689)

RASMUSSEN, J. O. (See MORRISSEY, LBL-8964)

RASMUSSEN, John O. (See NAKAI, K., LBL-10936)

RASMUSSEN, J. O. (See NEESE, R. E., no LBL number)

RASMUSSEN, J. O. (See VAN BIBBER, K., LBL-8939)

RATTAZZI, G. U. (See SCHMITT, R. P., LBL-9512)

RAUSCHER, Elizabeth A. (See RAMON, Ceon, LBL-9752)

REGIMBART, R. (See SCHMITT, R. P., LBL-9512)

REMAUD, B. and E. S. Hernandez
Damping of the Wave Packet Motion in a General Time-Dependent Quadratic Field
LBL-9506, September 1979
Journ. of Phys.

REMAUD, B. (See HERNANDEZ, E. S., LBL-9558)

REMAUD, B. (See HERNANDEZ, E. S., LBL-9761)

RICHARDSON, L. W., G. J. Wozniak, M. R. Maier and L. G. Moretto
Neutron-Gamma Discrimination Using NaI(Tl) Scintillators with Application for Measurement of the Gamma-Ray Multiplicity Distribution in Heavy-Ion Reactions
LBL-10146, November 1979
Nucl. Inst. and Meth.

RITTER, H. G. (See MAIER, M. R., LBL-10062)

ROULET, C. P. (See HILLIS, D. L., LBL-9519)

ROY, R. (See STEPHENSON, E. J., LBL-9531)

SALAMON, Michael H.
A Range-Energy Program for Relativistic Heavy Ions in the Region 1 < E < 3000 MeV/amu
LBL-10446, January 1980)

SANDOVAL, A.
4π Physics
LBL-10721, March 1980
Presented at the Workshop on Nuclear Dyanmics, Granlibakken, Lake Tahoe, Nevada, March 24-28, 1980

SANDOVAL, A., H. H. Gutbrod, W. G. Meyer, A. M. Poskanzer, R. Stock, J. Gosset, J.-C. Jourdain, C. H. King, G. King, Ch. Lukner, Nguyen Van Sen, G. D. Westfall, and K. L. Wolf
Spectra of p, d, and t from Relativistic Nuclear Collisions
LBL-8771, September 1979
Phys. Rev. C21 (1980) 1321

SANDOVAL, A. (See W. G. Meyer, LBL-9151)

SASAO, M. (See NAKAI, K., LBL-10936)

SCHMITT, R. P., G. J. Wozniak, G. U. Rattazzi, G. J. Mathews, R. Regimbart and L. G. Moretto
Fast Particle Emission in the Deep Inelastic Reaction $^{nat}Cu + ^{20}Ne$ at 12.6 MeV/Nucleon
LBL-9512, January 1980
Phys. Letts.

SCHMITT, Richard P. (See MORETTO, Luciano G., LBL-8656)

SCHNETZER, S. (See TANIHATA, LBL-9352)

SCHRÖDER, W. U., J. R. Birkelund, J. R. Huzenga, W. W. Wilcke and J. Randrup
Effect of Pauli Blocking on Exchange and Dissipation Mechanisms Operating in Heavy-Ion Reactions
LBL-10529, October 1979
Phys. Rev. Letts. 44 (1980) 308

SCHROEDER, L. S. (See GEAGA, J. V., LBL-10265)

SCHROEDER, L. S. (See VAN BIBBER, K., LBL-8939)

SCOTT, D. K. (See VAN BIBBER, K., LBL-3939)

SCOTT, D. K. (See WESTFALL, G. D., LBL-9926)

SEABORG, Glenn T.
The New Elements
LBL-11364, 1980
American Scientist 68 (1980) 279

SEABORG, Glenn T.
The Periodic Table, Tortuous Path to Man-Made Elements
LBL-9074
Chem. Engin. News 57 (1979) 46

SEABORG, G. T. (See LOVELAND, W., LBL-10010)

SEABORG, G. T. (See MORRISSEY, D. J., LBL-8964)

SEABORG, G. T. (See MORRISSEY, D. J., LBL-8983)

SEN, S. T. (See MA, A. Y., LBL-9689)

SHAPIRO, G. (See TANIHATA, LBL-9352)

SHIH, S. (See HILLIS, D. L., LBL-9519)

SHOTTER, A. C. (See WESTFALL, G. D., LBL-9926)

SIEMENS, Philip J.
Heavy Ion Collisions
LBL-9595, December 1979
Presented at the Eighth International Conference on High Energy Physics and Nuclear Structure, Vancouver, BC, Canada, August 1979

SILVA, R. J. (See NITSCHKE, J. M., LBL-10173)

SLOBODRIAN, R. J. (See LAMONTAGNE, C. R., LBL-8555)

SOBOTKA, L. G., G. J. Mathews, and L. G. Moretto
A Theoretical Investigation of Shell Effects in Deep Inelastic collisions
LBL-8512, May 1979
Zietschrift fur Physik A<u>292</u> (1979) 191

SOMERVILLE, L. P.
New Spontaneous Fission Activities Produced in the Bombardments of $^{248}_{96}$Cm and $^{249}_{97}$Bk by $^{13}_{6}$C, $^{15}_{7}$N, $^{16}_{8}$O, and $^{18}_{8}$O Ions
LBL-9754, September 1979
Further Directions in Studies of Nuclei far from Stability. J. H. Hamilton, et al., (eds.) North-Holland Publ. Company 337 (1980)

SOMERVILLE, L. P. (See NITSCHKE, J. M., LBL-10173)

STAHEL, Dieter Paul
Nuclear Reactions Producing ^{2}He and Excited States of ^{4}He as Unbound Outgoing Systems
LBL-9706, September 1979
Ph.D. thesis

STAHEL, D. P., R. Jahn, G. J. Wozniak and Joseph Cerny
Charge-Exchange Reaction (d, ^{2}He)
LBL-8636, May 1979
Phys. Rev. C<u>20</u> (1979) .680

STEINBERG, E. P. (See LOVELAND, W., LBL-i0010)

STEINER, H. (See TANIHATA, LBL-9352)

STEPHENS, F. S.
Gamma-Rays from Deep Inelastic Collisions
LBL-10356, January 1980
Presented at the Varenna Conf.rence, Varenna, Italy, July 9-25, 1979

STEPHENS, F. S.
Nuclear Structure at High Angular Momentum
LBL-10957, June 1980
Presented at the Nuclear Physics Workshop, Tandar Project, Comision Nacional de ˈrergia Atomica, Argentina, April 7-18, 1980

STEPHENS, F. S.
Phenomena at Very High Spins
LBL-10645, March 1980
Presented at the Conference on Band Structure and Nuclear Dynamics, New Orleans, Louisiana, February 27-March 1, 1980

STEPHENS, F. (See DIAMOND, R. M., LBL-10325)

STEPHENS, F. (See HILLIS, D. L., LBL-9519)

STEPHENS, F. (See WARD, D., no LBL number)

STEPHENSON, E. J., H. E. Conzett, R. M. Larimer, B. T. Leemann, R. Roy and P. von Rossen
Tensor Analyzing Powers in ^{4}He(d,d)^{4}He Elastic Scattering between 17 and 45 MeV
LBL-9531, August 1979
Phys. Rev. C21 (1980) 44

STEVENSON, J. D., P. B. Price and M. P. Budiansky
Imaging and Identification of Relativistic Projectile Fragments with Lexan Spectrometry
LBL-10054, October 1979
Nucl. Inst. and Meth.

STOCK, R. (See SANDOVAL, A., LBL-8771)

STOKSTAD, R. G. (See RAE, W. D., LBL-11135)

SWIATECKI, W. J.
The Dynamics of Nuclear Coalescence or Reseparation
LBL-10911, June 1980
Presented at the Nobel Symposium on High-Spin States, Orenas, Sweden, June 22-25, 1980; and submitted to Physica Scripta

SWIATECKI, W. J. (See MYERS, W. D., LBL-9306)

SWIATECKI, W. J. (See RANDRUP, J., LBL-10495)

SYMONS, T. J. M. (See RAE, W. D., LBL-11135)

SYMONS, T. J. M. (See WESTFALL, G. D., LBL-9926)

TA-Chung, Meng (See KO, Che-Ming, LBL-8933)

TANIHATA, I., S. Nagamiya, O. Chamberlain, M.-C. Lemaire, S. Schnetzer, G. Shapiro and H. Steiner
Negative Pion Production by 800 MeV/A C, Ne, and Ar Beams
LBL-9352, June 1979
Phys. Lett. 87B (1979) 349

TANIHATA, I. (See CHIBA, J., LBL-8699)

TANIHATA, I. (See NAKAI, K., LBL-10936)

THOMAS, Kenneth Eugene, III
Transfer Products from the Reactions of Heavy Ions with Heavy Nuclei
LBL-9886, November 1979
Ph.D. thesis

TIEDJE, J. M. (See FIRESTONE, R. B., LBL-10919)

TREUHAFT, R. N. (See GEAGA, J. V., LBL-10265)

TREUHAFT, R. (See VAN BIBBER, K., LBL-8939)

VAN BIBBER, K., D. L. Hendrie, D. K. Scott, H. H. Wieman, L. S. Schroeder, J. V. Geaga, S. A. Chessin, R. Treuhaft, J. Y. Grossiord, J. O. Rasmussen and C. Y. Wong
Evidence for Orbital Dispersion in the Fragmentation of ^{16}O at 90 and 120 MeV/Nucleon
LBL-8939, March 1979
Phys. Rev. Letts. 43 (1979) 840

VAN BIBBER, K., W. Pang, M. Avery and E. Bloemhof
Use of a Streamer Chamber for Low Energy Nuclear Physics
LBL-9979, October 1979
Invited talk at the Nuclear Science Symposium, San Francisco, California, October 17-19, 1979
IEEE Trans. on Nucl. Sci. NS-27 (1980) 86

Author Index